Prediction of solubility and diffusion properties of pesticides in polymers

Muro Sunè, Nuria; Gani, Rafiqul

Publication date:
2006

Document Version
Publisher's PDF, also known as Version of record

Prediction of solubility and diffusion properties of pesticides in polymers

Ph.D. Thesis

Núria Muro Suñé
CAPEC
Department of Chemical Engineering
Technical University of Denmark

August 2005

Preface

This thesis is submitted in partial fulfilment of the requirements for the Ph.D. degree at the Technical University of Denmark (Danmarks Tekniske Universitet).
This work has been carried out from August 2002 to July 2005 at the Department of Chemical Engineering (Institut for Kemiteknik) under the supervision of Professor Rafiqul Gani.
The project has been financed by Syngenta and the PMILS European project, to whom the author is very grateful.
I would like to thank my supervisor for granting me the opportunity to work on this project, and for the time dedicated to the work, as well as the inputs and the discussions along the way.
Furthermore, special acknowledgements to Dr. Gordon Bell for the enormous help, dedication and advice received, and thanks to Dr. Ian Shirley, for the ideas and discussions throughout the project.
Also, I want to recognize the help received from Dr. Grozdana Bogdanic.

Finally, a number of people have been very important during these years, and I would specially like to thank:

- Michael, for bringing me back to the real world.
- My parents and the rest of my family and friends back home. Moltes gràcies per ser sempre a l'altra banda del telèfon.
- Mauricio, Edgar and Jorge for your extraordinary patience and great help.
- Mariana for the enormous moral support.
- Jose, Jaime, and many other friends for reminding me that there are other things besides work.
- Jan, Jacob og Steen, tak for alt.

August 2005

Núria Muro Suñé

Summary

In the agrochemical industry, the use of controlled release technology for the delivery of pesticides to the environment has numerous advantages, from optimized delivery of the Active Ingredient (AI) to reduction of possible hazards to humans and the environment. The ability to model and study the delivery of AIs from controlled release devices is a very useful tool in product design where different pesticide-polymer combinations need to be tested to obtain the desired release behaviour. A model-based analysis of the release from different product alternatives provides, therefore, significant reduction of time and economical resources usually needed for the experimental measurements.

The objective of this thesis is to develop controlled release mathematical models and integrate them with predictive models for the estimation of the properties required by the release models. With this, the delivery of an AI from a specific controlled release device can be studied without the need, in principle, of additional experimental measurements.

According to the stated objectives, a model for the release of AIs from a microcapsule device has been developed, tested and further extended to include important special effects observed during the initial periods of delivery. The critical properties that control the delivery of an AI from a controlled release device have been identified as the solubility and the diffusivity (of the AIs) and therefore predictive models for their estimation are proposed.

For the study of the solubility of the AIs in the polymers, an approach involving the estimation of activity coefficients of the compounds in polymers is suggested. A group contribution based model for the estimation of these activity coefficients is selected and further developed to allow for the calculations involving the complex pesticide molecules. In the case of the diffusion coefficient, the predictive model is based on the free volume theory of diffusion, with special attention to its application to large molecules representative of pesticides.

The property models for solubility and diffusivity are integrated with the release model, and used to study the release behaviour of typical industrial pesticides encapsulated within microcapsules. With this, the overall performance of the predictive property models and the release models is assessed. Additional examples highlight that the developed models can also be applied to the release of pharmaceutical AIs.

Finally, the basis for a predictive model-based analysis of the release behaviour of different pesticide-polymer alternatives has been established through a systematic study of the important issues, such as, need for predictive models and data needed for their development and verification.

Resumé på Dansk

Anvendelse af teknologier til kontrolleret frigivelse af et pesticid til omgivelserne har stort potentiale for den kemiske industri i forbindelse med produkter til landbrugssektoren. Denne teknologi muliggør en optimering af udskillelsen af et aktivt stof, samt en reduktion af de mulige skadelige påvirkninger stoffet måtte have på miljøet og mennesker. Evnen til at simulere og analysere den kontrollerede frigivelse/udskilning af et aktivt stof er meget anvendelig i produkt design fasen, hvor mange kombinationer af pesticider og polymerer testes for at opnå den ønskede tidsafhængige frigivelse/udskilningsadfærd. En modelbaseret analyse af den kontrollerede frigivelse fra de mulige produkt kombinationer vil signifikant reducere de økonomiske omkostninger og tidsforbruget, der er forbundet med eksperimentelle undersøgelser.

Formålet med denne afhandling er at udvikle matematiske modeller for kontrolleret frigivelse og integrere dem med prædiktive modeller, der kan estimere de, for frigivelsesmodellerne relevante, fysiske egenskaber for blandingerne. Denne metode vil principielt medføre at frigivelsen af et aktivt stof fra et specifikt medie kan studeres uden brug af yderligere eksperimentelle målinger.

I relation til det erklærede formål er en model for kontrolleret frigivelse af et aktivt stof fra mikrokapsler blevet udviklet. Modellen er valideret og videreudviklet til at beskrive de særlige fænomener der indtræffer i den første fase af frigivelsen. De mest afgørende egenskaber der begrænser frigivelsen af et aktivt stof fra et medie er identificeret til at være opløselighed og diffusion af det aktive stof. Prædiktive modeller til estimation af disse egenskaber er derfor fremsat.

Til beregning af opløseligheden af det aktive stof i polymerer fremsættes en metode hvor aktivitetskoefficienterne af stofferne i polymerblandingen beregnes. En model baseret på gruppebidragsprincippet er blevet valgt og videreudviklet, hvormed det er gjort muligt at inkludere komplekse stoffer som pesticider i opløslighedsberegningerne. Den prædiktive model for diffusion er baseret på 'free volume' diffusionsteorien, med speciel henblik på anvendelse for store molekyler. Med store molekyler menes pesticider.

Modellerne til forudsigelse af opløselighed og diffusions egenskaber er blevet integreret i frigivelsesmodellen, som er blevet anvendt i studiet af udskilningen fra industrielt fremstillede mikrokapsler indeholdende et pesticid. De prædiktive og de kontrollerede frivelsesmodeller er blevet bedømt på basis af disse resultater. Derudover gives der eksempler på at modellen kan bruges til at forudsige udskilning af aktive stoffer i problemstillinger fra den farmaceutiske industri.

Endeligt er der på baggrund af det ovenstående arbejde blevet udarbejdet en

systematisk fremgangsmåde med hensyn til kritiske faser i modelopbygningen. Den indeholder retningslinier for hvilke data, der skal bruges til udvikling af de forskellige modeller, samt metoder til at validere dem.

Contents

List of Figures

List of Tables

1

Introduction

Controlled release technology was initially developed in the pharmaceutical industry with the aim of producing oral drug forms that could keep an effective drug level in the body, avoiding at the same time, side effects caused by the administration of these drugs.
In the agrochemical area the continuous need for better pest control was at first overcome with the use of more powerful agents but with the increasing environmental regulations this became unviable. Besides, in the applications where protection from pests is required for extended periods of time the conventional methods of application of pesticides (such as spraying the solution over the crop) may not be good enough because the pesticide might not be delivered at the desired site, and it might not last long enough to accomplish the protection of the crop. In these situations, considerable improvement can be achieved by using controlled release technology for the pesticide delivery to the environment. With this, the amount of pesticide used, as well as the number of times it needs to be applied on the crop is significantly reduced. As the pesticide is usually encapsulated within a polymer membrane, there is also a reduction with respect to environmental hazards and human toxicity.
This thesis is focused on the applications related to the agrochemical area, but the developments are considered extendable to the pharmaceutical industry.
Within the field of controlled release technology the design of a product that can provide the desired Active Ingredient (AI) release behaviour is a critical step. Different combinations of AIs with polymers and solvents, as well as different types of products must be experimentally tested to find the appropriate alternative for the application of interest. A significant reduction of the expensive and time consuming experimental work can be achieved through an initial examination of alternatives through model-based simulations.
The global objective of this thesis, involves the development and implementation of mathematical models to study the release of AIs from controlled release devices, that are predictive. This will allow the study of the effect of design and physicochemical parameters on the release of the AI from controlled release devices. A mathematical model for the release of AI from a microcapsule has been developed for the illustration of this aspect of the work. The model is at the same time extended to include some effects related to the history of the system (storage time and use) that affect the initial periods of release of the AI when applied in the environment.

Controlled release technology commonly involves a pesticide AI that is encapsulated or incorporated within a polymeric material, the release being generally controlled by Fickian diffusion through the polymer. The actual release rate depends mainly on thickness, area and permeability of the membrane. While the thickness and area of the membrane can be determined by the experimental procedure, the permeability depends on the compounds present in the system. The permeability is directly dependent on the solubility (through the partition coefficients) and the diffusivity of the pesticide in the polymer. These properties are therefore the ones needed by the mathematical release model in order to study the AI release from a particular device and for different pesticide-polymer systems.

An important number of mathematical models have been developed in the literature to study the release from different types of controlled release devices. The shortcoming here is the fact that the model parameters (partition and diffusion coefficients) are generally obtained from fitting of experimentally measured release data for the system of interest. Consequently, the development of models that can predict the diffusivity and solubility properties of AIs in polymers would be a significant contribution in the field of product design. The development of predictive models for these properties that can be applied to a wide range of AIs and polymers is the main objective of this thesis. The incorporation of these models within the controlled release models will allow the study of the AI delivery from different AI-polymer and product alternatives without the need of experimental work, that is, in a completely predictive manner.

More specifically, the objective of this thesis is to develop predictive models for the diffusivity and the solubility of AIs in polymers that can be used for the large and complex pesticide molecules. Also, it should be possible to integrate these models with the mathematical release models so that the delivery of an AI to the environment can be studied in a completely predictive manner.

In order to model the partition coefficients in a predictive manner, an approach is proposed to obtain them from activity coefficient values of the AIs in the solvents and in the polymers. Focus is given to the model for estimation of activity coefficients of AIs in polymers. The selected model is the GC-Flory EoS, which is a simple activity coefficient model based on a group-contribution approach, with an existing parameter table that provides accurate and predictive results for solvent(small molecules)-polymer systems. This is a particularly interesting approach when dealing with systems that involve pesticides, given that no experimental data of the actual system of interest is required as input data, (apart from molecular structure, temperature and composition) which is generally a major problem for these systems. The initial shortcomings of the model are related to the relatively reduced group parameter table that can only describe a few of the complex pesticide AIs. The model then, needs to be extended so that the activity coefficient calculations can be performed for a much wider range of AIs. The model parameters for the new groups are estimated from low molecular weight compounds and then tested with systems involving polymers. The extended parameter table allows for the calculation of activity coefficients

for a greater number of pesticides and polymers used in the field of controlled release of agrochemicals.
On the other hand, a predictive model for the estimation of diffusion coefficients of AIs in polymers is also needed. The model selected for further development is derived from the free volume theory of diffusion, which is based on the assumption that diffusion is controlled by the availability of free volume in the polymer. The model takes into account the molecular size and shape (asymmetry) of the compounds which is the most important feature when dealing with larger molecules. The model has been widely used, but mainly for relatively small molecules (compared to the pesticide AIs). Once again, the fact that the compounds of interest are pesticide AIs needs to be considered since their diffusive behaviour will differ from that of small and simple molecules. The challenge is then to apply the predictive form of the model to the large and complex pesticide molecules and compounds that can be considered equivalent. The model parameters are estimated from pure component properties (no diffusivity data is needed) for a significant number of large compounds in different polymers and the model predictions are analyzed. The model predictions are also analyzed for some compounds and polymers related to controlled release applications.
Finally, the predictive property models are integrated with the mathematical release models in order to study the delivery of the AIs from controlled release devices in a predictive manner. This needs to be analysed through experimental data of release of pesticide AIs to assess the applicability of the integrated models within the field of controlled release technology.
According to the above explanations, the thesis is divided into five chapters. In Chapter 2, the modelling aspects involved in controlled release technology are introduced. In this chapter, the model developed for the study of AI release from a microcapsule is presented together with its extension to deal with more detailed aspects of the actual release behaviour, that is, the initial periods of lag time and burst release. The mathematical release model and its extensions are illustrated through three different case studies highlighting the main aspects of their application. That is, the performance of the model to reproduce the experimental release data, as well as its ability to account for some factors that affect the delivery of the AI, such as, the size of the microcapsule and the thickness of the membrane. In Chapters 3 and 4, the predictive property models are presented. In Chapter 3, the approach proposed for the estimation of partition coefficients through activity coefficients is described. The property model used to estimate the activity coefficients in polymers is presented together with the details of the extension performed that now allows for estimations for a wider range of complex molecules. The applicability of this approach is highlighted through several sample calculations involving complex molecules as well as pesticides of interest. At the same time, some improvements achieved through the extension of the model are also highlighted. In Chapter 4, the approach used for the predictive estimation of diffusion coefficients of AIs in polymers is described. The extended property model and its

predictive abilities are analysed for an important number of complex molecules and the model parameters obtained. The applicability and predictability of the model are studied with several systems involving the diffusion of pesticides in polymers. Chapter 5 contains the integration of the predictive property models with the microcapsule release model, illustrated through three case studies that highlight the applicability of this methodology mainly in the agrochemical area (with two examples involving pesticides), but also in the pharmaceutical field (through an example of drug release). Finally, in Chapter 6, the final conclusions of the work are provided together with some ideas for future work to further improve the models and their integration.

2

Controlled Release

2.1 Introduction to controlled release technology

i) What is controlled release technology? Why use it?

The basic definition of controlled release technology is that it involves a product that is specifically designed to provide the delivery of an Active Ingredient (AI) to a specified target and with a desired rate and duration.

This technology was initially developed by the pharmaceutical industry where the need to control the amount of drug delivered as well as the localization of the dose application appeared as critical factors. The benefits in this area are significant given that an effective level of drug is kept in the body and thereby side effects caused by administration of high doses of drug are avoided. These advantages lead to a relatively fast and broad development of the controlled release technology in this field.

In the agricultural area the advantages of using this technology are similar but the product design and fabrication costs limited the development of complex devices for the controlled release of AIs. In this field the use of conventional methods for application of pesticides (for example solution spraying) may not be good enough when long term protection is needed due to the pesticide AI not being delivered at the desired site and being lost through wash-off, evaporation, and degradation, for example. Considerable improvements can be achieved by using controlled release systems for the AI delivery into the environment. Through these devices, the amount of pesticide used as well as the number of applications needed is significantly reduced (optimization of the dose). An illustration of the advantages of having a controlled release system is presented in Fig. 2.1 with respect to the concentrations of AI in the environment. It can be observed in the figure that with common applications very high levels of AI are initially achieved that can exceed the toxic level and then, a rapid decrease of the concentration occurs (due to degradation or other effects) that brings the levels below the minimum effective level. These undesired effects are avoided with the controlled release system that quickly provides the desired concentration and this is then maintained over time. This is possible by having a delivery rate that is close to that of removal of the AI. With this figure, it is

also illustrated how possible damages, due to overdosing, to the environment and humans, are avoided through this technology.

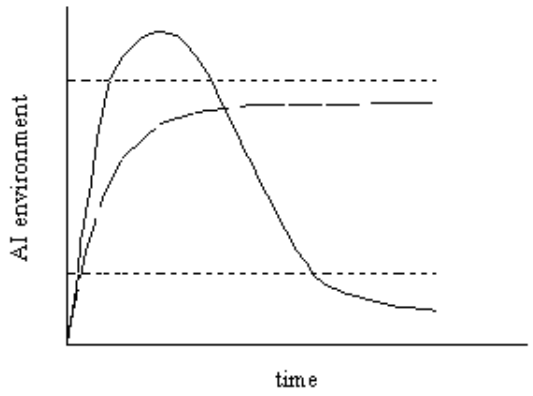

Figure 2.1: Comparison of AI concentrations in the environment with a common application (—) and with a controlled release application (– –). The dotted lines (- - -) represent the minimum effective level (lowest) and the toxicity limit (highest).

In controlled release technology there is obviously also some disadvantages that need consideration, for example, the higher cost of preparation and processing, the fate of the polymer matrix and the effect of product additives on the environment.

ii) Types of controlled release devices

Within the area of controlled release technology several kinds of products have been developed and used. Different factors can determine the choice of a specific product for a given application, such as cost, AI properties or biodegradability, but generally, one of the most important is the release rate required for the particular application. A constant release rate is considered, in general, one of the most desirable, and this corresponds to a zero order release rate. In many cases the devices provide a release rate that is proportional to the amount of AI still left in the reservoir and varies exponentially over time, this is equivalent to a first order release rate, which is useful for a great number of applications. And finally, another very common release rate order found in several applications is the square-root of time dependence. The different release rate orders are illustrated through Fig. 2.2 where the mass of AI released (M_r) is plotted as a function of time (t) for each of the cases mentioned above.

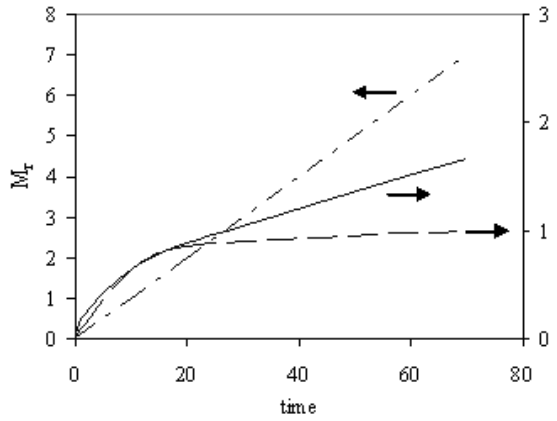

Figure 2.2: Plot of the mass of AI released (M_r) over time for different release rate orders. (– - –) Zero order; (– –) First order; (—) Square-root of time order.

The different release rate orders are summarized in Table 2.1, with the expressions of time dependence for the release rates (dM_r/dt) and mass of AI released (M_r). For each of them some examples of types of products that present these release rate order are also given. Further explanations of the products will be provided below.

Table 2.1: Release rate orders: expressions for time dependence and examples of products.

Order	$\mathbf{d}M_r/dt$	$M_r(t)$	**Examples**
Zero	k_0	$k_0 t$	Reservoir with membrane and constant activity source
First	$k_1\ M_r(t)$	$M_{total}(1 - exp(-k_1 t))$	Reservoir with membrane and non-constant activity source
Square root	$k_2/\sqrt{t}$	$2k_2\sqrt{t}$	Reservoir without membrane Erodible systems Monolithic (dispersed) and non-erodible

k_0, k_1 and k_2: constants
M_{total}: total mass of AI

The main types of controlled release products existing are listed in Table 2.2 together with some examples of commercially available products found within each type. It is important to mention that, in general terms, the controlled release devices are formed by the AI incorporated within a polymer matrix by using different technologies to bring and maintain them together.

These devices can first be classified into two big groups according to the mechanism that controls the release of the AI, that is, either diffusion (Diffusion or physical systems) or erosion and chemical reactions (Chemical systems), even though in the latter it is very common to find a combination of the two mechanisms. Within these groups, further classification is possible based on the manner in which the AI is incorporated in the polymer matrix. In the reservoir systems the AI is completely enclosed in a permeable polymer membrane (as in microcapsules) while in the monolithic systems it is incorporated (either dissolved or dispersed) within the polymer matrix. The latter are the simplest and therefore least expensive types, but they require more polymer than the reservoir systems.

Reservoir
Within the reservoir systems, there are those with a rate-controlling membrane where the rate of delivery is determined by the geometry of the device (membrane thickness and area) and the permeability of the polymer membrane (dependent on both diffusivity and solubility). These can provide either zero- or first-order release depending on the initial concentrations inside the device. Another type within these systems involves those without a rate-controlling membrane, such as the hollow fibers. In these devices the AI is retained by capillarity or embedded in the pores. They can be considered as a type of monolithic device except that the interaction between the AI and the polymer is minimal. The release rate in these systems is a square-root of time dependence.

Monolithic
The monolithic systems can also be further divided into those having the AI dissolved within the polymer matrix or dispersed (above the solubility limit) in the polymer. In both cases the rate of release depends on the nature of the polymer, geometry of the device and also on the AI loading achieved, together with the parameters mentioned above (solubility, diffusivity). The release rate order is a square-root of time but in the dissolved type it decreases exponentially (first order) in the last period of the delivery. In some cases the polymer membrane degrades during usage, leading to the so-called erodible systems where release is controlled by a combination of diffusion and erosion mechanisms. Finally, in some cases the release occurs due to the penetration of a compound within the device, through a leaching mechanism.

The laminated structures can also be considered within the monolithic type. Here the AI is incorporated in a polymer layer surrounded by two (or more) outer layers and the AI permeates through one or all of them. The release depends on the same parameters mentioned for monolithic systems and the rate can be pseudo-zero order when the reservoir layer is similar to the outer layers or square-root of time combined with first-order when they are different from each other.

Others
Another type of physical methods to be mentioned are the osmotic pumps where release occurs due to the osmotic pressure gradient established from water diffusion through the membrane. Membrane permeability is therefore the determining factor in these systems and the release rate can be of zero or first order depending on the presence (or not) of excess solid. The last type involves the use of ion-exchange resins where the AI is adsorbed and release will depend on pH and electrolyte concentration.

Swelling systems
In the swelling systems the polymers involved tend to absorb the solvent they are in contact with given their thermodynamic compatibility. That would be the case of water swelling hydrophilic polymers (for example PHEMA) or organic solvents otherwise. The release of the AI depends then on its solubility in the solvent within the polymer and that is where it diffuses through. In other cases the diffusion mechanism through the polymer is modified from Fickian to anomalous diffusion, for example when cross-linking is increased, due to relaxation mechanisms occurring in the polymer. The permeability can then be varied through use of different degrees of hydration of the polymer.

On the other hand, within the chemical systems, the release is not necessarily controlled by diffusivity but also erosion. It is important that the polymer be compatible with the environment and that the degradation rate is in accordance with the required duration of the device. In the cases where the AI is immobilized by binding to the polymer (pendant-chain systems) the release rates are controlled by the nature of the bond, of other functional groups, among others, and then moisture or light can be the mechanisms that activate the release. In this work the focus is on the diffusion-controlled devices so the latter will not be further treated.

Table 2.2: Different types of controlled release products.

Controlling mechanism				
Diffusion or physical systems			**Examples**	**AI**
Reservoir	With rate-controlling membrane	Micro- and macro-encapsulation	TopNotch	Acetochlor
			Fultime	Acetochlor (inside)/ Atrazine(outside)
			Icon or Demand	λ-cyhalothrin
			Karate	λ-cyhalothrin
		Membranes	HERCON	
	Without rate-controlling membrane	Hollow fibers	Attract NKill	Insect phermononones
			Conrel	Gossyplure (pheromone)
		Ultramicroporous cellulose triacetate	Poroplastic	
			Sustrelle	
		Porous polymeric substrates and foams	TTS	Drugs
Monolithic	Dissolved	Non-erodible	Sergeant Collars	Flea and tick control
		Erodible[(1)]	Dexon	
		Environmental agent ingression		
	Dispersed	Non-erodible	Dursban	Larvicide
		Erodible		
		Environmental agent ingression	BioMet SRM	
Porous	(Higuchi derivation)		TTS	Drugs
Laminated	Similar reservoir and outer layers		Staph-Chek	Antibacterial
			Insectape	Propoxopur, Diazinon or Chlorpyrifos
			Roach-tape	
	Dissimilar reservoir and outer layers		Luretape	Pheromone
Others	Osmotic pumps		Oros	Drugs, hormones, antigens
			Alzet	
	Asdorption onto ion-exchange resins		Tussionex	Chlorpheniramine
			Penntuss	Codeine, Chlorpheniramine
Swelling systems			PHEMA	biomedical applications - soft contact eye lenses
Chemical systems				
Chemical erosion of polymer matrix		Heterogeneous	Tox-Hid	Warfarin (rodenticide)
		Homogeneous	Brocon CR	Nasal descongestant
Biological erosion of polymer matrix		Heterogeneous		
		Homogeneous		
Pendant-chain systems				

[(1)] Release rate is not controlled by diffusion but erosion speed

2.2 Controlled release modelling

2.2.1 Introduction

Given the advantages provided by controlled release technology in different fields and the possibilities offered in design of better optimized products, a large amount of work has been done on studying the different types of systems both through experimental work (Shulkin et al. [1], Park et al. [2], Zulfiqar et al. [3], among many others) and through mathematical modeling. The focus of this section is on the modeling part. This is due to the fact that the availability of mathematical models that can predict the release behavior of AIs from different fabricated devices is a very interesting tool in product design, even though in the current state, not all the variables or parameters of the models are at hand so a certain amount of experimental work is still required.

The most representative models for describing controlled release of AIs have been provided in several compilations by Peppas et al. [4], Comyn [5] and Kydonieus et al. [6] and more recently reviewed by Siepmann et al. [7]. A brief overview of the existing mathematical models for AI release from different types of products will be presented here. However, instead of analyzing the accuracy or complexity (as it has been done in the cited literature), focus is given to analyzing the models in terms of the variables and parameters appearing in them, in order to discern which of them are (or can be) fixed from the fabrication conditions and which are properties of the compounds (AI, polymer) and need to be obtained independently.

In general terms, the factors affecting the release of the AIs include the solubility and diffusivity of the AI in the polymer together with geometric parameters (such as area, membrane thickness), concentrations, and in some cases porosity related parameters (for example tortuosity). The first group (solubility and diffusivity) depend mainly on the properties and characteristics of the solute (molecular weight, shape, etc.) and the polymer (glass transition temperature, chemical functionality, stiffness), but are also affected by the presence of fillers or codiffusants. The rest of the parameters (except maybe porosity) can, in general, be determined from the experimental conditions established for the fabrication of the device. The identification of the different variables that will be presented here is then used to recognize the convenience for property models to estimate those parameters that are not fixed from the experimental conditions. With these, the study of the release behavior of different alternatives for a product could be done without any need of experimental measurements, at least during the initial stages of design.

2.2.2 The models

The models considered for this analysis/overview are presented in Table 2.3 for the main types of different devices with their corresponding equations. The release rate order is identified as well as the variables of the models, which are

classified into those that are fixed from the experimental conditions (Exp) and those that depend on the properties of the compounds (Properties).

A great number of models are available in the literature for the release from different products, geometries, etc. (Peppas et al. [4]). Most of these models are based on the same principles of diffusion-controlled release but may also include extra terms to account for dissolution of the AI and/or the polymer, swelling of the polymer membrane, non-constant diffusion coefficient, etc. Some of these models have been reviewed by (Siepmann et al. [7]), but they are not considered here given that the parameters to be identified are not much different than those obtained from the basic models listed in Table 2.3 (or combinations of those) and thus not relevant for this analysis. The same applies for different geometries within a same product type, where the models might slightly differ but the parameters are equivalent, so only a chosen geometry is detailed.

Table 2.3: Controlled release models for different types of devices and their equations.

Diffusion or physical systems		**Equations**		**Release rate order**	**Parameters**	
		General (dM/dt)	**Detailed (M(t))**		**Exp**	**Prop.**
Reservoir	Constant activity source	$\frac{dM}{dt} = \frac{-DKA}{h}(C_r - C_d)$	$M = \frac{4\pi r_o r_i DK}{r_o - r_i}(C_d - C_r)t$ *(sphere)*	Zero	$C_r, C_d,$ r_o, r_i	D K
	Non-constant activity source	$\frac{dM}{dt} = \frac{-DKA}{h}(M_r/V_r - M_d/V_d)$	$M = M_{total}\left[1 - \exp\left(\frac{-ADK}{V_r h}\right)t\right]$	First	h, V_r M_{total} A	D K
	Membrane: Porous	*(see Porous systems)*				
	Membrane: Non-porous	$\frac{dM}{dt} = \frac{DA}{h}(C_s - KC_r)$	$M = \frac{DKA}{h}(C_s - KC_r)t$	Zero, First	A, h, C_s C_r, C_d	D K
		$\frac{dM}{dt} = \frac{DKA}{h}(C_d - C_r)$	$M = \frac{DKA}{h}(C_d - C_r)t$			
Monolithic (dissolved AI)	Non-erodible (spheres): *General equation*	$M = M_{total}\left[1 - \frac{6}{\pi^2}\sum_{n=1}^{\infty}\frac{1}{n^2}\exp\left(\frac{-Dn^2\pi^2}{r^2}t\right)\right]$			M_{total},r	D
	i) early times ($M/M_{total} < 0.5$)	$\frac{dM}{dt} = 3M_{total}\left[\left(\frac{D}{\pi r^2 t}\right)^{1/2} - \frac{D}{r^2}\right]$	$M = M_{total}\left[6\left(\frac{D}{\pi r^2}t\right)^{1/2} - \frac{3D}{r^2}t\right]$	$\sqrt{t}$		
	ii) late times ($M/M_{total} > 0.5$)	$\frac{dM}{dt} = M_{total}\frac{6D}{r^2}\exp\left(\frac{-\pi^2 D}{r^2}t\right)$	$M = M_{total}\left(1 - \frac{6}{\pi^2}\exp\left(\frac{-\pi^2 Dt}{r^2}\right)\right)$	First		
	Erodible	$\frac{dM}{dt} = BC_0A$	$M = M_{total}t/t_\infty$ M_{total}	Zero	C_0, A t_∞	
Monolithic (dispersed AI)	Non-erodible	$\frac{dM}{dt} = \frac{A}{2}\left(DC_s\frac{(2C_0 - C_s)}{t}\right)^{1/2}$	$M = A\left(DC_s(2C_0 - C_s)t\right)^{1/2}$	$\sqrt{t}$	A, C_s C_0	D

Exp.: From experiment, Prop.: Properties

Diffusion or physical systems		**Equations**		**Release rate order**	**Parameters**	
		General (dM/dt)	**Detailed (M(t))**		**Exp**	**Prop.**
Porous	*(Higuchi derivation)*	$\frac{dM}{dt} = \frac{A}{2}\left[\frac{2D_w \varepsilon C_s C_0}{\tau t}\right]^{1/2}$	$M = A\left[D_w \frac{\varepsilon}{\tau} C_s (2C_0 - \varepsilon C_s)t\right]^{1/2}$	$\sqrt{t}$	A, C_s C_0, ϵ, τ	D_w
Laminated (monolithic dissolved)	Similar reservoir and outer layers	$\frac{dM}{dt} = \frac{8DM_{total}}{h^2}\exp\left(\frac{-\pi^2 D}{h^2}t\right)$	late time approximation: $M = M_{total}\left(1 - \frac{8}{\pi^2}\exp\left(\frac{-\pi^2 D}{h^2}t\right)\right)$	1st or $\sqrt{t}$	M_{total} h	D
	Dissimilar reservoir and outer layers	$\frac{dM}{dt} = \frac{DA}{h}(C_s - KC_r)$	$M = \frac{DKA}{h}(C_s - KC_r)t$	Pseudo -zero	$A,\ h$ C_r, C_s	D K
Others	Osmotic pumps	$\frac{dV}{dt} = \frac{A}{h}L_p\left[\sigma\left(\pi_2 - \pi_1\right) - \left(p_2^H - p_1^H\right)\right]$		Zero (1st)	A, h	L_p
Swelling systems		$M = M_{total}\left[1 - \frac{8}{\pi^2}\sum_{n=0}^{\infty}\frac{1}{(2n+1)^2}\exp\left(\frac{-(2n+1)^2\pi^2 T}{h^2}t\right)\right]$ $T = \int_0^t D(t)dt$		Zero (slab)	h	$D(t)$
Chemical systems						
Chemical erosion of polymer matrix	Heterogeneous	$\frac{dM}{dt} = k_e A_e C_0$	$M = M_{total}\left[1 - \left(1 - \frac{k_e}{C_0 l}t\right)^n\right]$	-	k_e, C_0, l M_{total}	-
Biological erosion of polymer matrix	Homogeneous	$\frac{dM}{dt} = M_{total}k_h C_0 e^{-k_h t}$	-	-	M_{total} C_0, k_h	-
Pendant-chain systems		$\frac{dM}{dt} = nk_r A C_0$	-	-	k_r A, C_0	-

Exp.: From experiment, Prop.: Properties

How are the models derived?

In order to provide a better understanding of the model equations that are given in Table 2.3, a brief explanation of their derivation is provided. Consider the basic scenario of diffusion of an AI from a donor or reservoir comparent to a release medium, through a polymeric membrane, as in Fig. 2.3.

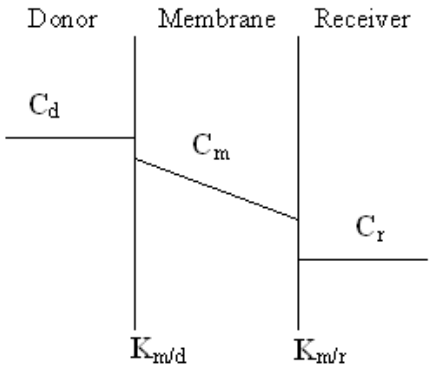

Figure 2.3: Basic scenario for diffusion of an AI from the donor to the receiver compartment.

The release models are derived from the basic assumption that most controlled release devices can be described through Fickian diffusion, which is valid for rubbery polymers, that is, above the glass transition temperature. The model equations are then derived from Fick's first and second laws of diffusion, represented by Eqs. 2.1 and 2.2, respectively.

$$J = -AD\frac{\partial C_m}{\partial x} \tag{2.1}$$

$$\frac{\partial C_m}{\partial t} = D\frac{\partial^2 C_m}{\partial x^2} \tag{2.2}$$

Equation 2.1 relates the flux (J) of AI to the concentration gradient ($\partial C_m/\partial x$) through a constant that is the diffusion coefficient (D). Here, A, is the area through which diffusion occurs. This equation has been reduced to one dimension by considering the assumption that diffusion occurs through thin membranes and it can therefore be considered only along the x-axis. At the same time the diffusion coefficient has been considered independent of concentration, which is a good assumption for dilute systems but might need to be revised for concentrated solutions.

In Eq. 2.2 the rate of change in concentration ($\partial C_m/\partial t$) is observed to be proportional to the rate of change in the spatial concentration gradient ($\partial^2 C_m/\partial x^2$) again through the diffusion coefficient.

For reservoir systems the above equations are solved by considering constant flux and the appropriate initial and boundary conditions detailed in 2.3 to 2.5, to obtain the equation for the flux of AI (Eq. 2.6). Note that 2.4 and 2.5 consider the definitions of partition coefficients due to different physicochemical characteristics of the polymer membrane and the solvents in the donor and receiver compartments.

$$t = 0, \qquad 0 = x = h, \qquad C_m = 0 \tag{2.3}$$

$$t > 0, \qquad x = 0, \qquad C_m = KC_d \tag{2.4}$$

$$t > 0, \qquad x = h, \qquad C_m = KC_r \tag{2.5}$$

$$J = -\frac{DA}{h} K \left(C_r - C_d\right) \tag{2.6}$$

Then the flux is expressed in terms of the mass of AI released (M_r) and the general expression for AI delivery from controlled release devices is obtained (Eq. 2.7).

$$J = \frac{dM_r}{dt} = -\frac{DA}{h} K \left(C_r - C_d\right) \tag{2.7}$$

In these systems there is a distinction to be made regarding the concentration of AI in the donor compartment (C_d). In the case where this concentration is maintained constant (constant activity source) zero-order release is observed, but on the other hand, if the AI is available in solution below saturation (non-constant activity source), the donor concentration is not constant and a first order release is observed. Note that the equations for a constant activity source in the table are provided for a spherical geometry.

In the case of monolithic systems of the dissolved type, the model equations are obtained from Fick's laws (Eqs. 2.1 and 2.2) that can be solved for different geometric shapes under different initial and boundary conditions (Crank [8]) through the technique of separation of variables, for example. These equations are usually simplified by considering only the important terms in the early or later periods of delivery. The case of laminated systems with similar inner and outer layers can be modeled with the equations derived from this same approach but for a different geometry than the above, while the ones with dissimilar layers are equivalent to the reservoir models.

Again the dissolved monolithic systems approach is used for swelling systems with the added consideration of the variation of the diffusion coefficient over time due to the swelling of the polymer.

Finally, for the dispersed monolithic systems the model commonly used is obtained from the pseudo-steady state approximation by Higuchi [9], using Fick's first law under a number of assumptions. Using a similar approach the equations for porous systems were also derived by Higuchi, [10] taking into

account the void fraction and tortuosity of the polymer. A similar equation is obtained.

The model equations for the last group of products (Osmotic pumps and Chemical systems) are derived in a different manner given that the controlling mechanism is not the diffusion through the polymer but other factors, or at least a combination of other factors plus diffusion. These are only briefly discussed here because of their applicability, mainly when combined with the previously mentioned models (for reservoir, monolithic, etc.) but without further detail given that the parameter identification study is based on the purely diffusive systems (in polymer).

The model equation for the osmotic pumps takes into account the volume change in flow of water through the membrane due to an osmotic pressure gradient. In the chemically controlled systems the equations consider the process of polymer dissolution and define the erosion rate by taking into account the changes in the area available for degradation. Finally, within this type, the pendant chain systems are governed by reaction kinetics and therefore a complete other topic not to be treated here.

2.2.3 The model parameters

In Table 2.3, a classification of the model variables has been provided. In general terms, the variables controlling the delivery are the same or equivalent in all the devices where diffusion is the controlling mechanism. These are, the geometric parameters (area, thickness and volumes) together with the concentrations of AI inside and outside the device and the total mass of AI in the system. The values for these variables are predetermined from the experimental conditions of fabrication (of the product) and therefore no further considerations are needed. On the other hand, the properties of the compounds that determine the release and that are in principle independent of the controlled release product, are also found to be common in almost all the release models. These are the diffusivity and the partition coefficients, which are, in fact, usually unknown.

This means that, in the study of the release of an AI from a particular device through mathematical models, once all the application conditions are known, the lack of values for the diffusivity and the partition coefficients is the only impediment to performing a fully model-based analysis (or fully predictive analysis). Therefore, the development of property models that can predict the diffusion and the partition coefficient of the compounds involved in a controlled release product together with their integration with the mathematical models for release, would be a very valuable tool for the design process, allowing for the evaluation of several alternative combinations of AI and polymers with different controlled release devices through computer-aided simulations. This is the reason for the study of the predictive property models studied in chapters 3 and 4 that are finally integrated with the controlled release models (chapter 5).

2.3 The microcapsule model

2.3.1 The basic microcapsule model

i) Theory about microcapsules

In order to illustrate the controlled release modelling and later on the integration of property prediction within this frame (chapter 5), a specific type of controlled release devices has been chosen, the microcapsules. These devices can be modelled in a relatively simple manner and the parameters/properties of interest in this study can be clearly identified and distinguished from other effects. For example in monolithic systems the amount of AI loaded within the device depends on the solubility of the AI in the polymer and consists only of a part of the AI initially introduced. Therefore further considerations are needed before studying the release behaviour of the AI. This is not the case of microcapsules, where the amount of AI encapsulated is practically the whole of what is originally introduced. Given that the focus of this work is on the release part and not on the fabrication process, the microcapsules are considered to be the most appropriate and representative of the different types of devices available.

Definition of microcapsule

A microcapsule consists of an AI enclosed within a polymer membrane, as shown in Fig. 2.4. The microcapsule is then put in contact with a fluid, the release medium, where the AI is delivered. The AI in the microcapsule core can be present in the form of solid particles, liquid, or dispersions of solids in liquids. Together with the AI, other compounds (additives) are generally found in the core, such as emulsifiers or solvents. The polymer membrane forming the microcapsule wall must be, among other things, chemically compatible with the AI and non-reactive with it. The membrane can be natural or synthetic, porous or non-porous polymer, that is subject to cross-linking and plasticization and provides the capsule with strength, as well as flexibility, stability and a certain impermeability. Some polymers commonly used in these applications are polyethylene (PE), polystyrene (PS), polyesters, polyureas and polyurethanes to name a few. A requirement for these polymer membranes is that they form a cohesive film with the AI.

The microcapsules have a size ranging from tenths of micrometers to about a thousand micrometers, and sizes over 2000 μm are considered macrocapsules, which present the same behaviour as the microcapsules. The wall thickness depends on the microcapsule size and the ratio of polymer formed with respect to the quantity of AI encapsulated. The thickness generally represents about 5 to 25% of the total microcapsule weight. The advantages of having an AI within a reservoir device apply entirely to microcapsule devices with the add-on that microcapsules can be diluted in water or liquid fertilizers and then applied

using the conventional methods.

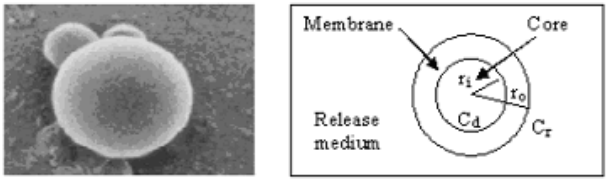

Figure 2.4: Microcapsule illustration: picture (left) and schematic representation (right).

There is a very large number of processes through which microcapsules can be produced. These processes can be classified basically into three main groups: Chemical, Physicochemical and Physical methods. In the Chemical methods the core material is emulsified or dispersed in an immiscible continuous phase and then the interfacial polymerization reaction (generally polycondensation) takes place at the surface of the capsules to form the polymer membrane. It is suitable mainly for encapsulation of liquids. In the second group, the physicochemical methods, after creating the emulsion or dispersion of the core material into the continuous phase in which the wall material is dissolved, this wall material is made to physically separate from the continuous phase and deposit around the particle. In the last type, the physical methods, the wall and core material are physically brought together and the wall flows around the particle to form the microcapsule. Different methods are found within each group, and they are listed in Table 2.4, which also provides an idea of the range of microcapsule sizes that can be obtained from each method.

Table 2.4: Microcapsule preparation methods (Vandegaer [11]), and microcapsule sizes obtained thereby

	Size (μm)
Chemical	$1 - > 1000$
Interfacial polymerization	
In-situ polymerization	
Insolubilization	
Physicochemical	$< 1 - 1000$
Aqueous and organic phase separations	
Interfacial deposition	
Spray-drying	
Physical	1-10 or 40-1000
Electrostatic	
Physical vapour-deposition	
Fluidized-bed spray coating	

Finally some examples of commercial microencapsulated products are presented in Table 2.5 with information of the components and the polymers.

Table 2.5: Commercial microencapsulated products

Product name	**AI**	**Polymer**
Temp SC	Cyfluthrin	Polyurea
Racer	Fluorochloridone	Polyurea
Suspend CS	Deltamethrin	Polyurea
3M	Pheromone	-
Debcote	Fertilizer	-

ii) Release behaviour and modelling

In this section the model to study the release of an AI from a microcapsule is presented. It is well known that the release of an AI is affected by several parameters, related to:

i) the geometry of the device: for example an increase in wall thickness or microcapsule size causes a reduction of the release

ii) properties of the polymer membrane, such as cross-linking, crystallinity, density and orientation, all of them reducing the release as they increase.

iii) plasticization of the membrane, better solubility of the AI in the polymer or higher temperatures, that can enhance the delivery.

Therefore a mathematical model for these systems must be able to account for all these factors (or as many of them as possible).

1. The microcapsule model

The microcapsule model presented here is based on the equations for non-constant activity source (Table 2.3 in section 2.2.2) that are applicable when the AI is available in solution in the core, below saturation conditions (Comyn [5]). These equations provide a first-order type of release which is in fact the one usually observed in common microcapsule applications. The model has been further developed in two main aspects that are discussed below.

a) In the first place, to take into account the differences between the solvents or solutions in the core and that used as release medium. That is, in the literature models presented before (Non-constant activity source reservoirs in Table 2.3), a single partition coefficient is generally used, defined as in Eq. 2.8, while in the model developed here, two different partition coefficients are considered as in Eqs. 2.9 and 2.10.

$$K = \frac{C_m}{C_d} = \frac{C_m}{C_r} \tag{2.8}$$

$$K_{m/d} = \frac{C_m}{C_d} \tag{2.9}$$

$$K_{m/r} = \frac{C_m}{C_r} \tag{2.10}$$

From this consideration (two different partition coefficients) the model equations are then derived from Fick's laws of diffusion in a similar manner as illustrated previously (section 2.2.2) and the complete derivations are given in Appendix A. The rate of change of AI concentration with time is obtained in the donor compartment (C_d, Eq. 2.11) and in the receiver or release medium (C_r, Eq. 2.12).

$$\frac{dC_d}{dt} = -\frac{DA}{hV_d} K_{m/d} C_{d,initial} \times \exp\left(-\frac{DAK_{m/d}}{V_r h}\left(\frac{K_{m/r}}{K_{m/d}} + \frac{V_r}{V_d}\right) t\right) \tag{2.11}$$

$$\frac{dC_r}{dt} = \frac{DA}{V_r h} K_{m/d} C_{d,initial} \times \exp\left(-\frac{DAK_{m/d}}{V_r h}\left(\frac{K_{m/r}}{K_{m/d}} + \frac{V_r}{V_d}\right) t\right) \tag{2.12}$$

Equations 2.11 and 2.12 contain the assumption that diffusion occurs through a film that is thin enough so that diffusion can be considered one-dimensional, and that the diffusion coefficient is independent of concentration. The concentrations are mainly affected by two properties related to the AI and the polymer, the diffusion coefficient of the AI in the polymer (D) and the partition coefficients between the membrane and the donor ($K_{m/d}$) and the receiver ($K_{m/r}$). The model equations also take into account the geometric parameters affecting the release, that is surface area (A), membrane thickness (h), microcapsule volume (V_d) together with the initial concentrations in the core ($C_{d,initial}$) and the volume of the release medium (V_r).

b) The second aspect that has been introduced in this model is related to the representation of the different sizes of microcapsules present in solution through a normal distribution function (Eq. 2.13).

$$F(r;\mu;\sigma) = \int_{-\infty}^{r'} \frac{1}{\sqrt{2\pi}\sigma} \exp\left(-\frac{(r-\mu)^2}{2\sigma^2}\right) dr \tag{2.13}$$

Equation 2.13 represents the normal distribution function for the microcapsule radius (r) applied with a specified mean distribution value (μ) and standard deviation (σ).

The total model (Eqs. 2.11 to 2.13) consists then of a macroscopic part that accounts for the number of microcapsules and their sizes and a microscopic part that accounts for the actual release from the microcapsules.

2. Model analysis and solution strategy

The controlled release model is analysed in terms of number and types of variables and equations. The controlled release model represented by Eqs. 2.11 to 2.13 corresponds to a DAE (differential-algebraic equations) system where the different types of variables are listed in Table 2.6.

Table 2.6: Classification of the variables of the model

Input/ Design Variables	**Calculated variables**	**Parameters (Constitutive variables)**	**Independent variable**	**Dependent /State variables**
$r_{min}, r_{max}, r_{step}$	r_{mean}	$K_{m/d}, K_{m/r}$	t	C_d
σ, μ	V_i, A_i	D		C_r
$C_{d,initial}, V_d$	$\%particles_i, N_{p,i}$			
V_r, h	$M_{initial}, \Delta M_i,$ ΔM_{total},%release			

The controlled release model analysis shows that the model equations can be solved for the dependent state variables, given their initial values at time t_0, the values for the design variables, and the parameters or constitutive variables (or models representing them). Also the equation set can be decomposed into two sub-models:

Sub-model I: Solve Eq. 2.13, to generate the size distribution data for a specified number of microcapsules.

Sub-model II: Solve Eqs. 2.11, 2.12, plus associated constitutive equations for each microcapsule size.

Solution strategy for Sub-model I:

For given values of maximum and minimum microcapsule radius (r_{max} and r_{min} respectively), together with a radius increment (r_{step}), the number of microcapsule sizes (n_f) for which the normal distribution (Eq. 2.13) needs to be evaluated is calculated through Eq. 2.14.

$$n_f = \frac{|r_{max} - r_{min}|}{r_{step}} \tag{2.14}$$

The distribution function (Eq. 2.13) is now solved n_f times to generate a profile of percentage of particles (or number of particles, $N'_{p,i}$). From these values a total donor volume ($V_{d,calc}$) is calculated according to Eq. 2.15.

$$V_{d,calc} = \sum_{i} N'_{p,i} V_i \tag{2.15}$$

As the total donor volume (V_d) is usually known (see Table 2.6), the number of particles of each size ($N_{p,i}$) is revised according to the specified donor volume, with Eq. 2.16.

$$N_{p,i} = N'_{p,i} \frac{V_d}{V_{d,calc}} \tag{2.16}$$

Solution strategy for Sub-model II:

Using the size distribution data for the microcapsules, and initial values for the dependent variables, Eqs. 2.11, 2.12 plus associated constitutive equations are solved for each microcapsule size. The additional constitutive equations are derived for the variables listed as 'calculated' in Table 2.6. For each microcapsule size, an average radius is calculated (r_{mean}, Eq. 2.17), which provides the area (A_i, Eq. 2.18) and the volume (V_i, Eq. 2.19) of each microcapsule.

$$r_i = r_{mean,i} = \frac{r_{\min,i} + r_{\max,i}}{2}; \mathrm{i} = 1, \mathrm{n_f} \tag{2.17}$$

$$A_i = 4\pi r_i^2; \mathrm{i} = 1, \mathrm{n_f} \tag{2.18}$$

$$V_i = \frac{4}{3}\pi r_i^3; \mathrm{i} = 1, \mathrm{n_f} \tag{2.19}$$

From the initial concentration in each microcapsule ($C_{d,initial}$), which is assumed equal for all the microcapsules), the total initial mass ($M_{initial}$) is calculated, as:

$$M_{initial} = \sum_{i} C_{d,initial} V_i N_{p,i} \tag{2.20}$$

The mass change (ΔM_i), the total mass change (ΔM_{total}) and the release percentage (%release) are obtained through the following equations respectively.

$$\Delta M_i = C_{d,i} V_i N_{p,i} \tag{2.21}$$

$$\Delta M_{total} = \sum_{i} \Delta M_i \tag{2.22}$$

$$\%release = 100 \left(M_{initial} - \Delta M_{total} \right) / M_{initial} \tag{2.23}$$

Note that Eqs. 2.11-2.12, 2.17-2.19 and 2.21 are solved for each microcapsule size, while Eqs. 2.20, 2.22 and 2.23 are solved once for the total set of microcapsules. That is, the controlled release model consists of 2*n_f ODE's (Ordinary Differential Equations), plus 4*n_f+3 algebraic equations (AE's), not counting the constitutive model equations. Note that Eqs. 2.11-2.12 can also be converted to their analytical AE forms and the resulting AE-system solved as a function of time.

3. Model solution: case study

In this section the mathematical model for release of AIs from microcapsules is tested with experimental data through a case study, in order to assess its performance and ability to take into account some of the factors affecting the release of the AI.

In this case study the AI encapsulated is Salbutamol sulphate [51022-70-9], which is an adrenoceptor agonist drug that is used for treating asthma. The advantages of having this drug encapsulated are related to its relatively high water solubility and how, through encapsulation, a sustained or delayed delivery can be achieved.

The microcapsules are formed with an Ethyl cellulose polymer wall, by an emulsion-solvent evaporation process. The composition and concentrations in the microcapsules are taken from the same reference as the experimental release data as a function of time (Amperiadou et al. [13]). Most parameters that are fixed by the experimental conditions, design parameters, are directly extracted from the same publication, while some others need to be calculated. That is the case of the thickness of the microcapsule membrane. This is obtained from the percentage of wall material with respect to the amount of core material ($wall\%$), as defined by Eq. 2.24. Then, using the definition of thickness (Eq. 2.25) and the volume, a relationship is derived to calculate the thickness of the membrane, see Eq. 2.26.

$$wall\% = 100 \times \frac{M_{polymer}}{M_{polymer} + M_{core}} \tag{2.24}$$

$$h = r_o - r_i \tag{2.25}$$

$$r_i = \left[r_o^3 \left(1 - \frac{wall\%}{100} \right) \right]^{1/3}, \text{and :}$$

$$h = r_o - r_i = r_o - \left[r_o^3 \left(1 - \frac{wall\%}{100} \right) \right]^{1/3} \tag{2.26}$$

The objective of this case study is not to assess the property prediction capabilities but to show that with the appropriate parameters the model can reproduce the experimental data. The values of the parameters defined as constitutive variables (D, $K_{m/d}$ and $K_{m/r}$) used here are those that best fit the experimental data. It is worth mentioning that Amperiadou et al. [13] analyzed

the release behaviour in terms of the release rate orders, with a kinetic model of the type shown in Eq. 2.27. Amperiadou et al. [13] conclude that a first order release rate is in general the most appropriate to represent the experimental data, but no attempt is made to provide a theoretically or physically derived model with the corresponding meaningful physical parameters (such as D, $K_{m/d}$ and $K_{m/r}$).

$$M = M_0 \exp(-k_1 t) \tag{2.27}$$

Finally, all the data required for the mathematical model is summarized in Table 2.7 for the three different scenarios that have been investigated.

Table 2.7: Summary of the input data required for the mathematical release model.

Variable	**Case 1**	**Case 2**	**Case 2 (aggregates)**	**Case 3**
AI : polymer	1:1	1:3	1:3	1:1
h (m)	1.083×10^{-4}	1.287×10^{-4}	1.287×10^{-4}	5.964×10^{-5}
r_{max} (m)	6.75×10^{-4}	5.25×10^{-4}	1.58×10^{-4}	5.25×10^{-4}
r_{min} (m)	3.00×10^{-4}	1.50×10^{-4}	5.25×10^{-4}	7.50×10^{-5}
r_{mean} (m)	5.25×10^{-4}	3.48×10^{-4}	1.22×10^{-3}	2.89×10^{-4}
σ	7.50×10^{-5}	7.50×10^{-5}	2.63×10^{-4}	7.50×10^{-5}
r_{step} (m)	1.00×10^{-5}	1.00×10^{-5}	1.00×10^{-5}	1.00×10^{-5}
$D(m^2/s)$	5.21×10^{-14}	5.21×10^{-14}	5.21×10^{-14}	1.36×10^{-14}
$K_{m/r}$	2×10^{6}	2×10^{6}	2×10^{6}	2×10^{7}
$K_{m/d}$	90	90	90	90
$V_r(m^3)$	2.50×10^{-4}	2.50×10^{-4}	2.50×10^{-4}	2.50×10^{-4}
t (s)	28800	28800	28800	28800
$C_{d,initial}(g/m^3)$	5.685×10^{5}	3.063×10^{5}	3.063×10^{5}	5.500×10^{5}
$V_d(m^3)$	3.166×10^{-6}	1.959×10^{-6}	1.959×10^{-6}	3.273×10^{-6}

Three different cases are chosen to illustrate the release model, two of them prepared under the same conditions (regarding stirring, as reported in Amperiadou et al. [13]), cases 1 and 2, but having different sizes and membrane thicknesses and the last one, case 3, prepared under different conditions. The fact that the microcapsules are prepared under the same conditions or not, is assumed to derive into different membrane morphologies and thus properties, therefore the parameters needed to fit the release data with the model are expected to be equal when the microcapsules are prepared under the same conditions, but different when these are modified.

A special case is found when studying case 2, for which Amperiadou et al. [13] have reported the formation of aggregates of smaller microcapsules. This phenomenon has been taken into account in the mathematical model by increasing the size (radii) of the capsules so as to consider the release from aggregates in-

stead of small microcapsules and the parameters are also reported in Table 2.7.

The model equations are then solved by setting the appropriate values of the diffusion and partition coefficients. The calculated values for the AI released in each of the cases are plotted in Fig. 2.5 together with the experimental values.

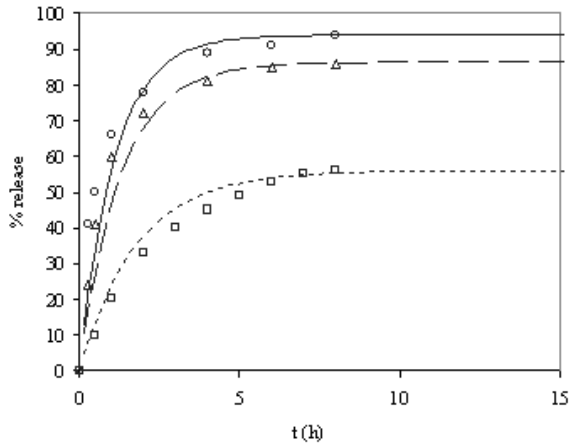

Figure 2.5: Comparison of experimental and estimated Salbutamol sulphate release values as a function of time. Experimental data: (∘) Case 1, (□) Case 2, (△) Case 3. Predicted release: (—) Case 1, (- - -) Case 2, (– –) Case 3.

It can be observed that the tendencies presented by the experimental data are well reproduced by the model, that is, for example, the increase of thickness and size of the capsules from case 1 to 2, supposes a significant reduction in the amount of AI released. Case 3 cannot be included in this comparison because the morphology of the polymer membrane is different, affecting therefore the diffusion and solubility properties of the AI in the polymer. This case is reported to show that these differences can also be taken into account by using different values of the parameters but still the same mathematical release model.

The results are considered satisfactory because even though small deviations from the experimental data are observed (mainly in the initial period of the delivery), the overall release values are well reproduced. These deviations can therefore be attributed to possible experimental errors that are particularly sensitive in the initial period of release, or inaccuracies in the values of the design variables used in the mathematical model, given that for example the normal distribution provides an approximation to the real size distribution of microcapsules with slight deviations as can be observed for the last case studied in Fig. 2.6.

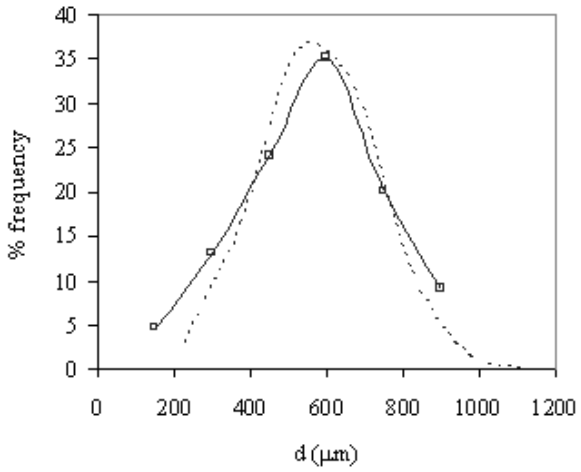

Figure 2.6: Comparison of distribution of microcapsule sizes from experiment (– □ –) and that obtained through normal distribution (- - -) for Case 4.

2.3.2 Model extension: burst and lag time effects

1. The extended model

For many microcapsule devices, the release can be accurately modelled with controlled release models, similar to the basic model above, when the release rate of the AI is of the first-order type (as shown above and in the case studies in chapter 5) and all the needed model parameters are available. A more complex model is therefore, in principle, not required for these specific applications. Even so, controlled release models can be further refined in order to predict more accurately the initial periods of delivery as part of the total release behaviour. In this initial period, before an eventual steady-state is achieved, it is necessary to account for the history of the system. That is, the so-called burst and lag time effects. These phenomena depend mainly on the diffusivity of the solute in the polymer, the thickness of the membrane and the storage as well as usage conditions.

The burst effect occurs when, for example, the devices are stored for a period, giving time for the AI to diffuse into the polymer membrane and saturate it. Then, when the system is used the initial delivery rate from the microcapsule becomes greater than that of the steady state, producing thereby the burst effect. This can be observed in commercially available products. On the other hand, if there is no lapse between fabrication and use of the device, the active ingredient does not have time to partition into the membrane and there is a delay before the steady state gradient is reached, this is the lag time effect and it occurs for example when novel devices are being tested.

The general equations to model these effects (Eqs. 2.28 and 2.29, for burst and lag time effect respectively) are taken from Kydonieus et al. [6] and the variation of the mass in the receiver as a function of time is derived, where it can be observed that the two phenomena are equivalent but with opposite signs.

$$\frac{J}{J_{\max}} = 1 + 2\exp\left(\frac{-DK_{m/d}\pi^2 t}{h^2}\right)$$
$$\rightarrow M_r(t) = J_{\max}A\left[t + \frac{2}{\alpha'}\left(1 - \exp\left(-\alpha' t\right)\right)\right] \quad (2.28)$$
$$\frac{J}{J_{\max}} = 1 - 2\exp\left(\frac{-DK_{m/d}\pi^2 t}{h^2}\right)$$
$$\rightarrow M_r(t) = J_{\max}A\left[t - \frac{2}{\alpha'}\left(1 - \exp\left(-\alpha' t\right)\right)\right] \quad (2.29)$$

where,

$$\alpha` = \frac{D\pi^2}{h^2}K_{m/d} \quad (2.30)$$
$$J_{\max} = \frac{DC_{d,initial}}{h}K_{m/d} \quad (2.31)$$

The second term (exponential term) takes into account the burst and lag time effects respectively, while the first term is an indicator of zero-order release rate, then Eqs. 2.28 and 2.29 are only applicable for the initial period and not for the rest of the delivery in the cases treated in this work because the microcapsules handled usually present first-order release rate. Therefore, Eqs. 2.28 and 2.29 have been modified (see Eqs. 2.32 and 2.33) in order to give a first-order release rate after the initial burst or lag time periods. These derivations are provided in Appendix B.

$$M_r(t) = \frac{V_r C'_{d,initial}}{\left(K_{m/r}/K_{m/d} + V_r/V_d\right)}\left(1 - \exp(-\alpha t)\right)$$
$$+ J_{\max}A\frac{2}{\alpha'}\left(1 - \exp\left(-\alpha' t\right)\right) \quad (2.32)$$
$$M_r(t) = \frac{V_r C'_{d,initial}}{\left(K_{m/r}/K_{m/d} + V_r/V_d\right)}\left(1 - \exp(-\alpha t)\right)$$
$$- J_{\max}A\frac{2}{\alpha'}\left(1 - \exp\left(-\alpha' t\right)\right) \quad (2.33)$$

where,

$$\begin{aligned} \alpha &= \frac{DA}{V_r h} K_{m/d} \left(\frac{K_{m/r}}{K_{m/d}} + \frac{V_r}{V_d} \right) \\ \alpha' &= \frac{D\pi^2}{h^2} K_{m/d} \\ J_{\max} &= \frac{DC_{d,initial}}{h} K_{m/d} \end{aligned}$$

It is important to note that the initial concentration used ($C'_{d,initial}$) in Eqs. 2.32 and 2.33 is not the total concentration but a modified one, where the mass released by either burst or lag effect is subtracted (or added respectively) in order to comply with the mass balances.

$$C'_{d,initial} = \frac{M'_{d,initial}}{V_d} \tag{2.34}$$

where, $M'_{d,initial} = M_{d,initial} - M_{burst/lag,\infty}$

and, $M_{burst,\infty} = \frac{2}{\alpha'} J_{\max} A$

$M_{lag,\infty} = -\frac{2}{\alpha'} J_{\max} A$

2. Case studies: burst and lag time effects

The purpose of this section is to present two case studies to illustrate the need and application of the models for lag time (Case study 1) and burst (Case study 2) effects respectively. Through the case studies, the need for development of the model equations to represent the first order release rate instead of a zero-order is also demonstrated. Neither of the two cases studies presented involve pesticide molecules but since the purpose is to illustrate the burst and lag release models, these other systems where the phenomena are observed can be used given that they are equivalent to studying the release of a pesticide AI from a microcapsule.

Case study 1

This case study is based on the experimental release data published by Lukaszczyk et al. [12] where several of the parameters affecting the AI release have been experimentally studied but no modelling attempt has been made. The system studied consists of Codeine [76-57-3], which is a narcotic analgesic drug used mainly to alleviate pain, that is encapsulated together with an ion-exchange resin acting as a carrier, within polyurea microcapsules. The microcapsule wall is formed by water promoted polyreaction of the monomer Methyl Diphenyl

Diisocyanate (MDI, CAS nr: 101-68-8) that can produce a cross-linked polymer.

The composition of the microcapsules is taken from the literature (Lukaszczyk et al. [12]) together with the conditions at which the release experiments were performed. These data, as well as the rest of the data that is required by the mathematical release model is summarized in Table 2.8 for the case investigated. Note that this same literature data is later used (chapter 5) to illustrate the final integration of the methodology through different scenarios, but here only one of them is used where the lag time effects were observed.

As some of the data needed by the model was not available, their values have been assumed (marked in italics in the table). This is the case of the dimensions (and size distribution) of the capsules, which have been fixed based on knowledge of commercially available microcapsules. The microcapsule sizes are then used to calculate the microcapsule wall thickness through the wall percentage ($wall\%$) in the same manner as explained in the previous case study. With respect to the properties of the system (D, $K_{m/r}$ and $K_{m/d}$) the same values have been used as in chapter 5 where details on how these are obtained are given. It is not further explained here because the focus of this section is the release model and not yet the property models.

Table 2.8: Summary of the input data required for the mathematical release model.

Variables	**Values**
MDI/resinate	0.25
h (m)	6.72×10^{-9}
r_{max} (m)	$\mathit{329}\times10^{-9}$
r_{min} (m)	$\mathit{29}\times10^{-9}$
r_{mean} (m)	$\mathit{129}\times10^{-9}$
σ	$\mathit{3}\times10^{-8}$
r_{step}(m)	$\mathit{1}\times10^{-8}$
D(m^2/s)	1.027×10^{-19}
$K_{m/r}$	2.67
$K_{m/d}$	0.138
V_r(m^3)	400×10^{-6}
t (s)	12600
$C_{d,initial}$(g/m^3)	324.72×10^{3}

Finally, the release of Codeine from the polyurea microcapsules is calculated with the mathematical release model and the results are compared with the experimental data in Fig. 2.7 and Fig. 2.8. The first step is to show, in Fig. 2.7, how the appropriate model is the first-order release rate to represent these experimental data and not the zero-order one, so the need for the modification of the of the original equations is confirmed. In this case the results obtained with the burst model are also plotted even though this phenomena is not taking place, just for illustration purposes.

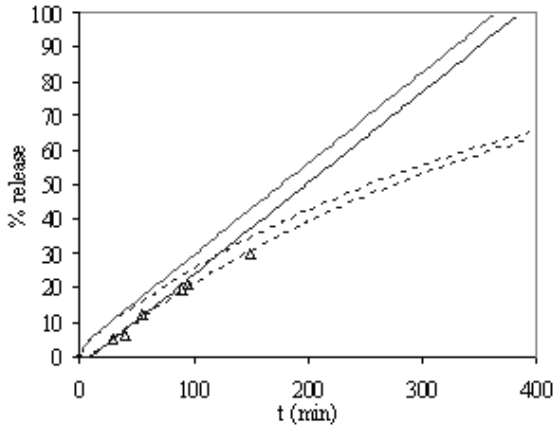

Figure 2.7: Comparison between the original and the modified model equations. Where: (—) Burst and lag (original equations, Eqs. 2.28 and 2.29), (- - -) Burst and lag (modified equations, Eqs. 2.32 and 2.33).

In the second place, Fig. 2.8 shows how a better representation of the experimental data is achieved in the initial period of release by using the lag time model. Different values of the partition coefficient have been used within the basic first order model and none of them succeeded to represent the initial delivery behaviour, so the lag model needs to be used.

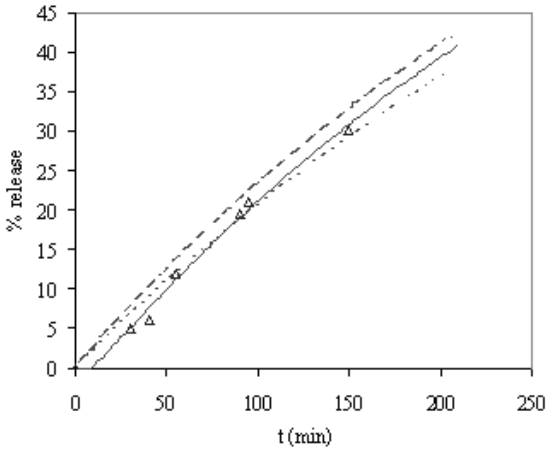

Figure 2.8: Predicted release of AI as a function of time compared with experimental data (△) for the different release models. Where: (– –) first order release ($K_{m/d}$=0.138), (- - -) first order release ($K_{m/d}$=0.12), (—) lag effect.

Finally, the goodness of the predicted release values confirms the fact that the behaviour of microcapsule devices can be reproduced without the need of more complicated models.

Case study 2

This second case study is based on the experimental release data published by Bachtsi et al. [14] where again some of the parameters affecting the release of an AI from microcapsules were studied through experiments and an attempt to correlate the data to a simple first order kinetic model was made. The experimental data could not be fitted to the mentioned model so this was empirically modified to obtain a final semi-empirical equation (Eq. 2.35). The equation is though not explained in terms of physically meaningful parameters.

$$M_t/M_\infty = a + b\left(1 - e^{-Kt}\right) \tag{2.35}$$

This is the difference with the treatment provided in this section where a model derived from physical phenomena is used and an explanation is provided (the burst effects) for the empirical modification introduced originally by the authors.

This case study involves the release of Santosol oil, a commonly used solvent which consists of a mixture of terphenyls and quatraphenyls, from Polyvinyl alcohol (PVA) microcapsules. These microcapsules are prepared by simple coacervation and the oil is then released in an aqueous solution of SDS (Sodium Dodecyl Sulphate) surfactant. Here, again, the focus is not on the prediction of the properties (D, $K_{m/r}$ and $K_{m/d}$) but on the release model, so these variables are used to fit the model to the experimental data. The remaining model variables are obtained from the literature (Bachtsi et al. [14]) with the appropriate calculations when needed. All of the variables needed for the release calculations are summarized in Table 2.9.

Table 2.9: Input data required for the mathematical release model.

Variable	**Values**
h (m)	2.317×10^{-5}
r_{max} (m)	5.50×10^{-4}
r_{min} (m)	6.50×10^{-5}
r_{mean} (m)	4.00×10^{-4}
σ	8.00×10^{-5}
r_{step} (m)	1.00×10^{-5}
D(m^2/s)	6.64×10^{-15}
$K_{m/r}$	2.67
$K_{m/d}$	50
$V_r(m^3)$	2.00×10^{-4}
t (s)	10800
$C_{d,initial}(g/m^3)$	3.92×10^{7}

Again the two models are used, first order and burst model, to study the release from the microcapsules and compare them with the experimental data in Fig. 2.9. From this figure it is clear that a better representation of the initial release behaviour is achieved with the burst model and in the later release period the models perform equally good (as expected).

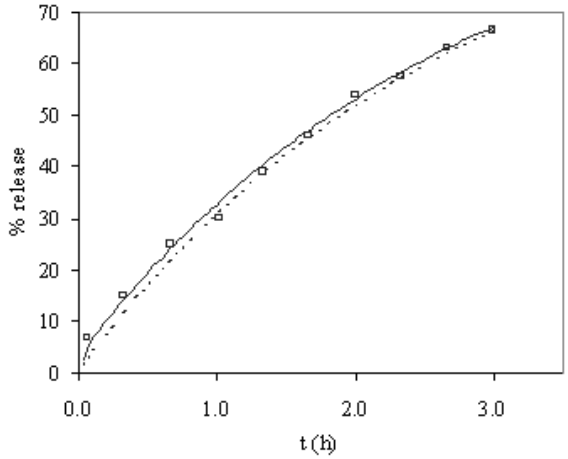

Figure 2.9: Predicted release of AI as a function of time compared with experimental data (□).For the different release models. Where: (- - -) first order release, (—) lag effect.

Once more it has been proved that release of AIs from microcapsules can be studied with these relatively simple mathematical models.

Nomenclature

List of symbols

A	Surface area through which diffusion takes place
A_e	Area available for erosion
B	Surface degradation rate
C_d	Concentration of AI in the donor
$C_{d,initial}$	Initial concentration of AI in the donor
C_m	Concentration of AI in the membrane
C_r	Concentration of AI in the receiver
C_s	Saturation solubility of AI in polymer
C_0	Total initial concentration of AI (dissolved and dispersed)
d	Diameter
D	Diffusion coefficient
D_w	Diffusion coefficient in water
h	Thickness of the microcapsule wall
J	Flux
J_{max}	Steady-state flux
k_e	Erosion constant
k_h	Surface hydrolisis constant
k_r	Rate constant for hydrolisis reaction
K	Partition coefficient of the AI between the polymer membrane and the donor or receiver compartment.
$K_{m/d}$	Partition coefficient of the AI between the donor and the polymer membrane
$K_{m/r}$	Partition coefficient of the AI between the polymer membrane and the release medium
l	Radii of a sphere (in chemical erosion equations)
L_p	Mechanical permeability coefficient (in osmotic pumps)
M	Mass
M_d	Mass of AI in the donor
$M_{initial}$	Initial mass of AI
M_r	Mass of released AI
M_{total}	Total mass of AI
n_f	Number of points to evaluate the function
N_p	Number of particles
p_2^H, p_1^H	Hydrostatic pressure
r	Microcapsule radius
r	Integration limit for microcapsule radius, see Eq. (1)
r_o	Outer (external) radius
r_i	Internal radius
t	Time
t_∞	Time to total erosion
V	Volume

V	Molar volume of the solvent (water in osmotic pumps)
V_d	Donor volume
V_r	Receiver volume
x	Distance along x-axis

Greek letters

ΔM	Mass change (g)
ϵ	Porosity
μ	Mean value in the normal distribution
$\pi_2 - \pi_1$	Osmotic pressure at equilibrium
σ	Standard deviation (in the normal distribution)
σ	Reflection coefficient (measure of leakiness of the membrane, in osmotic pumps)
τ	Tortuosity

Subscripts

0	Initial
∞	Total
calc	Calculated (value)
d	Donor
exp	Experimental (value)
i	Microcapsule internal radii
initial	Initial value
m	Membrane
max	Maximum
mean	Mean value
min	Minimum
o	Microcapsule outer radii
r	Release medium
step	Step size (increment)
total	Total value

Abbreviations

PHEMA	poly(2-hydroxyethyl methacrylate)

References

[1] Shulkin, A., Stöver, H.D.H, Polymer microcapsules by interfacial polyaddition between styrene-maleic anhydride copolymers and amines, *J. Membrane Sci.* 2002, 209, 421-432.

[2] Park, Y. J., Nam, K.H., Ha, S.J., Pai, Ch.M., Chung, Ch. P., Lee, S.J. Porous poly(L-lactide) membranes for guided tissue regeneration and controlled drug delivery: membrane fabrication and characterization, *J. Control. Release* 1997, 43, 151-160.

[3] Zulfiqar, M., Quddos, A., Zulfiqar, S. Release of Tritium-labeled estradiol steroids from fully swollen hydrogels of polyurethane networks, *J. Appl. Polym. Sci.* 1994, 51, 2001-2005.

[4] Peppas, N.A., Controlled drug bioavailability, vol. 1 (p. 203-237), *Mathematical modeling of diffusion processes in drug delivery polymeric systems.* New York, Wiley, 1984.

[5] Comyn, J., *Polymer permeability.* Elsevier, NY, 1985.

[6] Kydonieus, A.F., *Controlled release technologies: methods, theory and applications*, CRC Press, Inc. Boca Ratón, Florida, 1980.

[7] Siepmann, J., Peppas,N.A., Modeling of drug release from delivery systems based on hydroxypropyl methylcellulose (HPMC), *Adv. Drug Deliver. Rev.* 2001, 48, 139-157.

[8] Crank, J., *The mathematics of diffusion*, Oxford, 1956.

[9] Higuchi, T., Rate of release of medicaments from ointment bases containing drugs in suspension, *J. Pharm. Sci.* 1961, 50(10), 874.

[10] Higuchi, T., Mechanism of sustained action medication, *J. Pharm. Sci.* 1963, 52, 1145.

[11] Vandegaer, J.E., *Microencapsulation. Processes and applications.* ACS Symposium series, Plenum Press, New York, 1973.

[12] Lukaszczyk, J. and Urbas,P. , Influence of the parameters of encapsulation process and of the structure of diisocyanates on the release of codeine from resinate encapsulated in polyurea by interfacial water promoted polyreaction, *React. Funct. Polym.* 1997, 33, 233-239.

[13] Amperiadou, A., Georgarakis, M., Controlled release salbutamol sulphate microcapsules prepared by emulsion solvent-evaporation technique and study on the release affected parameters, *Int. J. Pharm.* 1995, 115, 1-8.

[14] Bachtsi, A.R, Kiparissides,C., Synthesis and release studies of oil-containing poly(vinyl alcohol) microcapsules prepared by coacervation, *J. Control. Release* 1996, 38, 49-58.

3

Partition coefficient

3.1 Property definition and theory

i) Definition and thermodynamic approach

One of the variables that influence the release of an Active Ingredient (AI) from a controlled release device is the partition coefficient ($K^{AI}_{p/solv}$). This variable represents the equilibrium distribution of the AI between the polymer membrane and the solvent, in the inner core or outside the device (release medium) as defined by Eq. 3.1.

$$K^{AI}_{p/solv} = \frac{x^{p}_{AI}}{x^{solv}_{AI}} \tag{3.1}$$

This definition is derived from the equilibrium condition of a component i (the AI) distributed between two liquid phases, I and II, corresponding to the polymer and solvent phases respectively, given by Eq. 3.2 in terms of the chemical potential (or activities).

$$\mu^{I}_{AI} = \mu^{II}_{AI} \qquad (or\ the\ equivalent: a^{I}_{AI} = a^{II}_{AI}) \tag{3.2}$$

The definition of activity in terms of mole and weight basis, respectively, is given as,

$$a^{I}_{AI} = x^{I}_{AI}\gamma^{I}_{AI} = w^{I}_{AI}\Omega^{I}_{AI} \tag{3.3}$$

The liquid-liquid equilibrium relation, on a weight basis, is therefore given as,

$$w^{I}_{AI}\Omega^{I}_{AI} = w^{II}_{AI}\Omega^{II}_{AI} \tag{3.4}$$

Then, from Eq. 3.4 the ratios of weight fractions and activity coefficients in each phase are considered to define the partition coefficient (Eq. 3.5), which is equivalent to Eq. 3.1 by replacing the compositions in weight fractions to mole fractions.

$$K^{AI}_{I/II} = \frac{w^{I}_{AI}}{w^{II}_{AI}} = \frac{\Omega^{II}_{AI}}{\Omega^{I}_{AI}} \tag{3.5}$$

Note that the polymer is considered as a liquid phase and liquid-liquid equilibrium is used. This is a common assumption for amorphous polymers (Baner et al. [1]). Also for convenience, the weight units will be used hereafter.

ii) Background literature

Partition coefficients of active ingredients distributing between a solvent and a polymer phases have been studied by several investigators (Pitt et al. [2], Jenke et al. [3]) resulting in measured data for $K^{AI}_{p/solv}$ and correlated models. Thermodynamics based predictive models for estimation of partition coefficients can be found mainly in the field of fragrances, aroma and flavour compounds (Tse et al. [4], Baner et al. [1], Peppas and Peppas [5]) and only in a few of these cases it is related to the application in controlled release of the AI of interest (Peppas and Peppas [5]). While these earlier works are somewhat closer to the objective of this thesis, it is worth noting that the types of compounds that have been treated are much simpler than those commonly employed in the pesticide area. These compounds are usually represented by one single functional group, while pesticide compounds are in most of the cases larger and represented by several different functional groups. In Table 3.1, a comparison is presented of some representative compounds (found in the published papers) with some pesticides that are used in commercial microcapsules (Scher et al. [6]).

As can be seen from Table 3.1, the compounds treated in previous studies all have one single functional group (with one exception of a compound with two functional groups), while the pesticide compounds shown have at least three different functionalities. Besides that, the molecular weights of compounds in the literature range in general from 100 to 200 g/mol (with few exceptions) while the pesticides are in general bigger, with molecular weight over 250 g/mol. It is considered therefore that more work is needed in this area given the great number of applications containing highly complicated molecules.

Table 3.1: Comparison of compounds treated in the literature with some pesticide compounds.

Source	Compounds (solutes)	Type	Functional groups	Mw range (g/mol)
From existing literature:				
[4]	Benzyl alcohol n-Octanol Geraniol Farnesol	Alcohol	1 OH	108 222
[4]	Galaxolide	Ether	1 -O-	258.4
[1]	n-alkanes	Alkanes	-	170-310
[1]	d-limonene	Cycloalkene	-	136
[1]	Diphenylmethane	Aromatic	-	168
[1]	Eugenol	Alcohol + ether	1 OH 1 -O-	164
[1]	Menthol Phenyl ethyl alcohol Cis-3-hexen-1-ol	Alcohol	1 OH	156 122 100.16
[1], [5]	Linalyl acetate	Ester	1 -COO	197
[1]	Isoamyl Acetate			
[1]	Camphor	Cyclic ketone	1 -C=O	152
[1]	Diphenyl oxide	Ether	1 -O-	170
[5]	Carvone Jasmone	Cyclic ketone	1 -C=O	150-164
Pesticide systems:				
[6]	Acetochlor		-Cl, -C=O, -N, -O-	269.8
[6]	λ-cyhalothrin	Pyrethroid	-Cl, -COO, -O-, -CN, -F	449.86
-	Permethrin	Pyrethroid	-Cl, -COO, -O-	391.3

iii) Our approach to predict the partition coefficients

Controlled release devices involve a high degree of complexity at different levels when it comes to applying a thermodynamic model for the calculation of the partition coefficients. This degree of complexity is, for example, related to the number of compounds present in the formulation that can distribute into the polymer. A commercial formulation generally includes, apart from the AI, a solvent for this AI, one or more surfactants and other materials that might be required to stabilize the solution (Lo et al. [8]). In order to simplify the problem, the following assumptions are made:

i) The solution contained in the core of the release device is composed only of the solvent and the AI. This assumption is made on the basis that these are the major components, and the rest are only present in small quantities. This converts a multicomponent problem into a ternary mixture problem.

ii) The AI is the only component that distributes between the two phases (after the reduction of number of components, only solvent and polymer phases are to be considered). That is, the solvent (in the core or in the release medium) does not distribute into the polymer phase and vice versa. This assumption is convenient given that the thermodynamic models that have been considered for the calculation of the activity coefficients (see section 3.2) are reliable for estimation of activity coefficients of solvents in polymers but usually not so for estimation of the activity (or solubility) of polymers in solvents (Kontogeorgis et al. [9]), and therefore a possible source of error is avoided. This assumption would have to be revised in the case of hydrogel polymers, for example, polymers that swell in the presence of water.

Another issue that complicates the estimation of the activity coefficient of the AI in the polymer and solvent phases is the liquid-liquid equilibrium (LLE) calculation. LLE calculations in polymer systems can be rather difficult to solve in some cases (Heidemann and Michelsen [10]). In the case of pesticide compounds, for which no data is available, the factors causing these difficulties would be hard to identify, so the problem must be simplified. Another consideration with respect to LLE calculations (and distribution of components) involving polymers is the polydispersity effect (Chen [11]). When dealing with VLE none of the polymer will go to the vapour phase so there is only one polymer phase, but in the case of LLE the polymer may distribute between the two equilibrium liquid phases, consequently the molecular weight distribution of the polymer in the two phases can be different, therefore the incorporation of the distribution of chain lengths into the activity coefficient models needs to be considered. For this reason, infinite dilution conditions are considered for the AI in the solvent (both in the core and release medium) and in the polymer. This consideration converts the LLE calculation problem into simple activity coefficient estimation (given that the compositions are fixed), and it is generally applicable according to the following assumptions,

- the amount of AI in the formulation is generally small. This might have to be revised in some cases where the amounts of pesticide within the capsule are higher (this depends mainly on the strength of the AI, Chadwick et al. [12]). But in such cases, it can still be assumed that the ratio of AI in each of the phases is of the same order of magnitude.

- the volume of release medium is much greater than that of the microcapsules (infinite sink conditions).

- the polymer does not distribute into other phases.

The above assumptions (or in some cases equivalent) have also been considered by Baner et al. [1], Tse et al. [4] and Peppas and Peppas [5], and for purposes of comparison, are therefore considered valid.

The introduction of the infinite dilution assumption, leads to the calculation of the infinite dilution activity coefficient of the AI as,

$$\Omega_{AI}^{\infty} = \lim_{w_i \to 0} \Omega_{AI} \tag{3.6}$$

Combination of Eq. 3.6 with Eq. 3.5 provides the final expression for the partition coefficient (Eq. 3.7), that will be used hereafter.

$$K_{p/solv}^{AI} = \frac{\Omega_{AI}^{solv,\infty}}{\Omega_{AI}^{p,\infty}} \tag{3.7}$$

3.2 Evaluation of available models for estimation of activity coefficients in polymer systems

As concluded from the previous section the prediction of the partition coefficient is reduced to the estimation of the infinite dilution activity coefficients of the AI in each of the two phases, solvent and polymer. The solubility of AIs in well-known solvents has been widely studied because it is an important part of formulation design. Therefore the activity coefficient of the pesticide in the solvent can usually be calculated from experimental data (for example from Worthing [13]) through Eq. 3.8.

$$\Omega_{AI}^{\infty} = \frac{1}{w_{solv,AI}} \tag{3.8}$$

In the cases where experimental data is not available, a group-contribution based model such as UNIFAC can be used for these calculations. The UNIFAC models (Fredenslund et al. [14], Kang et al. [15]) have a large (group) parameter table that allows the estimation of activities for a wide range of compounds, including pesticides. As these models have been widely used and tested, further discussion of their suitability is not considered here.

On the other hand, there is a considerable lack of data related to the solubility of pesticides in polymers in the open literature. Therefore, attention is focused in this section on analyzing the models available for estimation of activity coefficients of AIs in polymer systems. This analysis differs from those available in numerous publications (Lee and Danner [16] and Danner and High [17]) with respect to the focus of the study. In general the interest has been put on the performance (predictive accuracy) of the models for different types of polymer-solvent systems, at various temperature and pressure conditions. The

analysis in this Ph.D. thesis, however, is directed to investigating the applicability of these models to pesticide compounds, usually represented by large and multifunctional molecules for which little data is available. Consequently, a major concern is whether the calculations can be done at all.

3.2.1 All polymer models

Innumerable efforts have been made to model phase equilibria of systems involving polymers. A brief overview is presented, not to provide an extensive review of models for polymer systems but to explain the choice of the model for pesticide-polymer systems. The models can be classified into different groups based on the theory used to derive them. In Table 3.2, six groups of model types are highlighted and their applicability to pesticide-polymer systems analyzed. The analysis considers the model parameters that are required, the data needed to estimate them and finally, whether these data are available for pesticide-polymer systems.

Table 3.2: Review of the available thermodynamic models and their applicability to pesticide-polymer systems.

Model	**Theory**	**Model Parameters / Properties**	**Obtained from**	**Availability for pesticides**
1. Lattice models				
Regular solution theory [18]	Based on solubility parameters	δ	Experiment	n/a
			Calculated GC	y (not reliable)
		$\tilde{V}_i$ pesticide	Experiment	y
		polymer	Calculated GC	
FH-model [19], [20]	Lattice theory	χ_{12}	Experiment (VLE data)	n/a
			Calculated: need δ	not reliable
			- Experiment	n/a
			- Calculated GC	y (not reliable)
		$\tilde{V}_i$ pesticide		y
		polymer		
Sanchez-Lacombe EoS [21]	Hole theory	ϵ^*	Experimental data:	
		v^*	Pesticide: $P_{vap}(T)$ (or $\rho(T)$)	n/a
		r	Polymer: $\rho(T,P)$	
			Mixture data ($\Delta H_{mix}, \Delta V_{mix}$)	n/a
Panayiotou-Vera EoS [22]	Lattice-Hole theory	$\epsilon_{ii}{}^*$	Experimental data	
		v^*	Pesticide: $P_{vap}(T)$	n/a
		k_{ij}	$\rho(T)$	n/a
			Polymer: PVT data: $\rho(T,P)$	
			VLE data	n/a
			Calculated: GC (High-Danner EoS)	

Model	**Theory**	**Model Parameters / Properties**	**Obtained from**	**Availability for pesticides**
2. Cubic EoS				
Van der Waals EoS [24]	Cubic EoS + G^E model	a b	Pesticide: Tc, Pc Polymer: ρ(T, P)	n/a
PR EoS [26]	FH model + Wong-Sandler mixing rules or $+G^E$ model	a b c_1, c_2, c_3	Pesticide: Tc, Pc ω Polymer: ρ(T,P)	n/a n/a
SRK EoS [27]	Cubic EoS + G^E model	a b	Pesticide: Tc, Pc Polymer: ρ(T,P)	n/a
3. GC Free-volume models				
UNIFAC-FV [28]	Lattice theory + Flory EoS	v_w (R_n), Q_n a_{nm} ρ(T of system): pesticide polymer	GC parameters GC parameters Experimental Calculated from GC Calculated from GC (GCVOL) from Tg [39]	y $y^{(1)}$ n/a
Entropic-FV [29], [30]	FH (with FV) + UNIFAC (residual /energetic term)	v_w (R_n), Q_n $a_{nm,1}$, $a_{nm,2}$ ρ(T of system): pesticide polymer	GC parameters GC parameters Experimental Calculated from GC Calculated from GC (GCVOL) from Tg [39]	y $y^{(1)}$ n/a

Model	Theory	Model Parameters / Properties	Obtained from	Availability for pesticides
Molecular-FV model				
Entropic-FV / UNIQUAC [30]	FH (with FV) + UNIQUAC (residual/energetic term)	$a_{nm,1}$, $a_{nm,2}$	Experimental VLE data of Molecules/segments involved	n/a
		v_w (R_n), Q_n	GC parameters	y
		ρ(T of system): pesticide	Experimental	
		polymer	Calculated from GC	
			Calculated from GC (GCVOL) from Tg [39]	
4. VdW models				
Flory EoS [31]	VdW model	C	Thermal expansion	n/a
		$s\eta$	Coefficient of compressibility	n/a
			Thermal pressure coefficient	n/a
GC-Flory EoS [32]	Flory EoS + local composition model GC-model	R_n, Q_n	GC parameters	y
		$C_{T0,n}$, $C_{T,n}$, C_n^0	GC parameters	$y^{(1)}$
		a_{nm}	GC parameters	$y^{(1)}$
5. Continuum model (Non-cubic EoS)				
SAFT EoS [33], [34]	Wertheim perturbation theory	m	P_{vap}(T)	n/a
		v^*	ρ(T)	n/a
		u^0/k	Polymers PVT or extrapolation from low Mw homologues	
		ϵ^{AB}/k		
		κ^{AB}		
		Association scheme		
		k_{ij}	VLE data of system	n/a

n/a: not available; y: available

(1) Not always available but can be estimated without need of pesticide data.

Based on the information in the table, the models are now discussed in terms of their applicability to the pesticide-polymer systems of interest.

The Regular Solution Theory (Hildebrand and Scott [18]) is one of the simplest models that can be used for systems including polymers. Due to its simplicity it is also very limited in its applicability, to non-polar or slightly polar compounds. Pesticide compounds contain, in general, several functional groups or atoms (Cl, F, N, O, ...) that provide them with a certain polarity, thereby making this model infeasible for them. In Table 3.3 the molecular formula of some of the commonly used pesticides in controlled release technology (Scher et al. [6]) is given to illustrate the different elements found in them. Also, the fact that some of the properties required for the calculations (solubility parameter and density) are not always available for these compounds (see also Table 3.3) is an inconvenience.

Within the group of models based on the lattice theory, the Flory-Huggins (FH) model (Flory [19] and Huggins [20]) is discarded as equilibrium data is not usually available to obtain the interaction parameter (χ_{12}), meaning that this would have to be estimated with the formula,

$$\chi_{12} = 0.35 + \frac{\tilde{V}_1}{RT}\left(\delta_1 - \delta_2\right)^2 \tag{3.9}$$

The above equation is not reliable, among other reasons, because the interaction parameter is known to be a function of concentration and temperature, but these are not taken into account by the equation. At the same time, some properties that are needed in this model (similar to the Regular Solution Theory) are not available for pesticide compounds.

In the case of EoS models (Sanchez-Lacombe (Lacombe and Sanchez [21]), Panayiotou-Vera (Panayiotou and Vera [22])) the main setback for their use in pesticide-polymer systems is that they require pure properties of the compounds of interest as a function of temperature (vapor pressure, liquid density) which are not always available for pesticides. Apart from that, mixture data is also required to determine the interaction parameters, and that again, is lacking for pesticide-polymer systems.

The models based on cubic EoS have been combined with G^E models (such as FH-model, UNIFAC-FV (Oishi and Prausnitz [28]), etc.) in order to obtain a predictive model. Therefore the aspects concerning the applicability of the G^E models discussed below, is also suitable here. The limitation in the use of these models in pesticide-polymer systems is the lack of critical properties data for the pesticide compounds that are necessary for the calculation of the EoS parameters.

The next group of models to be considered includes group-contribution based methods (including a free-volume term), which are the most promising models for use within the scope of this work. This is because they do not require data of the compounds of interest for the estimation of the model parameters, which is usually missing for pesticide compounds. They allow the calculation of activity coefficients of any molecule for which the molecular structure is known and can

be represented by the corresponding groups. These models are discussed separately, together with the GC-Flory EoS (Bogdanic and Fredenslund [32]) and the special case of Entropic-FV/UNIQUAC (Elbro et al. [30]), in section 3.2.2.

Finally, one of the models that have shown a high potential in terms of performance is the SAFT EoS (Huang and Radosz [33] and Chapman et al. [34]). The parameters required for this model are molecular parameters, which means that vapour pressure and liquid density data as a function of temperature are required for the compounds of interest, which, as mentioned above, is not readily available for pesticides. Also, an interaction parameter (k_{ij}) is needed in most cases to represent the phase behaviour accurately.

Table 3.3: Pesticide compounds (typical of controlled release, Scher et al. [6]) and properties from Tomlin [35]

Pesticide	**CAS nr**	**Formula**	$\rho, 20°C$ (g/cm^3)	$P_{vap}, 25°C$ **(mPa)**	δ	**Tc,** Pc
λ-cyhalothrin	91465-08-6	$C_{23}H_{19}ClF_3NO_3$	1.25	0.001	n/a	n/a
Thiamethoxam	153719-23-4	$C_8H_{10}ClN_5O_3S$	1.57	6.6×10^6	n/a	n/a
Permethrin	52645-53-1	$C_{21}H_{20}Cl_2O_3$	1.29	0.0025	n/a	n/a
Acetochlor	34256-82-1	$C_{14}H_{20}ClNO_2$	1.1221	6	n/a	n/a
Tefluthrin	79538-32-2	$C_{17}H_{14}ClF_7O_2$	1.48	8.4	n/a	n/a
Fluorochloridone	61213-25-0	$C_{12}H_{10}C_{l2}F_3NO$	1.19	0.44	n/a	n/a
Fonophos	944-22-9	$C_{10}H_{15}OPS_2$	1.16	28	n/a	n/a

The conclusion from the above discussion is that, within the wide variety of models presented, the majority are not feasible in practice for systems involving pesticides given that they require experimental data of the pure compounds (as a function of temperature) or mixtures, which is generally not available for these systems. The most promising are then the group-contribution based models as they require little or no data of the actual compound of interest.

3.2.2 Group Contribution-models and GC-Flory EoS

i) Group Contribution-approach

The type of models considered to have most potential in the study of pesticide-polymer systems are those based on the group-contribution (GC) approach. In general terms, this approach consists of representing the molecule of interest as constituted by different (pre-defined) groups such as -CH_2, -OH, etc. The parameters required for the estimation of the property (in this case activity coefficients) are group parameters and not molecular parameters (as in other models such as Sanchez-Lacombe EoS or Panayiotou-Vera EoS). The fact that they are group-parameters means that they are obtained from fitting data of compounds having the groups of interest, and not necessarily the actual compound of interest (in this case the model may be subject to larger errors). This solves the obstacle of lack of experimental data when dealing with pesticide containing systems. In general the GC-based models have some drawbacks, such

as the representation of isomers, which are described with the same groups and thus the same value for the property is obtained. Another type of mixtures that are problematic are those containing highly complex compounds, with several functional groups. This is precisely the case of pesticide compounds. The models for activity coefficients have been tested with compounds having one or at the most two functional groups but a thorough analysis of performance for more complex molecules (with many different functional groups) is generally not possible due to the lack of experimental data to compare with.

ii) Theory of the models

The first group of GC-models (UNIFAC-FV and Entropic-FV) are based on the UNIFAC models for low molecular weight compounds (Fredenslund et al. [14]). Here, the activity coefficient is calculated from two contributions (see Eq. 3.10), a combinatorial term that accounts for entropic effects (size and shape), and a residual or energetic term, that takes into account the molecular interactions.

$$\ln \gamma_i = \ln \gamma_i^{comb} + \ln \gamma_i^{res} \tag{3.10}$$

The extension of these models to polymer systems maintains the same residual or energetic term as the original UNIFAC models but the combinatorial term is modified to include the free volume effects, as shown in Eqs. 3.11 and 3.12 for UNIFAC-FV and Entropic-FV respectively. This modification is essential due to the fact that free volume differences are important in polymer solutions, that is, when the compounds in solution have very different sizes, as is the case for solvents and polymers.

$$\ln \gamma_i = \ln \gamma_i^{comb} + \ln \gamma_i^{res} + \ln \gamma_i^{fv} \tag{3.11}$$

$$\ln \gamma_i = \ln \gamma_i^{comb-fv} + \ln \gamma_i^{res} \tag{3.12}$$

The general definition of free volume is 'the volume allocated to the molecules for movement when their own volume is subtracted' (Kontogeorgis [36]). In practice the formulas/equations representing this free-volume differ for the various models (Kontogeorgis [36]) and in some cases (such as Flory EoS) does not even correspond to the volume. The volume of the molecule is also represented in different forms, even though they are all based on the Van der Waals volume (Kontogeorgis [36]). In the UNIFAC-FV model, the free-volume term is based on the Flory EoS (similarly to the GC-Flory EoS discussed in the next section) while in the Entropic-FV model it is similar to that of the FH-model. The fact that the residual terms are not modified implies that the energy interaction parameters of the existing UNIFAC models can be used in both cases. This is the major advantage of these models given that the parameter tables are very large and thus the parameter estimation procedure is avoided. An interesting modification, in terms of prediction accuracy, of the Entropic-FV

model is its combination with the residual term of UNIQUAC model, to give the so-called Entropic-FV/ UNIQUAC. While this is very convenient in terms of performance, it cannot be applied in this work because the parameters are not group-based anymore, but molecular (or segment) based, which leads to the need of experimental data for the compounds of interest, again the main obstacle of pesticide-polymer systems. The models considered (UNIFAC-FV and Entropic-FV) have certain drawbacks that make them inappropriate for the use in pesticide-polymer systems, and in this work, such as:

i) Not reliable at high dilution. As described in the methodology (section 3.1), this is the concentration range that is used in the scope of this work.

ii) Need of accurate density data for both pesticide and polymer at the temperature of interest. For the pesticide compounds this data is missing in many cases (as mentioned earlier). An important number of correlations is available for polymers (Zoller and Walsh [37]) but the problem in this case might be the fact that the polymer used for the controlled release device has a very specific structure (even though they belong to a general type of polymers for which the correlation is available) for which the experimental correlations might not be useful. In both cases (pesticide and polymer) group-contribution methods are available for the estimation of densities as a function of temperature (Marrero and Gani [41]) for pesticides and GCVOL (Elbro et al. [38]), and Van Krevelen method (Van Krevelen [39]), for polymers), but it has been shown (Lindvig et al. [40]) that the activity coefficient models are extremely sensitive to the values of density, so this is not a recommended option.

The last GC-model to be considered here is the GC-Flory EoS (Bogdanic and Fredenslund [32]), based on a modified form of the Flory EoS. The main advantage of this model over the other GC-models discussed above is the fact that it does not require density data for any of the compounds and thus it is completely predictive. Furthermore the parameters have been extensively tested with activity coefficient data of polymer systems at infinite dilution and satisfactory results have been obtained (Bogdanic and Fredenslund [32], and sections 3.3.3 to 3.3.7). The disadvantage of this model with respect to other GC-models is the size of the parameter table, which is much smaller. The model is, however, similar in terms of prediction accuracy as it has been shown by other researchers (see reviews by Lee and Danner [16], Danner and High [17]). Given the limitation of the number of parameters available, an extension of the model is required to include these complex pesticide molecules (as well as some polymers), which is the subject of the next section.

3.3 The GC-Flory EoS model and its extension

3.3.1 Introduction

i) The GC-Flory EoS model
The GC-Flory EoS model is based on a modified form of the Flory EoS combined with a local-composition group-contribution model (similar to UNIFAC-FV). Thanks to the inclusion of the equation of state the model is purely predictive and the activity coefficients can be estimated without need of any experimental data, and with only the information (apart from temperature and composition of the system) of the molecular structure of the solvent/pesticide and the polymer (repeat unit). Holten-Andersen et al. [42] first modified the Flory EoS to introduce the GC-approach, to make it applicable to the vapour phase and also for associating systems. The model was subsequently revised and improved by Chen et al. [43] but the parameter table provided was very limited. The final version of the model was developed by Bogdanic and Fredenslund [32], which is the model used in this work. The definition of groups corresponds to that of the UNIFAC model (Fredenslund et al. [14]) and it is worth noting that the best representation of the polymer is achieved by considering the number average molecular weight of the polymer (M_n) in the calculations, even if for large molecular weight the results become insensitive to the molecular weight values. Extensive tests of performance of this model have been conducted by Bogdanic and Fredenslund [32] as well as several literature reviews (for example, Lee and Danner [16], and Danner and High [17]). Therefore, it is not considered necessary to repeat these tests for the existing groups and an analysis of accuracy will only be presented for the new groups introduced in this work (next section). The equations of the model needed to calculate the activity coefficients are given in Table 3.4 and the model solution is now briefly discussed. The variables of the model are identified in order to determine the degrees of freedom (DOF), from subtracting the number of equations to the number of variables. These indicate the number of variables that need to be specified in the model (given in the last row in Table 3.4). The variables that need to be specified are the following:

i) Those given by the mixture conditions: temperature (T), pressure (P, P_i), compositions (x_i, n, n_i, w_i), and the times each subgroup appears in the compound (ν_n).

ii) Variables retrieved from the group parameter tables: $C_{To,n}$, $C_{T,n}$, C_n^0 , ϵ_{nm}, R_n, Q_n

iii) Model fixed constants: T_0, z, R

The number of main groups (MG), subgroups (SG) also needs to be given.

Table 3.4: List of the GC-Flory EoS model equations for calculation of activity coefficients

Eq. No.	Equation	Number of equations
P1	$\ln \Omega_i = \ln \Omega_i^{comb} + \ln \Omega_i^{fv} + \ln \Omega_i^{attr}$	NC
P2	$\ln \Omega_i^{comb} = \ln \frac{\varphi_i}{w_i} + 1 - \frac{\varphi_i}{x_i}$	NC
P3	$\Phi_i = \frac{x_i v_i^*}{\sum\limits_{j=1}^{NC} x_j v_j^*}$	NC
P4	$v_i^* = (1.448)(15.17) \sum\limits_{n=1}^{SG} v_n R_n$	NC
P5	$\ln \Omega_i^{fv} = 3(1 + C_i) \ln \left(\frac{\tilde{v}_i^{1/3} - 1}{\tilde{v}^{1/3} - 1} \right) - C_i \ln \frac{\tilde{v}_i}{\tilde{v}}$	NC
P6	$C_i = \sum\limits_{n=1}^{SG} v_n \left[C_{To,n} + C_{T,n} \left(\frac{1}{T} - \frac{1}{T_0} \right) + \sum\limits_{n=1}^{SG} \frac{R_n}{\sum\limits_{m=1}^{SG} R_m} C_n^0 \right]$	NC
P7	$\ln \Omega_i^{attr} = \frac{1}{2} z q_i \left\{ \frac{1}{RT} \left[\varepsilon_{ii}(\tilde{v}) - \varepsilon_{ii}(\tilde{v}_i) \right] + 1 - \ln \sum\limits_{j=1}^{NC} \theta_j \exp\left(-\Delta\varepsilon_{ji}/RT\right) - \frac{\sum\limits_{j=1}^{NC} \theta_j \exp(-\Delta\varepsilon_{ji}/RT) \Delta\varepsilon_{ji}}{\sum\limits_{k=1}^{NC} \theta_k \exp(-\Delta\varepsilon_{ki}/RT)} \right\}$	NC
P8	$q_i = \sum\limits_{n=1}^{SG} v_n Q_n$	NC
P9	$\varepsilon_{ji}(\tilde{v}) = \frac{\varepsilon_{ji}^0}{\tilde{v}}$	NC*NC
P10	$\varepsilon_{ii}(\tilde{v}) = \frac{\varepsilon_{ii}^0}{\tilde{v}}$	NC
P11	$\varepsilon_{ji}(\tilde{v}_i) = \frac{\varepsilon_{ji}^0}{\tilde{v}_i}$	NC*NC
P12	$\varepsilon_{ji}^0 = \sum\limits_{m=1}^{SG} \theta_m^{(i)} \sum\limits_{n=1}^{SG} \theta_n^{(j)} \Delta\varepsilon_{nm}$	NC*NC
P13	$\theta_n^{(i)} = \frac{v_n^{(i)} Q_n}{q_i}$	NC*SG
P14	$\Delta\varepsilon_{nm} = -\left[\varepsilon_{mm}\varepsilon_{nm}\right]^{1/2} + \varepsilon_{nm}$	MG*MG
P15	$\theta_i = \frac{x_i q_i}{\sum\limits_j x_j q_j}$	NC
P16	$\Delta\varepsilon_{ji} = \varepsilon_{ji} - \varepsilon_{ii} = \varepsilon_{ji}(\tilde{v}) - \varepsilon_{ii}(\tilde{v})$	NC*NC
P17	$P_i = \frac{nRT(\tilde{v}_i^{1/3} + C_i)}{v_i^* \tilde{v}_i \left(\tilde{v}_i^{1/3} - 1\right)} + \frac{E^{attr}(\tilde{v}_i)}{v_i^* \tilde{v}_i}$	NC
P18	$P = \frac{nRT(\tilde{v}^{1/3} + C)}{v^* \tilde{v} \left(\tilde{v}^{1/3} - 1\right)} + \frac{E^{attr}(\tilde{v})}{v^* \tilde{v}}$	1
P19	$C = \frac{1}{n} \sum\limits_{i=1}^{NC} n_i C_i = \sum\limits_{i=1}^{NC} x_i C_i$	1
P20	$v^* = \sum\limits_{j=1}^{NC} x_j v_j^*$	1
P21	$E^{attr}(\tilde{v}_i) = \sum\limits_{i=1}^{NC} \frac{1}{2} z q_i n_i \left\{ \varepsilon_{ii}(\tilde{v}_i) + \sum\limits_{j=1}^{NC} \theta_j \exp\left(-\Delta\varepsilon_{ji}/RT\right) \Delta\varepsilon_{ji} / \sum\limits_{k=1}^{NC} \theta_k \exp\left(-\Delta\varepsilon_{ki}/RT\right) \right\}$	NC
P22	$E^{attr}(\tilde{v}) = \sum\limits_{i=1}^{NC} \frac{1}{2} z q_i n_i \left\{ \varepsilon_{ii}(\tilde{v}) + \sum\limits_{j=1}^{NC} \theta_j \exp\left(-\Delta\varepsilon_{ji}/RT\right) \Delta\varepsilon_{ji} / \sum\limits_{k=1}^{NC} \theta_k \exp\left(-\Delta\varepsilon_{ki}/RT\right) \right\}$	1

NC: number of components; MG: number of main groups; SG: number of subgroups.

Total number of equations = 12NC + 4NCxNC + NCxSG + MGxMG + 4
Total number of variables = 10 [$\tilde{v}$,P, $E^{attr}(\tilde{v})$, C, v*,T_0, T, z, R, n] + (16NC+ 6SG) [Ω_i, Ω_i^{comb},ϕ_i, v_i*, Ω_i^{fv}, C_i, Ω_i^{attr}, $\tilde{v}_i$, q_i, $\epsilon_{ii}(\tilde{v})$,θ_i,P_i, $E^{attr}(\tilde{v}_i)$,x_i, n_i, w_i, R_n,$C_{T_0,n}$, $C_{T,n}$, C_n^0, Q_n, ν_n] +(4NCxNC + NCxSG + 2MGxMG) [$\epsilon_{ji}(\tilde{v})$, $\epsilon_{ji}(\tilde{v}_i)$, ϵ_{ji}^0,$\Delta\epsilon_{ji}$,$\theta^(i)$,$\Delta\epsilon_{nm}$, ϵ_{nm}]
DOF = 4NC + MGxMG + 6 + 6SG

An analysis of the model solution is done through the incidence matrix that contains the unknown variables (in the columns) and the equations (rows), and where (*) indicates a variable appearing in the corresponding equation. A square incidence matrix is obtained and given in Fig. 3.1. As observed from Fig. 3.1 a lower tridiagonal form of the incidence matrix cannot be obtained, which indicates that the equations cannot be solved directly or sequentially (as if it was a lower tridiagonal matrix) but an iterative procedure is needed for the variables and equations outside the lower tridiagonal matrix.

Eqs.	Unknown variables																					
	v_i^*	Ψ_i	q_i	$\theta_n^{(i)}$	q_i	$\Delta\varepsilon_{nm}$	ε_{ji}^0	$\Delta\varepsilon_{ji}$	$\varepsilon_{ji}(\tilde{\nu}_i)$	$\varepsilon_{ii}(\tilde{\nu})$	C_i	$E^{attr}(\tilde{\nu}_i)$	$\varepsilon_{ji}(\tilde{\nu})$	$\tilde{\nu}_i$	v^*	C	$E^{attr}(\tilde{\nu})$	$\tilde{\nu}$	Ω_i^{comb}	Ω_i^{fr}	Ω_i^{attr}	Ω_i
P4	*																					
P3	*	*																				
P8			*																			
P13			*	*																		
P15			*		*																	
P14						*																
P12				*		*	*															
P16								*	*	*			*									
P11							*							*								
P10							*			*								*				
P6											*											
P21					*			*		*		*		*								
P9							*						*					*				
P17	*										*	*		*								
P20	*														*							
P19											*					*						
P22			*		*			*		*							*					
P18															*	*	*	*				
P2		*																	*			
P5											*			*				*		*		
P7			*		*			*		*											*	
P1																						*

Figure 3.1: Incidence matrix of GC-Flory EoS model equations.

ii) Extension of the model

The subject of this section is the extension of the GC-Flory EoS model to include new groups that will allow the representation of some of the complex pesticide molecules of interest together with some of the polymers commonly used within the frame of controlled release technology. The introduction of new groups involves the estimation of the group parameters through the procedure described by Bogdanic and Fredenslund [32], which is highlighted in Fig. 3.2. The parameters to be estimated are the coefficients of the C-correlation (C(T)) for each subgroup n ($C_{T0,n}, C_{T,n}, C_{0n}$) and the interaction parameters between each of the main groups (ϵ_{nn} and ϵ_{nm}). R_n and Q_n are obtained from UNIFAC (Fredenslund et al. [14]) or else from Bondi [45]. This estimation procedure requires experimental data of low molecular weight compounds. In the first place, pure component properties are needed for compounds containing the groups to be estimated, that is, thermal expansivity (α) and enthalpy of vaporization (ΔH_{vap}) as a function of temperature [46]. At the same time, experimental mixture data is necessary, usually in the form of activity coefficient data of the low molecular weight compounds (Tiegs et al. [47] and Gmehling et al. [48]).

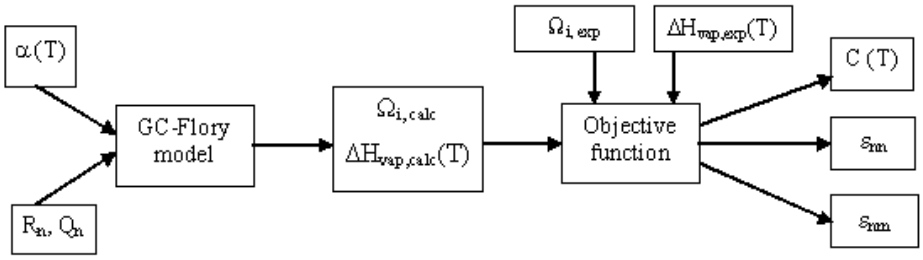

Figure 3.2: Scheme for the group parameter estimation procedure (R_n and Q_n are the hard core volume and surface area of new group n, respectively).

No polymer data is used for the estimation of the group parameters, therefore it is always necessary to test the applicability of the parameters obtained through comparison with experimental data involving polymers. In the ideal case, data of pesticide-polymer systems should be used for this analysis but since this data is not available, the check must be done with literature data including compounds that are represented with the new groups.

The extension of the model is limited to the compounds of interest in this work, that is, compounds used in controlled release technology. The range of pesticides used in this area covers a large variety of molecular structures, that is, a large number of different functional groups. Therefore the amount of groups that would need to be added is very important. This is illustrated in Table 3.5 where some active ingredients used in microcapsule formulations (Scher et al. [6]) are presented, together with their description in terms of groups.

Table 3.5: Pesticide active ingredients and their description in terms of groups (UNIFAC)

Pesticide	**CAS nr**	**Property**	**Product**	**Group description**	**Missing groups**
EPTC	759-94-4	Herbicide	Capsolane	CH_2 CON CH_2S	CON CH_2S
Fluorochloridone	61213-25-0	Herbicide	Racer ME	aCH CH_2 CH_2Cl CF_2 -Cl NCO	CF_2 -Cl NCO
Acetochlor	34256-82-1	Herbicide	TopNotch Fultime	CH_2 aCH CH_2O (N)CO CH_2Cl	(N)CO
Fonofos	944-22-9	Insecticide	Dyfonate	CH_2 aCH CH_2O aC-S- S P	aC-S- P=S
Tefluthrin	79538-32-2	Insecticide	Force Seed Treatment	CH_2 C=C aCH COO CF_2 aC-F Cl-(C=C)	CF_2 aC-F Cl-(C=C)
λ- cyhalothrin	91465-08-6	Insecticide	Icon (Demand) Karate	CH_2 C=C aCH COO aC-O $C \equiv N$ CF_2 Cl-(C=C)	aC-O $C \equiv N$ CF_2 Cl-(C=C)

In order to simplify and focus the work it was agreed to concentrate on a specific family of pesticides that is widely used in the field of controlled release technology. The chosen type of pesticides is the synthetic pyrethroids, and with that the number of different groups needed is reduced to some representative ones, that will still allow the study of an important number of compounds. This is illustrated in Table 3.6, where most of the pyrethroid compounds can be represented as soon as the groups considered for this extension are available.

Table 3.6: Pyrethroid active ingredients and their description in terms of main groups (UNIFAC)

Pesticide	**CAS nr**	**Property**	**Product**	**Group description**	**Missing groups**	
					Before extension	**After extension**
Permethrin	52645-53-1	Insecticide	AMBUSH	CH_2 C=C aCH COO aC-O Cl-(C=C)	aC-O Cl-(C=C)	
Cypermethrin	52315-07-8	Insecticide	Cymbush (&more)	CH_2 C=C aCH COO aC-O C ≡ N Cl-(C=C)	aC-O C ≡ N Cl-(C=C)	-
Phenothrin	26002-80-2	Insecticide	Sumithrin Neopitroid	CH_2 C=C aCH COO, aC-O	aC-O	-
Fenvalerate	51630-58-1	Insecticide (acaricide)	Sumicidin	CH_2 aCH COO aC-O aC-Cl , C ≡ N	aC-O C ≡ N	-
Fluvalinate	102851-06-9	Insecticide	Mavrik, Yardex	CH_2 aCH COO aC-O (C)NH C ≡ N aC-Cl, CF_2	aC-O CH-NH C ≡ N CF_2	C-NH(1)
Dimethrin	70-38-2	Insecticide	n/a	CH_2 aCH C=C, COO	-	-
Decamethrin	52820-00-5	Insecticide	Decis Delta	CH_2 C=C aCH COO aC-O, C ≡ N -Br	aC-O C ≡ N -Br	-Br
Resmethrin	10453-86-8	Insecticide	Chrysron Synthrin Termout	CH_2 C=C aCH COO, cy-O	cy-O	cy-O
Allethrin	584-79-2	Insecticide	Pynamin Forte Pyrotex	CH_2 C=C COO, cy-CO	cy-CO	cy-CO
Tetramethrin	7696-12-0	Insecticide	Neo-pynamin Chinethrin	CH_2 C=C COO cy-N, cy-CO	cy-N cy-CO	cy-N cy-CO
λ- cyhalothrin	91465-08-6	Insecticide	Icon (Demand) Karate	CH_2 C=C aCH COO aC-O C ≡ N CF_2 Cl-(C=C)	aC-O C ≡ N CF_2 Cl-(C=C)	-

(1) Available (parallel work [7])

The variety of polymers used in the area of controlled release of agricultural products (Baker et al. [49]) is a bit more limited (than that of pesticides), maybe not in terms of molecular structure but more regarding the number of different functional groups, which is in fact the concern when dealing with group-contribution models. These polymers are for example Poly(vinyl chloride), various rubbers (Baker et al. [49]), and for microcapsules, polyurea, polyesters, polyurethanes and polyamides are commonly used (Dahl and Simkin [50]), as shown in Table 3.7. Many of the groups needed to represent these polymers are already available in the original parameter table (Bogdanic and Fredenslund [32]), but a few important polymers in microencapsulation of pesticidal compounds such as polyureas, polyamides, polyurethanes, cannot yet be described (see Table 3.7). This is therefore another focus point for the extension of the GC-Flory EoS model that includes the addition of -CONH- group.

Table 3.7: Microencapsulated pesticides and polymer materials (Baker et al. [49])

Product	**Pesticide**	**Property**	**Polymer**	**Functional group**	**Missing groups**	
					Before extension	**After extension**
Penncap-M	Methyl parathion	insecticide	Nylon (Polyamide)	-CONH-	-CONH-	-
Knox-Out	Diazinone	insecticide	Nylon (Polyamide)	-CONH-	-CONH-	-
Dursban	Chlorpyrifos	insecticide	Polyurethane	-NH-COO-	(C)NH[(1)]	
Osmocoat	fertilizer	fertilizer	Resin			
Zeon, Icon	Cyhalothrin	insecticide	Polyurea	-NH-CO-NH-	-CONH-	-
					(C)NH[(1)]	
Force CS	Tefluthrin	insecticide	Polyurea	-NH-CO-NH-	-CONH-	-
					(C)NH[(1)]	
TopNotch	Acetochlor	herbicide	Polyurea	-NH-CO-NH-	-CONH-	-
					(C)NH[(1)]	

[(1)] Parallel work [7]

3.3.2 Results of the GC-Flory EoS model extension

In this section the new groups resulting from the extension of the GC-Flory EoS group parameter table are presented together with their corresponding parameters, both pure component and mixture, in Table 3.8 and Table 3.9, respectively.

As mentioned in section 3.3.1 the parameters for each group have been estimated from data of low molecular weight compounds, that is, no polymers are used within the parameter estimation procedure. In some cases the parameters have not been estimated (indicated by n/a in the tables) due to the lack of (enough) experimental mixture data of low molecular weight systems.

Table 3.8: Group R_n, Q_n and C values of the GC Flory EoS for the new group

Main group	**Subgroup**	R_n	Q_n	$C_{T0,n}$	$C_{T,n}$	C_n^0
aC-O	aC-O	0.6091	0.36	-0.2303	-201.8	-0.9068
aC-OH	aC-OH	0.8952	0.68	-0.2628	-133.5	0.1161
Cl-(C=C)	Cl-(C=C)	0.791	0.724	-0.1804	-5.7	0
CCN	CH_3CN	1.8701	1.724	0. 2479	-1.147	0
	CH_2CN	1.6434	1.416	0.1967	-1.147	0
	CHCN	1.416	1.104	0.1754	-1.147	0
	CCN	1.885	0.876	n/a	n/a	n/a
CF_2	CF_3	1.406	1.38	-0.3301	22.4	0
	CF_2	1.0105	0.92	0.182	22.4	0
CONH	CONH	1.3039	1.036	2.24	251.7	-0.9855

In order to ensure the applicability of these parameters when the systems involve polymers, they need to be tested for their performance in solvent-polymer systems for which experimental mixture data is available for compounds including the new groups.

In this work the compounds (i.e. solvent) of interest are the pesticide active ingredients for which no activity coefficient data is available in polymers. On the other hand, experimental data is available of infinite dilution activity coefficients of low molecular weight compounds (solvents) in polymers (Hao et al. (1992) and Danner and High (1993)), where the groups of interest (new groups) are present, either in the solvent or in the polymer. These data have therefore been used to compare with the estimations from the GC-Flory EoS model with the new parameters. An analysis of the results from these tests is provided within this section.

The first three groups presented (aCO, aCOH and Cl-(C=C)) are analysed together (section 3.3.3) given the small amount of experimental data available for the tests. The remaining groups are discussed separately given that more extensive tests could be performed that provide insights on the reliability of the estimated parameters.

The results of the test with polymer data are analysed through average de-

Table 3.9: Group-Interaction Parameters ϵ_{mm} and ϵ_{mn}, Calories/q-unit

	aC-O	aC-OH	Cl-(C=C)	CCN	CF_2	CONH
CH_2	928.8	306.9	6.881	84.35	24.94	55.62
aCH	970.7	282.9	-4.643	45.94	17.64	60.72
CH_2CO	732.8	-356.9	-41.85	-23.11	-99.63	-61.33
COO	-2638	-390.5	5.956	-46.83	-169.3	-207.7
COOH	239.9	-173.1	86.13	85.99	347.8	n/a
CH_2O	n/a	n/a	-112.8	28	-154.8	156.2
C=C	1153	232.8	-55.14	23.29	1.959	5.828
CCl	293.2	246.8	156.2	-12.04	144.8	n/a
CCl_2	n/a	n/a	n/a	-18.04	n/a	618.1
CCl_3	n/a	n/a	n/a	-26.89	n/a	-506.6
CCl_4	n/a	214.3	-4.14	53.7	n/a	n/a
ACCl	456.8	-395.1	n/a	57.34	22.58	n/a
CH_3OH	662.9	-227.3	89.48	41.35	n/a	-699.5
OH	-1038	n/a	231	217.4	-20.8	n/a
H_2O	n/a	566	n/a	179	566.9	-494.9
aC-O	-611.8	1261	4.36	730.9	n/a	n/a
aC-OH		-1336	n/a	n/a	n/a	n/a
Cl-(C=C)			-631.9	32.21	-22.3	-110.8
CCN				-1201	n/a	-124.1
CF_2					-344	n/a
CONH						-4213
(C)3N				-117.7	n/a	n/a
(C)NH				n/a	n/a	n/a
CNH_2				24.3	n/a	n/a

viations from the experimental data in relative (AAD%, see Eq. 3.13) and absolute (Abs, see Eq. 3.14) terms, where N corresponds to the number of systems for which experimental data was available. The temperature range of the experimental polymer data is also provided.

$$AAD\% = \frac{1}{N}\sum_{i}^{N}\frac{\left|\Omega^{\infty}_{1,i,pred} - \Omega^{\infty}_{1,i,\mathrm{exp}}\right|}{\Omega^{\infty}_{1,i,\mathrm{exp}}} * 100 \tag{3.13}$$

$$Abs = \frac{1}{N}\sum_{i}^{N}\left|\Omega^{\infty}_{1,i,pred} - \Omega^{\infty}_{1,i,\mathrm{exp}}\right| \tag{3.14}$$

Note that one of the new groups, aCOH, is not commonly found in pesticide molecules but its inclusion is necessary as it often appears in the mixture experimental data used for estimating other group parameters (aCO), thus the aCOH parameters are required as intermediates to obtain other parameters. This is the case of 2-methoxy phenol. It is also important to note that all

the experimental data available for polymer systems (and therefore used in the polymer tests) is at infinite dilution concentrations of the solvent. The estimation of activity coefficients is usually expected to be better in the non-dilute regions (as mentioned in section 3.2.2).

3.3.3 New groups: aC-O, aC-OH and Cl-(C=C)

In this subsection the analysis of the reliability of the parameters estimated is presented for the first three new groups. In the first place the temperature range of validity of the pure component parameters (Table 3.8) is indicated in Table 3.10 for each of them. The numerical results of the tests with polymer systems are given in Tables 3.11 to 3.13.

Table 3.10: Temperature range of validity for the pure component parameters of each group

Main group	Subgroup	T (K)
aC−O	aC−O	293.15 − 473.15
aC−OH	aC−OH	323.15 − 453.15
Cl−(C=C)	Cl−(C=C)	273.15 − 373.15

Table 3.11: Group-Interaction Parameters ϵ_{mm} and ϵ_{mn}, Calories/q-unit

	aC-O	**Polymer test**		
		N	**AAD (%)**	**Abs**
CH_2	928.8	5	40.2	5.33
aCH	970.7	20	12.96	0.72
CH_2CO	732.8	1	20.22	1.36
COO	-2638	n/a	-	-
COOH	239.9	n/a	-	-
CH_2O	n/a	n/a	-	-
C=C	1153	n/a	-	-
CCl	293.2	n/a	-	-
CCl_2	n/a	n/a	-	-
CCl_3	n/a	n/a	-	-
CCl_4	n/a	n/a	-	-
ACCl	456.8	1	34.32	1.61
CH_3OH	662.9	n/a	-	-
OH	-1038	n/a	-	-
H_2O	n/a	n/a	-	-
aC-O	-611.8			
	Total	27	19.97	-
T =	423.7-513 K			

Table 3.12: Group-Interaction Parameters ϵ_{mm} and ϵ_{mn}, Calories/q-unit

	aC-OH	**Polymer test**		
		N	**AAD (%)**	**Abs**
CH_2	306.9	3	30.74	1.94
aCH	282.9	n/a	-	-
CH_2CO	-356.9	n/a	-	-
COO	-390.5	3	7.92	0.2
COOH	-173.1	n/a	-	-
CH_2O	n/a	n/a	-	-
C=C	232.8	n/a	-	-
CCl	246.8	2	41.38	4.3
CCl_2	n/a	n/a	-	-
CCl_3	n/a	n/a	-	-
CCl_4	214.3	n/a	-	-
ACCl	-395.1	n/a	-	-
CH_3OH	-227.3	n/a	-	-
OH	n/a	n/a	-	-
H_2O	566	n/a	-	-
aC-O	1261	n/a	-	-
aCOH	-1336			
	Total	8	25.09	
T	373.15-463 K			

From Tables 3.11 to 3.13 it can be observed that, even though the amount of parameters that have been estimated is fairly high, relatively few of them can actually be tested against experimental data of polymer systems (due to the lack of the same). The results of the polymer tests are satisfactory for those group parameters for which more data is available to compare with. In some cases (such as CCl - Cl-(C=C)) the results of the polymer test are not good, but given the little amount of data available, no final conclusions can be made. This applies also in general to the aCOH group parameters.

These results are better analysed graphically through Fig. 3.3, where the experimental and predicted values for polymer-solvent systems including these three groups have been plotted together. In this plot, the diagonal is shown since it represents the points where the experimental and estimated values are identical. Then, the points below the diagonal indicate underprediction by the model, while those above the line indicate overpredictions. This representation gives a very clear picture of the performance of the model.

Table 3.13: Group-Interaction Parameters ϵ_{mm} and ϵ_{mn}, Calories/q-unit

	Cl-(C=C)	**Polymer test**		
		N	**AAD (%)**	**Abs**
CH_2	6.881	n/a	-	-
aCH	-4.643	5	30.54	1.18
CH_2CO	-41.85	n/a	-	-
COO	5.956	2	22.53	0.7
COOH	86.13	n/a	-	-
CH_2O	-112.8	13	41.61	0.75
C=C	-55.14	n/a	-	-
CCl	156.2	2	74.05	3.12
CCl_2	n/a	n/a	-	-
CCl_3	n/a	n/a	-	-
CCl_4	-4.14	n/a	-	-
ACCl	n/a	n/a	-	-
CH_3OH	89.48	n/a	-	-
OH	231	n/a	-	-
H_2O	n/a	n/a	-	-
aC-O	4.36	n/a	-	-
aCOH	n/a	n/a	-	-
Cl-(C=C)	-631.9			
(C)3N	n/a	n/a	-	-
CNH	n/a	n/a	-	-
CNH_2	n/a	n/a	-	-
	Total	22	31.41	
T	298.15-502.58 K			

From Fig. 3.3 it is observed that the model, generally slightly underpredicts the values of the infinite dilution activity coefficients, while only a few cases are overpredicted. The results can be considered acceptable for the purposes of this work, due to the qualitatively good accuracy of the predictions (majority of points near the diagonal, and the scatter is not very large), and also taking into account that all the comparisons are made at infinite dilution concentrations, where the model is not expected to have an optimal performance. The compounds involving the aromatic ether group (aCO) were originally described by the aliphatic ether group (CH_2O). The introduction of this new aCO group represents a significant improvement in the activity coefficient estimations for this type of compounds. This will be presented in section 3.4.

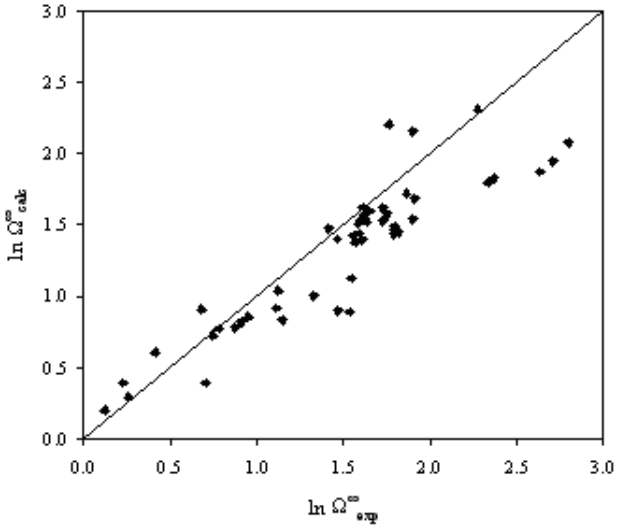

Figure 3.3: Comparison of experimental and predicted data for polymer systems. Compounds containing the groups aCO, aCOH and Cl-(C=C).

3.3.4 New group: CC≡N

In this section the results from the polymer tests for the nitrile group are presented. It is worth mentioning that from the UNIFAC group definitions (Fredenslund et al. [14]) this main group is constituted by four different subgroups, but in this work one of them is not considered for the parameter estimation, that is, the CC≡N, given that absolutely none of the required experimental data has been found in the literature including this subgroup. The pure component parameters for this group (Table 3.8) are valid for the range of temperatures from 273 to 433 K. In Table 3.14 the interaction parameters for this main group are given together with the results from the test with polymer systems where the new parameters have been applied. The range of temperatures of the polymer systems used for the tests is 323.15 - 502.58 K.

Table 3.14: Group-Interaction Parameters ϵ_{mm} and ϵ_{mn}, Calories/q-unit

	CCN	**Polymer test**		
		N	**AAD (%)**	**Abs**
CH_2	84.35	4	> 100	-
aCH	45.94	28	23.57	8.9
CH_2CO	-23.11	3	15.22	1.22
COO	-46.83	42	22.6	2.97
COOH	85.99	n/a	-	-
CH_2O	28	23	73.81	3.14
C=C	23.29	4	81.31	22.35
CCl	-12.04	11	32.2	6.63
CCl_2	-18.04	3	30.7	1.4
CCl_3	-26.89	3	53.28	2.19
CCl_4	53.7	n/a	-	-
ACCl	57.34	3	40.17	1.83
CH_3OH	41.35	1	16.07	3.47
OH	217.4	1	78.1	32.8
H_2O	179.0	n/a	-	-
aC-O	730.9	n/a	-	-
aCOH	n/a	n/a	-	-
Cl-(C=C)	32.21	n/a	-	-
(C)3N	-117.7	n/a	-	-
CNH	n/a	n/a	-	-
CNH_2	24.3	n/a	-	-
CCN	-1201			
Total[(1)]		118	37.05	5.18

[(1)]Neglecting the CH_2 and OH results.

Regarding the polymer systems studied, it is worth mentioning that in some cases (concerning the groups CH_2O and CCl_3) the number-average molecular weight of the polymer (Mn) is not provided in the experimental data. In these cases the viscosity-average molecular weight (Mv, for the CH_2O compounds) and weight-average molecular weight (Mw, for the CCl_3 compounds) have been used respectively, which can be the cause of the high errors reported in the activity coefficient calculations. With respect to the results involving CH_2 group alone (systems involving alkanes in Polyacrylonitrile), these appear to be significantly wrong. The reason for these results can be found in the very high values for the activity coefficient (Ω^{∞}), that is the high non-ideality of the systems. It has been shown (Kontogeorgis [36]) that these systems are very difficult to predict with UNIFAC-based models. Besides that, the CH_2-CCN interaction parameter takes part in most of the other tests presented in Table 3.14, where good results have been obtained. Therefore the previous three points are not considered an indication of non-reliability of this parameter. Another point

to be mentioned is the high deviations obtained in the systems including the CCN-C=C interaction parameter, this can be due to:

i) the experimental data used in the parameter estimation (for this group) has a very limited temperature range, causing problems when the calculations are performed out of this range, as is the case for the polymer systems.

ii) the fact that the subgroup CH=CH is not part of the compounds used in the estimation procedure but on the other hand it appears in the polymer systems used in the tests, but it is not well represented here by the main group parameter.

Finally, the bad results of the systems including the parameter CCN-OH are not considered of importance given that a single data point is available, so the results are not representative.

To conclude this subsection, the experimental and estimated values of the activity coefficients are compared in Fig. 3.4. From this plot the results are considered satisfactory given that all the points (except for the three mentioned systems involving only CH_2-CCN) are located close to the diagonal, without much scattering, which implies that the experimental and predicted values are close to each other. No indication of over- or under-predictive tendencies can be observed from the plot.

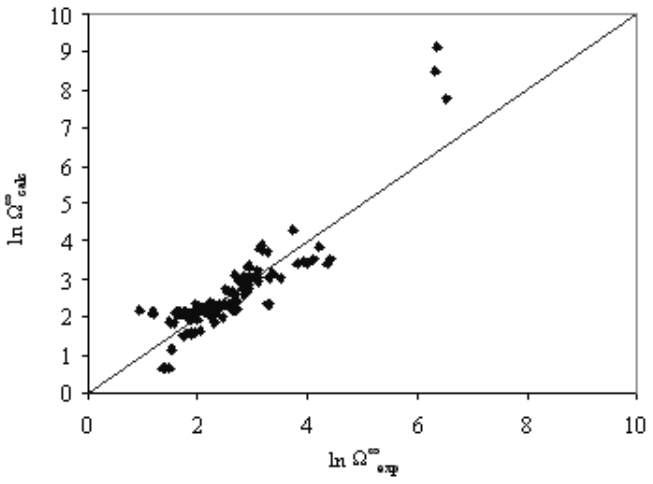

Figure 3.4: Comparison of experimental and estimated values for polymer systems (compounds containing the the CCN group).

3.3.5 New group: CF_2

In this part the tests with polymer systems involving the fluoride group are presented. The pure component parameters for this group (Table 3.8) are

valid within the range of temperatures from 253.15 to 353.15 K. It is worth noting here, that in UNIFAC the CF_2 main group is used to represent, not only linear compounds but also fluoride groups attached to a cyclic carbon, like in octafluorocyclobutane. In this work this has been modified given that the inclusion of cyclic compounds in the parameter estimations caused large deviations, therefore these compounds were excluded and cannot, in principle, be represented with the CF_2 main group presented here.

The interaction parameters estimated for this group are provided in Table 3.15 together with the results of their testing with systems involving polymers, within the range 343.15 - 493.15 K. In this specific case the two sources of data for these polymer systems (Hao et al. [51] and Danner and High [17]) do not entirely agree in the values reported for the infinite dilution activity coefficients and therefore the values of the deviations are reported for both of them, for the DECHEMA (Hao et al. [51]) data set at first, and in parentheses for the HPST (Danner and High [17]) data set.

Table 3.15: Group-Interaction Parameters ϵ_{mm} and ϵ_{mn}, Calories/q-unit.

	CF_2	**Polymer test**		
		N	**AAD (%)**	**Abs**
CH_2	24.94	56 (71)	65.02 (82.09)	87.31 (124.9)
aCH	17.64	11	21.6 (36.32)	3.72 (7.26)
CH_2CO	-99.63	11 (7)	63.07 (31.8)	4.95 (2.6)
COO	-169.3	44 (24)	18.48 (31.73)	1.01 (4.3)
COOH	347.8	-	-	-
CH_2O	-154.8	1 (with CH_2O)	27.7	0.47
C=C	1.959	n/a	-	-
CCl	144.8	n/a	-	-
CCl_2	n/a	n/a	-	-
CCl_3	n/a	n/a	-	-
CCl_4	n/a	n/a	-	-
ACCl	22.58	1	2.28	0.25
CH_3OH	n/a	n/a	-	-
OH	-20.8	12	33.8	2.5
		2 (with COO)	*185.96*	*10.4*
H_2O	566.9	n/a	-	-
aC-O	n/a	n/a	-	-
aCOH	n/a	n/a	-	-
Cl-(C=C)	-22.3	n/a	-	-
(C)3N	n/a	n/a	-	-
CNH_2	n/a	n/a	-	-
CCN	n/a	n/a	-	-
CF_2	-344			
Total (DECHEMA)(*)		70	31.5	1.97
Total (HPST) (*)		55	32.58	5.26

(*) Neglecting the CH_2 results.

From the tests done in polymer systems the following points need to be discussed:

i) The estimation of activity coefficients of systems involving alkanes and PVDF are significantly wrong. Given that the number of systems involved is very high, this is further studied in section 3.3.6.

ii) For two systems involving the OH-CF_2 and COO-CF_2 parameters (marked in italics in the table) the estimations are not accurate. But only two points are tested, while the OH-CF_2 parameter has been used for the test in twelve other systems providing satisfactory results, therefore the inaccurate results can be neglected.

iii) The COOH-CF_2 parameter cannot be used for systems containing 2 COOH groups (one in each of the compounds of the binary).

Again the results of the polymer tests are illustrated graphically through the plot of the experimental values against the predicted ones in Fig. 3.5. From the plot it can be observed that while most of the points are close to the diagonal, some of the systems are underpredicted, these are the alkanes-PVDF sytems mentioned above that will be discussed separately. Otherwise the results are considered satisfactory.

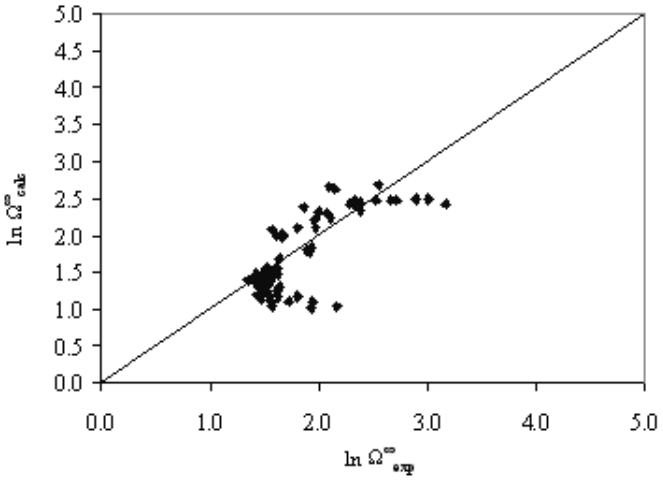

Figure 3.5: Comparison of experimental and estimated values for compounds including the CF_2 group.

3.3.6 Further analysis of the systems with very bad performance (CF_2): Alkanes - PVDF

i) Analysis of the experimental data

The first problem encountered when dealing with these systems is related to the experimental data given that the two sets available provide different values of the activity coefficients at infinite dilution. A comparison between the two sets is shown in Fig. 3.6 which includes the alkanes from n-pentane to n-dodecane, and n-tetradecane. The diagonal indicates the line where the values of the two sets would be identical and therefore it highlights the differences in the values from the two sets of data.

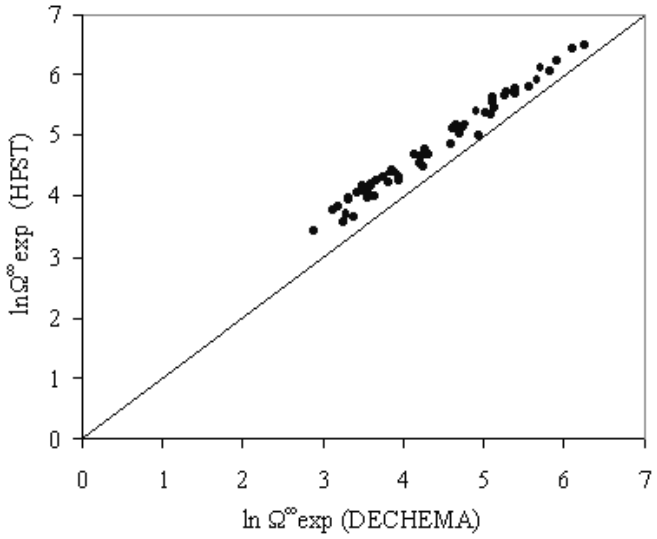

Figure 3.6: Comparison of the experimental data sets from DECHEMA and from HPST for activity coefficients at infinite dilution of alkanes (from n-pentane to n-dodecane, and n-tetradecane) in PVDF at different temperatures (•). Solid line indicates the diagonal.

ii) Performance of the GC-Flory EoS with each of the data sets

The estimation of activity coefficients with GC-Flory EoS, for the systems involving alkanes and PVDF are significantly wrong. The reason for these bad results can be found in the very high values for the activity coefficient (Ω^{∞}) that is, the high non-ideality of the systems. It has been shown (Kontogeorgis [36]) that these systems are very difficult to predict with UNIFAC-based models, they cannot be represented as it will be shown in the following section.

iii) Analysis of the same systems with GC-Flory EoS and other UNIFAC-based thermodynamic models: UNIFAC-FV and Entropic-FV.

A comparison of the experimental data with those estimated with each of the three chosen models for this analysis is highlighted in Fig. 3.7. The comparison is shown with only one of the data sets since the trend of the deviations between experimental and calculated data is equivalent for the two sets of experimental data with the models.

As observed from Fig. 3.7, the predictions from Entropic-FV and GC-Flory EoS are equivalent with respect to the behaviour of the deviations from the experimental data. For the GC-Flory EoS, as the activity coefficient values increase, the predicted ones seem to give a constant value, underpredicting in

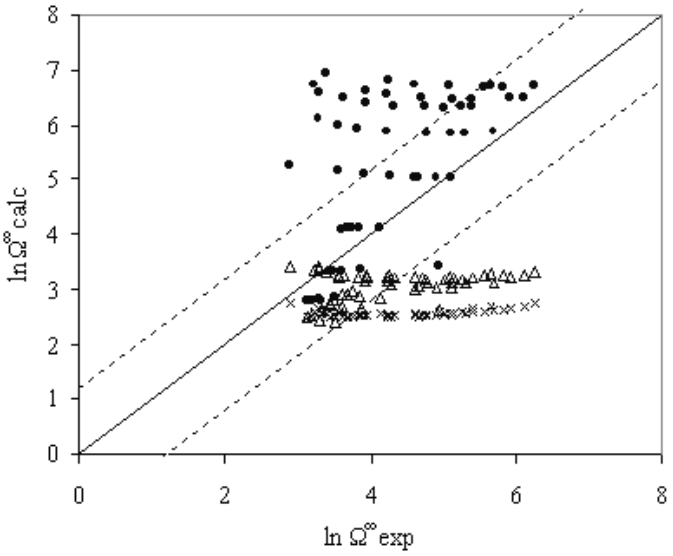

Figure 3.7: Experimental data from DECHEMA. (•) UNIFAC-FV, (△) Entropic-FV, (x) GC-Flory EoS, (- - -) range of confidence, 15%.

almost all the cases, while those of UNIFAC-FV are spread and in the majority of the cases overpredict the experimental values. Therefore the Entropic-FV and GC-Flory EoS models will be analysed together and the UNIFAC-FV separately. The fact that these systems cannot be represented by UNIFAC-based models in general has now been proven given that the models perform equally bad (represented by the values outside the range of confidence). This indicates that the problem does not lie on the value for the estimated parameter but on the systems and the model. A further analysis is though provided in order to evaluate where each of the models is more reliable for this type of systems.

a) Analysis of UNIFAC-FV performance

In Fig. 3.8 the same systems discussed previously are plotted but only the values predicted with UNIFAC-FV are compared with the experimental values. A distinction is made between the alkanes smaller or equal to n-octane, and those larger than that. This is an interesting observation given that the deviations from the experimental data are much smaller for the higher alkanes. This is related to the fact that the experimental values of the infinite dilution activity coefficient increase with increasing the number of carbons in the alkane. As mentioned before, this model tends to overpredict the activity coefficients, therefore, as these values increase (with increasing number of carbons), the deviations are reduced. At the same time, the activity coefficient values predicted by the model decrease significantly with an increase of temper-

ature, thus becoming closer to the experimental values that are less dependent on temperature. This is why the deviations of the model are smaller at high temperatures, when the system is closer to ideality.

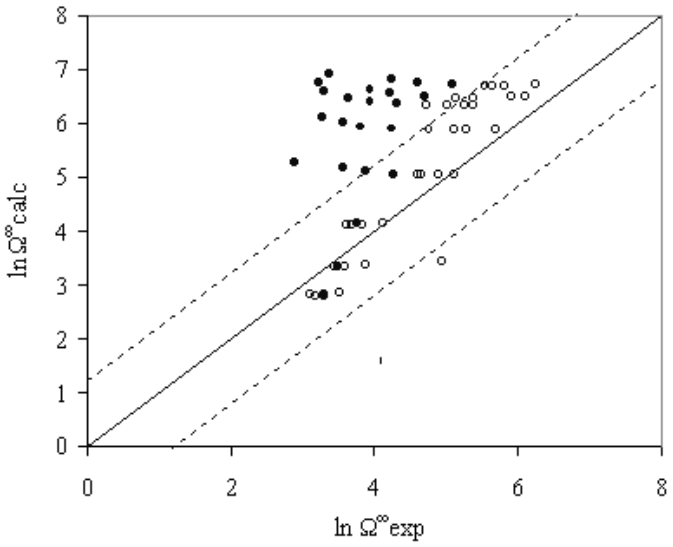

Figure 3.8: (•) Small alkanes (From pentane to octane), (○) Big alkanes (from nonane to dodecane, and tetradecane).

b) Analysis of Entropic-FV and GC-Flory EoS performance

In this case the predictions of the two models have been compared with experimental data and plotted together in Fig. 3.9 for all the systems. The range of confidence has been extended to 25% (the original being 15%) given the bad performance of the models. As it can be seen in Fig. 3.9(a) many of the points are still outside the range of confidence, these correspond to the systems of larger alkanes (from octane and larger) and low temperatures ($T < 448.15K$). Therefore, in the other figure (Fig. 3.9(b)) these values have been removed. Summarizing, in this case the performance of the models is good for the lower alkanes, and also for the larger alkanes at high temperatures ($T \geq 448.15K$). In these cases the situation is the opposite compared to the UNIFAC-FV, because these models tend to underpredict the activity coefficients. The calculated values are almost constant with temperature while the experimental ones decrease with temperatures, thus the values get closer at high temperatures, which is also the range where the system is less non-ideal.

To conclude, the performance of three different UNIFAC-based models has been analyzed for the systems involving alkanes and PVDF. The performance of

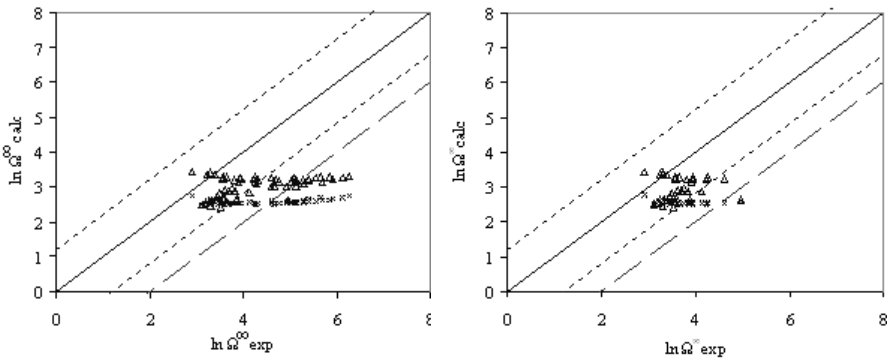

(a) All data (all alkanes at all temperatures) (b) All alkanes, the ones greater than octane (this included), at T=448.15 K.

Figure 3.9: (△) Entropic-FV, (x) GC-Flory EoS.

the models is in general inaccurate, but it improves in some specific situations. UNIFAC-FV provides slightly better predictions of the activity coefficients for larger alkanes and high temperatures, while the other two models (Entropic-FV and GC-Flory EoS) are better for smaller alkanes, but also at high temperatures.

3.3.7 New group: CONH

The last group introduced in this model extension is the CONH. The pure component parameters given at the beginning of this section (Table 3.8) are valid for temperatures between 303 and 463 K. In this section the objective is to present the results from the tests with polymer systems done to analyze the reliability of the parameters. The experimental data available is that reported by Newman and Prausnitz [52] for the activity coefficients of several compounds in the polyamide Epotuf 37-612. The specific structure of this polymer and its molecular weight is though not provided. This presents a difficulty in the estimation of the activity coefficients through the model. Epotuf polymers are obtained from fatty acids they are therefore, in principle, constituted by a linear chain, without phenyl groups. Based on this, the chemical structure of this polymer is assumed as that of Nylon 6 in order to perform the calculations with the model. With respect to the molecular weight of the polymer, a high value is assumed (Mw = 1.8×10^7) given that at high molecular weights the activity coefficient values become independent of the polymer molecular weight, and therefore this will not affect the calculations. These experimental data cover the range of temperatures from 348.15 to 473.15 K. A few more experimental data are available from Bonifaci and Ravanetti [53] for systems consisting of aromatic compounds in Nylon 6, within the range of temperatures from 523 to 563 K. The numerical results of the tests with the mentioned polymer data are provided in Table 3.16.

Table 3.16: Group-Interaction Parameters ϵ_{mm} and ϵ_{mn}, Calories/q-unit.

	CONH	**Polymer test**		
		N	**AAD (%)**	**Abs**
CH_2	55.62	n/a	-	-
aCH	60.72	23	29.76	2.48
CH_2CO	-61.33	13	38.69	3.35
COO	-207.7	n/a	-	-
COOH	n/a	n/a	-	-
CH_2O	156.2	12	26.31	2.27
C=C	5.828	n/a	-	-
CCl	n/a	n/a	-	-
CCl_2	618.1	n/a	-	-
CCl_3	-506.6	6	88.9	1.93
CCl_4	n/a	n/a	-	-
ACCl	n/a	n/a	-	-
CH_3OH	-699.5	n/a	-	-
OH	n/a	n/a	-	-
H_2O	-494.9	n/a	-	-
aC-O	n/a	n/a	-	-
aCOH	n/a	n/a	-	-
Cl-(C=C)	-110.8	n/a	-	-
(C)3N	n/a	n/a	-	-
CNH	n/a	n/a	-	-
CNH_2	n/a	n/a	-	-
CCN	-124.1	7	71.57	10.65
CF_2	n/a	n/a	-	-
CONH	-4213			
	Total[(1)]	55	36.44	3.68

[(1)]Neglecting the CCl_3 results.

As can be extracted from the table, very few of the group parameters can actually be tested given the reduced amount (or variety) of measured data containing the CONH group. In general terms, the results are considered satisfactory with the exceptions of the CCl_3 and CCN group parameters where high deviations from the experimental data are observed. In the case of CCl_3, the high values of the relative deviation are partially due to the very small values of the activity coefficients, while the absolute deviations are actually small. It is difficult to extract any final conclusions given the assumptions that have been made (polymer structure and molecular weight) in order to do the model calculations, so the parameter values are kept and further testing is encouraged if more experimental data becomes available.

Finally, the comparison of experimental and predicted activity coefficient

values is illustrated in Fig. 3.10. Here it is clearly observed that the model underpredicts the activity coefficient values for all the systems included in this study. The values are though close to the diagonal and not scattered, with the exception of the bad results involving the CCN group parameter (CCl_3 systems not represented). The fact that all the predictions present the same deviation from the experimental data indicates that if the actual structure of the polymer was known and used for the model estimations, possibly better results could be obtained.

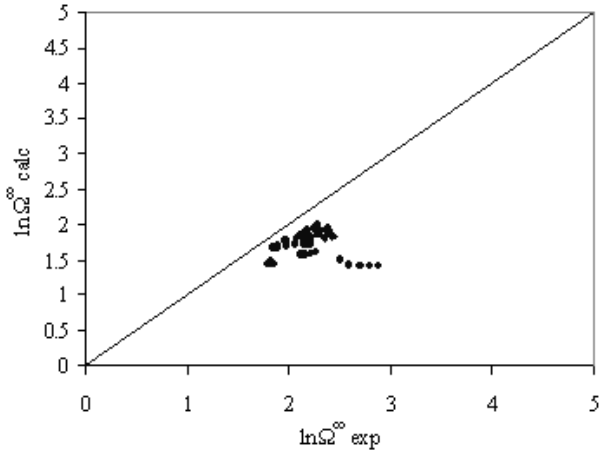

Figure 3.10: Comparison of experimental and estimated values for compounds including the CONH group.

3.4 Improvements of the model and further studies

3.4.1 Improvements in the aromatic ether group

The new estimated parameters have been evaluated for aromatic ethers, given that a better representation of these compounds has been achieved with one of the new groups. Some aromatic ethers could be represented already with the original parameter table (Bogdanic and Fredenslund [32]), through the ether group (CH_2O), but now they can also be described with the new 'aromatic-ether' group (aC-O), and the results of the activity coefficient estimation are considerably better. Table 3.17 shows both the relative (AAD%) and absolute errors (Abs) obtained from estimating the infinite dilution activity coefficients of 20 systems consisting of Anisole in Polystyrene (experimental data from DECHEMA, Hao et al. [51]), where Anisole can be represented with the

CH_2O group from Bogdanic and Fredenslund [32] (a), or with the aCO group presented in this paper (b) (see Table 3.17).

Table 3.17: Group description and error comparison with the two different sets of parameters

	error in Ω^{∞}		Group description
	AAD (%)	Abs.	
(a) OLD	40.13	2.1	1 CH_3O, 1 AC, 5 ACH
(b) NEW	14.76	0.78	1 CH_3, 5 ACH, 1 aC-O

In Fig. 3.11 the logarithm of the experimental activity coefficients versus the logarithm of the predicted values is shown for both possible group representations (a) and (b). The dotted lines are drawn to show the delimitation of the range of confidence. The diagonal line is shown to help the analysis of the results, where the points over the diagonal are over predictions of the model, while the ones below are under prediction of the experimental results.

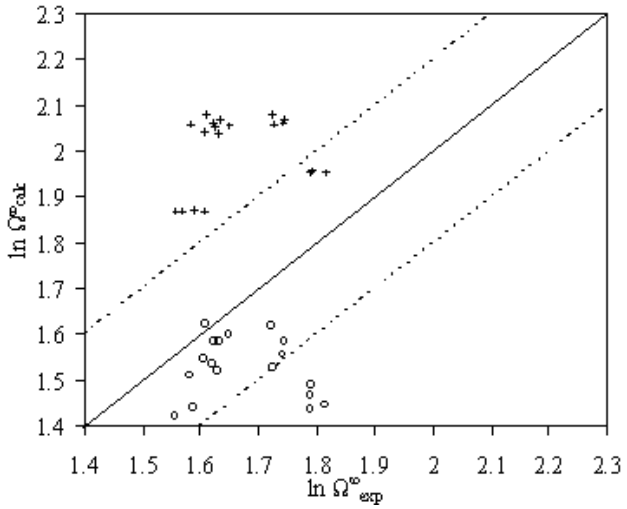

Figure 3.11: Comparison of estimated of solvent-polymer activity coefficients with the two different sets of parameters. (+) Old groups (a); (o) New groups (b). Range of confidence (- - -). Outliers: PS (Mw=4000). Range of confidence considered: 7%.

In case (a) the majority of the points fall outside the range of confidence while for (b), there are only a few points that are not within this range. These points are outliers, according to an analysis of the experimental data, as can be seen in Fig. 3.12.

In the figure above, the experimental data for the Polystyrene with Mw = 4000, is observed to be much higher than the rest, even though the molecular

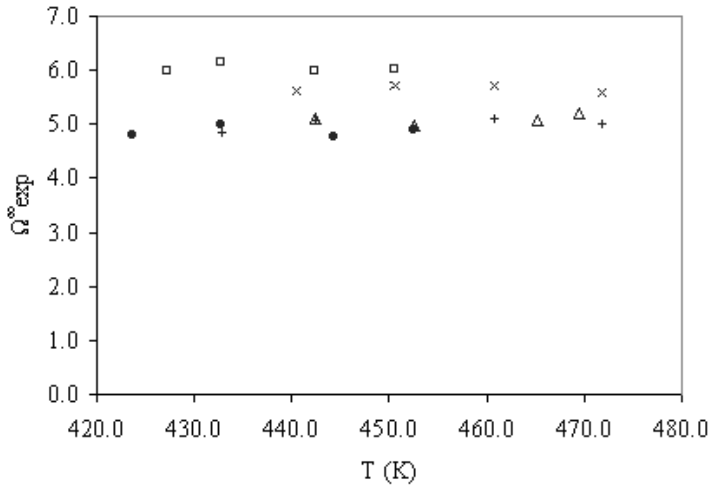

Figure 3.12: Plot of the experimental infinite dilution activity coefficients as a function of temperature for Anisole-Polystyrene, for different molecular weights of the polymer: (•) Mw=2200; (□) Mw=4000; (△) Mw=17500; (x) Mw=107000; (+) Mw=1800000.

weight is significantly lower, while the rest of the data lie approximately in the same range of values for the activity coefficients.

Summarizing, as observed from both the table and the figure, the improvement is remarkable when representing the anisole with the new aromatic ether (aC-O) group.

3.4.2 Alkanes-Polystyrene systems study

Introduction

In this section the performance of the GC-Flory EoS model is analysed for alkane-polystyrene systems. In addition, results from other models UNIFAC-FV (Oishi and Prausnitz [28]) and PC-SAFT (Gross et al. [54] and Gross et al. [55]) have also been compared. It appears that the GC-Flory EoS model is unable to represent the experimental data with the parameters estimated from low molecular weight compounds. The UNIFAC-FV and the PC-SAFT (without any interaction parameters) did not perform very well either. Using, however, some of the polymer data to re-estimate the group parameters (of ACH), it was possible to represent the infinite dilution data). It is not clear, however, if these parameters would be valid for other applications. More work is needed to establish this. The details of this study are given below.

Tests with alkane-PS systems:

The GC-Flory EoS model has now been tested with alkane-polystyrene systems for which it is observed that the temperature dependence of the activity coefficients cannot be reproduced by the model. It is in fact opposite to that of the measured data, as shown in Fig. 3.13.

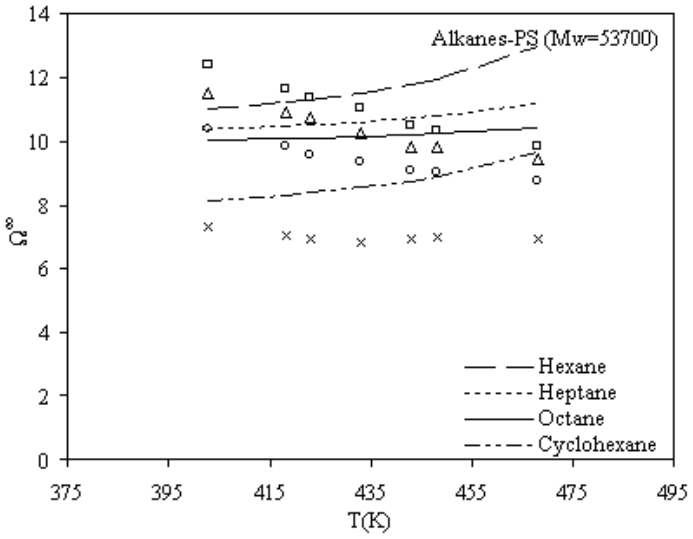

Figure 3.13: Comparison of experimental and estimated (with GC-Flory EoS) values of infinite dilution activity coefficients as a function of temperature. Experimental data from (Hao et al. (1992)): (□) Hexane, (△) Heptane, (o) Octane, (x) Cyclohexane.

In order to evaluate this problem some systems with the same constituting groups (aCH, CH_2) but where these are present either in the polymer or in the solvent (i.e. alkanes-PE, aromatics-PS and aromatics-PE) have been tested with the objective to find out if it is a general problem of the interactions of these two groups. The results of this test are shown in Fig. 3.14, where it can be observed that the estimations are very bad when the ACH group is part of the polymer repeat unit but not when it is part of the solvent. The analysis is presented in the form of a comparison between experimental and calculated data and not as a function of temperature for clarity purposes. From this it can be concluded that this opposite temperature dependence is a specific problem of the alkanes-PS systems, i.e. presence group CH_2 in the solvent and group aCH in the polymer.

Test of infinite dilution data with other models:

These problematic systems have been tested with two other models, UNIFAC-

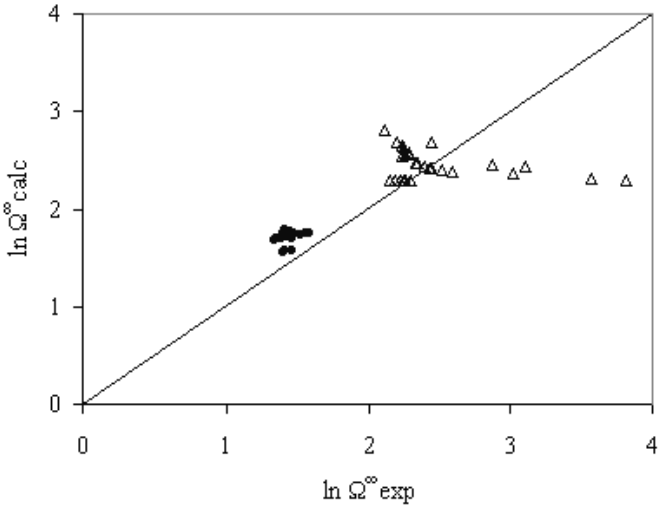

Figure 3.14: Comparison of experimental and calculated values of infinite dilution activity coefficients for the case when the ACH group is in the solvent (•) or in the polymer (△).

FV (Oishi and Prausnitz [28] with parameters reported in Danner and High [17]) and PC-SAFT (from ASPEN, with parameters from Gross et al. [54] and Gross et al. [55]), without any interaction parameter, and some of the results are presented here (Fig. 3.15).

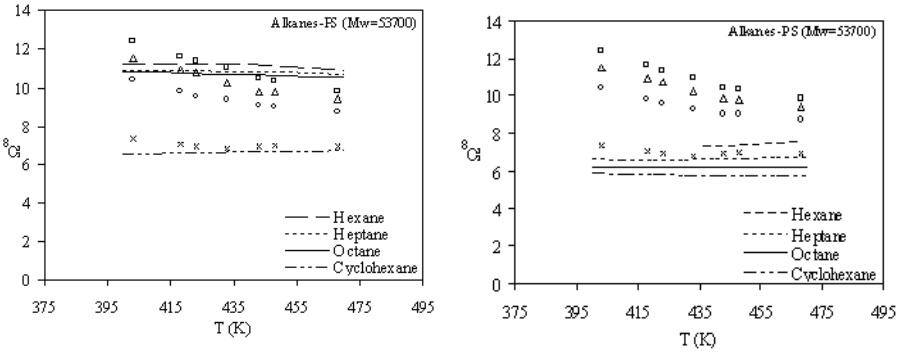

(a) Estimations with UNIFAC-FV. (b) Estimations with PC-SAFT.

Figure 3.15: Comparison of experimental and estimated infinite dilution activity coefficients. Experimental data:(□) Hexane, (△) Heptane, (○) Octane, (x) Cyclohexane.

As seen from the figure, none of these models can reproduce the temperature behaviour of the infinite dilution activity coefficients, even though the results do not present an opposed behaviour as in the GC-Flory EoS model, but very inaccurate in the case of PC-SAFT. It is important to observe that when the alkane becomes bigger (more than 9 carbon atoms), these problems with the temperature dependency are diminished, even though the activity coefficient values are still quite inaccurate.

Try to re-estimate the parameters using low molecular weight compounds:

The pure component properties of both alkanes and PS have also been tested in order to analyse if the error is due to a bad correlation of those. But this is not the case. The re-estimation of the parameters from low molecular weight compound data has been attempted but no improvements achieved.

From the experimental data available (of low molecular weight compounds) it can be observed that the activity coefficients of these systems do not have a strong temperature dependency, in fact they are almost constant with temperature, so this could be the reason why they can not represent the behaviour of the polystyrene systems.

Try to re-estimate the parameters using polymers:

After the lack of success in the previous studies, we try to assess the capabilities of the model in correlating these alkane-PS systems, by fitting part of the polymer data (heptane and nonane with PS) and estimating the rest (octane and hexane). The results are shown in Table 3.18 and Fig. 3.16.

Table 3.18: Estimated values of the parameters (systems used: nonane, heptane + PS)

ACH-ACH	ACH-CH_2	$C_{T0,n}$(ACH)	$C_{T0,n}$(AC)	$C_{T,n}$	C_n^0
-264.2	-10.82	-0.04287	-0.03	-19.53	4.868

As seen from the Fig. 3.16, the temperature behaviour of the activity coefficients for these systems has been significantly improved with the new parameters, with respect to the original ones. In the previous correlation of the polymer data only infinite dilution data has been used in order to focus on the study of the temperature dependence. A more exhaustive study would be needed in order to obtain the final improved parameters for these systems, but this was not the purpose of this work.

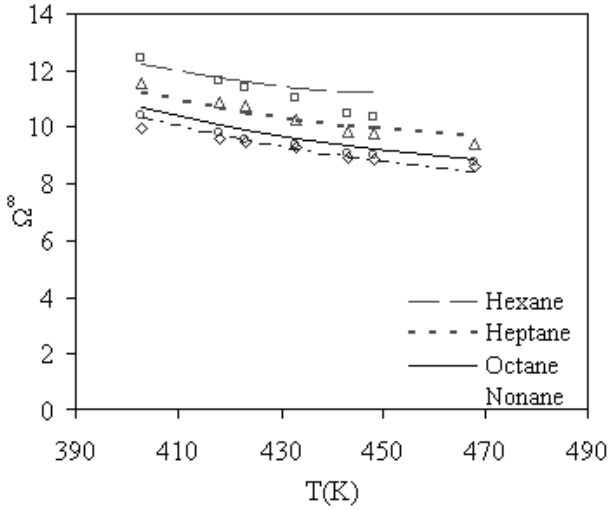

Figure 3.16: Estimation (heptane and nonane) and prediction (octane, hexane) results with the new parameters. Experimental data: (□) Hexane, (△) Heptane, (○) Octane, (◇) Nonane.

3.5 Application of the partition coefficient approach and extended model

This last section is aimed at providing some examples of, in the first place (3.5.1), the calculations of partition coefficients using the approach presented in the beginning of this chapter (section 3.1) and secondly (3.5.2), the extension of the activity coefficient model (presented in sections 3.2 and 3.3) applied to some pesticide compounds of interest.

3.5.1 Calculation of partition coefficients: comparison with available experimental data and other approaches

In this part the objective is to analyze the performance of the suggested approach for calculation of partition coefficients of Active Ingredients (AIs) between solvents and polymers by comparison with experimental data from the literature and other approaches that have been proposed.

Note that the systems of interest in this work include pesticide AIs for which no data of partition coefficients can be found in the literature. It is therefore that the approach is not tested here with pesticide AIs but with other relatively complex compounds for which measured data has been reported. This study is based on the data published by Baner et al. [1] where values of the partition coefficients have been reported for a number of flavour and aroma compounds. Baner et al. [1] applied the Regular Solution Theory (discussed in section 3.2)

with solubility parameters estimated from group-contribution methods (Hoy [57], Van Krevelen and Hoftyzer [58] and Fedors [59], [60]) to estimate the partition coefficients and compared them with the experimental data.

In this work the purely predictive approach described in section 3.1 has been applied to the same compounds. In these cases the activity coefficients of the AIs in the solvents (Methanol and Ethanol) have been estimated with two UNIFAC methods: the UNIFAC VLE - 3 param (Larsen et al. [56]) and the KT-UNIFAC (Kang et al. [15]), while the activity coefficient in the polymers have been estimated with the GC-Flory EoS model where some of the new groups (presented in section 3.3) have been used (in the compounds: Diphenyl oxide and Eugenol). These results are shown in Fig. 3.17 together with the predictive approach suggested by Baner et al. [1].

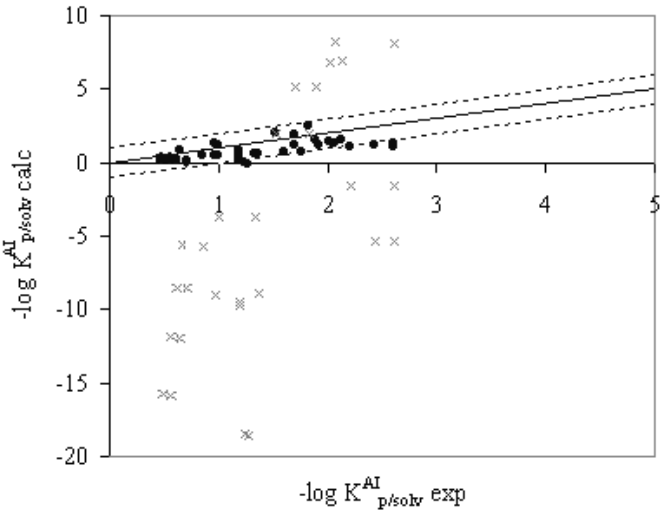

Figure 3.17: Comparison of experimental (Baner et al. [1]) and calculated values of the partition coefficient. Calculated values from: (x) Baner predictions without empirical correction; (•) Approach suggested in this work.

In Fig. 3.17, it can be observed that without use of any experimental data the improvement is very significant with respect to using the Regular Solution Theory as in Baner et al. [1] for which very bad results were originally obtained.

In Fig. 3.18 the results obtained with the approach presented in this work are plotted separately. The results with two of the models that can be used for the estimation of activity coefficients in the solvents (UNIFAC and KT-UNIFAC) are shown and similar performance is observed in the cases that can be compared.

In the mentioned reference (Baner et al. [1]), an empirical correction based on

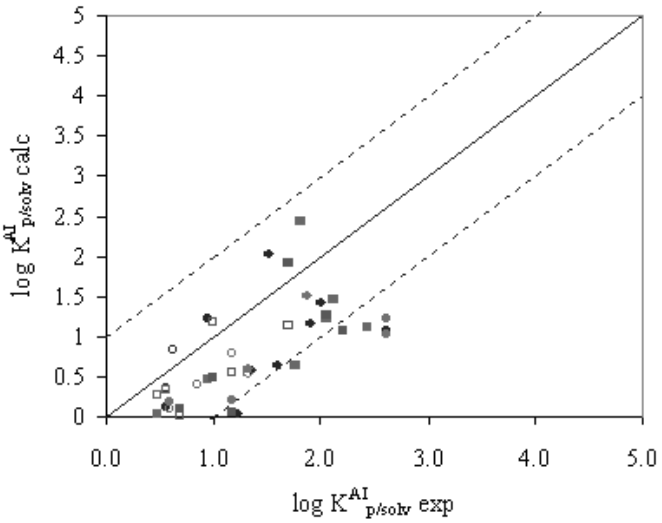

Figure 3.18: Calculated (using GC-Flory EoS, and 2 UNIFAC methods: (•,■) for UNIFAC VLE 3p (○,□) for KT-UNIFAC) and experimental Baner et al. [1] values of partition coefficients between polymer (•,○ PE and ■,■ PP) and solvent (Methanol and Ethanol).

the experimental values of the partition coefficients is introduced to reduce the high deviations obtained in the original predictions, which therefore no longer represented a predictive approach. The values obtained from this method are shown in Fig. 3.19 together with the predictions obtained from the approach of this work.

From this plot, it can be observed that the performance of Baners approach, with empirical correction is similar to the pure prediction from this work. In some cases the calculated results are very accurate (points close to the diagonal) while in others they are more imprecise (points outside the dotted lines representing the range of confidence), and this behaviour occurs with both approaches. But the most important point here is that in Baners approach the partition coefficient experimental data has been used to correct the values, while in the approach of this work the values are pure predictions, the results from this work are thus quite remarkable, given that they perform as good as an empirically adjusted model.

In this approach though, there is room for improvement in the predictions. It has originally been suggested (in the description of the approach) that in the cases where experimental data of the AI solubility in the solvents is available (common case in pesticide area) this would be used. A sample case where this can be done (with the compounds from the previous study) is that of the

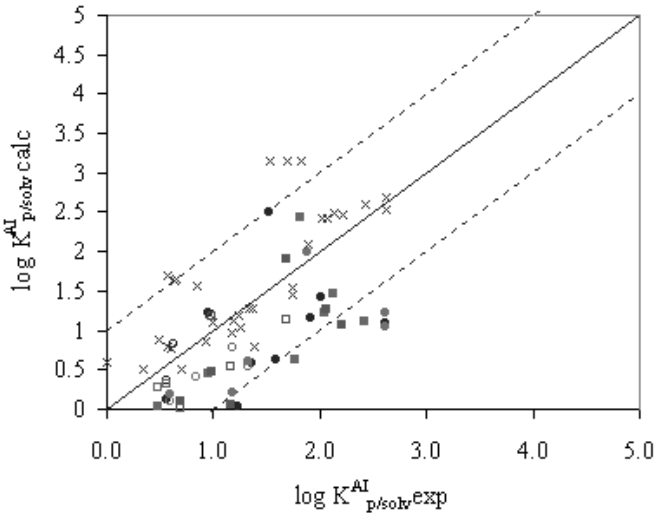

Figure 3.19: Calculated (using GC-Flory EoS, and 2 UNIFAC methods: (•,■) for UNIFAC VLE 3p (○,□) for KT-UNIFAC) and experimental Baner et al. [1] values of partition coefficients between polymer (•,○ PE and ■,■ PP) and solvent (Methanol and Ethanol). (x) Baner predictions with empirical correction.

Isoamyl Acetate partition between ethanol and polymer, given that data is available for the solubility of this compound in ethanol (Kharin et al. 1971). The results are presented in Table 3.19, where the estimated partition coefficient is compared with the experimental value reported in Baner et al. [1] and the agreement is very good. As an indication of the goodness of the prediction the calculated values from Baner et al. [1], including the empirical correction are also reported. Again the two models have a similar performance even though one of them is purely predictive (this work) and the other one makes use of experimental data of the partition coefficients.

Table 3.19: Partitioning of Isoamyl Acetate between solvent (Ethanol) and two different polymers. Comparison of estimated and experimental values.

Polymer	$LogK_{p/solv,exp}$	$LogK_{p/solv,calc}$	$LogK_{p/solv,calc}(*)$
LDPE	-1.337	-1.288	-1.276
PP	-1	-1.165	-1.102

(*) Baner, with empirical correction.

Finally to confirm the good results provided by this approach another small set of data is tested (Kydonieus [62]). In this case the solutes (or AIs) partition between water and Polyethylene (PE) at 40 °C. The activity coefficients come

from estimations (UNIFAC VLE-3p in water, GC-Flory EoS in PE). The results are shown in Table 3.20 where they are compared with the experimental data, and once again the agreement is remarkable within the two.

Table 3.20: Partitioning of different solutes (AIs) between solvent (Water) and PE. Comparison of estimated and experimental values.

AI	**CAS nr**	$\Omega^{\infty}_{\mathrm{AI,solv}}$	$\Omega^{\infty}_{\mathrm{AI,pol}}$	$\mathrm{LogK_{p/solv,exp}}$	$\mathrm{LogK_{p/solv,calc}}$
Acetophenone	98-86-2	161.62	39.63	0.5	0.61
Benzoic acid	65-85-0	42.81	5.42	0.796	0.898
4-methylacetophenone	122-00-9	273.44	25.88	1.097	1.024

3.5.2 Examples of application to systems involving pesticides

In this section the aim is to study the performance of the model presented in the previous sections (GC-Flory EoS) for the compounds of interest, that is, the pesticide AIs.

The procedure used for this purpose is the study of the solubility behaviour of pesticides in polymers in a qualitative manner, through two different models and making use of some well-known rules of thumb (Lindvig et al. [63]). The models to be used are the GC-Flory EoS model for prediction of activity coefficients at infinite dilution and the Flory-Huggins (FH) model based on the Hansen solubility parameters (including the correction proposed by Lindvig et al. [63]). Other UNIFAC-based models have been considered for purposes of comparison but the fact that some important groups (such as aCO) and interaction parameters (several of the CF_2 group) are missing for the description of these compounds, makes it difficult to obtain an accurate and complete analysis. Therefore only the results for one of the pesticides (Dimethrin) that could be fully characterized with the UNIFAC-FV model is shown for comparison. The indications obtained from the empirical rules of thumb with respect to the AI solubility in polymers are given in Table 3.21 (Lindvig et al. [63]), with respect to the infinite dilution activity coefficient values (Ω^{∞}_{AI}) and the FH interaction parameter (χ_{12}) values.

Table 3.21: Rules of thumb as indicators of solubility

Activity coefficient models	**FH parameter**	**Solublity indication**
$\Omega^{\infty}_{\mathrm{AI}} \leq 6$	$\chi_{12} \leq 0.5$	Complete miscibility
$\Omega^{\infty}_{\mathrm{AI}} > 8$	$\chi_{12} > 0.5$	Immiscibility

The study has been performed for the AIs of interest, the pyrethroid compounds and their solubility in some of the polymers commonly found in controlled release technology. The results are presented in Table 3.22 for all the

pesticides in each of the polymers, and with the mentioned calculated properties and parameters.

Table 3.22: Results of the calculations of activity coefficients (GC-Flory EoS and UNIFAC-FV model) and FH-interaction parameters for several pesticide AIs in four different polymers (T = 298.15 K).

	GC-Flory EoS		Flory-Huggins		UNIFAC-FV	
	Ω_{AI}^{∞}		χ_{12}		Ω_{AI}^{∞}	
Pesticide AI	**Polymer: PE**					
Permethrin	299.53	NS	1.46	NS		
Cypermethrin	1218.75	NS	2.06	NS		
Phenothrin	102.33	NS	1.21	NS		
Fenvalerate	1869.18	NS	1.88	NS		
Dimethrin	17.51	NS	0.85	NS	6.8071	NA
Pesticide AI	**Polymer: Nylon 6**					
Permethrin	15.7	NS	1.26	NS		
Cypermethrin	17.98	NS	1.14	NS		
Phenothrin	10.66	NS	0.9	NS		
Fenvalerate	50.48	NS	1.24	NS		
Dimethrin	8.48	NS	1.34	NS		
Pesticide AI	**Polymer: PVC**					
Permethrin	17.98	NS	1.69	NS		
Cypermethrin	10.36	NS	1.39	NS		
Phenothrin	3.97	S	2.25	NS		
Fenvalerate	0.65	S	1.65	NS		
Dimethrin	28.25	NS	1.84	NS	3.6742	S
Pesticide AI	**Polymer: PBMA**					
Permethrin	0.96	S	0.66	NS		
Cypermethrin	1.07	S	0.51	NS		
Phenothrin	0.65	S	1.06	NS		
Fenvalerate	0.7	S	0.61	NS		
Dimethrin	11.2	NS	0.78	NS	3.1198	S

S: solubility, NS: non-solubility, NA: no answer

In the light of these results the agreement between the GC-Flory EoS and the other models (mainly the FH-model) can be studied.

In the case of PE, both models predict non-solubility of all the AIs in the polymer, and in both cases Dimethrin is the compound that is closer to the solubility/non-solubility limit, having the lowest Ω_{AI}^{∞} and χ_{12} values. In this case the UNIFAC-FV does not provide an answer given that the values of Ω_{AI}^{∞} are between the two limits (6 and 8). For Nylon 6 again both models agree in the fact that none of the AIs are soluble in the polymer, and UNIFAC-FV cannot be used here given that it cannot describe this specific polymer.

The next polymer studied is the PVC, where the models do not agree any-

more. The FH-model predicts non-solubility of all the AIs in this polymer, while the GC-Flory does not. It predicts immiscibility for the first two AIs (Permethrin and Cypermethrin) and Dimethrin in PVC (like the FH-model) but for the two remaining compounds it predicts solubility, as opposed to the FH-model predictions. Here, the UNIFAC-FV is in disagreement with the other two models for the Dimethrin. The disagreement (of solubility/non-solubility) obtained from the calculations with PVC can be attributed to the fact that PVC is a polar polymer (more than the other polymers studied here) and this causes additional complications in the accuracy of the model predictions.

Finally, the solubility of the AIs in PBMA is observed. Here, the FH-model results in some values close to the limit of 0.5 (Permethrin, Cypermethrin and Fenvalerate) where the GC-Flory EoS predicts miscibility. On the other hand they agree with respect to the non-miscibility of Dimethrin, where once again UNIFAC-FV predicts the opposite behaviour.

It is worth mentioning that in the cases where the UNIFAC-FV could be used for the calculations, the prediction of the miscibility behaviour was always in disagreement with the other two models. In Lindvig et al. [63] an important number of systems were tested for which experimental data were available with respect to their solubility in polymers, and the predictions done with these three models. The conclusions of this study are that while the GC-Flory EoS and the FH models provide the most number of correct answers (regarding solubility/non-solubility), the UNIFAC-FV is the least reliable, which is in agreement with the results presented above, therefore the fact that the two other models agree is considered a good indicator of good performance in this analysis.

Summarizing, final conclusions cannot be made with respect to the qualitative prediction of solubility of pesticide AIs in polymers until some experimental data becomes available, but as stated above, the agreement between the two models is considered as an indicator of good prediction.

3.6 Conclusions

In this chapter a predictive approach has been proposed to estimate the partition coefficients of AIs between polymers and solvents that are needed in modelling of controlled release devices.

The approach makes use of activity coefficient estimations, applied to the complex and large pesticide molecules that have not been treated before in the literature.

The discussion has then been focused on finding an appropriate thermodynamic model to estimate the activity coefficients of pesticides in polymers. Models that are generally considered accurate for other applications have been not been considered due to the special nature of the AI-polymer systems. The model chosen for these calculations (GC-Flory EoS) allows for the estimation of these activity coefficients without need of any experimental data, that is,

in a completely predictive manner, when the needed group-parameters are all available.

Given the complexity of the pesticide molecules, not all the groups (and parameters) needed to represent them were available in the GC-Flory EoS model therefore, an extension of the model has been performed. The new groups available are: aCO, aC-OH, Cl-(C=C), CCN, CF_2 and CONH.

With the addition of the new parameters a wide range of pesticide compounds (mainly pyrethroids) can now be represented, as well as some polymers that are commonly used in controlled release, such as polyamides.

The parameters estimated have been analyzed for their reliability in prediction of activity coefficients of solvent-polymer systems in general. For each of the new groups a significant number of parameters has been estimated, but the tests with polymer systems could not be performed with all of them due to the lack of experimental data. Overall, the results from the tests with polymer systems are satisfactory with a few exceptions that have been treated with detail (alkanes in PVDF, for example).

A significant improvement in the description and model performance for aromatic ethers has been achieved through the introduction of the new aCO group in the parameter table of the GC-Flory EoS model.

In the last part of this section the performance of the proposed approach to calculate partition coefficients has been studied and compared with previous work and experimental data from the literature. The improvement considering that this is an entirely predictive approach is significant. This is a very encouraging result for the application of the mentioned predictive approach to the systems of interest.

Finally a qualitative analysis of the solubility of pesticides in polymers has been presented, where the GC-Flory EoS model shows good agreement (based on rules of thumb) with previously analysed models (from the literature). To conclude, a predictive approach has been presented and tested, with the corresponding model extension that allows the use in complex molecules (where it was not possible earlier). The applicability and predictive features of the model and of the approach have been analysed separately with satisfactory results.

Nomenclature

List of symbols

a	Energy parameter
a_i^α	Activity of component i in phase α
a_{nm}	Interaction parameters (n, m are main groups in UNIFAC-FV and GC-Flory EoS)
$a_{nm,1}, a_{nm,2}$	Interaction parameters with T-dependency (n, m are main groups in Entropic-FV)
$a_{nm,1}, a_{nm,2}$	Segmental interaction parameters with T-dependency (n, m are segments in Entropic-FV/UNIQUAC)
b	Co-volume parameter
C	Measure of flexibility and rotation (in VdW model)
C	Temperature dependent molecular external degrees of freedom parameter (GC-Flory EoS)
C_i	Number of external degrees of freedom associated with component i
c_1, c_2, c_3	Constants of the Mathias-Copeman correlation
$C_{To,n}, C_{T,n}, C_n^0$	Degree of freedom parameters
E	Energy (per mol) that a molecule needs to overcome attractive forces which constrain it to its neighbours (cal/mol)
k_{ij}	Binary interaction parameter
$K_{p/solv}^{AI}$	Partition coefficient of the AI between the solvent and the polymer phases
m	Number of segments per molecule (molecular size parameter)
Mn	Number average molecular weight
Mv	Viscosity average molecular weight
Mw	Molecular weight
n	Total number of moles of the system
n_i	Number of moles of component i
P	Pressure
Pc	Critical pressure
P_{vap}	Vapor pressure
q_i	Surface area of component i
Q_n	Surface area of group n (normalized Van der Waals surface area, UNIFAC)
r	Number of sites occupied by the molecule
R	Gas constant
R_n	Hard-core volume of group n (normalized Van der Waals volume, UNIFAC)
$s\eta$	Interaction energy of molecule per segment
T	Temperature
Tc	Critical temperature
Tg	Glass transition temperature
T_0	Reference temperature (298.15 K)
u^0/k	Segment energy parameter
v	Molar volume of the system , in GC-Flory EoS
v_i	Molar volume of component i, in GC-Flory EoS

$\tilde{v}$	Reduced volume of the system
$\tilde{v}_i$	Reduced volume of pure component i
v^*	Closed packed volume of a segment (in Sanchez-Lacombe)
	Molecular hard-core volume or reference volume (in Panayiotou-Vera)
v^*	Segment size parameter (in SAFT EoS)
v_i^*	Molar hard-core volume of component i, in GC-Flory EoS
$v_w, (R_n)$	Van der Waals volume for subgroup k
w_i	Weight fraction of component i
w_i^α	Weight fraction of component i in phase α
$w_{solv,AI}$	Solubility of component i (in weight fraction)
x_i	Molar fraction of component i
x_i^α	Mole fraction of component i in phase α
z	Coordination number (z=10)

Greek letters

α	Thermal expansivity
χ_{12}	Flory-Huggins interaction parameter
δ	Solubility parameter
ΔH_{vap}	Enthalpy of vaporization
ΔH_{mix}	Heat of mixing
$\Delta V mix$	Volume of mixing
$\Delta\epsilon_{ji}$	Interaction energy parameter
$\Delta\epsilon_{nm}$	Interaction energies between unlike groups n and m
$\epsilon_{nm}, \epsilon_{mm}$	Interaction energies between groups
$\epsilon_{ji}(\tilde{v})$,$\epsilon_{ji}(\tilde{v}_i)$	Energy interaction parameters
ϵ^*	Interaction energy of lattice per site (in Sanchez-Lacombe)
ϵ_{ii}^*	Molecular interaction energy parameter
ϵ^{AB}/k	Association energy
ϕ_j	Volume fraction of component j
φ_i	Segment volume fraction of component i
γ_i	Activity coefficient of component i (mole basis)
γ_i^α	Activity coefficient of component i in phase α (mole basis)
κ^{AB}	Volume of association
μ_i^α	Chemical potential of component i in phase α
$\nu_n^{(i)}$	Number of groups n in component i
θ_i	Surface area fraction of component i
ρ	Density
ω	Acentric factor
Ω	Activity coefficient (weight-basis)
Ω_i	Activity coefficient (weight basis) of component i
Ω_i^{attr}	Attractive contribution to the activity coefficient
Ω_i^{comb}	Combinatorial contribution to the activity coefficient
Ω_i^{fv}	Free-volume contribution to the activity coefficient
Ω_i^α	Activity coefficient of component i in phase α (weight basis)

Ω_{AI}^{∞}	Activity coefficient of component i at infinite dilution (weight basis)

Subscripts

I, II	phase
AI	Active Ingredient
$calc$	Calculated
exp	Experimental
i, j	Component i and j respectively
m, n	Group of type m, n
p	Polymer
$pred$	Predicted
$solv$	Solvent

Superscripts

α, I, II	phase
$attr$	Attractive
$comb$	Combinatorial
fv	Free-volume
(i)	Compound i
p	Polymer
$solv$	Solvent
res	Residual
∞	Infinite dilution

List of abbreviations:

AAD	Absolute average deviation
Abs	Absolute deviation
FH	Flory-Huggins
N	Number of systems
PAN	Poly(acrylonitrile)
PBMA	Poly (butyl methacrylate)
PE	Polyethylene
PVC	Poly (vinyl chloride)
PVDF	Poly (vinylidene fluoride)

References

[1] Baner, A.L., Piringer, O.G., Prediction of solute partition coefficients between polyolefins and alcohols using the regular solution theory and group contribution methods, *Ind. Eng. Chem. Res.* 1991, 30, 1506-1515.

[2] Pitt, C.G., Bao Y.T., Andrady, A.L., Samuel, P.N.K., The correlation of polymer-water and octanol-water partition coefficients: estimation of drug solubilities in polymers, *Int. J. Pharm.* 1988, 45, 1-11.

[3] Jenke D.R., Kenley, R.A., Hayward, D.S., Interactions between polymeric containers and their contained solution: Modeling of polymer-water solute partitioning via coupled solvent-water partition coefficients, *J. Appl. Polym. Sci.* 1991, 43, 1475-1482.

[4] Tse,G., Blankschtein,D., Shefer,A., Shefer,S., Thermodynamic prediction of active ingredient loading in polymeric microparticles, *J. Control. Release* 1999, 60, 77-100.

[5] Peppas, N.A. and Brannon-Peppas,L., Controlled release of fragances from polymers: I. Thermodynamic analysis, *J. Control. Release* 1996, 40, 245-250.

[6] Scher H.B., Rodson M., Kuo-Shin L., Microencapsulation of pesticides by interfacial polymerization utilizing Isocyanate or Aminoplast chemistry, *Pestic. Sci.* 1998, 54, 394-400.

[7] Kouskoumvekaki, I. A. and Abildskov, J., Thermodynamic modeling as a tool in the design of microparticle controlled-delivery systems (2005) (under preparation).

[8] Lo, R.J.R., Chen, J.L., Scher, H.B, Van Koppenhagen, J.E., Shirley, I.M., *Dry water-dispersible compositions of microencapsulated pesticides* US Patent 6,555,122 (2003).

[9] Kontogeorgis, G.M., Models for polymer solutions, Chapter 7 in *Computer aided property estimation for process and product design*. Editors G.M. Kontogeorgis and R. Gani, 2004.

[10] Heidemann, R.A. and Michelsen, M.L., Instability of successive substitution. *Ind. Eng. Chem. Res.* 1995, 34, 958-966.

[11] Chen, F., *Prediction of phase equilibria for mixtures with polymers*. PhD thesis, 1991.

[12] Chadwick, P.R, Jeffries, D.A, *Pesticidal Compositions*. US Patent 5,229,122 (1993).

[13] Worthing, C.R., *The pesticide manual. A world compendium.* 6th Ed. The British Crop Protection Council., Croydon, 1979.

[14] Fredenslund, Aa., Gmehling, J. and Rasmussen, P., *Vapor-Liquid Equilibria using UNIFAC.* Elsevier Scientific Publishing Company, 1977.

[15] Kang, J.W., Abildskov,J., Gani,R., Cobas,J., Estimation of Mixture Properties from First- and Second-Order Group Contributions with the UNIFAC Model, *Ind. Eng. Chem. Res.* 2002, 41(13), 3260.

[16] Lee, B., Danner, R.P., Prediction of infinite dilution solvent activity coefficients in polymer solutions: comparison of prediction models, *Fluid Phase Equilibr.* 1997, 128, 97-114.

[17] Danner, R.P. and High,M.S., *Handbook of polymer solution thermodynamics* American Institute of Chemical Engineers, NY, 1993.

[18] Hildebrand, J. and Scott, R., *Solubility of non-electrolytes.* 3rd. ed. Reinhold, New York, NY, 1949.

[19] Flory, P.J., *J. Chem. Phys* 1941, 9, 660.

[20] Huggins, M.L., *J. Chem. Phys* 1941, 15, 225.

[21] Lacombe, R.H. and Sanchez, I.C., Statistical thermodynamics of fluid mixtures, *J. Phys. Chem.*, 1976, vol. 80, 23.

[22] Panayiotou, C.P. and Vera, J.H., Statistical thermodynamics of r-mer fluids and their mixtures, *Polym. J.*, 1982, 14, 681.

[23] High, M.S. and Danner, R.P., A group contribution equation of state for polymer solutions, *Fluid Phase Equilibr.*, 1989, 53, 323-330.

[24] Kontogeorgis, G., Harismiadis, V.I., Fredenslund, Aa., Tassios, D.P, Applications of the van der Waals equation of state to polymers. I. Correlation, *Fluid Phase Equilibr.*, 1994, 96, 65-92.

[25] Louli, V. and Tassios, D., Vapor-Liquid equilibrium in polymer-solvent systems with a cubic equation of state, *Fluid Phase Equilibr.*, 2000, 168, 165-182.

[26] Orbey H., Chen, Ch. and Bokis, C.P. An extension of cubic equations of state to vapor-liquid equilibria in polymer-solvent mixtures, *Fluid Phase Equilibr.* 1998, 145, 169.

[27] Orbey H., Bokis, C.P. and Chen, Ch., Equation of state modeling of phase equilibrium in the low-density polyethylene process: the Sanchez-Lacombe, Statistical Associating Fluid Theory and Polymer-Soave-Redlich-Kwong equations of state, *Ind. Eng. Chem. Res.* 1998, 37, 4481-4491.

[28] Oishi, T. and Prausnitz, M., Estimation of solvent activities in polymer solution using a group-contribution method, *Ind. Eng. Chem. Proc. D. D.*, 1978, 17 (3), 333.

[29] Kontogeorgis, G., Fredenslund, Aa. and Tassios, D.P, Simple activity coefficient model for the prediction of solvent activities in polymer solutions, *Ind. Eng. Chem. Res.* 1993, 32, 362.

[30] Elbro, H., Fredenslund, Aa. and Rasmussen,.P, A new simple equation for the prediction of solvent activities in polymer solutions, *Macromolecules*, 1990, 23, 4707.

[31] Flory, P.J., Orwoll, R.A. and Vrij, A., Statistical thermodynamics of chain molecule liquids. I. An equation of state for normal paraffin hydrocarbons., *J. Am. Chem. Soc.* 1964, 86, 3507.

[32] Bogdanic,G. and Fredenslund,Aa., Revision of the Group-contribution Flory equation of state for phase equilibria calculations in mixtures with polymers. 1.Prediction of Vapor-Liquid equilibria for polymer solutions, *Ind. Eng. Chem. Res.* 1994, 33, 1331-1340.

[33] Huang, S.H. and Radosz, M., Equation of state for small, large, polydisperse and associating molecules, *Ind. Eng. Chem. Res.* 1990, 29, 2284-2294.

[34] Chapman, W.G., Gubbins, K.E., Jackson, G. and Radosz, M., New reference equation of state for associating fluids, *Ind. Eng. Chem. Res.* 1990, 29, 1709-1721.

[35] Tomlin, C.D.S., *The pesticide manual*. 13th edition, British Crop Protection Council, Farnham, 2003.

[36] Kontogeorgis, G.M., notes from the Ph.D. Summer School: *Phase Equilibria in the Chemical, Biochemical and Petroleum Industries*, 2003.

[37] Zoller, P., Walsh, D. J. *Standard PVT Data for Polymers* Technonomic Publishing Company: Lancaster, PA, 1995.

[38] Elbro, H.S., Fredenslund, Aa. and Rsmussen, P., Group contribution method for the prediction of liquid densities as a function of temperature for solvents, oligomers and polymers, *Ind. Eng. Chem. Res.* 1991, 30, 2576.

[39] Van Krevelen, *Properties of polymers. Their correlation with chemical structure, their numerical estimation and prediction from additive group contributions*. Elsevier, Amsterdam, 1990.

[40] Lindvig, Th., Hestkjær, L.L., Hansen, A.F., Michelsen, M.L., Kontogeorgis, G.M., Phase equilibria for complex polymer solutions, *Fluid Phase Equilibr.* 2002, 663, 189-197.

[41] Marrero, J. and Gani, R., Chapter 3: Pure component property estimation: Models and Databases, in *Computer Aided Property Estimation for Process and product design*. Ed. Kontogeorgis, G.M. and Gani, R., Elsevier, 2004.

[42] Holten-Andersen, J., Rasmussen, P., Fredenslund, Aa. Phase Equi- libria of Polymer Solutions by Group Contribution. 1. Vapor- Liquid Equilibria. *Ind. Eng. Chem. Res.* 1987, 26, 1382.

[43] Chen,F., Fredenslund,Aa. and Rasmussen,P., Group-contribution Flory equation of state for Vapor-Liquid equilibria in mixtures with polymers, *Ind. Eng. Chem. Res.* 1990, 29, 875-882.

[44] Fredenslund, Aa., Gmehling, J., Rasmussen, P. *Vapor-Liquid Equilibria Using UNIFAC*. Elsevier Scientific: New York, 1977.

[45] Bondi, A., *Physical properties of molecular crystals, liquids and glasses*. John Wiley & Sons, New York, 1968.

[46] *DIPPR Tables of Physical and Thermodynamic Properties of Pure Compounds*. AIChE: New York, 1998.

[47] Tiegs,D., Gmehling,J., Medina,A., Soares,M., Bastos,J., Alessi,P., Kikic,I., *Activity coefficients at infinite dilution*. vol. IX, Parts 1 and 2, DECHEMA. Chemistry data series, 1986.

[48] Gmehling,J., Onken,U., Weidlich,U., *Vapor-Liquid equilibrium data collection* Vol. I, Part 2d, DECHEMA. Chemistry data series, 1982.

[49] Baker, R. W., *Controlled release of biologically active agents*. 1987.

[50] Dahl,G., Simkin,J. *Microencapsulated Pyrethroids*, USpat 4,670,246, 1987.

[51] Hao,W., Elbro,H.S., Alessi,P., *Polymer solution data collection* Part 2+3 (vol. 14), DECHEMA. Chemistry data series, 1992.

[52] Newman,R.D. & Prausnitz,J.M., Polymer-solvent interactions from gas-liquid chromatography, *Paint Research Institute*, 1973, Proceedings Nr. 105, vol. 45, no. 585.

[53] Bonifaci,L. and Ravanetti,G., Measurement of infinite dilution diffusion coefficients of e-caprolactam in Nylon 6 at elevated temperatures by inverse gas chromatography, *J. of Chromatoghr.* 1992, 607, 145-149.

[54] Gross,J., Sadowski,G., Perturbed-Chain SAFT: An equation of state based on a perturbation theory for chain molecules *Ind. Chem. Eng. Res.* 2001, 40, 1244-1260.

[55] Gross,J., Sadowski,G., Application of the Perturbed-Chain SAFT equation of state to associating systems, *Ind. Chem. Eng. Res.* 41 (2002) 1084-1093.

[56] Larsen, B.L., Rasmussen, P. and Fredenslund, Aa. A modified UNIFAC group-contribution model for prediction of phase equilibria and heats of mixing, *Ind. Chem. Eng. Res.* 1987, 26, 2274.

[57] Hoy, K.L., *The Hoy tables of solubility parameters*. Union Carbide Corp.: South Charleston, WV, 1985.

[58] Van Krevelen, D.W. and Hoftyzer, P.J. *Properties of polymers. Their correlation with chemical structure*. Elsevier, Amsterdam, 1976.

[59] Fedors, R.F.A., A method for estimating both the solubility parameters and molar volumes of liquids, *Polym. Eng. Sci.* 1974a, 14, 2, 147-154.

[60] Fedors, R.F.A., A method for estimating both the solubility parameters and molar volumes of liquids Supplement , *Polym. Eng. Sci.* 1974a, 14, 6, 472.

[61] Kharin, S. E., Perelygin, V. M., Volkov, A. G., *Izv. Vyssh. Uchebn. Zaved., Pishch. Tekhnol.* 1971, 6, 119.

[62] Kydonieus, A.F., *Controlled release technologies: methods, theory and applications*. CRC Press, Inc. Boca Ratón, Florida, 1980.

[63] Lindvig, T., Michelsen, M., Kontogeorgis, G., A Flory-Huggins model based on the Hansen solubility parameters, *Fluid Phase Equilibr.* 2002, 203, 247-260.

4

Diffusion coefficient

4.1 Property definition and theory

i) Definition and approach

The diffusion coefficient of the Active Ingredient (AI) in the polymer membrane is another of the variables that have an important effect on the release of the AI from the device where it is contained. It is a measure of the rate of transfer of AI through the polymer membrane due to a concentration gradient.

In general terms, the diffusivity of the molecules is affected by several factors, such as temperature and pressure, as well as the properties or characteristics of the diffusant (size and concentration) and the medium, the polymer molecular weight, glass transition temperature and morphology (crystallinity, cross-linking density and swelling). Other factors that can influence the diffusion of the AI molecules is the addition of fillers (decreasing the diffusivity) or plasticizers (increasing the diffusivity).

The objective of this chapter is to describe a predictive method for the estimation of diffusion coefficients of AIs in polymers. It is important that the above mentioned factors (or at least as many of them as possible) can be taken into account through a model so that their immediate effect on the release of AI from controlled release devices can be assessed.

In the controlled release models the equations are derived from Fick's laws of diffusion (see chapter 2) and the diffusion coefficients involved are the so-called mutual diffusion coefficients (D_{12}). In this chapter subscript 1 refers to the AI and subscript 2 to the polymer. As indicated by Eq. 4.1, the mutual diffusion coefficient is related to the self-diffusion coefficient of each of the components of the system (D_1 and D_2), through the chemical potential gradient.

$$D_{12} = \frac{D_1 x_2 + D_2 x_1}{RT} \left(\frac{\partial \mu}{\partial \ln x_1} \right)_{T,P} \tag{4.1}$$

D_1 is the actual measure of the mobility of the diffusant molecules (AI) within the polymer membrane, which in AI-polymer systems is much larger than the self-diffusion coefficient of the polymer molecules (D_2). Therefore by considering D_2 to be negligible, Eq. 4.1 is simplified to obtain,

$$D_{12} = \frac{D_1 x_2}{RT} \left(\frac{\partial \mu}{\partial \ln x_1} \right)_{T,P} \tag{4.2}$$

Equation 4.2 is only strictly valid at the limit of solvent infinite dilution ($x_1 \rightarrow 0$), but its use is commonly accepted for all the concentration range since D_2 is usually not known (Zhong et al. [60]).

The chemical potential (μ) and the activity (a) are related through,

$$\mu_1 = \mu_1^0 + RT \ln a_1 \tag{4.3}$$

Where,

$$a_1 = x_1 \gamma_1 \tag{4.4}$$

Replacing the chemical potential (Eq. 4.3) in Eq. 4.2 gives,

$$D_{12} = D_1 x_2 \left(\frac{\partial \ln a_1}{\partial \ln x_1} \right)_{T,P} \tag{4.5}$$

Replacing the activity (Eq. 4.4) in Eq. 4.5 gives,

$$D_{12} = D_1 x_2 \left(1 + \frac{\partial \ln \gamma_1}{\partial \ln x_1} \right)_{T,P} \tag{4.6}$$

Through the introduction of a thermodynamic model for the activity (coefficient) term, such as those described in Chapter 3, and a model for the estimation of the self-diffusion coefficient (see the next section), the mutual diffusion coefficient can then be calculated.

ii) Background literature (Diffusion in controlled release)

Diffusion coefficient is an important parameter in the field of controlled release and its effect on the release behaviour is generally studied through experimental observations.

Experimentally measured release data (or mass transfer data) has been used to regress, in an appropriate mathematical model, the values of the parameter of interest, in this case the diffusion coefficients. Examples of application can be found in food packaging, pharmaceutical and agrochemical industries (Hoon [1], Ferrara et al. [2], Goydan et al. [13]). In some cases the parameter values have been correlated to provide an empirical equation for the diffusivity (Kou et al. [3]), taking into account the temperature effects (Ferrara et al. [2], Foldes [4], Goydan et al. [13]), concentration variations (Gao et al. [5]) and membrane swelling (Chen and Lostritto [11]).

Other aspects of polymer morphology have also been experimentally assessed (Chen and Lostritto [11] and Kagayama et al. [12]). The influence of specific plasticizers has been empirically studied in the field of pesticide controlled release (Shailaja et al. [6]) and the diffusion coefficient correlated as a function

of plasticizer concentration (Shailaja et al. [7]). A few attempts have also been made in the field of drug release to use empirical equations for the estimation of diffusivities, either as a function of concentration of the compounds in the formulation (Gao et al. [5]) or of AI properties, such as size or molecular weight (Pitt et al. [8]), that are then used to study the AI release behaviour.

Another area where the mass transfer in polymers and therefore the diffusivities of the compounds are of interest, is that of protective clothing (Goydan et al. [14],[15]), where also empirical correlations have been developed for estimation of diffusion coefficients through polymers as a function of solute properties such as molecular weight (Goydan et al. [14]) or other molecular structural parameters (Goydan et al. [15]).

The use of an empirical equation for the estimation of diffusion coefficients has several limitations as they are generally only applicable to a specific polymer and a limited number of compounds. Consequently, the predictive ability of these correlations is severely limited. Besides, the fact that a minimum number of measured data is required to obtain the correlation does not reduce the needed experimental work. Therefore, the introduction of a completely predictive model, that is applicable to complex AIs, is a very interesting concept when the lack of experimental data is a recurring problem.

The idea of applying free volume concepts for the prediction of diffusion coefficients required by the controlled release mathematical models has been suggested by Fan et al. [9] and Amidon et al. [10]. The development of a completely predictive model for the estimation of diffusion coefficients has, however, not yet been found for controlled release technology related to the pharmaceutical and agrochemical industries.

iii) Approach for estimation of diffusion coefficients

Several considerations need to be taken into account when analysing the models to be used for the prediction of diffusion coefficients in controlled release applications.

i) Fickian diffusion: The fact that Fick's laws of diffusion are the basis for the derivation of most of the controlled release models (at least the ones considered in this work) limits the temperature range of the models given that the assumption of Fickian diffusion is usually applicable above the glass transition temperatures of the polymers. Consequently, in the controlled release systems, glassy polymers are not considered. That is, the temperature of the systems considered must be above the glass transition temperature of the polymer. With this assumption, the problem of dealing with the complex behaviour of glassy polymers (relaxation phenomena, Fan et al. [9]), is avoided.

ii) The polymer membrane is considered to be macroscopically homogeneous, that is, non-porous. In this case, diffusion is not limited by the pore size and related factors, such as porosity, pore orientation and distribution.

iii) Infinite dilution of the AI (diffusing compound): In controlled release applications the polymer (diffusing medium) is expected to be mechanically stable and therefore only the region of concentrated polymer needs to be accounted for. The AI (diffusing compound), on the other hand, is assumed to be at infinite dilution conditions. Then, the estimation of the diffusion coefficient is basically determined by the self-diffusion coefficient (see Eqs. 4.5 and 4.6). The term accounting for the thermodynamic activity becomes less important due to the AI-polymer interactions being dramatically reduced. Therefore, predictive models for self-diffusion coefficient are the ones that need to be analyzed (see next section).

iv) The solvent present in the core of the controlled release device is not considered to affect the AI diffusion coefficient. This is because the solvent used is usually not soluble in the polymer, so it does not partition at all into the membrane thereby not affecting the AI diffusivity once it is in the membrane.

v) Pressure effects: Given that the applications of controlled release of pesticides are at atmospheric pressure, the pressure dependence does not need to be considered in the calculations.

4.2 Evaluation of currently available models

4.2.1 Introduction

This section provides an analysis of some of the currently available models for the estimation of diffusivities of low molecular weight compounds (the AIs) in polymers. In principle, for the calculation of the mutual diffusion coefficient, two types of models are needed: (i) a thermodynamic model for the activity and, (ii) a model for the self-diffusion coefficient. In this section though, only self-diffusion coefficient models are treated as the thermodynamic models for activity have been discussed earlier in Chapter 3.

For the estimation of self-diffusion coefficients, the models are analyzed and assessed in terms of their applicability to pesticide controlled release systems. In addition to the factors already discussed in section 4.1 (pressure dependence and glassy polymers), other aspects to be taken into account are the following:

i) Predictive ability of the model: This is an important factor as the main objective of this work is the prediction of properties (variables) needed by the controlled release models. Therefore, empirical correlations are not an option, even though they are discussed in order to provide an overview of the available approaches and because they provide important insights about the dependencies of diffusivities on specific parameters.

ii) Temperature dependence of the model: Temperature is important because it affects significantly the values of the diffusion coefficients. In controlled

release applications, where the devices are subject to environmental conditions and their variations, temperature dependence becomes an important effect to be considered.

iii) Performance at high polymer concentrations: In controlled release applications the concentration range of interest is the high polymer concentrations and therefore, the models that are only valid for dilute polymer solutions are not considered.

iv) Applicability to large and complex molecules: For small molecules, diffusion takes place through molecular jumps from one cavity to another. Consequently, the diffusion coefficient and the activation energy are concentration-independent, and the latter is also independent of temperature. On the other hand, for the diffusion of large molecules there might be need for the polymer segments to be redistributed in order to accommodate the big molecules if the cavity is not big enough. In this case, both the diffusion coefficient and the activation energy become functions of concentration and temperature, which is usually the case of pesticide compounds. Therefore models that take into account molecular size and structure become very interesting.

Since numerous and extensive reviews of polymer diffusion theories and models are available in the literature (for example, Crank [19], Masaro et al. [20]), the evaluation of the existing models will be presented in the light of the above observations and only an overview will be provided of the main theories in order to assess the applicability of a few selected models for the specific systems of interest (pesticide controlled release devices).

4.2.2 Overview of diffusivity models

The models discussed below are grouped in terms of their theoretical basis.

i) Arrhenius and empirical models

The Arrhenius theory has been widely employed to describe the temperature dependence of the diffusion coefficient (Gao et al. [5]). This is an empirical correlation, with no predictive capabilities, but on the other hand, useful to obtain information about the behaviour of the systems. Other empirical models (Petit et al. [22]) have tried to reproduce the effect of the size of the diffusing molecules, together with the temperature dependence of the systems. These models are not considered in this work, mainly due to their lack of predictive potential. Also, their limited range of applicability, only to dilute polymer concentrations, makes them unsuitable for their use in controlled release studies.

ii) Obstruction and hydrodynamic theories

A few attempts have been made to develop models for the self-diffusion coefficient on the basis of the obstruction effects presented by the polymer molecules due to their significantly lower mobility (relative to solute molecules). The obstruction concept considers the tortuosity of the polymer through an increased diffusion path length of the solutes. Several models have appeared based on this concept (Maxwell-Fricke model (Waggoner et al. [23]), Mackie-Meares model (Mackie et al. [24]), among others) which account for the concentration dependence as well as the shape of the molecules. These models though, are not valid for large compounds or for high polymer concentrations, and therefore, not useful for the systems of interest in this work. Another group of models were derived on the basis of hydrodynamic interactions, and with the same limitations as above. This theory takes into account the friction between the solute and the polymer. As an example of models within this theory, the Phillies model (Phillies et al. [25]) and the Gao and Fagerness model (Gao et al. [21]) can be mentioned. These models are also not suitable for the purposes of this work, due to their limitations and empirical nature.

iii) Zone theory

Another series of models have been developed based on the zone theory of Barrer et al. [30], which was originally proposed by Barrer to account for the activation energies required for diffusion. It was reformulated by Bueche et al. [32], to apply the energy fluctuation theory, while Brandt et al. [31] attempted to provide a molecular model to estimate these activation energies. These models though, are unlikely to give acceptable results when applied to bigger molecules since they were only tested for gases (H_2, He, ...), which makes them inappropriate for the systems of interest in this work.

iv) Enskog theory

One of the theories that have shown potential for predictive capabilities is the modified Enskog theory (MacElroy et al. [26]). According to this theory, the particle diffusing is described as a rigid sphere that flows through a polymer solution. It uses the kinetic theory to account for momentum transfer between the spheres, and based on the assumption that the solute only interacts with part of the polymer chain at one time, the diffusion coefficient is scaled with respect to part of the polymer chain. The diffusivity equation contains concentration terms as well as the molecular radii of each of the compounds. This model, with the molecular radii fitted to experimental data, has been applied by Waggoner et al. [23] for study of diffusion in polymer networks. The model can be made predictive by obtaining the value for the radii through molecular modelling generated data. Zhu et al. [27] studied the molecular size and shape effects on the diffusivity and analysed the possible approximations for the shape

of the molecule (cylindrical rods or conical sections) that would provide a good description of the diffusion coefficient. They however, did not present any predicted results. Even though this model had promising predictability features, it was also shown (Waggoner et al. [23]) that a good fit could only be provided at low concentrations of the polymer, which is an impediment for its use in controlled release studies.

v) Molecular theories

An interesting approach for the AI-polymer systems that deserves special attention is provided by the molecular theories. The models employing molecular theories take into account, in a detailed manner, the motions and local interactions of the diffusant molecules and the polymer segments. Here, the diffusivity of the molecules depends on the activation energy, the diffusant jumping distance and frequency, which are then related to molecular parameters of both the diffusant and the polymer. The theory takes into account the fluctuation of the polymer segments that allow the diffusive jumps through the available voids.

The best known model based on the molecular theory is the one reported by Pace and Datyner (Pace et al. [28],[29]). Earlier models (Meares et al. [33], Barrer et al. [30], Brandt et al. [31], Kumins et al. [34], Kumins et al. [35], DiBenedetto et al. [36]) have been used to relate the activation energies of diffusion to polymer structure and diffusant diameters but they are, in general, unable to correlate the concentration and temperature dependence of the diffusivity. Besides, they are limited to small and simple molecules (such as inert gases, O_2, N_2, ...). Pace and Datyner on the other hand, attempted to develop a predictive model that would take into account the concentration and temperature dependencies (through explicit expressions) which could be used for both simple and complex diffusants.

The Pace and Datyner model (based on DiBenedetto et al. [36]) is a statistical mechanical model based on the physico-chemical properties of the system. The basic assumptions of the model are:

i) Semi-crystalline order in the amorphous regions of the polymer.

ii) The chain bundles are considered to be locally parallel along distances of several nanometers.

iii) The coordination numbers are assumed to be 4 for the amorphous region and 6 for the crystalline region.

iv) A diffusing molecule can diffuse through the amorphous polymer phase,
(a) along the axis: this accounts for the jumping distance of the diffusant and it takes place until a barrier is encountered (entanglement, crystallite, cross-link, ...)
(b) perpendicular to the axis: this accounts for the activation energy and

jumping frequency and is the rate limiting step.

The main drawback of this model, with respect to the objectives of this work, is the fact that it is actually not completely predictive because at least two parameters (the root-mean-square displacement between jumps and the chain displacement) cannot be obtained from first principles.

Apart from this, some other parameters may need further assumptions and considerations that require knowledge of the detailed structures of the compounds (such as the angle between molecular axis), which may be unavailable for the pesticide-polymer systems of interest. Other drawbacks involve the fact that the model has not been extensively tested to prove its applicability (large compound diffusion only studied in Poly(ethylene terephtalate) and Polyisoprene).

vi) Free volume theory

The last group of models to be considered in this overview are the ones based on the free-volume theory. The basis of the free volume theory lies on the assumption that the mobilities of both the diffusant and the polymer molecules are primarily determined by the free volume in the system. The variation of the diffusion coefficient as a function of concentration and temperature is introduced through the effect of these variables on the free volume of the system. That is, an increase in the diffusant concentration and/or in the temperature, causes an increase in the free volume and thus the diffusivity also increases. Also, the free volume theory can be considered applicable when there is sufficient contact and overlapping of the polymer molecules, that is, at high polymer concentrations, which is the range of interest in controlled release systems.

The derivation of the free volume theory for diffusion in polymers has its origin in Cohen et al. [37] who developed the free volume concept for self-diffusivity in van der Waals liquids. According to this theory, diffusion occurs due to local density fluctuations that provide holes where the diffusant molecule can jump into. Several theories have been derived from this concept and extended to diffusion in polymers. As an example, Paul [38], suggested a predictive model for diffusion coefficient estimation in amorphous polymers. The only experimental data required by the model are viscosity, critical volume of the pure solvent and specific volume of the mixture. That is, binary diffusivity data is not needed. The model, even though especially promising with respect to predictive capabilities, does not perform well at high polymer concentrations and is therefore not applicable for controlled release uses.

Another model that stems from the Cohen-Turnbull theory is the Vrentas-Duda free-volume model (Vrentas and Duda [39],[40]). A great effort has been put to improve and extend the model and its predictive capabilities, and thereby it is the most suitable for the applications of interest in this work. This is due to the fact that the complexity of the molecules (pesticide AIs) can be

accounted for and all the parameters of the model can be predicted without the need for binary transport data. It is therefore selected for further development and use.

Another widely used model that makes use of the free volume concept is the one by Fujita [41]. This model is an extension of the Doolittle model ([43], [44]) for the temperature dependence of the viscosity of pure liquids, to polymer-solvent binary systems at temperatures above glass transition. The mobility of the molecules is taken as inversely proportional to the viscosity (Stokes law). The parameters of the equation are to be obtained from mobility data as a function of concentration and it is therefore, an empirical correlation model with no predictive capabilities.

Other models have been derived from the Fujita approach, such as Yasuda et al. [45], but further detail is not considered necessary given that, as the Fujita model, it is an empirical approach and is not applicable for the systems of interest here.

The three principal models developed from the free volume concept are presented in Table 4.1 which highlights the differences and similarities between them. This further illustrates the choice of the Vrentas-Duda model for the purposes of this work.

Table 4.1: Table of comparisons of the main FV models.

Aspects	**Fujita [41]**	**Paul [38]**	**Vrentas and Duda [39],[52]**	**Vrentas and Duda [61],[66]**
Apply for		Fickian diffusion Amorphous polymers		
Polymer concentration range (ϕ_2)	Semi-dilute polymer solutions	0 - 0.9	$\phi_2 > 0.9$	$\phi_2 > 0.9$
Nr. of parameters	4	3	$10^{(1)}$	10
Experimental data required	D(ϕ_i) at each T	η_i(T) V_{c_1} ρ_{mix}	ρ_i (T) η_i(T) D (T), at least 3 points $\chi(for D_{12})$	ρ_i (T) V_{c_1} η_i(T) $\chi(for D_{12})$
FV distribution	Random among all units	Random among all units	Equally among all units (random in [66])	
Major limitation	Assumed: $M_{1j} = M_{2j}$ Correlation	Concentration range	Need D (T) data	Estimations inaccuracies (in parameters)

(1) In Fujita [42] 8 parameters are mentioned. χ_{12} is not considered because it is only needed for mutual diffusion calculations. And E is grouped with D_0.

In Table 4.2 the choice of the free volume-based models over the molecular theories is illustrated through a summary of their applicability, parameters needed and availability and their main limitations.

Table 4.2: Table of comparisons of the Vrentas-Duda FV model with Pace and Datyner

	Pace and Datyner [28],[29]	**Vrentas and Duda [39],[52]**	**Vrentas and Duda [61],[66]**
Apply for	Mainly crystalline polymers	Fickian diffusion Amorphous polymers	
Polymer concentration range (ϕ_2)	High polymer concentrations	$\phi_2 > 0.9$	
Nr. of parameters	$\sim 14^{(1)}$	10	10
Experimental data required	Molecular parameters and properties	ρ_i(T) η_i(T) D (T), at least 3 points $\chi(for D_{12})$	ρ_i(T) V_{c_1} η_i(T) $\chi(for D_{12})$
FV distribution	n/a	Equally among all units (random in [66])	
Major limitation	2 of the parameters cannot be obtained from molecule. Need to be adjusted	Need D (T) data	Estimations inaccuracies (in paramters)

(1) There is two possible formulations, for which the number of parameters needed may vary slightly.

Finally, the combination of molecular theories with the free volume theory resulting into the so-called Hybrid models (Kiparissides (2003) and Doong and Ho [47]) is an attempt worth mentioning. These models attempt to overcome the gaps in the free volume theory based models and at the same time avoid the complexities inherent in the molecular models. The two types of models are combined through one of the terms of the free-volume theory (the pre-exponential term) that is estimated here through molecular parameters of the polymer and the solute by applying the molecular theory. The free volume expressions for temperature and concentration dependence are employed in these models. Here, the limitations in predictability that the molecular theories present are still inherent and the models have only been applied as correlations of experimental data. Therefore, this type of models is at the moment not interesting for the application in prediction of pesticide diffusivities in polymers.

To conclude, an overview of the main models available has been provided in this section. It is clear that, even though a significant number of models exist, they present limitations that make them useless for the purposes of this work.

That is, applicability limited to small compounds or low polymer concentration region, for example. The choice of the free volume-based models for further development has been highlighted.

4.3 The Vrentas-Duda free volume model

i) Theoretical basis

This model is based on the principles of the free volume effects. The free volume concept arises from the distinction of the volume of a liquid into two different types: (i) the volume occupied by the molecules, which can generally be assumed as the volume of the equilibrium liquid at absolute zero temperature, and (ii) the volume surrounding these molecules, or non-occupied volume, that is the free volume. The latter is being continuously redistributed in the space as no energy is required for this to occur. The average free volume per molecule is defined by Eq. 4.7, which is the difference between the occupied volume ($\overline{v}_o$) and the average volume in the liquid ($\overline{v}$).

$$\bar{v}_{FV} = \bar{v} - \bar{v}_o \tag{4.7}$$

As mentioned above, in these models diffusion is considered to be limited by the availability of free volume and according to Cohen-Turnbull [37], a diffusion jump occurs if a free volume hole of sufficient size is available and if the void left by the diffusing molecule is then filled by another one.

The basis for this model was first established by Vrentas and Duda [39],Vrentas et al. [52], who derived it as an extension to polymer systems of the Cohen-Turnbull [37] free volume (FV) theory for hard-sphere liquids. Some assumptions are made when the FV is applied to polymer systems, these are:

i) the occupied volume (defined as the volume at 0 K) is independent of the polymer molecular weight.

ii) the temperature dependence of the diffusion is dependent on the size of the diffusing molecule and not on the polymer (Frenkel [51]), as opposed to the considerations made by Cohen et al. [37].

In the Vrentas-Duda model the FV is defined by taking into account two effects due to an increase of the temperature: first an expansion of the polymer which generates the so-called *interstitial free volume* and secondly, the formation of voids or holes, that provide for the *hole free volume*. Diffusion will only occur through the second type of FV given that it requires little or no energy for redistribution, as opposed to the interstitial FV.

ii) Vrentas and Duda model

The equation obtained from the derivation (at constant pressure) to estimate

the self-diffusion coefficient (Eq. 4.8) represents the fact that the diffusion process depends on the probability that the diffusing molecule has sufficient energy to overcome the attractive forces that hold it to its neighbours (first exponential term) and the probability that a density fluctuation provides a hole that is large enough for the molecule to jump into (second term). It is important to note that this second term reflects the different approach taken by Vrentas and Duda with respect to Cohen and Turnbull's original formulation. In Eq. 4.8 the pre-exponential term (D_0) is not a strong function of temperature compared to the exponential term and it can therefore be considered constant.

$$D_1 = D_0 \exp\left(\frac{-E}{RT}\right) \exp\left(\frac{-\gamma\left(w_1\tilde{V}_1^* + w_2\xi\tilde{V}_2^*\right)}{\bar{V}_{FH}}\right) \tag{4.8}$$

where,

$$\bar{V}_{FH} = w_1 K_{11}\left(K_{21} - T_{g1} + T\right) + w_2 K_{12}\left(K_{22} - T_{g2} + T\right) \tag{4.9}$$

For the mutual diffusion coefficient, D_{12}, Duda et al. [54] proposed the use of the Flory-Huggins model [55],

$$D = D_1\left(1-\phi_1\right)^2\left(1-2\chi\phi_1\right) \tag{4.10}$$

The final mutual diffusion coefficient model consists of the following parameters: $D_0, E, \gamma, \tilde{V}_i^*, \xi, K_{1i}, K_{2i}$ and χ. Equation 4.10 contains the implicit assumption that the self-diffusion coefficient of the polymer is negligible. Also, the dependence on concentration and temperature of the Flory-Huggins parameter (χ) is neglected. Note that Vrentas et al. [52] originally suggested the use of a more complex thermodynamic model, the Flory model [53] for the mutual diffusion coefficient calculation.
The model based on the early version of the Vrentas-Duda FV model (Vrentas and Duda [39],Vrentas et al. [52] and Duda et al. [54]) is not predictive in the sense that some diffusivity data (at least three data points at different temperatures) is required for the estimation of some of the model parameters.

iii) Zielinski and Duda model

Zielinski and Duda [61] proposed a different set of estimation methods for the parameters of the mutual diffusion coefficient model (Eqs. 4.8-4.10), resulting in a predictive form of the model, where experimental diffusivity data is not needed. This is possible given that all the parameters have a physical meaning and can thus be estimated through some properties of the compounds involved, such as density and viscosity.

It is worth mentioning that in order to simplify the estimation of the parameters and achieve the predictive model Zielinski and Duda assumed that the energy effects are negligible (as seen in Table 4.3) and obtained Eq. 4.11 thereby.

$$D_1 = D_0 \exp\left(\frac{-\left(w_1\tilde{V}_1^* + w_2\xi\tilde{V}_2^*\right)}{w_1\frac{K_{11}}{\gamma}\left(K_{21} - T_{g1} + T\right) + w_2\frac{K_{12}}{\gamma}\left(K_{22} - T_{g2} + T\right)}\right) \quad (4.11)$$

This assumption is the cause of the temperature limitation of the model, valid from the glass transition temperature (Tg) and within a range of a 100°C above this value (Tg + 100°C, or 150°C). This is due to the fact that at higher temperatures the energy effects become more important and diffusion is no longer dominated by the free volume effects. These temperature limitations also result from the fact that the thermal expansion coefficients are approximated to average values over the temperature interval.

According to the Zielinski and Duda [61] model, the model parameters are obtained as follows:

- The specific critical hole free volume required for a jump ($\tilde{V}_i^*$) is approximated to the volume of the compound at 0 K. This volume can be estimated through group-contribution methods (Sugden et al. [48] and Blitz et al. [49]), therefore the only information required is the structure of the molecule.

- The free volume parameters for the solvent and the polymer (K_{1i}/γ, K_{2i}): In the case of the polymer molecules, the FV parameters can be obtained directly from the WLF equation parameters (C_{1j}^{WLF}, C_{2j}^{WLF}), if these are available for the polymer of interest (Ngai et al. [50]),

$$\frac{\gamma\tilde{V}_j^*}{K_{1j}} = 2.303 C_{1j}^{WLF} C_{2j}^{WLF} \quad (4.12)$$

$$K_{2j} = C_{2j}^{WLF} \quad (4.13)$$

  Else these parameters are estimated, as for the solvent, by fitting viscosity at low temperatures,

$$\ln\left(\eta/\eta_{T_{gj}}\right) = \frac{\gamma\tilde{V}_j^*/K_{1j}}{(K_{2j} - T_{gj}) + T} \quad (4.14)$$

- The pre-exponential factor (D_0) can be calculated from Dullien's expression (Eq. 4.15) using experimental data for specific volume (or density) of the solvent as a function of temperature and the critical volume of the solvent (Vc).

$$\ln\left(\frac{0.124 * 10^{-16}\tilde{V}_c^{2/3}RT}{\eta_1 M w_1 \tilde{V}_1}\right) = \ln D_0 - \frac{E\left(w_1 \to 1\right)}{RT} - \frac{\gamma\tilde{V}_1^*/K_{11}}{K_{21} + (T - T_{g1})} \quad (4.15)$$

In Eq. 4.15, the energy term ($E(w_1 \sim 1)$) is usually neglected.

- The ratio of jumping units (ξ) is defined by Eq. 4.16. The jumping units are parts of the molecules which are capable of essentially independent movement over short distances.

$$\xi = \frac{\tilde{V}_1^*}{\tilde{V}_{2j}^*} \tag{4.16}$$

In the case of small or symmetric molecules $\tilde{V}_1^*$ can be approximated by V_1 (0 K) and $\tilde{V}_{2j}^*$ is provided by some correlations with polymer properties (Eqs. 4.17 and 4.18), obtained from data within the range: 200 K $\leq$ $\mathrm{Tg_2}$ $\leq$ 380 K.

$$\tilde{V}_{2j}^* \left(cm^3/mol\right) = 0.6224 T_{g2}\,(\mathrm{K}) - 86.95 \tag{4.17}$$

$$\tilde{V}_{2j}^* \left(cm^3/mol\right) = 11.018 \exp\left(0.0074 \times T_{g2}\,(\mathrm{K})\right) \tag{4.18}$$

- The energy effects (E) are assumed negligible.

- The Flory-Huggins parameter (χ) needed for the calculation of the mutual diffusion coefficient can be obtained from the semi-empirical relation in Eq. 4.19.

$$\chi = 0.35 + \frac{\tilde{V}_1}{RT}\left(\delta_1 - \delta_2\right)^2 \tag{4.19}$$

Table 4.3 gives a list of the parameters required in the Zielinski-Duda model pointing out how they are determined and the experimental data needed. The main difference with the earlier versions (Vrentas and Duda [39],Vrentas et al. [52] and Duda et al. [54]) is related to the estimation of the parameters D_0 and ξ (and E when applicable) that originally required diffusivity data.

Table 4.3: Parameters of the Vrentas-Duda FV model (version by Zielinski and Duda [61])

Parameter	**Obtained**	**Data needed**
$\tilde{\mathrm{V}}_{\mathrm{i}}^*$	$\mathrm{V_i}$(0K), GC method	Molecular structure
$\mathrm{K_{1i}}/\gamma, \mathrm{K_{2i}}$	Solvent: Eq. 4.14	η(T), low T
	Polymer: i) Eqs. 4.12, 4.13	$\mathrm{C_{1j}^{WLF}}, \mathrm{C_{2j}^{WLF}}$
	ii) Eq. 4.14	η(T)
D_0	Eq. 4.15	$\tilde{\mathrm{V}}_1$(T) , Vc
ξ	Eq. 4.16	$\tilde{\mathrm{V}}_{\mathrm{2j}}^*$ (Eq. 4.17, 4.18 and Tg)
E	Assumed negligible	-
χ	Experimental	Solubility data
	Eq. 4.19	$\delta_{\mathrm{i}}, \tilde{\mathrm{V}}_1$

Assumptions in parameters estimation

Note that the assumption of infinite dilution of the diffusing compound ($\phi_1 \rightarrow 0$) is made, and consequently, the mutual diffusion coefficient is obtained directly from the self-diffusion coefficient ($D = D_1$).
In order to summarize this part, all the assumptions made in the derivation of the predictive Zielinski and Duda model are listed in Table 4.4.

Table 4.4: Table with all assumptions (in Zielinski and Duda [61])

Implicit assumptions (general of FV model)
• The mutual diffusion coefficient is related theoretically to the solvent and polymer self-diffusion coefficients through an expression developed by Bearman [67].
• The FV is equally distributed among polymer and solvent molecules.
• The contribution of polymer self-diffusion coefficient to the mutual diffusion coefficient is negligible.
• The volumes of the polymer and the solvent are presumed to be additive (without a volume change on mixing)
• Thermal expansion coefficients are approximated by average values over the temperature intervals of interest, and assumed independent of molecular weight.
• Constant pressure.
• γ and E can be assumed constant with the premise that the domains of the polymer molecules overlap and the environment experienced by a solvent molecule does not change significantly.
• Pre-exponential term (D_0) is constant (independent of temperature).
Specific assumptions (for solution) in Zielinski and Duda [61]
• The Flory-Huggins model [55] accurately describes the diffusant activity.
• The Flory-Huggins interaction parameter is considered independent of concentration and temperature.
• The energy effects are considered negligible (E = 0).
Limitations:
• The temperature range of applicability is: Tg < T < Tg + 100°C (or 150 °C in Zielinski and Duda [61]
• Non-glassy polymers(1)
• Not-predictive for large/asymmetric molecules.

(1) Other versions of the model have been applied to glassy polymers (see below)

Other modifications of the theory

As mentioned in the previous section the Vrentas-Duda FV model (Duda et al. [54]) has been extensively studied, further modified and extended by several authors. Three such extensions are briefly discussed below.

The extension of the model to deal with glassy polymers, that is, in systems where the temperature is below the glass transition of the polymer was initially

introduced by Vrentas and Duda [57] and later studied by Romdhane et al. [58].

Furthermore, different thermodynamic models to relate the mutual and the self-diffusion coefficient have been applied in substitution of the Flory-Huggins model. Kim et al. [17] implemented two versions of the UNIFAC-FV model, while Liu et al. [18] suggested the introduction of the Entropic-FV model. In the same area, Vrentas and Vrentas [59] have recently proposed a methodology to obtain the mutual diffusion coefficient from the self-diffusion coefficient without the use of thermodynamic models. Finally, a recent publication reports the inclusion of pressure dependence of the diffusion coefficient (Zhong et al. [60]) through the effect of pressure on the specific volume of both the polymer and the solvent. This is calculated with the hole theory equation of state (SHT EoS).

Extended version of the Zielinski and Duda model

The Zielinski and Duda model though very promising is still limited to small molecules with respect to its predictive capabilities. This is noticeable in the calculation of the ratio of molar jumping units of the solvent and the polymer. Here, the solvent is assumed to jump as a single unit and thereby the volume of the jumping unit is approximated as the volume at 0 K ($\xi = \xi_L$). This applies in general for small molecules but it has been shown (Ju et al. [62], Vrentas et al. [63], Arnould et al. [64]) that larger molecules present a different behaviour and this identified by $\xi < \xi_L$. This behaviour was initially attributed to segmentwise movement of the molecule (Vrentas and Vrentas [65]), that is, the diffusing unit corresponds to only a part of the molecule. This was observed in compounds of long and flexible chain (such as long alkanes) and considered to be highly dependent on the polymer through which diffusion takes place (Vrentas and Vrentas [65]). These observations make it very complicated to develop a predictive model given that the jumping unit of the solvent could be different for each solvent-polymer system.

Another possible explanation was provided by Vrentas et al. [66] where the occurrence of $\xi < \xi_L$ was explained by a variation in the distribution of the hole free volume, where large molecules would attract more of this FV creating a large site for the molecule to jump into as a single unit. This is in fact a relaxation of one the initially made assumptions (see Table 4.4) where the distribution of the hole FV was considered independent of the type of molecules involved (solvent and polymer).

The Zielinski and Duda FV model has been re-derived by Vrentas et al. [66] (in the same terms as the original model) to take into account the effect of the molecular size and shape on the diffusion coefficient, with the considerations of hole free volume accumulation, occurring under the circumstances explained above.

The main equations for the model are thus the same as the original Zielinski

and Duda FV model (Eqs. 4.8 to 4.11), with the only difference that a new form for the calculation of the ratio of molar jumping units (ξ) is introduced (Eq. 4.20) given that this is the parameter through which the molecular size influences the value of the diffusion coefficient.

$$\xi = \frac{\tilde{V}_1^*}{\tilde{V}_2^*}\psi \tag{4.20}$$

$$\psi = \frac{1}{1 + \tilde{V}_1^*/\tilde{V}_2^* \, (1 - 1/(B/A))} \tag{4.21}$$

The ψ parameter then takes into account the asymmetry of the molecule (Eq. 4.21) through the aspect ratio (B/A) of the molecule. This aspect ratio is obtained from the approximation of the molecular jumping unit of the solvent to a rectangular parallelepiped, where A is the side of the cross-section and B the height. Therefore for a symmetric molecule B/A $\rightarrow$ 1 and $\psi = 1$, so the ratio of jumping units is the same as in the original model: $\xi = \xi_L$. Further details on the calculation of the aspect ratio are given later in Appendix E. The final equation for the ratio of jumping units (Eq. 4.22) is obtained by combining Eqs. 4.20 and 4.21.

$$\xi = \frac{\xi_L}{1 + \xi_L \, (1 - 1/(B/A))} \tag{4.22}$$

where, $\xi_L = V_1(0K)/\tilde{V}_2^*$

The final model (hereafter referred to as 'Extended FV model') is then constituted by Eqs. 4.10 and 4.11, with the parameters reported in Table 4.3, and the additional aspect ratio parameter (B/A). The equations needed to estimate the model parameters are Eqs. 4.12 and 4.13 (or Eq. 4.14 if the WLF parameters are not available) to obtain the free-volume parameters, Eq. 4.15 for the pre-exponential factor and Eqs. 4.17, 4.18, 4.20 and 4.21 (or the equivalent 4.22) to obtain the ratio of molar jumping units, and Eq. 4.19 for the Flory-Huggins interaction parameter.

4.4 Extended FV model: Analysis and Application

In this section the Extended FV model presented in section 4.3 is analysed for its application to complex molecules that represent pesticide Active Ingredients. Before that though, a sensitivity analysis of the model parameters is presented.

4.4.1 Parameter sensitivity study

The procedure to obtain each of the parameters of the Extended FV model has been presented in the previous section together with the experimental data of pure compound properties required for their estimation. The pesticide data needed are basically specific volume and viscosity as a function of temperature, and critical volume. These data are not generally available (from measurements) for pesticides so they must be obtained from predictions (more details in section 4.4.2). Then, these predicted property values (specific volume, viscosity, etc.) are subject to inaccuracies, which will affect the estimated values of the model parameters and therefore the diffusivity values obtained from the Extended FV model. It is then the subject of this section to analyse how these possible inaccuracies in the property values (specific volume, viscosity and critical volume) will affect the model parameters and the calculated diffusivities.

The sensitivity analysis is performed for the model parameters that require experimental (or in this case estimated) input data of the pesticide, that is: $K_{1i}/\gamma, K_{2i}$, D_0, ξ and χ. This is illustrated in Table 4.5, where each parameter is related to the experimental data, the equations needed to estimate it and the data sources that will be used for this specific study.

Table 4.5: Experimental data and equations needed for the estimation of the model parameters

Parameter	**Obtained**	**Data needed**	**Data from**
$K_{1i}/\gamma, K_{2i}$	Solvent: Eq. 4.14	η(T), low T	DIPPR correlation
D_0	Eq. 4.15	$\tilde{V}_1$(T)	DIPPR correlation
		Vc	Experiment[(2)]
χ	Eq. 4.19	δ_i	Experiment[(1)]
		$\tilde{V}_1$	DIPPR

[(1)] Brandrup et al. [68]
[(2)] Smith et al. [69]

The effect of deviations of the experimental data is evaluated on the final values predicted for the self-diffusion coefficient (except for the Flory-Huggins parameter that only influences the mutual diffusion coefficient), given that the same effect is then experienced by the mutual diffusion coefficient.

The analysis is performed on the system Ethylbenzene (EB)-Polystyrene (PS), a system that has been widely studied, for which diffusivity data is available and also the values of all the parameters are known (Zielinski and Duda [61]). Moreover, the experimental data required for estimation of each of the parameters can be obtained from the literature and the sources are indicated in Table 4.5. The parameter values for the solvent (not for the polymer) that will be used as a reference are not the ones provided by Zielinski and Duda [61],

but the ones estimated with the experimental data available to us (Table 4.6). This is due to the fact that the values of the solvent parameters are different, either due to the estimation method or to the experimental data.

Table 4.6: Extended FV model parameters for the system Ethylbenzene (EB)-Polystyrene (PS)

Compound	$\tilde{V}_i^*$ (cm^3/g)	$K_{1i}/\gamma \times 10^3$ (cm^3/gK)	$K_{2i} - Tg_i$ **(K)**	$D_0 \times 10^3$ (cm^2/s)	ξ	**E**	χ
EB	0.946	1.40	-104.15	1.09	0.69	0	0.363
PS[a]	0.85	0.582	-327	-			

[a] Taken from Zielinski and Duda [61]

The values predicted for the diffusion coefficient are very similar, but not identical, with either set of parameters as can be seen in Fig. 4.1. Since variations on the property data are to be made, to observe their effect on the diffusion coefficients, this can only be done by taking as a reference the parameter values and diffusivities obtained from the same experimental data for which the variations are to be made.

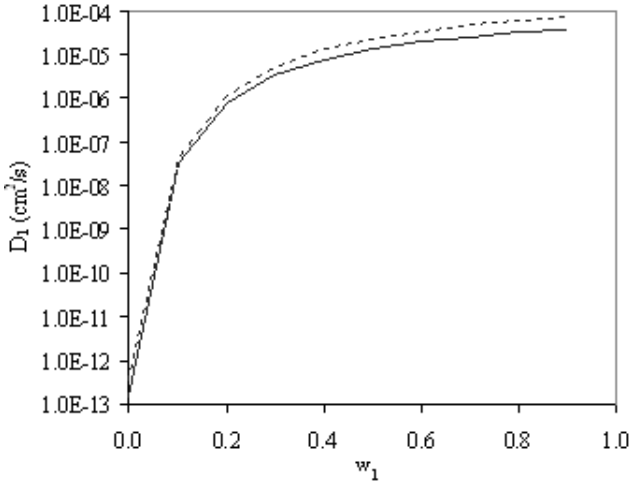

Figure 4.1: Comparison of predictions with the parameters from Zielinski and Duda [61] (—) and the ones of this work (- - -).

The analysis of the effect of inaccuracies in the property values on the model parameters and diffusivities will be presented first for the temperature dependent properties (specific volume and viscosity) in (a), and secondly, for the temperature independent data (critical volume, solubility parameters, aspect ratio) in (b). Note that, even though the solubility parameters are temperature dependent, they are used in the Extended FV model at a single temperature,

therefore their temperature dependence is not relevant for this analysis.

(a) Effect of temperature dependent properties on diffusivity

The parameters estimated from temperature dependent data are: the free volume parameters (K_{1i}/γ, K_{2i}), obtained from viscosity-temperature data, and the pre-exponential factor (D_0) estimated from viscosity-temperature data and also specific volume-temperature data. Two types of inaccuracies in the values of these properties are considered:

Case (i): The property value is always under - or over-predicted but the temperature dependence of the property (viscosity or specific volume) is well reproduced.

Case (ii): The temperature dependence of the property is not well described.

To simulate these inaccuracies (and their effect on diffusivity), the reference (experimental) values are modified as follows:

Case (i): A constant value (corresponding to 25% of the reference property value) is added or subtracted to the reference. This is illustrated in Fig. 4.2(a) and Fig. 4.3(a) for the specific volume and viscosity respectively.

Case (ii): A function is added to the reference values to modify their temperature dependence. This is shown in Fig. 4.2(b) and Fig. 4.3(b) for the specific volume and viscosity respectively.

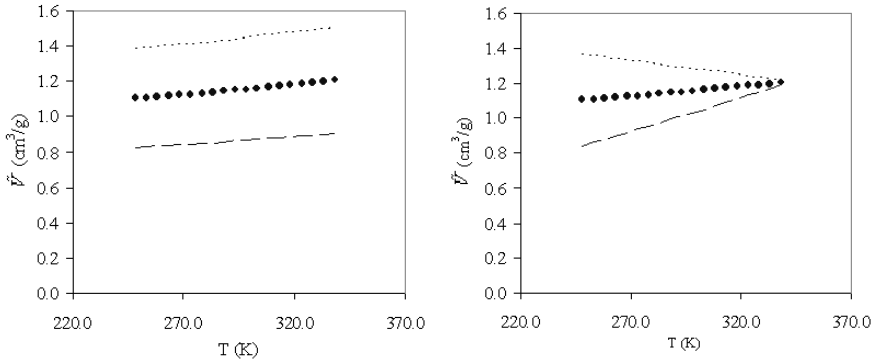

(a) Case (i) (b) Case (ii)

Figure 4.2: Temperature dependence of specific volume ($\tilde{V}$). Where: (•) Reference (Experimental data); (- - -) +25 %; (– –) -25 %.

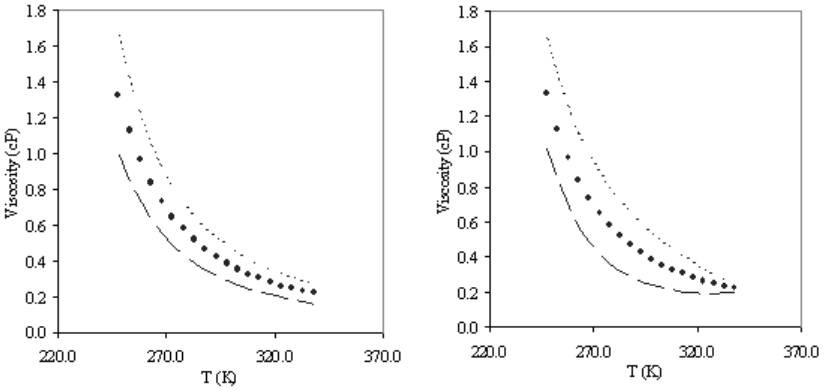

(a) Case (i) (b) Case (ii)

Figure 4.3: Temperature dependence of viscosity. Where: (•) Reference (Experimental data); (- - -) +25 %; (– –) -25 %.

Results of case (i):

The effect of inaccuracies in the specific volume and in the viscosity is observed on the free volume parameters (K_{1i}/γ, K_{2i}) and on the pre-exponential factor (D_0). This is presented in Table 4.7 together with their effect on the calculated diffusivites, evaluated through the average deviation from the reference values (Fig 4.1). Note that remaining parameters (E, ξ and χ) are not affected by these variations and their values are the same as in Table 4.6.

Table 4.7: Ethylbenzene parameters and average deviations obtained from variations (case (i)) in experimental data of specific volume and viscosity.

Exp. data	$\tilde{V}_i^*$ (cm^3/g)	$K_{1i}/\gamma \times 10^3$ (cm^3/gK)	$K_{2i} - Tg_i$ **(K)**	$D_0 \times 10^4$ (cm^2/s)	**AAD%**
reference	0.946	1.40	-104.15	10.9	
+25% $\tilde{V}$	0.946	1.40	-104.15	8.73	20.0
-25% $\tilde{V}$	0.946	1.40	-104.15	14.6	-33.3
+25% Viscosity	0.946	1.40	-103.10	8.55	20.5
-25% Viscosity	0.946	1.40	-104.15	14.6	-33.4

From Table 4.7 it can be observed that the pre-exponential factor is the only parameter affected by these inaccuracies in the specific volume and viscosity. The deviation in both properties affects the final calculated diffusivities in the same manner and magnitude, as seen from the AAD% values reported.

Results of case (ii):

The effect of a wrong temperature dependence of the specific volume and the viscosity on the estimated model parameters is shown in Table 4.8, together with the effect on the calculated diffusivities (through AAD%).

Table 4.8: Ethylbenzene parameters and average deviations obtained from variations (case (ii)) in experimental data of specific volume and viscosity.

Exp. data	$\tilde{V}_i^*$ (cm^3/g)	$K_{1i}/\gamma \times 10^3$ (cm^3/gK)	$K_{2i} - Tg_i$ **(K)**	$D_0 \times 10^4$ (cm^2/s)	**AAD%**
reference	0.946	1.40	-104.15	10.9	
+25% $\tilde{V}$	0.946	1.40	-104.15	9.92	-9.05
-25% $\tilde{V}$	0.946	1.40	-104.15	12.4	13.5
+25% Viscosity	0.946	1.40	-107.20	8.91	-21.5
-25% Viscosity	0.946	1.40	-98.42	14.0	39.3

In this case, deviations in the viscosity and the specific volume affect the free volume parameters (K_{2i}) and the pre-exponential factor (D_0). The deviations in the viscosity however, have a much greater effect on the calculated diffusivities (as seen from the AAD% values).

(b) Effect of non-temperature dependent properties on diffusivity:

Now the variations in the remaining properties (critical volume, aspect ratio and solubility parameters) are analysed in terms of their effects on the diffusivity values. It is worth noting that the variation of the ratio of jumping units (ξ) used is 15%, caused by a 25% variation on the aspect ratio (B/A, which is the actual 'experimental' value). In the case of the Flory-Huggins interaction parameter (χ), the variation is only 15% because the data at high concentrations is very sensitive to this value. The variation of the value of this parameter does not affect the self-diffusion coefficient but the mutual diffusion coefficient (see Eqs. 4.8 to 4.10), therefore the effects are analysed for the latter. The experimental data used to calculate the Flory-Huggins interaction parameter are the solubility parameters. This parameter does not play a role in the systems of interest in this work, given that the concentrations of interest have been limited to low (infinite dilution) values for the solvent, where this parameter has no effect. Even so, the sensitivity analysis has been done given that it can become relevant in the case that a higher concentration would need to be considered.

It is worth noting that deviations in the value of the critical volume affect the model parameters as well as the calculated diffusivites, while changes on the ratio of jumping units (ξ) and the Flory-Huggins parameter (χ) only affect the diffusivities. The model parameters and the average deviations from the reference diffusivities are given in Table 4.9.

Table 4.9: Ethylbenzene parameters and average deviations obtained from variations in experimental data of Vc, ξ and χ.

Exp. data	$\hat{V}_i^*$ (cm^3/g)	$K_{1i}/\gamma \times 10^3$ (cm^3/gK)	$K_{2i} - Tg_i$ **(K)**	$D_0 \times 10^4$ (cm^2/s)	**AAD%**
reference	0.946	1.40	-104.15	10.9	
+25% Vc	0.946	1.40	-104.15	12.7	16.1
-25% Vc	0.946	1.40	-104.15	9.01	-17.4
+15% ξ	0.946	1.40	-104.15	10.9	-33.6
-15% ξ	0.946	1.40	-104.15	10.9	306.7
+15% χ	0.946	1.40	-104.15	10.9	-13.9
-15% χ	0.946	1.40	-104.15	10.9	13.9

From Table 4.9 it is observed that deviations on the ratio of molar jumping units have a much greater effect on the calculated diffusivities than the critical volume or the Flory-Huggins parameter, and especially when the deviations are negative. In the cases of the ratio of molar jumping units and the Flory-Huggins parameter, the variations in their values have different effects over the concentration range. This is illustrated in Fig. 4.4.

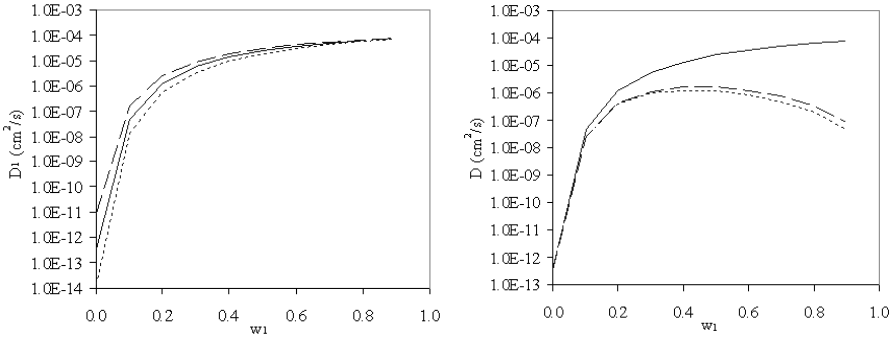

(a) Variations of ±15% in ξ

(b) Variations of ±15% in χ

Figure 4.4: Effect of variations of ξ (on the self-diffusion coefficient) and χ (on the mutual diffusion coefficient). Where: (—) Reference; (- - -) +15 %; (– –) -15 %.

In Fig. 4.4 it is observed that in the case of the ratio of jumping units (Fig. 4.4(a))) the effects on the diffusivity are higher at low concentrations of the solvent, while the Flory-Huggins parameter has a significant effect on the mutual diffusion coefficient at high concentrations (Fig. 4.4(b))).

Summary and conclusions:

The effect of deviations or inaccuracies in the property values (specific volume, viscosity, etc.) on the self-diffusion coefficient (and mutual diffusion coefficient in the case of χ) has been summarized in Table 4.10 and for clarity purposes plotted in Fig. 4.5.

Table 4.10: Summary table of the effects of experimental data deviations on the self-diffusion coefficients (and mutual diffusion coefficient in the case of χ).

Exp. data	**AAD%**	
Variation 25%	**+**	**-**
$\tilde{V} - T$	-20	33.3
Viscosity-T	-20.5	33.4
Vc	16.1	-17.4
Variation 15%	**+**	**-**
ξ	-33.6	306.7
χ	-13.9	13.9

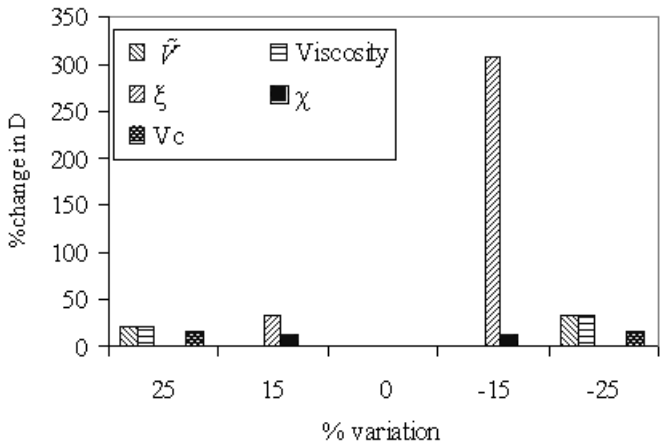

Figure 4.5: Effect of variations in the parameters and properties on the diffusivity.

To conclude, it can be observed that even high inaccuracies (up to 25%) in the temperature dependent properties (viscosity and density) do not cause a much higher error in the estimation of the diffusion coefficient. While the diffusivity is significantly more sensitive to deviations in the calculation of other parameters, such as the ratio of jumping units (obtained from the aspect ratio, B/A, where this one carries a 25% error).

4.4.2 Application of the model to complex molecules: regression of model parameters

The Extended FV model (from section 4.3) is the selected model. Although Vrentas et al. [66] treated a number of compounds (see Table 4.11), they cannot be considered representative for pesticide molecules (Table 4.12), which is the subject of this study.
In Table 4.11, the nature of the compounds studied by Vrentas et al. [66] is presented, in terms of the different families of compounds treated (alkanes, aromatics, etc.), with some representative examples of each type, the range of volumes of the compounds at absolute zero temperature and their molecular structures. This gives an idea of the size of the compounds.
In Table 4.12 the same type of information is provided but now including the compounds of interest in this work. The first observation to be made is the increased complexity of the compounds in Table 4.12 with respect to the previous ones (Table 4.11), regarding the functionalities and the molecular structure. And in the second place the range of molar volumes (at 0 K) is significantly bigger for the compounds in Table 4.12. These observations indicate that the fact that the model can be applied to large and complex molecules needs to be tested and validated, and this is the objective of this section. In order to prove the validity of the model to complex molecules, two types of tests have been considered:

- The first involves the appropriateness of the Extended FV model to describe the diffusion behaviour of the systems under study, that is, verify the ability of the model to correlate the temperature dependence of diffusivity and therefore indicate whether the model is applicable to these systems.
- The second step is the evaluation of the predictive capabilities of the model regarding molecules that are significantly more complex (and larger) than the ones originally studied by Vrentas et al. [66].

In order to do this analysis the need for a large amount of experimental data of diffusion coefficients as a function of temperature and/or concentration arises. As mentioned earlier, this amount of data is currently not available for pesticide compounds. In order to overcome this difficulty, a wide literature search has been performed, and data for a number of different systems, such as dye molecules (Table 4.12) that are comparable to pesticide compounds in terms of of size and complexity has been compiled and used in this study. For a few pesticide systems for which experimental data is available, the applicability of the Extended FV model will be tested, in the second part of this section (4.4.2.2). In the third part of this section (4.4.2.3) results from a study of some compounds found in controlled release literature and for which some data of diffusion coefficients has been reported at a single temperature are presented.

This is an interesting part of the application of the free volume model since it involves polymers that are used in the field of interest of this work, such as polyureas.

Table 4.11: Compounds treated in Vrentas et al. [66].

Group	**Compounds**	**V (0 K)** (cm^3/mol)	**Representative structures**
Small compounds	Methanol, Acetone	30 ∼ 55	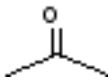
Aromatics	Benzene, Ethylbenzene, Xylenes, Triisopropylbenzene, ...	70 ∼ 199	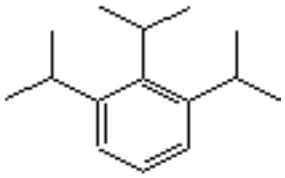
Acetates	C1 ∼ C5	63 ∼ 117	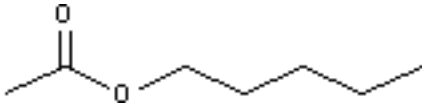
Alkanes	C6 ∼ C10	98 ∼ 152	
Branched alkanes	2-methylpentane, 2,3-dimethylbutane, ...	95	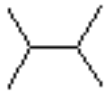
Alkenes	1-hexene, 1,4-hexadiene, ...	87 ∼ 91	

Table 4.12: Dye and pesticides compounds to be treated in this work

Group	**Compounds**	**V (0 K)** (cm^3/mol)	**Representative structures**
Dyes [62]	PNA, PAAB, Yellow 7	106 ∼ 233	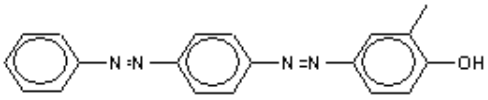
Dyes [73]	Orange 3, Red 1		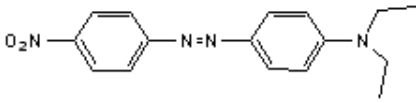
Dyes [73]	Red 4, Dye I, Dye II	180 ∼ 243	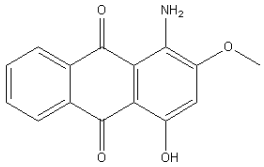
Dyes [72]	TTI, ONS A, ONS B, ONS N, ...	188 ∼ 382	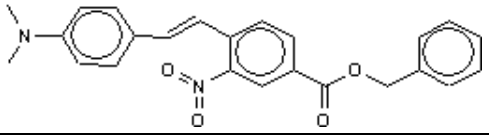
Pesticides	Permethrin, λ-cyhalothrin,...	280 ∼ 307	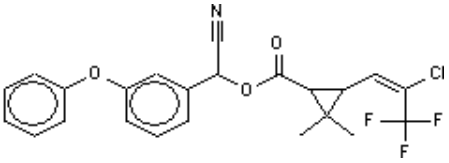
Pesticides	Thiamethoxam	180	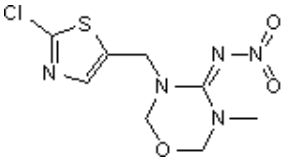
Drugs	Codeine	299	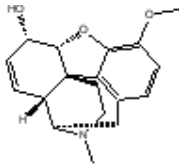

4.4.2.1 Complex molecules (non-pesticides)

In this section the results of the analysis of the Extended FV model applied to complex molecules (not pesticides) are presented.

Analysis of correlative ability

First the correlative capabilities of the Extended FV model are analysed. The compiled experimental data (diffusion coefficients as a function of temperature in the limit of zero diffusant concentration) is fitted to the Extended FV model. The fitted model parameters include the pre-exponential factor (D_0) and the ratio of jumping units (ξ) for each system evaluated and they are reported in Table 4.13. These parameters will be used in the following analysis as experimental values.

The estimation of these parameters includes the assumption of infinite dilution conditions for the diffusant molecule, and the equation to be fitted is Eq. 4.23 (derived from Eq. 4.11). For the systems reported in Table 4.13 this assumption has been reported and also used in some of the cases.

$$\ln D_1 = \ln D_0 - \frac{-\xi \tilde{V}_2^*}{\frac{K_{12}}{\gamma}\left(K_{22} - T_{g2} + T\right)} \tag{4.23}$$

As pointed out earlier, as $D \rightarrow D_1$ at infinite dilution (see Eq. 4.10), the Flory-Huggins interaction parameter (χ) is not needed. As the glass transition temperature of the polymer is important (defines the temperature limit of the model), these values are listed in Table 4.13.

Table 4.13: Table with the parameters of the Extended FV model obtained from experimental data fitting of diffusivity as a function of temperature.

Source	**Solvent**	**Polymer**	**T range data (K)**	Tg_2 **(K)**	$D_0(cm^2/s)$	ξ
[70],[71]	PNA	PS	388 - 423	373	4.49×10^{-5}	0.48
[70],[71]	PAAB	PS	387 - 443		4.94×10^{-4}	0.698
[70],[71]	Disp. Yellow 7	PS	403 - 443		3.81×10^{-4}	0.799
[72]	TTI	PC	423 - 453	423	3.79×10^{-4}	0.754
[72]	ONSN	PC	423 - 453		1.13×10^{-3}	0.867
[72]	ONSB	PC	423 - 453		7.95×10^{-4}	0.852
[72]	ONSA	PC	423 - 453		1.31×10^{-2}	1.113
[72]	TTI	PS	412 - 452	373	5.43×10^{-4}	0.834
[72]	TTI	PES	412 - 452	355	1.87×10^{-3}	0.789
[72]	TTI	PMMA	412 - 452	390	2.74×10^{-4}	0.87
[72]	TTI	PEMA	412 - 452	335	5.36×10^{-3}	0.796
[73]	Orange3	PET-B	384 - 434	346.6	3.00×10^{-4}	0.806
[73]	Red1	PET-B	400 - 454		2.87×10^{-4}	0.871
[73]	Disp. Yellow 7	PET-B	400 - 476		1.71×10^{-5}	0.773
[73]	Disp. Yellow 7	PET-A	400 - 476		6.93×10^{-7}	0.449
[73]	Disp. Yellow 7	PET-D	400 - 476		1.52×10^{-4}	0.95
[73]	PNA	PET-B	346 - 400		1.29×10^{-5}	0.489
[73]	PNA	PET-A	357 - 435		2.92×10^{-7}	0.255
[73]	Red4	PET-A	384 - 455		4.49×10^{-7}	0.338
[73]	Red4	PET-D	384 - 455		2.94×10^{-4}	0.904
[74]	Disp. Yellow 7	iPP (A)	323 - 423	253	1.10	1.685
[74]	Dye I	iPP (A)	323 - 423		5.28×10^{-2}	1.19
[74]	Dye II	iPP (A)	323 - 423		4.39×10^{-3}	1.027
[74]	Dye I	iPP (A)	323 - 423		2.69×10^{-1}	1.308
[74]	Dye II	iPP (A)	323 - 423		2.94×10^{-1}	1.337
[74]	Disp. Yellow 7	iPP (B)	323 - 423	253	5.45×10^{-4}	2.327
[74]	Dye I	iPP (B)	323 - 423		5.42×10^{-3}	1.245
[74]	Dye I	PE (A)	344 - 384	148	28.1	3.594
[74]	Dye I	PE (B)	344 - 384	148	1.74×10^{-2}	2.793
[62]	PNA	PVAc	353 - 413	305	7.54×10^{-2}	0.854
[62]	PAAB	PVAc	353 - 423		1.17×10^{-1}	0.934
[62]	Disp. Yellow 7	PVAc	353 - 423		4.94×10^{-2}	1.1
[75]	PAAB	Nylon 6	323 - 343	273.15	7.60×10^{-7}	1.008

In all of the cases presented in Table 4.13, the experimental data could be correlated with the Extended FV model and the parameters obtained. As an example to illustrate the good correlation obtained with the Extended FV model, the experimental diffusivity data has been plotted (see Fig. 4.6) together with the correlated values for three dyes diffusing in PS (Masuko et al.

[71]) where the parameters obtained correspond to those in Table 4.13. The correlation results for the remaining systems are not provided given that they are equivalent to these.

The conclusion from this part is that the Extended FV model provides a good description of the systems involving large and complex molecules.

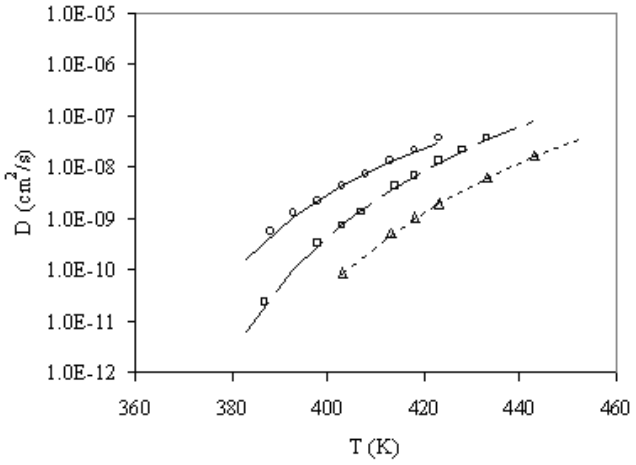

Figure 4.6: Comparison of experimental values with correlation using the free volume model with the parameters reported in Table 4.13, for the diffusion of three dyes in PS. Experimental points: (o) PNA; (□) PAAB, (△) Disperse Yellow 7. Correlation results: (—) PNA; (– –) PAAB, (- - -) Disperse Yellow 7.

Analysis of predictive capabilities

The next step is to evaluate the predictive capabilities of the free volume model, especially with respect to the shape of the molecules. In this context the parameter values estimated above from diffusivity data (Table 4.13) are now considered as experimental values. Together with the systems in Table 4.13 and in order to provide a more complete study of the predictive capabilities of the model, data from additional systems, presented in Table 4.14, is included. For these systems, again, experimental data of diffusivity as a function of temperature is available and thus these are fitted to the model (in the same manner as above) to obtain the necessary parameters (D_0 and ξ). These new systems are interesting, even though they do not involve complex or large molecules, because they include some polymers that have not been previously considered (Balashova et al. [76]) and also for completeness of the study reported by Vrentas et al. [66].

Table 4.14: Table with the parameters of the Extended FV model obtained from experimental data fitting of diffusivity as a function of temperature.

Source	**Solvent**	**Polymer**	**T range data (K)**	Tg_2 **(K)**	$D_0(cm^2/s)$	ξ
[76]	NMP	PSF	473 - 523	459	1.50×10^{-5}	0.286
[76]	γ-butyrolactone	PSF	473 - 523		1.79×10^{-5}	0.271
[76]	acetic acid	PSF	473 - 523		1.22×10^{-5}	0.199
[76]	propionic acid	PSF	473 - 523		1.77×10^{-5}	0.246
[76]	THF	PSF	473 - 523		1.64×10^{-5}	0.259
[40]	Methyl acetate	PMA	289 - 336	276	6.31×10^{-2}	0.626
[40]	Ethyl acetate	PMA	286 - 391		3.98×10^{-2}	0.638
[40]	Propyl acetate	PMA	?		1.59×10^{-2}	0.638
[40]	Butyl acetate	PMA	?		3.16×10^{-2}	0.688

Finally, some additional systems for which experimental data of diffusivity is not available but the value of the parameters (ξ) have been reported, have also been included in this analysis (see Table 4.15). Note that these systems can only be used to analyse the predictions of the ratio of jumping units, and not the pre-exponential factor, which is not available.

Table 4.15: Table with the parameters of the Extended FV model obtained from the literature.

Source	**Solvent**	**Polymer**	ξ
[40]	n-Butane	PIB	0.958
[40]	iso-Butane	PIB	1
[40]	n-pentane	PIB	0.918
[40]	iso-pentane	PIB	1.04
[40]	Neopentane	PIB	1.03
[40]	n-dodecane	PIB	0.907
[40]	n-hexadecane	PIB	0.908
[40]	1,1-diphenylethane	PIB	0.946
[40]	cyclohexane	PIB	0.897
[40]	2,2,5-trimethylhexane	PIB	0.981
[77]	n-hexane	PIB	0.94
[77]	n-heptane	PIB	1.05
[77]	n-octane	PIB	1.07

Some temperature dependent data of the diffusivity of complex molecules (Foldes [78], Foldes [4], Bonifaci et al. [79]) which is available was actually not used since the temperatures of the experiments are very high, implying that the energy effects would be dominant in the diffusion process, instead of the effect of the free volume.

Pure prediction of the model parameters:

The parameters of the model are now estimated in a purely predictive manner according to the procedure summarized in section 4.3 (Tables 4.3 and 4.5). This is combined with the pure prediction of the ratio of molar jumping units (ξ) by taking into account the molecular shape (as described in the last part of section 4.3). The experimental data required for the estimation of all the model parameters is listed in Table 4.16 together with the sources and methods used to obtained each of them.

Table 4.16: Experimental data required by the model and sources to obtain them

Property	**Source/Method**
η(T) solvent	GC methods (CSGC-VK, Yinghua et al. [81])
$\tilde{V}$(T)	GC method (Marrero and Gani [82])
$C_{1j}^{WLF}, C_{2j}^{WLF}$	Ngai et al. [50], Zielinski and Duda [61]

All the model parameters obtained are reported in Table 4.17 for the diffusant molecules and in Table 4.18 for the polymers. For some of the systems in Table 4.15 the pure component model parameters (D_0, K_{11}/γ, K_{21}) are not estimated given that,

i) The pre-exponential factor (D_0) cannot be compared with experimental data because this is not available.

ii) The free volume parameters (K_{11}/γ, K_{21}) are already available in the literature (Shapiro et al. [83]).

Finally the predictions of the ratio of jumping units are given in Table 4.19 for each of the systems studied, together with the values of the pre-exponential factor.

Table 4.17: Table with the parameters of the Extended FV model for diffusant molecules.

Solvent	**Mw (g/mol)**	V(0K) (cm^3/g)	$K_{11}/\gamma \times 10^3$ (cm^3/gK)	$K_{21} - Tg_1$ **(K)**	$D_0(cm^2/s) \times 10^4$	**B/A**
PNA	138.12	0.77	1.40	-159.43	1.83	1.463
PAAB*	197.24	0.78	1.43	-115.57	0.287	2.148
Disp. Yellow 7*	316.36	0.74	1.35	-204.77	0.146	2.925
TTI	256.38	0.73	1.38	-167.7	1.37	1.342
ONSN	293.32	0.78	1.47	-159.21	16.2	1.66
ONSB	402.44	0.77	1.44	-163.4	12.2	1.577
ONSA*	506.55	0.75	1.42	-235.81	2.05	1.496
Orange3*	242.23	0.74	1.32	-312.6	0.282	2.347
Red1*	298.34	0.79	1.48	-263.84	0.492	2.179
Red4	269.25	0.67	1.57	-322.58	0.306	1.306
Dye I	293.36	0.78	1.59	-307.2	3.54	1.547
Dye II	307.39	0.79	1.60	-318.4	3.05	1.476
NMP	99.13	0.86	1.92	-139.53	1.31	1.185
γ-butyrolactone	86.09	0.77	1.45	-788.31	0.124	1.167
acetic acid	60.05	0.76	1.41	-118.71	3.38	1.234
propionic acid	74.08	0.82	1.49	-99.96	2.47	1.395
THF	72.11	0.91	1.67	-45.59	1.90	1.223
Methyl acetate	74.08	0.85	0.934	-24.63	14.4	1.319
Ethyl acetate	88.11	0.88	1.38	-36.04	3.34	1.364
Propyl acetate	102.13	0.9	1.67	-66.43	2.33	1.681
Butyl acetate	116.16	0.92	1.69	-89.21	2.35	1.888

Some comments need to be made with respect to the estimations of the previous parameters:

i) In some cases (marked with *) the compounds could not be fully described by the group contribution methods for estimation of viscosity. The calculations have been done even though a group was missing in the molecule representation and the free volume parameters are given in Table 4.17. This can be the cause of some inaccuracies in the prediction of the pre-exponential factor because the free-volume parameters take part in the calculation for this last one.

ii) In some of the published data (Ito et al. [73]) the diffusivity values are given for several samples of the same polymer, having different properties (generally different crystallinities). No explanation or additional information is provided of these differences in the properties. The different degrees of crystallinity of the polymer are considered to be mainly related to its mobility and this is reflected in the diffusivity model (Extended FV model) through the size of the polymer jumping unit ($\tilde{V}^*_{2j}$).

Table 4.18: Table with the parameters of the Extended FV model for polymers.

Polymer	$K_{11}/\gamma \times 10^4$ (cm^3/gK)	$K_{21} - Tg_1$ **(K)**	C_1^{WLF}	C_2^{WLF} **(K)**	Tg_2 **(K)**	$\tilde{V}^*_{2j}$ (cm^3/gK)
PS	5.68	-327	13.78	46	373	174.12
PC	5.82	-370.8	10.4	52.2	423	252.08
PES	4.50	-286.9	12.38	68.1	355	174.12
PMMA	4.00	-319.9	12.21	70.1	390	184.74
PEMA	3.08	-269.5	17.62	65.5	335	121.55
PET-B	3.84	-303.97	17.7	42.63	346.6	128.77
PET-A	3.84	-303.97	17.7	42.63	346.6	-
PET-D	3.84	-303.97	17.7	42.63	346.6	-
iPP (A)	5.17	-205.4	18.24	47.6	253	70.52
iPP (B)	5.17	-205.4	18.24	47.6	253	-
PE (A)	8.44	-161.15	n/a	n/a	148	32.94
PE (B)	8.44	-161.15	n/a	n/a	148	-
PVAc	4.45	-258.2	15.59	46.8	305	88.8
Nylon 6	39.5	-296.35	3.55	26.8	273.15	82.97
PSF	4.34	-410	15.1	49	459	329.02
PMA	3.98	-231	18.13	45	276	96.6
PIB	2.59	-100.6	16.63	104.4	205	-

Therefore the different degrees of crystallinity of this polymer have been taken into account by calculating different polymer jumping units for each of the samples ($\tilde{V}^*_{2j}$). In order to do these calculations, one of the diffusant-polymer systems is taken to be the reference, that is Disp. Yellow 7 in PET-B. This choice is based on the fact that Disp. Yellow 7 has been studied in a number of other polymers with good results, and also the majority of the compounds in Ito et al. [73] have been studied in this sample (PET-B), again with satisfactory results. The value of the polymer jumping unit for PET-B is therefore not modified. Then, based on the values of the ratio of jumping units (ξ) obtained from correlation of diffusivity data (Table 4.13) for Disp. Yellow 7 in each of the remaining PET samples (A, D), and the aspect ratio of Disp. Yellow 7, the value of the polymer jumping units ($\tilde{V}^*_{2j}$) can be back-calculated for these other PET samples, using the definition of ξ_L (Eq. 4.24) in Eq. 4.22.

$$\xi_L = \frac{V(0K)}{\tilde{V}^*_{2j}} \tag{4.24}$$

The results of accounting for the different properties of the polymer samples in this manner are satisfactory for PET and the values of the polymer jumping units obtained are reported in Table 4.20.

Table 4.19: Table with the predicted parameters of the Extended FV model for the systems studied.

Source	**Solvent**	**Polymer**	$D_0(cm^2/s)$	ξ
[70],[71]	PNA	PS	1.83×10^{-4}	0.613
[70],[71]	PAAB	PS	2.87×10^{-5}	0.695
[70],[71]	Disp. Yellow 7	PS	1.46×10^{-5}	0.798
[72]	TTI	PC	1.37×10^{-4}	0.84
[72]	ONSN	PC	1.62×10^{-3}	0.853
[72]	ONSB	PC	1.22×10^{-3}	1.067
[72]	ONSA	PC	2.05×10^{-4}	1.259
[72]	TTI	PS	1.37×10^{-4}	0.975
[72]	TTI	PES	1.37×10^{-4}	1.035
[72]	TTI	PMMA	1.37×10^{-4}	0.924
[72]	TTI	PEMA	1.37×10^{-4}	1.11
[73]	Orange3	PET-B	2.82×10^{-5}	0.772
[73]	Red1	PET-B	4.92×10^{-5}	0.921
[73]	Disp. Yellow 7	PET-B	1.46×10^{-5}	0.827
[73]	Disp. Yellow 7	PET-A	-	-
[73]	Disp. Yellow 7	PET-D	-	-
[73]	PNA	PET-B	1.83×10^{-4}	0.652
[73]	PNA	PET-A	7.40×10^{-6}	0.265
[73]	Red4	PET-A	3.06×10^{-5}	0.439
[73]	Red4	PET-D	6.69×10^{-3}	1.336
[74]	Disp. Yellow 7	iPP (A)	1.46×10^{-5}	1.042
[74]	Dye I	iPP (A)	3.54×10^{-4}	1.509
[74]	Dye II	iPP (A)	3.05×10^{-4}	1.631
[74]	Dye I	iPP (A)	3.54×10^{-4}	1.509
[74]	Dye II	iPP (A)	3.05×10^{-4}	1.631
[74]	Disp. Yellow 7	iPP (B)	1.46×10^{-5}	1.042
[74]	Dye I	iPP (B)	5.42×10^{-3}	1.245
[74]	Dye I	PE (A)	3.54×10^{-4}	2.657
[74]	Dye I	PE (B)	3.54×10^{-4}	2.657
[62]	PNA	PVAc	1.83×10^{-4}	0.865
[62]	PAAB	PVAc	2.87×10^{-5}	0.899
[62]	Disp. Yellow 7	PVAc	1.46×10^{-5}	0.963
[75]	PAAB	Nylon 6	2.87×10^{-5}	0.695
[76]	NMP	PSF	1.31×10^{-4}	0.249
[76]	γ-butyrolactone	PSF	1.24×10^{-5}	0.196
[76]	acetic acid	PSF	3.38×10^{-4}	0.136
[76]	propionic acid	PSF	2.47×10^{-4}	0.175
[76]	THF	PSF	1.90×10^{-4}	0.193
[40]	Methyl acetate	PMA	1.44×10^{-3}	0.572
[40]	Ethyl acetate	PMA	3.34×10^{-4}	0.652
[40]	Propyl acetate	PMA	2.33×10^{-4}	0.701
[40]	Butyl acetate	PMA	2.35×10^{-4}	0.733

Table 4.20: Polymer jumping units for each PET sample

Polymer	**Sample**	$\tilde{V}^*_{2j}$
PET	A	366.38
	B	128.77
	C	n/a
	D	92.12

iii) Okajima et al. [74] reported experimental data for diffusion of dye compounds in isotactic PP, but since the parameters needed by the free volume model (WLF constants) are only available for atactic PP, these are the ones used. In the correlation of experimental diffusivity data the values obtained for the pre-exponential factor (Table 4.13) are abnormally high, greater than 10^{-3}, when usually they are less than or equal to 10^{-3}.

Another indicator of a possible problem is the fact that while the prediction of the compound Disp. Yellow 7 in other polymers (PET and PS) are very good, these are significantly wrong for PP when comparing the predictions (Table 4.19) with the experimentally obtained parameter values (for D_0 and ξ). This brings the discussion back to the question of what is the most appropriate description of the polymer behaviour.

In the isotactic polymer the pendant groups are all located in the same side therefore it presents a higher ordering than the atactic one, where the pendant groups are randomly located. It is therefore more likely for an isotactic polymer to form packed structures and crystals, and from that it is expected that it will present different diffusive properties than the atactic one. The atactic form of PP is more amorphous than the isotactic one, thus by introducing the crystallinity effects the value of the pre-exponential factor would decrease and be closer to the predicted one.

In this study this cannot be further analysed because of the unavailability of the WLF parameters ($C^{WLF}_{1j}, C^{WLF}_{2j}$) for the isotactic polymer, and these systems are therefore not included in the next analysis of the results.

In order to evaluate the predicted results the values of the parameters obtained from experimental diffusivity data (Table 4.13 to 4.15) have been compared with those obtained from pure prediction (Table 4.17 to Table 4.19) in Fig. 4.7 for the ratio of jumping units and in Fig. 4.8 for the pre-exponential factor.

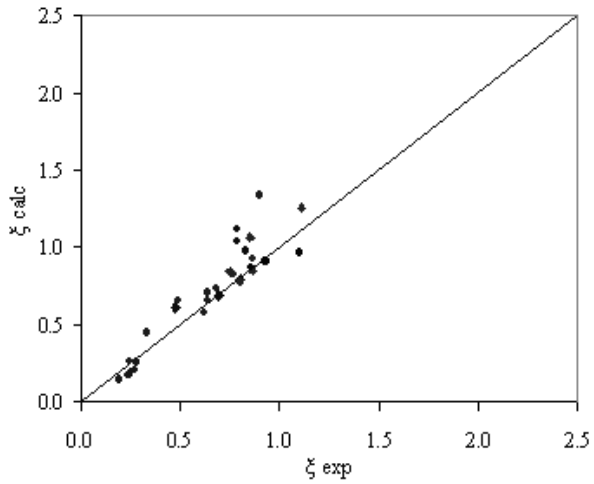

Figure 4.7: Comparison of experimental and predicted values of the ratio of jumping units.

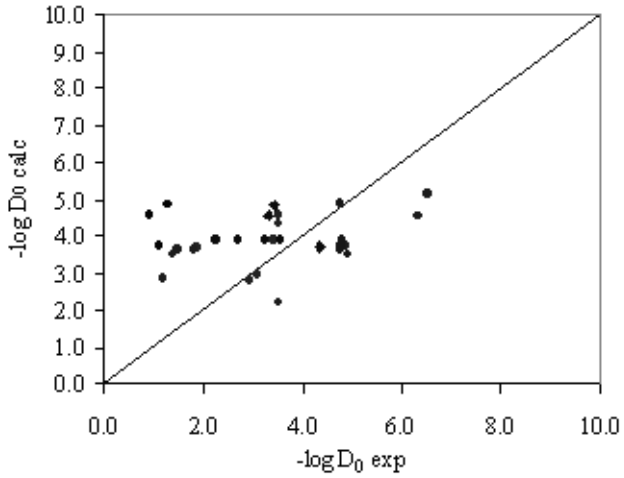

Figure 4.8: Comparison of experimental and predicted values of the pre-exponential factor (D_0 in cm^2/s).

As it can be seen from the plots the results for the ratio of jumping units (Fig. 4.7) are in general very good. This is the parameter that takes into account the shape of the molecules, it is therefore the most significant when moving from relatively small and simple molecules (in the existing literature) to larger and more complex molecules, as the ones in this work. A few points

are markedly overpredicted, that is for example the case of the dye Red 4 in PET (D). The inaccuracy in this value can be attributed to the considerations made for the different PET samples explained in (ii). Other inaccuracies in the values of the ratio of jumping units can be due to the values of the polymer jumping units that are currently obtained from experimental correlations as a function of the glass transition temperature of the polymer. There is room for improvement in this area as more data becomes available so the correlations represent a greater number of polymers.

This is in general a very encouraging result for the use of this predictive Extended FV model for complex molecules such as pesticides.

On the other hand, regarding the comparison of the experimental and predicted values of the pre-exponential factor, the results present a significant deviation for an important number of systems. This can be explained as follows: in the prediction of the pre-exponential factor (D_0), without use of diffusivity data, this parameter is considered to be a property of the solvent and is thus obtained only through values of pure component properties of the solvent. That is, it does not take into account any property or characteristic of the polymer or the solvent-polymer system. Alternatively, when the value of this parameter (D_0) is obtained from regression of the experimental diffusivity data, it might include extra effects (such as energy effects, even if not dominant) due to the form of the equation (Eq. 4.8) and the assumptions made. This aspect is better explained through an analysis of the model equations.

i) Analysis of energy effects:

With respect to the fitting of experimental diffusivity data, the original equation to be regressed is Eq. 4.25, obtained from Eq. 4.8 with the only assumption of infinite dilution of the diffusant compound, and applying the logarithms for illustration purposes.

$$\ln D_1 = \ln D_0 - \frac{E}{RT} - \frac{-\xi \tilde{V}_2^*}{\frac{K_{12}}{\gamma}\left(K_{22} - T_{g2} + T\right)} \tag{4.25}$$

For the regression of the pre-exponential factor (lnD_0), the energy term (E) in Eq. 4.25 is assumed negligible and the actual equation fitted is Eq. 4.23. If, on the other hand, this assumption (E=0) does not apply, the actual value of D_0 obtained from regression of diffusivity data ($D_1(T)$) comprises also this energy term (E) (see Eq. 4.25) and the actual parameter estimated is an average value, $D_{0,aver}$ (Eq. 4.26).

$$\ln D_{0,aver} = \ln D_0 - \frac{E}{RT} \tag{4.26}$$

Then the actual value of the pre-exponential factor (D_0) would be given by Eq. 4.27.

$$\ln D_0 = \ln D_{0,aver} + \frac{E}{RT} \tag{4.27}$$

Note that here the energy term refers to infinite dilution concentration of the solvent.

With respect to the prediction of the pre-exponential factor (D_0) from solvent properties, without use of diffusivity data, Eq. 4.15 is used (the previous Eq. 4.15 is given below for clarity purposes).

$$\ln\left(\frac{0.124 * 10^{-16}\tilde{V}_c^{2/3}RT}{\eta_1 M w_1 \tilde{V}_1}\right) = \ln D_0 - \frac{E\,(w_1 \to 1)}{RT} - \frac{\gamma\tilde{V}_1^*/K_{11}}{K_{21} + (T - T_{g1})}$$

Here again, an energy term appears, that is also neglected for the estimation of the pre-exponential factor (D_0). This energy term refers though to a pure solvent concentration, unlike the case above (estimation from diffusivity data). The differences in these energy terms are therefore likely to be the cause of the final deviations observed between the values of the pre-exponential factors obtained from either diffusivity data or pure prediction from solvent properties.

ii) Analysis of crystallinity effects:

In the case of possible deviations due to the crystallinity of the polymer, Lutzow et al. [80] added a tortuosity factor (τ) to the Extended FV model equation, that increases the diffusion path length, and then the model equation for diffusivity is given by,

$$D_1 = D_0 \exp\left(\frac{-\xi\tilde{V}_2^*}{K_{12}/\gamma\,(K_{22} - T_{g2} + T)}\right)\frac{1}{\tau} \tag{4.28}$$

where the energy term (E) has been neglected. Note that this equation is equivalent to Eq. 4.23 but with the additional tortuosity term.

Then, from estimation of the pre-exponential factor (D_0) using diffusivity data, the value obtained would correspond to an average value ($D_{0,aver}$) defined as,

$$\ln D_{0,aver} = \ln D_0 - \ln \tau \tag{4.29}$$

Then, the actual value corresponding to the pre-exponential factor would be given by,

$$\ln D_0 = \ln D_{0,aver} + \ln \tau \tag{4.30}$$

This tortuosity term though, does not appear when the pre-exponential factor is obtained from pure prediction (Eq. 4.15). So, again, these differences can be the cause of the deviations between the parameter values obtained from diffusivity data or the ones from pure prediction.

Summarizing, in the same manner as explained above, any other characteristics of the polymer (such as cross-linking) will implicitly be captured in the value of the pre-exponential factor obtained from the correlation of the diffusivity data. In some of the cases studied here, this is a known effect given that different samples of the same polymer are reported with different crystallinities (PET in Ito et al. [73]) and values of the pre-exponential factor are obtained for the same compounds having different orders of magnitude.

Therefore the imprecisions on the prediction of this parameter are not attributed to the fact that the model is applied to large and complex molecules but rather to the need of more detailed models to take into account crystallinity and cross-linking degrees of the polymer. This can specially be observed in the case of PP, where the necessary parameters are not available and those for atactic PP have been used to obtain the experimental value of the pre-exponential factor. Once again, if the parameters for the isotactic PP could be used, these would account for a higher crystallinity and the pre-exponential factor would decrease having a value closer to the predicted one.

4.4.2.2 Complex molecules: Pesticides

The main purpose of this study is the application of the predictive form of the free volume model (Extended FV model) to the estimation of diffusion coefficients of pesticide compounds in the polymers commonly used within controlled release technology. In this section, the applicability of the Extended FV model to pesticide compounds is assessed through the study of diffusion in two different scenarios.

In the first scenario, the analysis of two pesticides diffusing in synthetic polymers is done in the same manner as in section 4.4.2.1 given that two sets of temperature dependent diffusivity data are available. Through these data, the model parameters are estimated and compared with those predicted from pure component properties (without use of diffusivity data). The second scenario takes into account the diffusion of pesticide compounds through plant cuticles that can be modelled as a polymer. In this case, given the nature of the data, the analysis is presented through a qualitative study of the accuracy in the reproduction of the diffusion behaviour provided by the predictive form of the free volume model. The model parameters are not estimated from diffusivity data given that these values might not be representative. Therefore only the predicted parameters are provided. Note that in Appendix C the CAS numbers and names are provided for all the compounds used in this chapter.

i) Pesticides in synthetic polymers

System 1: λ-cyhalothrin in Poly(ethylene-co-vinyl acetate)

The first system to be studied is the diffusion of the insecticide λ-cyhalothrin (λ-cy) in Poly(ethylene-co-vinyl acetate) (PEVAc) polymers. PEVAc is a copolymer of Polyethylene (PE) and Poly(vinyl acetate) (VAc). The experimental data available (provided by Syngenta) consists of four data sets, where two different percentages of Vinyl Acetate (VAc) in the copolymer are represented, as well as, two different concentrations of the Active Ingredient (AI). These data sets are given in Table 4.21 and they have also been plotted in Fig. 4.9 to illustrate that the diffusion coefficient values do not depend either on the VAc content of the copolymer, or on the concentration of the AI (λ-cy). The latter observation leads to the validation of the infinite dilution assumption to be used in the model calculations. On the other hand, the fact that the VAc content does not affect the diffusivity values allows for the simplification of modelling the PEVAc copolymer as simply Polyethylene (PE). This is in fact a requirement in order to perform these calculations, since no data for the WLF parameters of the copolymer is available, and neither is any viscosity data to estimate them. The effect of having a certain amount of VAc instead of merely pure PE, provides the polymer with some amorphous character so diffusion is faster than in PE. This consideration does not contradict the fact that diffusivity is not affected by the percentage of VAc in the copolymer. Apparently, the presence of a certain amount of VAc in the polymer would modify its morphology, increasing the amorphous content and therefore the diffusivity of the AI. On the other hand, the addition of more VAc would not significantly modify the polymer structure once again, and therefore the diffusivities would not be further increased.

It is based on these considerations that the diffusivity values predicted through the Extended FV model (assuming PE) are expected to be lower than the experimental diffusivity values (in PEVAc).

Table 4.21: Variation of the diffusion coefficients with temperature. Experimental data for λ-cyhalothrin in PEVAc (from Syngenta).

T (K)	**D** (cm^2/s)			
	33%VAc 1% λ-cy	33%VAc 20% λ-cy	18%VAc 1% λ-cy	18%VAc 20% λ-cy
281.15	-	-	4.28×10^{-11}	4.90×10^{-11}
295.15	3.00×10^{-10}	2.10×10^{-10}	3.28×10^{-10}	1.10×10^{-10}
308.15	-	-	2.45×10^{-9}	-
318.15	-	-	2.10×10^{-9}	-
328.15	6.00×10^{-9}	6.00×10^{-9}	6.26×10^{-9}	5.40×10^{-9}

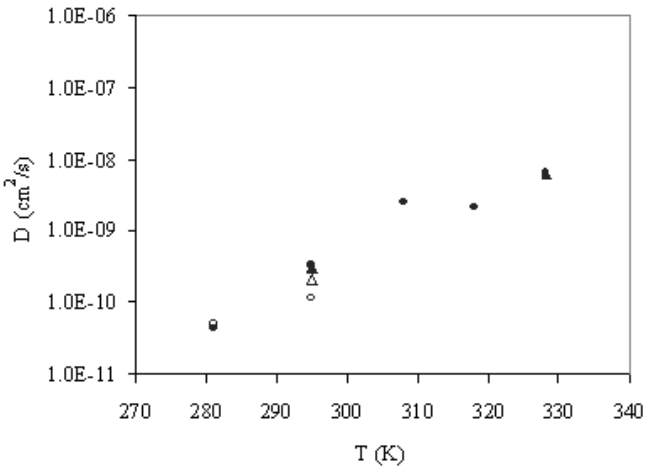

Figure 4.9: Experimental values of diffusion coefficients of λ-cyhalothrin in PEVAc as a function of temperature for four different data sets. (•) 1% λ-cyhalothrin, 18%VAc; (○) 20% λ-cyhalothrin, 18%VAc; (▲) 1% λ-cyhalothrin, 33%VAc; (△) 20% λ-cyhalothrin, 33%VAc. All % in weight.

Another aspect to be considered is the range of temperatures of the experimental data, which is 281 - 328 K for the λ-cyhalothrin in PEVAc system, with respect to the limitations imposed by the free volume model ($T < Tg_2 + 150K$). The glass transition of PEVAc (with 33% VAc) is approximately 178 K (Fornasiero et al. [84]) and then the experimental data is just within the limits ($Tg + 150 = 328$ K). This might be a problem due to the consideration of the polymer as a polyethylene that has a lower glass transition temperature (148 K), thus decreasing the upper limit of validity and indicating that the energy terms might become relevant. With the above considerations established the next step is the analysis of the performance of the Extended FV model in reproducing the behaviour of the λ-cyhalothrin diffusivity in this polymer (assumed as PE) by fitting the diffusivity data to the model and obtaining the model parameters (Eq. 4.23), reported in Table 4.22. A plot is presented in Fig. 4.10 to illustrate the good correlation obtained through the Extended FV model, as compared to the experimental values.

Table 4.22: Model parameters obtained from fitting of diffusivity data (Eq. 4.23)

Solvent	**Polymer**	**T range data (K)**	Tg_2 **(K)**	D_0 (cm^2/s)	ξ
λ-cyhalothrin	PE	281 - 328	148	1.94×10^{-3}	1.729

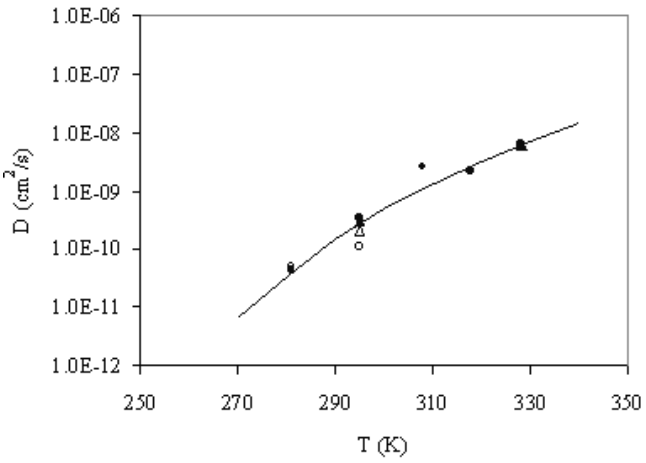

Figure 4.10: Comparison of experimental data (symbols) with correlation results (—).

After assessing the appropriateness of the Extended FV model for this system and obtaining the parameters from diffusivity data, the estimation of the model parameters in a purely predictive manner is attempted. For this, the same type and sources of data are used as detailed in section 4.4.1.

In these calculations, a Polyethylene (PE) polymer is used to model the diffusivity in PEVAc as explained and justified in the beginning of this study. In order to obtain the WLF parameters for PE, not available from the literature, a regression of temperature dependent viscosity data for High Density Polyethylene (HDPE) (Pearson et al. [85]) is performed. The obtained model parameters are presented in Table 4.23.

Table 4.23: Parameters obtained from pure prediction

Compound	V(0K) (cm^3/g)	K_{1i}/γ (cm^3/gK)	$K_{2i} - Tg_i$ **(K)**	D_0 (cm^2/s)	ξ
λ-cyhalothrin	0.68	1.36×10^{-3}	-206.46	4.75×10^{-5}	1.88
PE	1.03	8.44×10^{-4}	-161.15	-	

Summarizing, the parameters (D_0 and ξ) of the Extended FV model have been estimated first from fitting to experimental diffusivity data (Eq. 4.23) and then in a predictive manner from pure component properties. Results from each of these options have been highlighted in Tables 4.22 and 4.23, respectively.

By comparing the predicted values of the model parameters given in Table 4.23, with those estimated from diffusivity data (Table 4.22), it can immediately be observed that while the results for the prediction of the ratio

of jumping units (ξ) are quite accurate, the estimation of the pre-exponential factor (D_0) differs in approximately two orders of magnitude from the experimental value. This is not surprising since these inaccuracies have already been observed in section 4.4.2.1 for all types of molecules (not only large and complex ones). In this specific case, the energy effects could be related to the fact introduced above that the glass transition of the modelled polymer, PE, is smaller than that of the measured polymer, PEVAc, and thus the range of temperatures for which energy effects are negligible is exceeded, so the experimentally obtained value of the pre-exponential factor is not realistic.

One more consideration is the fact that PE is used to model an otherwise more amorphous polymer, PEVAc, and as expected, the predicted results underestimate the diffusivity values. This can be seen in Fig. 4.11, together with the remarkably good reproduction of the temperature dependence. In an attempt to confirm these observations, a correction of the pre-exponential factor has been performed according to the value estimated from diffusivity data (Table 4.22), that is, an increase of two orders of magnitude has been introduced ($D_0 = 4.75 \times 10^{-3} cm^2/s$). The goodness of the results obtained thereby is also shown in Fig. 4.11.

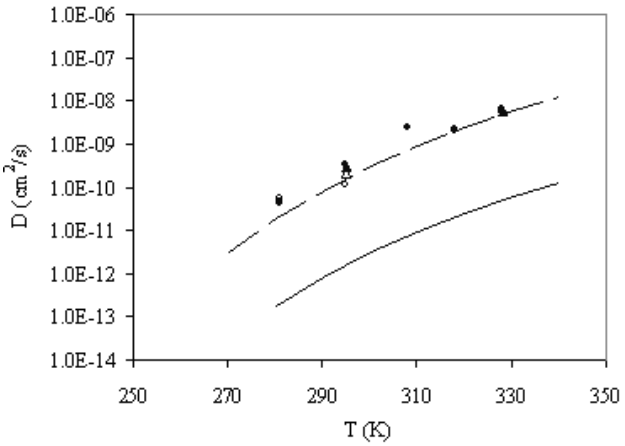

Figure 4.11: Comparison of experimental data (symbols) with predicted results (—), and prediction with correction of the pre-exponential factor (– –).

System 2: Permethrin in Polypropylene

The second system to be studied involves again an insecticide compound , Permethrin, diffusing through different samples of Polypropylene, isotactic (iPP, PP 42.786-1 and carpet PP) and syndiotactic (PP 45215-7). The experimental data (again provided by Syngenta) is reported in Table 4.24 and plotted in Fig. 4.12. The different samples of PP can be considered as one single type of

PP since isotactic and syndiotactic polymers both present an ordered structure (even though the location of the pendant groups is different) that confers them similar properties with respect to crystallinity. The temperature range of the experimental data is adequate in this case since the glass transition temperature of PP is 253 K, and the temperature span of the data is 277 - 353 K. The rest of the model assumptions are also valid for this case study.

Table 4.24: Variation of Permethrin diffusion coefficients with temperature in different PP samples. Experimental data (from Syngenta).

Polymer	**Type**	**T (K)**	**D** (cm^2/s)
iPP	isotactic	323.15	2.40×10^{-10}
		313.15	1.14×10^{-11}
		303.15	1.84×10^{-10}
		277.15	3.80×10^{-12}
PP 45215-7	syndiotactic	353.15	3.61×10^{-8}
PP 42.786-1	isotactic	353.15	1.91×10^{-8}
carpet PP	isotactic	353.15	9.01×10^{-9}
		333.15	5.96×10^{-9}

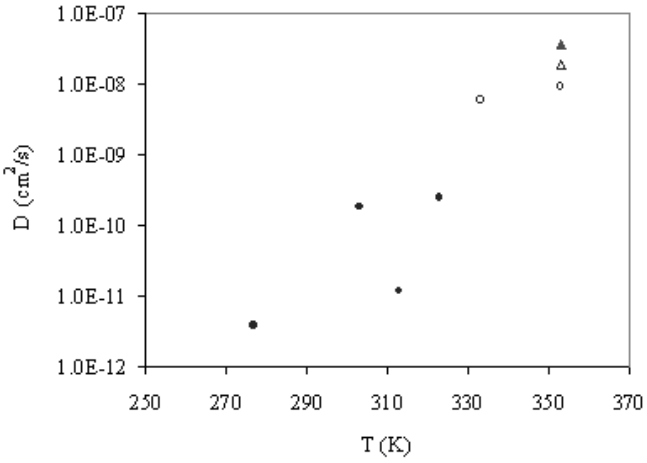

Figure 4.12: Experimental values of diffusion coefficients of Permethrin in different PP samples: (•) isotactic PP; (○) carpet PP; (▲) PP 45215-7; (△) PP 42786-1.

The applicability of the Extended FV model is tested by correlating the experimental data (Eq. 4.23) and obtaining the model parameters (D_0 and ξ). Due to the scattering observed in the experimental data, basically at low

temperatures (below 330 K), an added consideration needs to be made, that is, two different sets of data will be considered. Two different sets of parameters are then obtained, (i) by neglecting the lowest temperatures (277, 303 K) and (ii) neglecting the data at 313 and 323 K. A good fit is obtained with each of the cases respectively, and the estimated parameters are reported in Table 4.25, where it can be observed that the effect of considering one or the other data sets, changes dramatically the parameter values obtained, this must be regarded when analysing the results. The fit of the experimental data with each of the data sets is shown in Fig. 4.13.

The difference observed between the pre-exponential factors obtained from regression of each data set can be explained through the equation used to correlate the diffusivity data, Eq. 4.23. From Eq. 4.23 it can be observed that the values of the pre-exponential factor correspond to the intercept when the logarithm of the diffusion coefficient is plotted versus the reciprocal of the temperature. Then, from Fig. 4.13 (diffusivity as a function of temperature), the pre-exponential factors are already expected to be very different for each of the data sets.

In order to do the estimation of the Extended FV model parameters, the PP polymer has been modelled using the WLF constants for atactic PP (as in section 4.4.2.1) given that no data is available for either isotactic or syndiotactic forms of this polymer. The structures of these polymers are expected to have a high degree of ordering, packing and crystallinity, as opposed to the atactic forms, so their behaviour is expected to differ significantly. The pre-exponential values obtained would then have to be corrected with the crystallinity, implying a decrease in diffusivity and also a lower value of the pre-exponential factor.

Table 4.25: Parameters obtained from fitting of diffusivity data

Solvent	**Polymer**		**T range data (K)**	Tg_2 **(K)**	D_0 (cm^2/s)	ξ
Permethrin	PP	(i)	303.15-353.15	253	3.5	1.39
		(ii)	277.15-353.15	253	5.80×10^{-5}	0.6

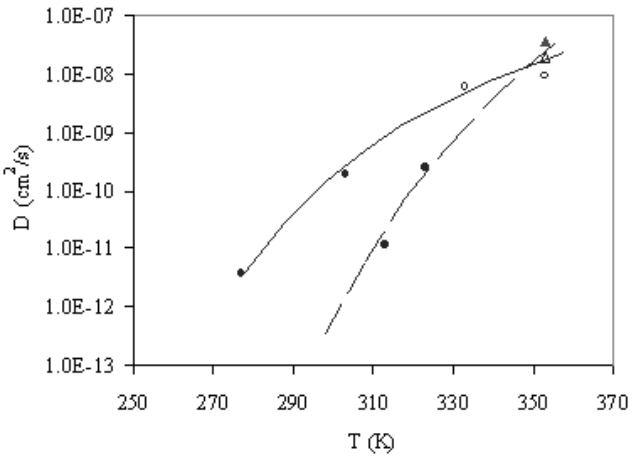

Figure 4.13: Comparison of experimental and correlated diffusion coefficients of Permethrin in different PP samples. Experimental values: (•) isotactic PP; (∘) carpet PP; (▲) PP 45215-7; (△) PP 42786-1. (– –) Correlated set (i); (—) Correlated set (ii).

Even with all the problems encountered so far, the prediction of the parameters is attempted by following the procedure summarized in section 4.3 and Table 4.3 and the results are given in Table 4.26.

Table 4.26: Parameters obtained from pure prediction.

Compound	V(0K) (cm^3/g)	K_{1i}/γ (cm^3/gK)	$K_{2i} - Tg_i$ **(K)**	D_0 (cm^2/s)	ξ
Permethrin	0.72	1.33×10^{-3}	-151.06	5.02×10^{-5}	1.731
PP	1.03	5.17×10^{-4}	-205.4	-	

These results can now be compared to the parameter values obtained from diffusivity data (Table 4.25). In each of the cases ((i) and (ii)) one of the two parameters (D_0 and ξ) is quite accurately predicted while the other is significantly wrong. No conclusions can be extracted as to which set of parameters and data is more representative of this system. These wrong predictions are immediately observed when plotting the predicted diffusivities together with the experimental data, as done in Fig. 4.14. Here it is observed that even though the values are significantly underpredicted, the temperature dependence of the diffusion coefficient seems to be appropriately described by the Extended FV model predictions.

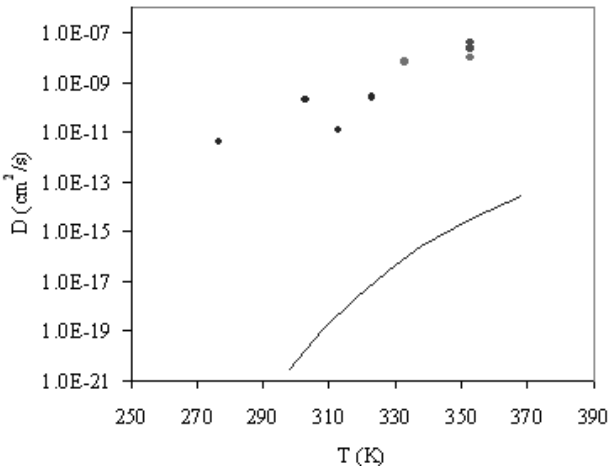

Figure 4.14: Comparison of experimental and predicted diffusion coefficients of Permethrin in different PP samples. Experimental values: (•) isotactic PP; (○) carpet PP; (▲) PP 45215-7; (△) PP 42786-1. (—) predicted.

The main cause to this important disagreement in the diffusion coefficient values is attributed to the different behaviour of atactic PP used to model the data and the isotactic PP used in the experimental measurements. This is reaffirmed by the fact that the same situation has previously been observed in similar systems (Okajima et al. [74]) with equivalent results.

ii) Pesticides in plant cuticles

Given the small amount of data on pesticide diffusion through polymers, the conclusions to be extracted on the performance of the predictive model cannot yet be established.

In order to further complement the previous analysis in section *(i)(Pesticides in synthetic polymers)*, the possibility of using data measured for pesticides diffusing through plant cuticles is studied. The data is available from different references, generally in the form of correlations either as a function of the molecular volume or temperature. In order to obtain experimental values that could be used for the purposes of this study, the two different types of correlations (with molar volume and with temperature) have been combined (as described in Appendix D) to provide the values of the diffusion coefficients as a function of temperature and for several different pesticides. It is worth noting here that the experimental correlations have been developed separately for different types of compounds, mainly aromatics and linear aliphatic compounds. This is a simple way to take into account the shape of the diffusants based on the experimental observations of linear molecules diffusing faster than

cyclic/aromatic ones. The range of molar volumes (V (0K)) for which these correlations have been developed is approximately 93 - 267 cm^3/mol.

Once the measured data of interest is obtained in the form of temperature dependent diffusivity data for different compounds, it will be qualitatively analyzed with respect to the predictive abilities of the Extended FV model.

The first consideration to be made regarding the modelling of these systems with the Extended FV model is the polymer that will be used to assimilate the plant cuticle. The fact that barley leaf wax is characterized by a chain-length distribution of n-alkanes (between 20 and 48 carbon atoms, Reynhardt et al. [86]), leads to a possible description as a Polyethylene polymer. The remaining assumptions commonly made for the Extended FV model calculations are also valid here. The concentration independence of the diffusion coefficient in these situations has been shown by Schreiber et al. [87].

Given the special nature of the diffusivity data a quantitative analysis will not be provided for these systems. That is, the model parameters will be estimated in a purely predictive manner and the results analyzed through a comparison of the predicted and the experimental diffusivities, as a function of temperature. For these systems though, the same model parameters (D_0, ξ) are not estimated from regression of the diffusivity data in order to compare them with the purely predicted ones. This is due to the fact that in these systems the pesticide does not diffuse through a synthetic polymer but through a plant cuticle. Then, the parameters that could be obtained from regression of these diffusivity data may implicitly contain additional properties of the cuticle (such as high crystallinity). Due to these special features of the membrane it is considered that the parameters might not be representative or adequate to be applied in other systems. It is therefore that these parameters are not estimated and only the purely predicted ones are reported since, even with their limitations, they are extendable to other systems.

i) Literature compounds: test

In this study the critical assumption is the modelling of a plant cuticle through a polyethylene polymer. In order to analyze and establish the deviations that can appear due to this consideration, a study is carried out with compounds for which the Extended FV model parameters are available (Zielinski and Duda [61]). Two different types of compounds are chosen, one of them aromatic (Toluene) and the other linear (n-hexane), to represent both types of experimental correlations. With these compounds, the diffusivity is predicted as a function of temperature and compared to that obtained from the experimental correlations. The parameters used are reported in Table 4.27 and the results of the comparison are shown in Fig. 4.15.

Table 4.27: Free volume parameters for solvent and polymer compounds studied.

Compound	V(0K) (cm^3/mol)	K_{1i}/γ (cm^3/gK)	$K_{2i} - Tg_i$ **(K)**	D_0 (cm^2/s)	ξ
Toluene	84.48	1.45×10^{-3}	-86.32	4.82×10^{-4}	2.56
Hexane	97.66	1.41×10^{-3}	-26.75	7.85×10^{-4}	1.7
Polyethylene	-	8.44×10^{-4}	-161.15	-	-

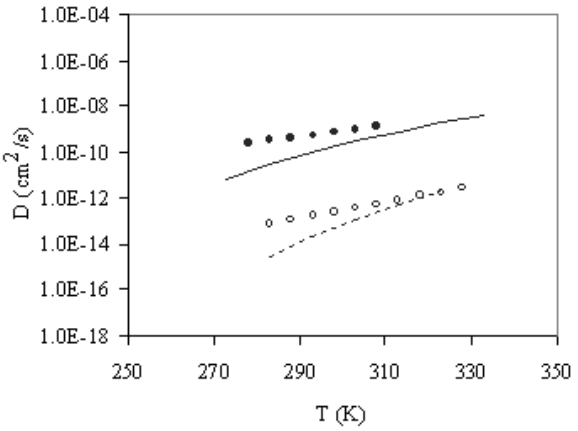

Figure 4.15: Plot of experimental data from correlations compared to Extended FV model predictions with known parameter values. Experimental correlation data for (○) Toluene, (●) n-hexane; FV calculations for (- - -) Toluene, (—) n-hexane.

As observed from Fig. 4.15, the values obtained from the Extended FV model predictions tend to underestimate the diffusivity at the lower range of temperatures while they get closer (in the case of the aromatic compound), to the experimental correlation values at higher temperatures. The temperature dependence of the diffusivity of the linear compound is very well reproduced by the free volume model and the values are underestimated for the whole temperature range. The inherent deviation existing between experiment and prediction is expected because of differences in the nature of the cuticle and the polyethylene used as a model. This nevertheless serves as a reference for the calculations (to be made below) involving pesticides, where similar deviations can be expected.

The next step is to apply the same comparisons to pesticide compounds. For this purpose, two sets, of four compounds each, have been chosen from the publications from where the experimental data was extracted (Schreiber et al. [87], Buchholz et al. [88], Baur et al. [89]).

The first set of compounds consists of relatively simple and small pesticides

with an aromatic base-structure while the second set includes more complex and generally larger compounds. The pure component experimental data needed for the estimation of the Extended FV model parameters has been extracted from different sources (group contribution methods) and when some uncertainties have been observed, mainly in viscosity estimations, the most consistent/appropriate values have been used.

i) 1st set of compounds

The first set of compounds is now analyzed. The parameter values obtained for this set of pesticides is summarized in Table 4.28, while in Fig. 4.16 the comparison between experimental and predicted diffusivity is highlighted. The pesticides in this set resemble the aromatic type of compounds, illustrated above through toluene. Here the deviations between experiment and prediction are totally equivalent to those of toluene (Fig. 4.15), except for Benzoic acid that is highly overpredicted and therefore needs special consideration. This indicates that the predictive methodology is reliable given that the results are totally comparable to the test ones where literature parameters were used.

Table 4.28: Values of the parameters required for the free volume calculations (set 1)

Compound	V(0K) (cm^3/mol)	K_{1i}/γ (cm^3/gK)	$K_{2i} - Tg_i$ **(K)**	D_0 (cm^2/s)	ξ
Benzoic acid	88.8	1.30×10^{-3}	-308.31	4.63×10^{-3}	1.869
2,4-D	134.4	1.12×10^{-3}	-205.95	7.88×10^{-6}	2.06
PCP	136.8	9.35×10^{-4}	-246.5	1.43×10^{-4}	2.552
Lindane	163.2	1.05×10^{-3}	-148.27	1.07×10^{-4}	2.586

The extremely high deviation of the predictions for Benzoic acid could be due to the fact that this compound is likely to form dimers at these conditions. This means that at least the aspect ratio and the molar volume (V(0K)) must be considered for the dimer. An attempt to take these factors into account through the Extended FV model has been done and the results are presented in Fig. 4.17.

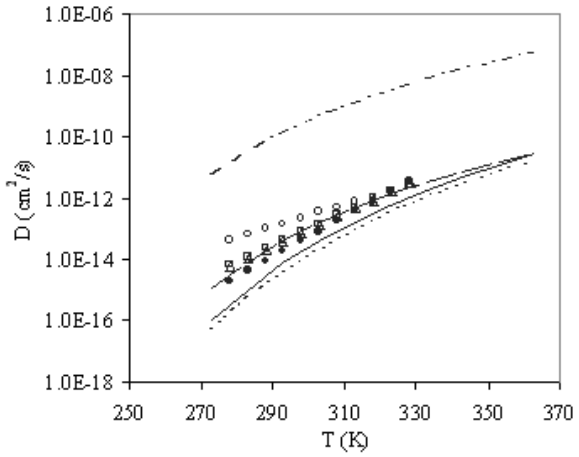

Figure 4.16: Plot of experimental data from correlations compared to Extended FV model. Experimental correlation data for (∘) Benzoic acid, (□) 2,4-D; (△)PCP; (•) Lindane. FV calculations for (– - –) Benzoic acid; (– –) 2,4-D; (—) PCP; (- - -) Lindane.

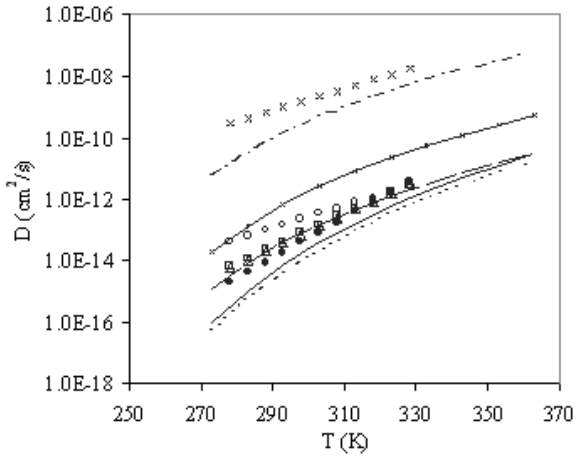

Figure 4.17: Plot of experimental data from correlations compared to Extended FV model. Experimental correlation data for (∘) Benzoic acid (Exp-1), (□) 2,4-D; (△)PCP; (•) Lindane. FV calculations for (– - –) Benzoic acid;(– x –) Benzoic acid dimer; (– –) 2,4-D; (—) PCP; (- - -) Lindane.; (x) Benzoic acid (Exp-2).

From Fig. 4.17 it can be seen that, even though there is an important improvement of the prediction, the model still overestimates the diffusivities. It

is likely that further considerations of the benzoic acid's dimerization are necessary. This is though a complex subject and will not be treated further here.

This disagreement with the Benzoic acid predictions can be approached from another angle. From the analysis above, it has been concluded that in the Extended FV model calculations, the Benzoic acid molecule considered is significantly smaller than the rest of compounds studied. On the other hand, from the point of view of the experimental data (used to compare the values), different correlations are available according to the different types of compounds diffusing (see Appendix D for details). While originally the experimental correlation obtained for pesticide compounds has been used (Exp-1 in Fig. 4.17), it might be interesting in the case of such a small molecule, to use the experimental correlation obtained for small cyclic compounds (see Exp-2 in Fig. 4.17). Now, it can be observed that the predictions from the Extended FV model without considering a Benzoic acid dimer, are much closer to this last set of experimental data (see Exp-2 in Fig. 4.17).

Finally, since the actual value of the diffusion coefficient of Benzoic acid is known to be $3.34\times10^{-13}\text{cm}^2/\text{s}$, which is close to that obtained for the dimer, the conclusion is that the explanations to these anomalies is the dimerization of this compound.

ii) 2nd set of compounds

The second part of this study deals with pesticides that are more complex in structure with respect to the first set, as well as larger in size (except for the IAA). The same procedure has been applied to predict and estimate the Extended FV model parameters and these are reported in Table 4.29. The diffusivity is calculated using the Extended FV model and compared to the experimental correlations in Fig. 4.18. The results vary significantly for these compounds. In the first place IAA is overestimated, but given the fact that this compound is an acid, the possibility of dimer formation arises, as in Benzoic acid above, and this would explain the significant overprediction. A treatment similar to that for Benzoic acid could be applied and similar improvements can be expected. This however, has not been done here given that it is equivalent to the previously mentioned Benzoic acid system. On the other hand, for the remaining pesticides (with a higher molar volume) the results are very accurate within the temperature range of interest. This result is very encouraging with respect to the use of the predicted parameters and the Extended FV model to describe the diffusion of large and complex pesticide molecules.

Table 4.29: Values of the parameters required for the free volume calculations (set 2)

Compound	V(0K) (cm^3/mol)	K_{1i}/γ (cm^3/gK)	$K_{2i} - Tg_i$ **(K)**	D_0 (cm^2/s)	ξ
IAA	130	1.24×10^{-3}	-255.19	1.60×10^{-4}	2.143
WL110547	192	1.35×10^{-3}	-14.25	1.24×10^{-4}	2.431
Bifenox	216	1.17×10^{-3}	-220.51	6.62×10^{-5}	2.513
Tebuconazole	241	1.38×10^{-3}	-221.52	2.12×10^{-5}	2.456

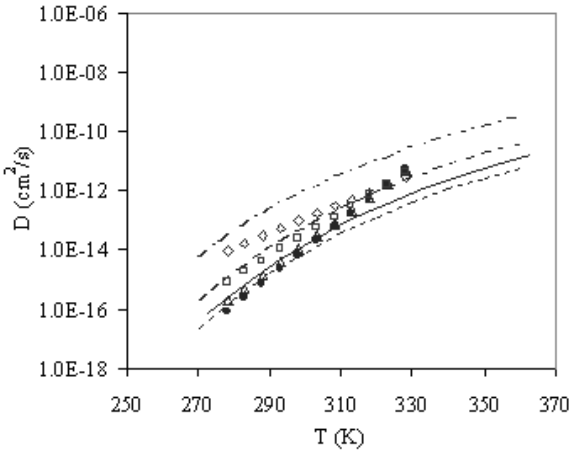

Figure 4.18: Plot of experimental data from correlations compared to Extended FV model. Experimental correlation data for (∘) IAA, (□) WL-110547; (△) Bifenox; (•) Tebuconazole. FV calculations for (– - –) IAA; (– –) WL-110547; (—) Bifenox; (- - -) Tebuconazole.

4.4.2.3 Controlled release related compounds

This last section concerning the application of the Extended FV model involves some systems for which diffusivity values are available at a single temperature. These systems are interesting from the point of view of controlled release technology, mainly with reference to the polymer that is used, given that the diffusing compounds are not specially large or complex. The experimental data is extracted from controlled release literature (Yadav et al. [90],[93], Kubo et al. [92]) and involves diffusion in a polyurea membrane, for which the Extended FV model has not yet been applied (to our knowledge). The experimental values are reported in Table 4.30. It is important to mention that the experimental values in the case of HMDA and cyclohexane, are reported for polymers of different crystallinities and in the case of DETA, the data is provided from two different sources. In order to model these systems additional assumptions

are needed since the WLF constants are not available for polyurea. In this situation the polyurea is then modelled as polyurethane, which is assumed to behave similarly with respect to the diffusive properties.

The permeabilities of Polyurethane and Polyurea have been reported [94] to be 0.08 g/100in^2 and 0.069 g/100in^2, respectively. These are observed to be very similar. In other literature on properties of polymers (Brandrup et al. [68]) some properties, such as glass transition temperature, are reported together for polyureas and polyurethanes, so it is difficult to extract more information on the differences between these two polymers. Therefore this assumption is considered valid and is afterwards proven to be a good supposition.

The rest of the free volume parameters, that is, for the pure compounds, and the ratio of jumping units, are calculated in the same manner and using the same experimental data as in the previous sections. The values for the diffusivity are estimated at the temperatures reported for the measured data and provided in Table 4.30. The values of the Extended FV model parameters estimated and used in these calculations are given in Table 4.31 for the diffusant compounds and for the polymer. The results are quite accurate in all of the cases and especially for HMDA. In all the cases the order of magnitude of the diffusion coefficient is correctly predicted and the small deviations observed can be attributed to the differences in the polymer properties mentioned before. These properties are not specified for the model polymer used in the predictions and therefore further considerations cannot be done. The results are therefore considered satisfactorily accurate.

Table 4.30: Results from the Extended FV model compared to the available experimental data for diffusion in Polyurea (Polyurethane).

Source	**Compound**	**T (K)**	$D_{exp}(m^2/s)$	$D_{pred}(m^2/s)$	**Obs**
[90]	HMDA	293	$0.8 \sim 99.0 \times 10^{-14}$	1.23×10^{-13}	Different crystallinities
[92]	DETA	298	$1.61 \sim 1.91 \times 10^{-13}$	8.69×10^{-14}	Different data sources
[93]	Cyclohexane	293	$0.55 \sim 3.45 \times 10^{-14}$	4.50×10^{-15}	Different crystallinities

Table 4.31: Values of the parameters required for the free volume calculations.

Source	**Compound**	V(0K) (cm^3/mol)	K_{1i}/γ (cm^3/gK)	$K_{2i} - Tg_i$ **(K)**	D_0 (cm^2/s)	ξ
[90]	HMDA	120.99	1.92×10^{-3}	-170.02	3.60×10^{-4}	0.95
[92]	DETA	102.3	1.83×10^{-3}	-119.31	2.56×10^{-4}	0.98
[93]	Cyclohexane	87.6	1.92×10^{-3}	-119.31	3.14×10^{-4}	1.19
All	Polyurea (Polyurethane)	148.8	3.23×10^{-4}	-181.4	- -	- -

4.5 Conclusions

In this chapter a predictive model has been presented and analysed, to estimate the diffusion coefficients of AIs in polymers, which are needed in the mathematical models for study of the AI release behaviour. The model used in this work (free volume based) has been selected after providing a brief overview of the models available for diffusion in polymers and based on the criteria determined by the type of systems to be treated, that is, controlled release applications of pesticides.

A detailed description of the model has been provided, including all the equations required, the parameters involved and the procedure to estimate them. Together with this, a parameter sensitivity analysis has been performed and the effect of parameters and properties on the final diffusivity values has been assessed. This is very helpful in the systems studied given that experimental data is not usually available for the estimation of the model parameters, and predicted values are used that might be a source of error in the final calculations. Therefore it is important to identify where this comes from.

The predictive model was originally derived for asymmetric molecules and applied to relatively large molecules (compared to previous literature). In this work though, the compounds of interest are much larger and complex, and therefore the model has been assessed for dye compounds, considered representative of the pesticide types. In the first place the ability of the free volume model to reproduce the temperature behaviour of diffusivity of these complex molecules has been successfully validated.

Then, the pure prediction of the parameters has been analysed. The prediction of the ratio of molar jumping units is the critical factor when extending the model from small to large molecules. After this analysis, it is confirmed that very satisfactory results are obtained for these complex molecules, and therefore this model can be used in pesticide systems. On the other hand, the prediction of the pre-exponential factor is problematic. The factors causing deviations from experimental values have been identified (they are related to crystallinity, energy effects, etc.) and the needed improvements proposed so that they can be used in a more reliable manner.

After analysing the model parameters, this has been applied to several systems involving the diffusion of pesticides in polymers. Again the results involve very accurate predictions of the ratio of jumping units, but some difficulties in obtaining the pre-exponential factor, as discussed before. The diffusion of pesticides has been further studied through the analysis of data on diffusion of pesticides in plant cuticles. The temperature dependence behaviour is very well reproduced by the Extended FV model, with a few exceptions that have been identified as compound dimerizations, therefore complicating the predictions.

Finally, the prediction of the diffusion coefficients of some compounds related to controlled release technology has also been performed and compared to experimental data. Very good results are obtained in these cases, which is

encouraging for using this predictive model together with the controlled release mathematical models.

Further studies based on accurate and detailed experimental data are needed to implement the proposed improvements.

Nomenclature

List of symbols

a_i	Activity of compound i
B/A	Aspect ratio of the molecule
$C_{1j}^{WLF}, C_{2j}^{WLF}$	WLF equation parameters. j = 1 for solvent; j=2 for polymer
D	Diffusion coefficient
D_0	Constant pre-exponential factor
D_i	Self-diffusion coefficient of compound i
D_{12}	Mutual diffusion coefficient
E	Energy (per mole) that a molecule needs to overcome attractive forces which constrain it to its neighbours
K_{1i}, K_{2i}	free-volume parameters of compound i
M_{1j}, M_{2j}	Molecular weight of the solvent and polymer jumping units, respectively
Mw_i	Molecular weight of component i
P	Pressure
R	Gas constant
T	Temperature
Tg_i	Glass transition temperature
$\overline{v}$	Average volume in the liquid
$\overline{v}_{FV}$	Average free volume of a molecule
$\overline{v}_o$	Occupied volume
V_c	Critical volume of the solvent
$\tilde{V}_c$	Specific critical volume of the solvent
$\overline{V}_{FH}$	Hole free volume
$\tilde{V}_i^*$	Critical hole free volume required for a jump
$\tilde{V}_i$	Specific volume of compound i
$V_i(0K)$	Volume of compound i at 0 K
$\tilde{V}_{2j}^*$	Volume of the polymer jumping unit
w_i	Weight fraction of component i
x_i	Mole fraction of compound i

Greek letters

χ	Flory-Huggins interaction parameter
δ_i	Solubility parameter of component i
ϕ_i	Volume fraction of component i
γ	Overlap factor (between 0.5 and 1), due to the same free volume being shared by more than one molecule
γ_i	Activity coefficient (mole basis) of compound i
η_i	Viscosity
$\eta(Tg_j)$	Viscosity at the reference temperature (generally Tg)
μ	Chemical potential
μ^0	Reference chemical potential

ρ_i	Density
τ	Tortuosity factor
ξ	Ratio of molar volumes for the solvent and the polymer jumping units

Subscripts

1	AI (or solute in general terms)
2	Polymer
$aver$	Average
exp	Experimental
FH	Hole free
FV	Free Volume
i	Compound
mix	Mixture
o	Occupied
$pred$	Predicted

References

[1] Hoon Han, J., Mass transfer modeling in closed systems for food packaging, particulate foods and controlled release technology, *Food Sci. Biotechnol.* 2004, 13(6) 700-706 .

[2] Ferrara, G., Bertoldo, M., Scoponi, M., Ciardelli, F., Diffusion coefficient and activation energy of Irganox 1010 in poly(propylene-co-ethylene) copolymers, *Polym. Degrad. Stabil.* 2001, 73, 411-416.

[3] Kou, J.H., Amidon, G.L., Lee,P.I., pH-dependent swelling and solute diffusion characteristics of Poly(Hydroxyethyl methacrylate-co-methacrylic acid) hydrogels, *Pharmaceut. Res.* 1988, 5, 9.

[4] Foldes,E., Transport of small molecules in Polyolefins. II. Diffusion and solubility of Irganox 1076 in Ethylene polymers, *J. Appl. Polym. Sci.* 1993, 48, 1905-1913.

[5] Gao, P., Nixon, P.R., Skoug, J.W., Diffusion in HPMC gels. II. Prediction of drug release rates from hydrophilic matrix extended-release dosage forms. *Pharmaceut. Res.* 1995, 12, 7.

[6] Shailaja, D., Yaseen M., Controlled release from PVC matrices: effect of four phtalate plasticizers on diffusion of THF, *Eur. Polym. J.* 1992, 28(11), 1321-1324.

[7] Shailaja, D., Merajuddin, S., Yaseen M., Comparative study of release kinetics of pheromone from polymer dispensers, *J. Appl. Polym. Sci.* 1997, 64, 1373-1380.

[8] Pitt, C.G., Bao Y.T., Andrady, A.Lb, Samuel, P.N.K., The correlation of polymer-water and octanol-water partition coefficients: estimation of drug solubilities in polymers, *Int. J. Pharm.* 1988, 45, 1-11.

[9] Fan, L.T., Singh, S.K., *Controlled release. A quantitative treatment.* Springer-Verlag, Berlin Heidelberg, 1989.

[10] Amidon, G.L., Lee, P.I. and E.M. Topp, *Transport processes in pharmaceutical systems.* Drugs and the pharmaceutical sciences vol. 102. New York, Marcel Dekker, 2000.

[11] Chen, S.X, Lostritto, R.T., Diffusion of Benzocaine in Poly(ethylene-vinyl acetate) membranes: Effects of vehicle ethanol concentration and membrane vinyl acetate content, *J. Control. Release* 1996, 38, 185-191.

[12] Kagayama, A., Mustafa, R., Akaho,E., Khawam,N., Truelove, J., Hussain, A., Mechanism of diffusion of compounds through ethylene vinyl acetate copolymers I. Kinetics of diffusion of 1-chloro-4-nitrobenzene, 3,4-dimethylphenol and 4-hexylresorcinol, *Int. J. Pharm.* 1984, 18, 247-258.

[13] Goydan, R., Schwope, A.D., Reid, R. C., Cramer, R. High-temperature migration of antioxidants from polyolefins, *Food Addit. Contam.* 1990, 7(3), 323-337.

[14] Goydan, R., Schwope, A.D., Reid, R.C., Krishnamurthy, S., Wong, K., Approaches to predicting the cumulative permeation of chemicals through protective clothing polymers, *Performance of protective clothing: second symposium, ASTM STP 989*, S.Z. Mansdorf, R. Sager, A.P. Nielsen, Eds., American Society for testing and materials, Philadelphia, 1988, pp.257-268.

[15] Goydan, R., Powell, J.R., Bentz, A.P., Billing, Jr., C.B., A computer system to predict chemical permeation through fluoropolymer- based protective clothing, *Performance of protective clothing: fourth volume, ASTM STP 1133*, J.P. McBriarty and N.W. Henry, Eds., American Society for testing and materials, Philadelphia, 1992.

[16] Schwope, A.D., Goydan, R., Ehntholt, D.J., Frank, U. And Nielsen, A.P., Resistance of glove materials to permeation by agricultural pesticides, *Performance of protective clothing: fourth volume, ASTM STP 1133*, J.P. McBriarty and N.W. Henry, Eds., American Society for testing and materials, Philadelphia, 1992.

[17] Kim, J.S., Lee, K.R., Prediction of mutual diffusion coefficient in polymer solution, *Polymer* 2000, 41, 8441-8448.

[18] Liu, Q.-L., Gao, H.-Q., Prediction of mutual-diffusion coefficients in polymer solutions using a simple activity coefficient model, *J. Membrane Scie.* 2003, 214, 131-142.

[19] Crank, J., *Diffusion in polymers.* London Academic Press, 1968.

[20] Masaro, L., Zhu, X.X., Physical models of diffusion for polymer solutions, gels and solids, *Prog. Polym. Sci.* 1999, 24, 731-775.

[21] Gao, P., Fagerness, P.E., Diffusion in HPMC gels. I. Determination of drug and water diffusivity by Pulsed-Field-Gradient Spin-Echo NMR, *Pharmaceut. Res.* 1995, 12, 7, pp. 955-964.

[22] Petit, J.-M., Roux, B., Zhu, X.X., Macdonald, P.M., A new physical model for the diffusion of solvents and solute probes in polymer solutions, *Macromolecules* 1996, 29, 6031-6036.

[23] Waggoner, R.A., Blum, F.D., MacElroy, J.M.D., Dependence of the solvent diffusion coefficient on concentration in polymer solutions, *Macromolecules* 1993, 26, 6841-6848.

[24] Mackie, J.S., Meares, P., The Sorption of Electrolytes by a Cation-Exchange Resin Membrane, 1955, 232 (1191), p. 485-498. In: *Proceedings of the Royal Society of London. Series A, Mathematical and Physical Sciences.*

[25] Phillies, G. D. J., Universal Scaling Equation for Self-Diffusion by Macromolecules in Solution, *Macromolecules* 1986, 19, 2367-2376.

[26] MacElroy, J.M.D., Kelly, J.J., Hindered diffusion of gases in 'leaky' membranes using the dusty gas model, *AIChE J.* 1985, 31 (1), p. 35-44.

[27] Zhu, X.X., Macdonald, P.M., Pulsed-Gradient Spin-Echo NMR measurements of the diffusion coefficients of ketones in Poly(methyl methacrylate), *Macromolecules* 1992, 25, 4345-4351.

[28] Pace, R.J. and Datyner, A., Statistical mechanical model of diffusion of complex penetrants in polymers. I. Theory, *J. Polym. Sci. A2* 1979, 17, 1675-1692.

[29] Pace, R.J. and Datyner, A., Statistical mechanical model of diffusion of complex penetrants in polymers. II. Applications, *J. Polym. Sci. A2* 1979, 17, 1693-1708.

[30] Barrer, R.M., Some Properties of Diffusion Coefficients in Polymers. *J. Phys. Chem.* 1957, 61, 178-189.

[31] Brandt, W.W. Model Calculation of the Temperature Dependence of Small Molecule Diffusion in High Polymers. *J. Phys. Chem.* 1959, 63, 1080-1084.

[32] Bueche, F. Segmental Mobility of Polymers near their Glass Temperature, *J. Chem. Phys.* 1953, 21, 1850-1855.

[33] Meares, P. The Diffusion of Gases through Polyvinyl Acetate. *J. Am. Chem. Soc.* 1954, 76, 3415-3422.

[34] Kumins C.A., Roteman J., Diffusion Of Gases And Vapours Through Polyvinyl Chloride-Polyvinyl Acetate Copolymer Films. 1. Glass Transition Effect. *J. Polym. Sci.* 1961, 55, 683-698.

[35] Kumins C.A., Roteman J., Diffusion Of Gases And Vapours Through Polyvinyl Chloride-Polyvinyl Acetate Copolymer Films. 2. The Effect Of Polymer Segment Mobility, *J. Polym. Sci.* 1961, 55, 699-711.

[36] DiBenedetto, A.T., Molecular Properties of Amorphous High Polymers. An Interpretation of Gaseous Diffusion through Polymers. *J. Polym. Sci. Part A* 1963, 1, 3477-3487.

[37] Cohen, M.H. and Turnbull, D., Molecular transport in liquids and glasses, *J. Chem. Phys.* 1959, 31(5), 1164-1169.

[38] Paul, C.W., A model for predicting solvent self-diffusion coefficients in non-glassy polymer/solvent solutions, *J. Polym. Sci. A2* 1983, 21, 425-439.

[39] Vrentas, J.S. and Duda, J.L., Diffusion in Polymer-Solvent systems. I. Reexamination of the free-volume theory. *J. Polym. Sci. A2* 1977, 15, 403-416.

[40] Vrentas, J.S. and Duda, J.L., Diffusion of large penetrant molecules in amorphous polymers, *J. Polym. Sci. A2*, 1979, 17, 1085-1096.

[41] Fujita, H., Diffusion in polymer-diluent systems, *Adv. Polym. Sci.* 1961, 3, 1-47.

[42] Fujita, H., Comments on free volume theories for polymer-solvent systems, *Chem. Eng. Sci.* 1993, 48, 17, 3037-3042.

[43] Doolittle, A.K., Studies in Newtonian flow. II. The dependence of the viscosity of liquids on free-space, *J. Appl. Phys.* 1951, 22, 1471-1475.

[44] Doolittle, A.K., Studies in Newtonian flow. III. The dependence of the viscosity of liquids on molecular weight and free-space (in homologous series), *J. Appl. Phys.* 1952, 23, 236-239.

[45] Yasuda H., Lamaze C.E., Ikenberry L.D., Permeability Of Solutes Through Hydrated Poloymer Membranes. I. Diffusion Of Sodium Chloride. *Makromol. Chem.* 1968, 118, 19-35.

[46] Kiparissides, C., Dimos, V., Boultouka, T., Anastasiadis, A. , Chasiotis, A., Experimental and theoretical investigation of solubility and diffusion of ethylene in semicrystalline PE at elevated pressures and temperatures. *J. Appl. Polym. Sci.* 2003, 87, 953-966.

[47] Doong, Sh. J., Winston Ho, W.S., Diffusion of hydrocarbons in Polyethylene, *Ind. Eng. Chem. Res.* 1992, 31, 1050-1060.

[48] Sugden, S., *J. Chem. Soc.* 1927, 1786.

[49] Blitz, W. *Rauchemie der Festen Stoffe.* Voss, Leipzig, 1934.

[50] Ngai, K.L. and Plazek, D.J. (Chapter 25: pag. 341-362) in: *Physical properties of polymers handbook.* Mark, J.E., Woodbury, NY. AIP Press, 1996.

[51] Frenkel, J. *Kinetic theory of liquids.* Dover, New York, 1955.

[52] Vrentas, J.S. and Duda, J.L., Diffusion in Polymer-Solvent systems. II. A predictive theory for the dependence of diffusion coefficients on temperature, concentration and molecular weight. *J. Appl. Polym. Sci. A2* 1977, 15, 417.

[53] Flory, P.J. Thermodynamics of polymer solutions, *Disc. Faraday Soc.* 1970, 49, 7.

[54] Duda, J.L., Vrentas, J.S., Ju, S.T., Liu, H.T. Prediction of diffusion coefficients for polymer-solvent systems, *AIChE J.* 1982, 28, 2, 279-285.

[55] Flory, P.J., *Principles of polymer chemistry.* Cornell University Press, Ithaca, NY, 1953.

[56] Ferry, J.D. *Viscoelastic properties of polymers.* 2nd. ed., Wiley NY, 1970.

[57] Vrentas,J.S., Duda,J.L., A free-volume interpretation of the influence of the glass transition on diffusion in amorphous polymers, *J. Appl. Polym. Sci.* 1978, 22, 2325-2339.

[58] Romdhane,I.H., Danner,R.P., Duda,J.L., Influence of the glass transition on solute diffusion in polymers by Inverse Gas Chromatography, *Ind. Eng. Chem. Res.* 1995, 34, 2833-2840.

[59] Vrentas,J.S. and Vrentas,C.M., Prediction of Mutual Diffusion Coefficients for Polymer-Solvent Systems, *J. Appl. Polym. Sci.* 2000, 77(14), 3195-3199.

[60] Zhong, Ch., Yang Ch. , Qu, Y., A modified Vrentas-Duda model for the correlation of the solvent self-diffusion coefficients in polymer solutions, *Polymer J.* 2001, 33, 11, 842-848.

[61] Zielinski, J.M. and Duda, J.L., Predicting polymer-solvent diffusion coefficients using free-volume theory, *AIChE J.* 1992, 38, 3, 405.

[62] Ju, S.T., Duda, L. Influence of temperature on the diffusion of solvents in polymers above the glass transition temperature, *Ind. Eng. Chem. Prod. R.D.* 1981, 20, 330-335.

[63] Vrentas,J.S, Duda,J.L. and Hou,A.C. Segmentwise diffusion in molten Polystyrene, *J. Appl. Polym. Sci.* 1986, 31, 739-745.

[64] Arnould,D., Laurence,R.L. Size effects on solvent diffusion in polymers, *Ind. Chem. Eng. Res.* 1992, 31, 218-228.

[65] Vrentas,J.S. and Vrentas,C.M., Influence of solvent size on the diffusion process for polymer-solvent systems. *J. Polym. Sci. Pol. Lett.* 1990, 28, 379-383.

[66] Vrentas, J.S., Vrentas,C.M. and N.Faridi, Effect of solvent size on solvent self-diffusion in polymer-solvent systems, *Macromolecules* 1996, 29, 3272-3276.

[67] Bearman, R.J., On the molecular basis of some current theories of diffusion, *J. Phys. Chem.* 1961, 65, 1961.

[68] Brandrup, J., Immergut, E.H., Grulke, E.A., *Polymer Handbook.* 4th ed., John Wiley & Sons, NY, 1999.

[69] Smith, J.M., Van Ness, H.C., Abbot, M.M., *Introduction to chemical engineering thermodynamics.* 5th ed., McGraw-Hill, Chemical Engineering Series, 1996.

[70] Vrentas,J.S., Liu,H.T., Duda,J.L., Effect of solvent size on diffusion in polymer-solvent systems, *J. Appl. Polym. Sci.* 1980, 25, 1793-1797.

[71] Masuko, T., Sato, M., Karasawa, M., Diffusion of disperse dye in atactic Polystyrene, *J. Appl. Polym. Sci.* 1978, 22,1431-1442.

[72] Ehlich, D. And Sillescu, H., Tracer diffusion at the glass transition, *Macromolecules* 1990, 23, 1600-1610.

[73] Ito,I., Okajima, S., Shibata,F., Studies on sublimation of Disperse dye out of dyed polymers. I. Rate of sublimation and amorphous transition points of Poly(ethylene terephtalate), *J. Appl. Polym. Sci.* 1970, 14, 551-571.

[74] Okajima,S., Sato,N., Tasaka,M. , Studies on sublimation of Disperse dye out of dyed polymers. II. Rate of sublimation and amorphous transition of Polypropylene, *J. Appl. Polym. Sci.* 1970, 14, 1563-1576.

[75] Sasaki,H., Honma,Y., Kidoh,H. and Karasawa,M., Temperature dependence of diffusion of a disperse dye in the multiple layers of a Nylon Fabric *J. Appl. Polym. Sci.* 1991, 42, 1745-1750.

[76] Balashova,I.M., Danner,R.P., Puri,P.S. , Duda,J.L., Solubility and diffusivity of solvents and nonsolvents in polysulfone and polyetherimide. *Ind. Chem. Eng. Res.* 2001, 40, 3058-3064.

[77] Jiang, W.H., Liu, H., Hu, H.J., Han, S.J., Infinite dilution diffusion coefficients of n-hexane, n-heptane and n-octane in PIB by inverse gas chromatographic measurements, *Eur. Polym. J.* 2001, 37, 1705-1712.

[78] Foldes,E., Transport of small molecules in Polyolefins. III. Diffusion of Topanol CA in Ethylene polymers, *J. Appl. Polym. Sci.* 1994, 51, 1581-1589.

[79] Bonifaci,L. and Ravanetti,G., Measurement ob infinite dilution diffusion coefficients of e-caprolactam in Nylon 6 at elevated temperatures by inverse gas chromatography, *J. Chromatoghr.* 1992, 607, 145-149.

[80] Lützow,N., Tihminlioglu,A., Danner,R.P., Duda,J.L., De Haan,A., Warnier,G., Zielinski,J.M., Diffusion of toluene and n-heptane in polyethylenes of different crystallinity, *Polymer* 1999, 40, 2797-2803.

[81] Yinghua,L., Peisheng,M., Ping,L., Estimation of liquid viscosity of pure compounds at different temperatures by a corresponding-states group contribution method, *Fluid Phase Equilibr.* 2002, 198, 123-130.

[82] Marrero, J. and Gani, R., Chapter 3: Pure cbmponent property estimation: Models and Databases, in *Computer Aided Property Estimation for Process and product design.* Ed. Kontogeorgis, G.M. and Gani, R., Elsevier, 2004.

[83] Shapiro,A., Davis,P.K., Duda,J.L. Chapter 9: Diffusion in multicomponent mixtures, in *Computer Aided Property Estimation for Process and product design.* Ed. Kontogeorgis, G.M. and Gani, R., Elsevier, 2004.

[84] Fornasiero, F., Olaya, M.M., Esprester, B., Nguyen, V., Prausnitz, J.M., Distribution coefficients and diffusivities in 3 polymers for 19 aqueous nonvolatile solutes, *J. Appl. Polym. Sci.* 2002, 85, 2041-2052.

[85] Pearson, D.S., Ver Strate, G., von Meerwall, E., Schilling,F.C. Viscosity and self-diffusion coefficient of linear polyethylene, *Macromolecules* 1987, 20, 1133-1141.

[86] Reynhardt, E.C., The role of hydrogen bonding in the cuticular wax of Hordeum vulgare L., *Eur. Biophys. J.* 1997, 26, 195-201.

[87] Schreiber,L. and Schnherr,J., Mobilities of organic compounds in reconstituted cuticular wax of Barley leaves: Determination of diffusion coefficients, *Pesti. Sci.* 1993, 38, 353-361.

[88] Buchholz, A., Baur,P., Schnherr, J., Differences among plant species in cuticular permeabilities and solute mobilities are not caused by differential size selectivities, *Planta* 1998, 206, 322-328.

[89] Baur,P., Buchholz,A., Schnherr,J., Diffusion in plant cuticles as affected by temperature and size of organic solutes: similarity and diversity among species, *Plant Cell Environ.* 1997, 20, 982-994.

[90] Yadav,S.K., Khilar,K.C. and Suresh,A.K. Microencapsulation in Polyurea shell: Kinetics and film structure, *AIChE J.* 1996, 42(9), 2616-2626.

[91] Yadav,S.K., Suresh, A.K. and Khilar,K.C. Microencapsulation in Polyurea shell by interfacial polycondensation, *AIChE J.* 1990, 36(3), 431-438.

[92] Kubo,M., Harada,Y., Kawakatsu,T. and Yonemoto,T. Modeling of the formation kinetics of Polyurea microcapsules with size distribution by interfacial polycondensation, *J. Chem. Eng. Jpn.* 2001, 34, 12, 1506-1515.

[93] Yadav,S.K., Khilar,K.C. and Suresh,A.K., Release rates from semicrystalline polymer microcapsules formed by interfacial polycondensation, *J. Membrane Sci.* 1997, 125, 213-218.

[94] http://www.generalpolymers.com/tech_lib/material_app.asp

5

Integration of property prediction with controlled release: case studies

5.1 Introduction

In Chapter 2 of this thesis, a brief review of the mathematical models available for controlled release products has been presented together with an identification of the variables (properties) that are critical for the majority of these models: partition coefficients and diffusion coefficients. The importance of developing predictive models to estimate these properties has also been highlighted. The release models and each of the property models have been presented and discussed in chapters 2, 3 and 4 respectively. The final step in the model development is the integration of the property prediction models with the controlled release models, and to show their applicability to different problems involving controlled release applications.

The integration of the models is done within the framework illustrated in Fig. 5.1, and at the same time its significance to product design is discussed here. From Fig. 5.1, the process of product design is illustrated through different steps of development. First of all, the AI of interest is chosen, together with a polymer to be used for the specific application. The combination of the AI and the polymer determines the properties of the system, that is, diffusivity and solubility, which play a very important role in the final release of the AI from the product. At the same (initial) level, a type of product is selected (microcapsule for example), which determines a number of parameters such as, geometry, size, etc. Then, in the analysis stage, the integration of the developed predictive property models with the mathematical release models allows the study of the release behaviour of this specifically designed product as a function of time.

By following this procedure, several alternatives of different AI-polymer and product combinations can be proposed and analysed to achieve the desired performance of the final product.

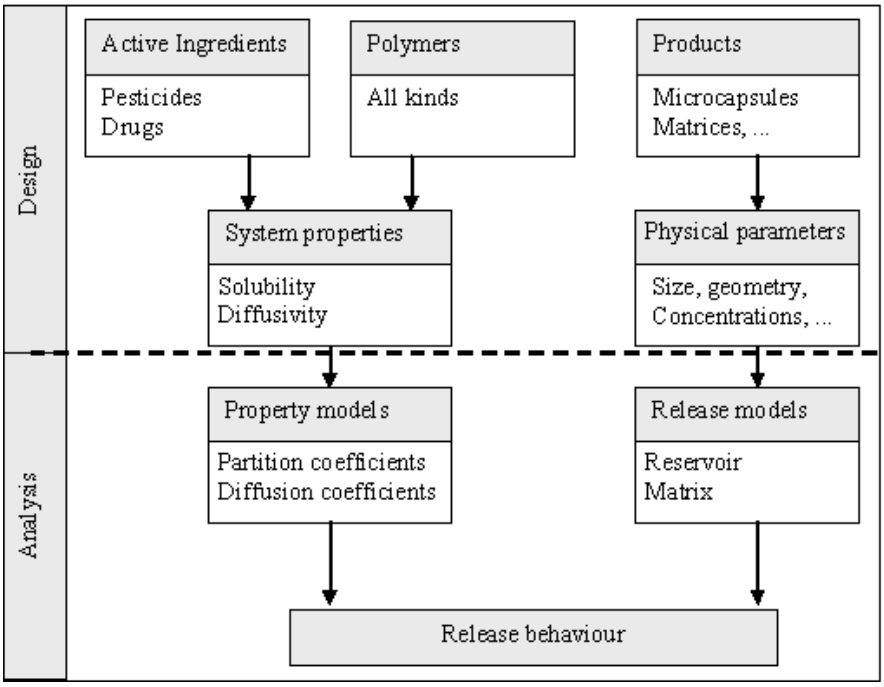

Figure 5.1: Framework for model-based design and analysis of AI release.

At this stage though, the validity and applicability of this framework needs to be assessed. Therefore, case studies are presented in this section highlighting the possibilities for property prediction together with the AI release calculations for systems where some experimental data is available in order to assess the reproducibility of the results.

The first two case studies involve the prediction of one of the parameters, the diffusion coefficient, which is then analyzed through some measured release data available given that no data for the actual parameter values is accessible. A drug compound is involved in the first example, which at the same time shows that the methodology can be applied out of the area of focus of this work (pesticides) and within, for example, the pharmaceutical field. The second example shows a similar analysis but now applied to the agrochemical area, which is the field of interest in this work, through use of a pesticide AI to evaluate the integration of property and release models. The last case study involves the implementation of all the predictive models described in this work and the analysis of their performance, again through measured data for the release of a pesticide compound.

5.2 Codeine case study: prediction of the diffusion coefficient

This case study involves the prediction of the diffusion coefficient (through the free volume model) together with the study of the release of a drug from a microcapsule.

The case study concerns the drug Codeine (CAS nr: 76-57-3) encapsulated within polyurea microcapsules. Note that this is the same system as Case study 1 in section 2.3.1. Experimental data of the release behaviour of the AI as a function of time is available from the literature (Lukaszczyk et al. [1]).

All the details on the microcapsule preparation, compositions and AI release conditions have been extracted from the literature (Lukaszczyk et al. [1]) and summarized in section 2.3.1. Therefore only details of the variables relevant for this specific case study are given here. All the values for the variables required by the controlled release mathematical model are summarized in Table 5.1 for the four different scenarios that have been investigated. The assumptions made previously in section 2.3.1 are also valid here.

Table 5.1: Summary of the input data required for the mathematical release model.

Variable	**Scenario 1**	**Scenario 2**	**Scenario 3**	**Scenario 4**
MDI/resinate	0.1	0.25	0.5	1
h (m)	2.86×10^{-9}	6.72×10^{-9}	12.23×10^{-9}	20.85×10^{-9}
r_{max} *(m)*	329×10^{-9}	329×10^{-9}	329×10^{-9}	329×10^{-9}
r_{min} *(m)*	29×10^{-9}	29×10^{-9}	29×10^{-9}	29×10^{-9}
r_{mean} *(m)*	129×10^{-9}	129×10^{-9}	129×10^{-9}	129×10^{-9}
σ	3×10^{-8}	3×10^{-8}	3×10^{-8}	3×10^{-8}
r_{step} *(m)*	1×10^{-8}	1×10^{-8}	1×10^{-8}	1×10^{-8}
$V_r(m^3)$	400×10^{-6}	400×10^{-6}	400×10^{-6}	400×10^{-6}
t (s)	12600	12600	12600	12600
$C_{d,initial}(g/m^3)$	358.44×10^{3}	324.72×10^{3}	280.697×10^{3}	220.825×10^{3}
$V_d(m^3)$	0.485×10^{-6}	0.536×10^{-6}	0.620×10^{-6}	0.788×10^{-6}

In each of the four scenarios the microcapsules present a different wall thickness, defined through a different monomer (MDI) to resinate ratio and calculated in the same manner explained in section 2.3.1.

The value of the diffusion coefficient of Codeine in polyurea is estimated through the Extended FV model described in section 4.3 of Chapter 4. In order to perform the Extended FV model calculations the WLF parameters (C_1^{WLF}, C_2^{WLF}) are required. For the specific polymer of interest (polyurea) these parameters or experimental data to estimate them (viscosity as a function of temperature) are not available. Therefore, the parameters of a polymer

assumed to have a similar behaviour, a polyurethane, are used (Ngai et al. [2]) in the same manner as in section 4.4.2.3 where this was proven to be a good approximation. The value of the diffusion coefficient is estimated at the temperature for which the release experiments are reported (310 K). The parameters of the Extended FV model that have been estimated with the predictive methodology are given in Table 5.2 together with the calculated value of the diffusion coefficient.

Table 5.2: Extended FV model estimated parameters (pure prediction) for Codeine in Polyurea (modelled as Polyurethane) and diffusion coefficient value at 310 K.

Compound	**V(0 K)**$\times 10^6$ (cm^3/mol)	$K_{1i}/\gamma \times 10^9$ (m^3/gK)	$K_{2i} - Tg_i$ **(K)**	D_0 (m^2/s)	ξ
Codeine	214.5	1.362	-132.75	5.142×10^{-8}	2.26
Polyurea	148.8	0.323	-181.4	-	-
D (m^2/s)= 1.027×10^{-19}					

The value of the diffusion coefficient is in principle considered to be the same for the four different scenarios because the polymer used is the same. Note however that, as different amounts of monomer have been used in the formation of the polymer membrane, it may affect the degree of cross-linking of the same and therefore the diffusivity value. This consideration might therefore have to be revised in the cases where the degree of cross-linking changes.

The partition coefficient values cannot be predicted through the property models because Codeine cannot be described with the groups that are currently available in the activity coefficient models. They are therefore obtained through other considerations.

The partition coefficient of Codeine between the polymer membrane (polyurea) and the release medium (water), $K_{m/r}$, can be adapted from that reported by (Kubo et al. [3]) for the partition of Diethylene triamine (DETA) also between water and polyurea. The partition coefficient is the relationship between the concentration of AI in the polymer membrane (C_m) and in the release medium (C_r), that is, $K_{m/r} = C_m/C_r$. Then, the validity of the assumption can be verified through the relative solubilities of each compound (Codeine and DETA) in the release medium (water) and the polymer membrane (polyurea) respectively, since these are the same in both cases. This is done through the solubility parameters, as shown in Table 5.3. From the table, the relative solubilities ($\Delta\delta$(I) − $\Delta\delta$(II)) are observed to be the same in both systems (with DETA and with Codeine), so the consideration of using the same partition coefficient is found to be valid.

Table 5.3: Relative solubilities of the compounds involved in the case study and those from Kubo et al. [3].

		δ_1 ($MPa^{1/2}$)	δ_2 ($MPa^{1/2}$)	$\Delta\delta$ ($MPa^{1/2}$)	$\Delta\delta(I) - \Delta\delta(II)$ ($MPa^{1/2}$)
I	DETA (1) - water (2)	25.8	47.9	22	-
II	DETA (1) - Polyurea (2)	25.8	32.76	6	16
I	Codeine (1) - water (2)	20	47.9	28	-
II	Codeine (1) - Polyurea (2)	20	32.76	12	16

$\Delta\delta = \delta_1 - \delta_2$

The value for the partition coefficient of Codeine between the polymer membrane and the donor (a resinate in this case), $K_{m/d}$, could not be obtained from the same source (Kubo et al. [3]) since the scenarios are not comparable. In this case, due to the binding of the drug to the resinate in the core, it is considered that the concentration inside (C_d) will be higher than in the membrane (C_m, then $C_d > C_m$). From the definition of the partition coefficient ($K_{m/d} = C_m/C_d$), the value of this parameter will then be less than unity. Then, the value assumed to model the release data for $K_{m/d}$ (0.12) can be considered qualitatively correct.

The values of the partition coefficients used for the different scenarios modelled are the same, since the donor and release mediums do not change. The values of the properties that will be used hereafter are summarized in Table 5.4.

Table 5.4: Properties required by the controlled release model

Variable	**All scenarios**	**Remarks**
$D(m^2/s)$	1.027×10^{-19}	Estimated
$K_{m/r}$	2.67	Adapted
$K_{m/d}$	0.12	Assumed

Finally, the release of Codeine from the polyurea microcapsules is calculated using the basic release model (section 2.3.1) for the four scenarios listed in Table 5.1 and the results obtained are plotted in Fig. 5.2. Note that one of these scenarios (scenario 2) was observed to present lag time effects, but the basic release model is used here (where these have not been considered).

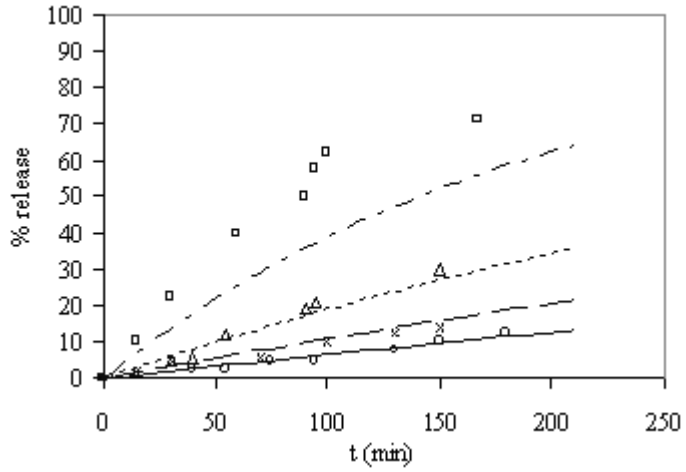

Figure 5.2: Comparison of experimental and estimated Codeine release values as a function of time. Experimental data: (□) Scenario 1, (△) Scenario 2, (x) Scenario 3, (○) Scenario 4. Predicted release: (– - –) Scenario 1, (- - -) Scenario 2, (– –) Scenario 3, (—) Scenario 4.

The performance of the release model with the predicted diffusion coefficient is very good in all the cases except in the case of the microcapsules with the smallest thickness (scenario 1). This can be attributed to different degrees of cross-linking of the polymer that would affect the value of the diffusion coefficient. For scenario 1, the amount of monomer forming the wall is lower than in the other cases, thereby reducing the degree of cross-linking and increasing the value of the diffusivity. In order to test this hypothesis, a study has been done to find the diffusion coefficient value that would best fit the experimental release data for each of the scenarios by keeping the rest of the variables fixed to the original values. The results are given in Table 5.5 and plotted in Fig. 5.3.

Table 5.5: Diffusion coefficient values for each scenario to fit release data.

Scenario	**MDI/resinate**	D(m^2/s)
1	0.1	1.59×10^{-19}
2	0.25	1.1×10^{-19}
3	0.5	1.027×10^{-19}
4	1	1.027×10^{-19}

It can be observed from these results that, as the amount of MDI-monomer increases (corresponding to an increase of the MDI/resinate ratio), the cross-linking of the polymer also increases while the diffusion coefficient decreases exponentially, confirming thereby the hypothesis.

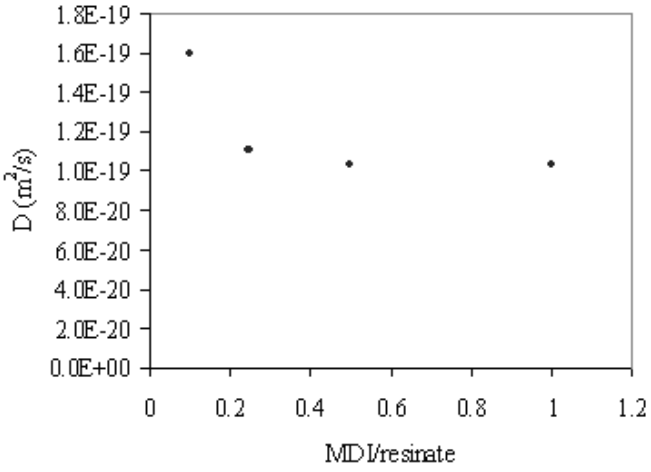

Figure 5.3: Values of the diffusion coefficients as a function of the monomer to resinate ratio.

Finally, the release results obtained with the new diffusivity values are given in Fig. 5.4 where the accuracy of the release model when the appropriate parameters are used is once more confirmed.

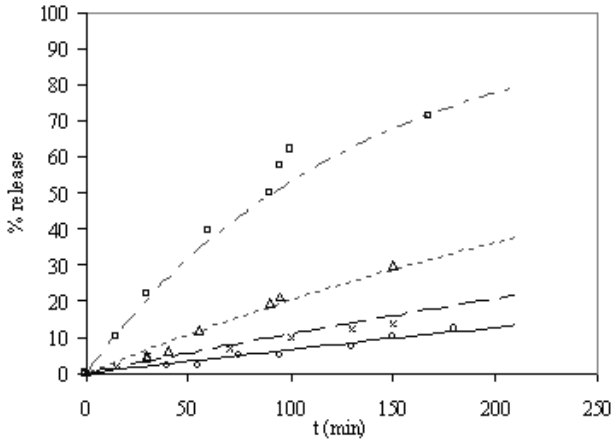

Figure 5.4: Comparison of experimental and estimated Codeine release values as a function of time. Experimental data: (□) Scenario 1, (△) Scenario 2, (x) Scenario 3, (○) Scenario 4. Predicted release: (– - –) Scenario 1, (- - -) Scenario 2, (– –) Scenario 3, (—) Scenario 4.

5.3 Agrochemical A case study: prediction of the diffusion coefficient

In this case study the estimation of the diffusion coefficient through the Extended FV model is again highlighted. No experimental data on the properties of the compounds could be found, but only measured data of release is available. Therefore the diffusivity predictions integrated within the mathematical release models are analysed through the measured release data. The scope of this case study is in general terms the same as that for the previous Codeine case study (section 5.2) but now the compound released is a pesticide AI.

The compound involved in this case study is Agrochemical A, which is encapsulated together with a solvent within polyurea microcapsules, to avoid fast removal, by leaching, from the environment (improve persistence). The polurea-based membrane used to encapsulate the Agrochemical A is formed through interfacial polycondensation of an isocyanate and a multifunctional amine to provide a polyurea membrane with a high degree of cross-linking. The reaction is illustrated in general terms in Fig. 5.5, and more details can be found for example in Kubo et al. [3] (even though the monomers used are different).

$$\underset{\text{isocyanate}}{-N=C=O} + \underset{\text{amine}}{-NH_2} \rightarrow \underset{\text{polyurea}}{-NH-CO-NH-}$$

Figure 5.5: Polycondensation reaction to form polyurea.

The compounds and their respective compositions used in the formulation of these microcapsules are listed in Table 5.6 for two different scenarios that consist of different percentages of wall material. Within each of these scenarios, several cases are investigated consisting of different microcapsule sizes.

Table 5.6: Formulation for the specific release experiments (quantities in mg).

	26.8 % wall	**30.5 % wall**
inside capsule (donor)		
Agrochemical A	6.25	6.25
Aliphatic solvent	7.81	7.15
capsule wall		
Isocyanate resin	4.688	5.36
Multifunctional amine	0.47	0.54
continuous phase		
Colloid stabilizer	2.812	2.81
Water	27.97	27.9
Total mg of microcapsules	50	50

In Table 5.7 some relevant information about the compounds present in the

formulation is provided.

Table 5.7: Summary of the compounds present in the formulation

Compound	**Details**
Agrochemical A	AI
Aliphatic solvent	Solvent (Mixture of fatty acids)
Isocyanate resin	Monomer
Multifunctional amine	Monomer
Colloid stabilizer	-
Water	Release medium

As mentioned above the reported release experiments were performed for different microcapsule sizes as well as thicknesses of the microcapsule wall. The Agrochemical A is then released into 50 mL of water at 20 °C. The values of the measured AI release as a function of time are provided in Table 5.8, with the first three cases having a 26.8% of wall material and the remaining four have 30.5% of wall material. The details on the sizes of each case studied are provided in Table 5.9.

Table 5.8: Experimental data of AI release as a function of time.

t (h)	**% release**						
	26.8 % wall			**30.5 % wall**			
	1	**2**	**3**	**4**	**5**	**6**	**7**
1	6.6	6.06	4.67	3.44	3	0	2.21
4	9.44	7.8	6.77	4.17	3.43	2.14	2.39
24	12.9	10.91	8.19	5.38	4.49	2.76	3.12
75	14.99	12.55	10.09	6.16	5.36	3.09	3.78
168	17.07	13.72	11.98	6.61	6.11	3.46	4.21
312	18.07	14.55	13.64	7	6.63	3.59	5.1

Table 5.9: Identification of each experiment.

Nomenclature	**d (μm)**	**wall %**
Case 1	13.09	26.8
Case 2	15.02	26.8
Case 3	16.4	26.8
Case 4	16.8	30.5
Case 5	20.1	30.5
Case 6	22.54	30.5
Case 7	26.35	30.5

The next step is the analysis of these data in terms of the mathematical model. From the previous description of the experiments, the values of the variables that are needed by the controlled release model can be obtained (details in the case study of section 2.3.1) and they are provided in Table 5.10 and Table 5.11 for the cases with 26.8% of wall material and 30.5% of wall material respectively, and for each of the scenarios to be studied. It is worth noting that the actual distribution of microcapsule sizes was not measured but it has been assumed on the basis of other studies (for example, Kubo et al. [3]).

Table 5.10: Summary of the input data required for the mathematical release model for the experiments with 26.8% wall.

Variable	**Case 1**	**Case 2**	**Case 3**
h (m)	0.557×10^{-6}	0.639×10^{-6}	0.698×10^{-6}
r_{max} (m)	13×10^{-6}	15×10^{-6}	16.4×10^{-6}
r_{min} (m)	3.25×10^{-6}	3.75×10^{-6}	4.1×10^{-6}
r_{mean} (m)	6.545×10^{-6}	7.51×10^{-6}	8.2×10^{-6}
σ	7×10^{-7}	7×10^{-7}	7×10^{-7}
r_{step} (m)	1.0×10^{-8}	1.0×10^{-8}	1.0×10^{-8}
$V_r(m^3)$	50×10^{-6}	50×10^{-6}	50×10^{-6}
t (s)	1123200	1123200	1123200
$C_{d,initial}(g/m^3)$	365217.5	365217.5	365217.5
$V_d(m^3)$	0.017×10^{-6}	0.017×10^{-6}	0.017×10^{-6}

Table 5.11: Summary of the input data required for the mathematical release model for the experiments with 30.5% wall.

Variable	**Case 4**	**Case 5**	**Case 6**	**Case 7**
h (m)	0.825×10^{-6}	0.987×10^{-6}	1.106×10^{-6}	1.293×10^{-6}
r_{max} (m)	16.8×10^{-6}	21×10^{-6}	22.54×10^{-6}	26.35×10^{-6}
r_{min}(m)	4.2×10^{-6}	5.25×10^{-6}	5.64×10^{-6}	6.59×10^{-6}
r_{mean} (m)	8.4×10^{-6}	10.05×10^{-6}	11.27×10^{-6}	13.175×10^{-6}
σ	7×10^{-7}	7×10^{-7}	7×10^{-7}	7×10^{-7}
r_{step} (m)	1.0×10^{-8}	1.0×10^{-8}	1.0×10^{-8}	1.0×10^{-8}
$V_r(m^3)$	50×10^{-6}	50×10^{-6}	50×10^{-6}	50×10^{-6}
t (s)	1123200	1123200	1123200	1123200
$C_{d,initial}(g/m^3)$	363948.7	363948.7	363948.7	363948.7
$V_d(m^3)$	0.017×10^{-6}	0.017×10^{-6}	0.017×10^{-6}	0.017×10^{-6}

In this case study not all the properties required by the controlled release model (diffusion and partition coefficients) can be predicted with the currently available property models due to the complexity of the AI and the monomer

molecules. Given this situation the value of the diffusion coefficient will be predicted and the values of the partition coefficients will be assumed in order to fit the release data and analyzed later on for consistency.

In the first place, the estimation of the diffusion coefficient in the polyurea membrane is done through the Extended FV model described in section 4.3. Again, polyurea is modelled as a polyurethane model polymer. The estimated parameters for the free volume model are listed in Table 5.12 together with the estimated value for the diffusion coefficient of Agrochemical A in polyurea (polyurethane) at the temperature of the experiments, that is, 293.15 K.

Table 5.12: Parameters obtained from pure prediction and diffusion coefficient value at 293.15 K.

Compound	**V(0 K)** (cm^3/mol)	K_{1i}/γ (cm^3/gK)	$K_{2i} - Tg_i$ **(K)**	D_0 (m^2/s)	ξ
Agrochemical A	187.5	1.207×10^{-3}	-148.97	1.92×10^{-8}	1.48
Polyurea (Polyurethane)	64.12	3.23×10^{-4}	-181.4	-	
D (m^2/s)= 5.8×10^{-17}					

The predicted value for the diffusion coefficient can be analyzed with respect to the values given in section 4.4.2.3 for DETA, cyclohexane and HMDA diffusing in polyurea (again modeled as polyurethane). These compounds are significantly smaller than Agrochemical A in terms of molar volume at 0 K ($\leq$ 115 cm^3/mol) and therefore expected to diffuse significantly faster, which is also predicted. Compared to the value obtained for Codeine, the faster diffusion of Agrochemical A can be explained due to the fact that Agrochemical A is a smaller and less bulky molecule.

For this example, the diffusion coefficient is considered to be the same for all the cases studied. This is a good approximation as the relative amount of polymer forming the wall (that defines the wall thickness) does not change significantly from one experiment to another and therefore the polymer morphology and properties (cross-link and crystallinity affecting the diffusion coefficient value) are expected to be quite similar.

With respect to the values of the partition coefficients ($K_{m/d}$ and $K_{m/r}$), the AI unfortunately, cannot be described by either of the group-contribution methods (KT-UNIFAC and GC-Flory EoS). The amount of groups missing for this compound is too high to do any attempts of calculations without the missing groups. Their values are therefore assumed and analyzed afterwards.

The final property values used for the release model calculations are summarized in Table 5.13.

Table 5.13: Properties required by the controlled release model

Variable	All scenarios with 26.8% wall	All scenarios with 30.5% wall	Remarks
D (m^2/s)	5.8×10^{-17}	5.8×10^{-17}	Estimated
$K_{m/r}$	9×10^{9}	2×10^{10}	Assumed
$K_{m/d}$	0.034	0.01	Assumed

After the assessment of all the parameters needed by the mathematical model, the calculations for controlled release can now be performed. From the experimental release data it can be observed that the amount of AI released increases very fast in the initial period of the delivery, which seems to be an indicator of burst effects. Therefore the mathematical model used to calculate the release of Agrochemical A from the microcapsules is that corresponding to burst combined with first order release described in section 2.3.2. The results of the calculations with the mentioned release model are plotted in Figs. 5.6 and 5.7 for the lower (Cases 1 to 3) and higher (Cases 4 to 7) wall percent, respectively, and compared with the experimental data for each of the cases.

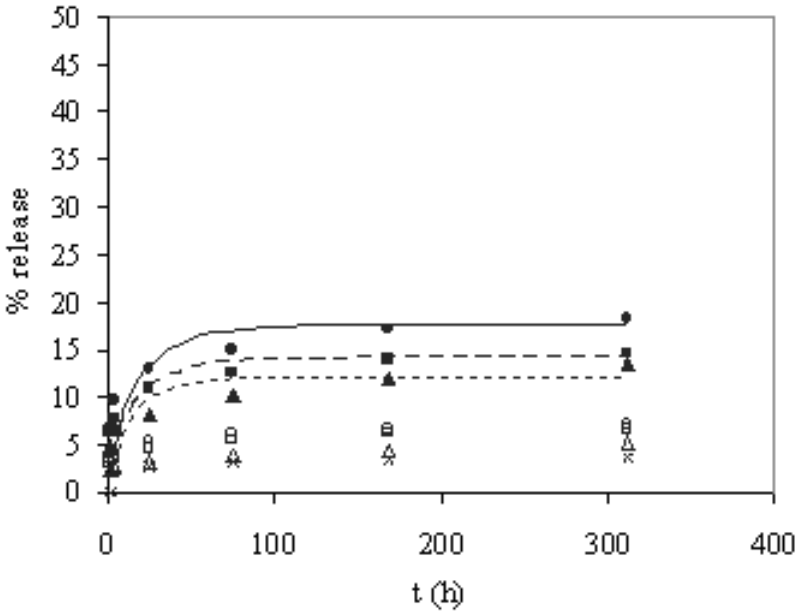

Figure 5.6: Comparison of model calculations and experimental data for the three cases with 26.8% wall. Experimental data: (•) Case 1, (■) Case 2, (▲) Case 3, (○) Case 4, (□) Case 5, (x) Case 6, (△) Case 7. Model calculations: (—) Case 1, (– –) Case 2, (- - -) Case 3.

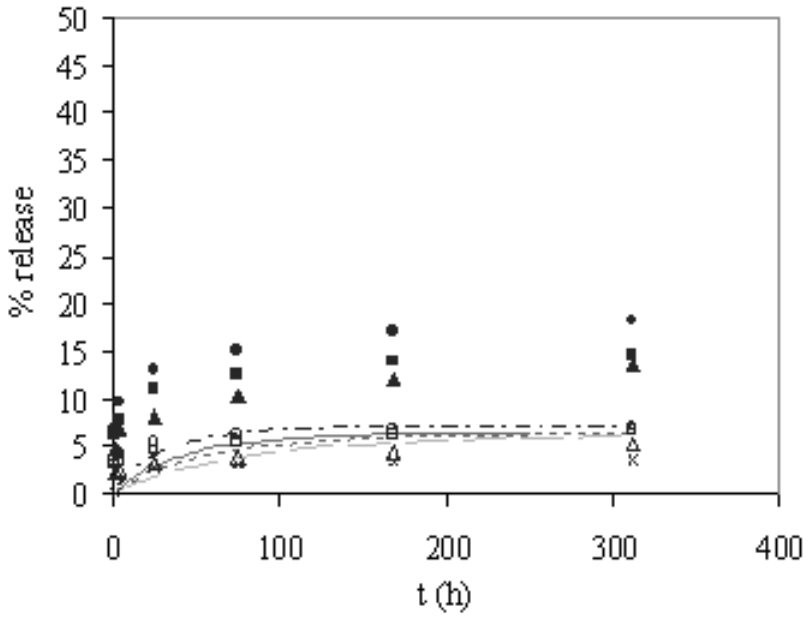

Figure 5.7: Comparison of model calculations for the cases with 30.5% wall. Experimental data: (•) Case 1, (■) Case 2, (▲) Case 3, (○) Case 4, (□) Case 5, (x) Case 6, (△) Case 7. Model calculations: (– - –) Case 4, (—) Case 5, (– –) Case 6, (- - -) Case 7.

From Figs. 5.6 and 5.7 it can be observed that for all the cases, (except 6 and 7 that will be analyzed later) the amounts of AI released can be matched with the appropriate partition coefficient values and the predicted diffusion coefficient. The initial period of delivery is not accurately reproduced by the model, even with use of the burst effect term in the model. This leads to the consideration that other effects are possibly occurring that have not been taken into account. A possible explanation comes from the fact that polyurea is a hydrophilic polymer, so it is likely that the water used as release medium penetrates into the polymer. This can lead to (i) swelling of the polymer, and (ii) release of part of the AI by diffusion through the water-filled pores. The first effect can have several consequences, for example, an increase of the membrane thickness that would explain the slow delivery through the whole release period. But swelling can also change the diffusion mechanism (Peppas et al. [5]) and the value of the diffusion coefficient is not a constant anymore but changes as a function of time. This is a very complex mechanism to model, and out of the scope of this work.

For cases 6 and 7, where the amount of AI released cannot be predicted on the same terms (or parameters) as those for case 4-5, deserve special attention. First of all, the microcapsules in case 7 have a greater wall thickness and mean

size than the ones in case 6, therefore the release from microcapsules in case 6 would be expected to be higher than the ones in case 7. The experimental release data show the opposite behaviour and therefore the model cannot reproduce these results. Another consideration to make is the fact that the amount of AI released is significantly overpredicted. Again the difference in size and thickness of cases 6 and 7 is equivalent to that between cases 4 and 5 but on the other hand there is a significant difference between the amount of AI released from case 5 and that from cases 6 and 7. Once more this is the reason why the model cannot reproduce accurately the experimental values.
A qualitative analysis of the partition coefficient values used to fit the release data is now attempted. This is, again, done through the solubility parameters of the compounds involved, and based on the fact that the closest the values of the solubility parameters, the better the solubility of the compounds. In Fig. 5.8, the relative solubilities of the compounds are illustrated through the solubility parameter values. Note that the solubility parameter of the aliphatic solvent is based on its main components, but since the exact composition is not known, this value can be subject to variations.

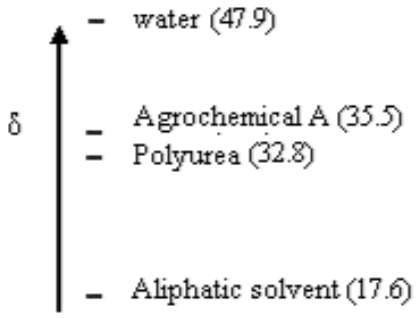

Figure 5.8: Scale of the solubility parameters (δ in $MPa^{1/2}$) for the compounds involved.

From Fig. 5.8, it is clear that Agrochemical A is significantly more soluble in the polyurea membrane than in water (the release medium), that is, $C_m > C_r$. This explains the high value of the partition coefficient between the membrane and the release medium ($K_{m/r}$), from the definition of this parameter ($K_{m/r} = C_m/C_r$). On the other hand, the partition coefficient of the AI between the polymer membrane and the donor ($K_{m/d}$) cannot be explained through Fig. 5.8. Here, the fact that the AI is initially in the core, with a very high concentration (given the small volume of the microcapsule), and none of the AI is in the membrane ($C_m < C_d$), provides the explanation for the partition coefficient being less than unity ($K_{m/d} = C_m/C_d$).

Finally, it should be noted that the difference in the partition coefficient values that match the release data in the two scenarios (different relative amounts of wall material) could be due to some variation in the polymer morphology

arising from the different composition of the microcapsules, which has not been taken into account in any way in the developed models.

5.4 λ-cyhalothrin case study

The final integration of the prediction of the two important constitutive variables (diffusion and partition coefficients), that play a role in the release of an AI from a microcapsule, is illustrated in this case study for a system involving a pesticide compound.

In this example the AI λ-cyhalothrin (CAS nr: 91465-08-6) is encapsulated together with a solvent, within polyurea microcapsules. λ-cyhalothrin is an acaricide and insecticide from the synthetic pyrethroids family. It is used to control a wide range of pests (beetle and butterfly larvae for example) in different crops (such as cotton and potatoes, among others). This is an AI that can cause paraesthesia, which is then avoided through encapsulation, at the same time achieving extended biological activity. The polyurea wall surrounding the AI and the solvent in the core is formed by interfacial polycondensation reaction of the polyfunctional isocyanate monomers, providing a highly cross-linked and thus very hard polymer. In this specific case the monomers used are Toluene diisocyanate (TDI) and Polymethylene polyphenylisocyanate (PMPPI) and the general form of the reaction is illustrated in Fig. 5.9. More details on the wall forming process can be found in Scher et al. [4]. The structure of the polymer resulting from each monomer is provided in Figs. 5.10(a) and 5.10(b), which will then be randomly mixed in the final polyurea wall.

$$\underset{\text{isocyanate}}{-N=C=O} + H_2O \rightarrow \underset{\text{carbamic acid}}{-NH-CO-OH-} \rightarrow \underset{\text{amine}}{-NH_2} + CO_2 \uparrow$$

$$\underset{\text{isocyanate}}{-N=C=O} + \underset{\text{amine}}{-NH_2} \rightarrow \underset{\text{polyurea}}{-NH-CO-NH-}$$

Figure 5.9: Polycondensation reaction to form polyurea.

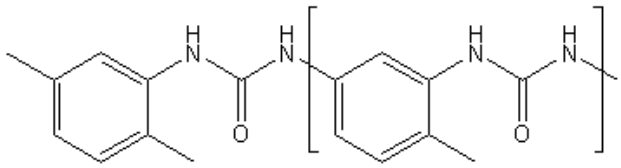

(a) Polyurea resulting from TDI.

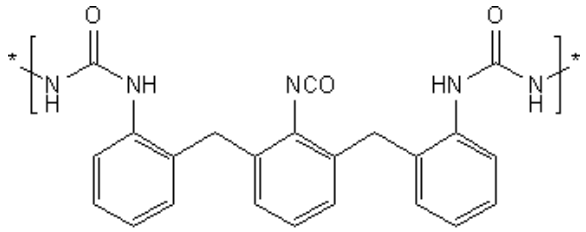

(b) Polyurea resulting from PMPPI

Figure 5.10: Polyureas obtained from each of the monomers

Details of the final formulation used to form the microcapsules in these experiments is given in Table 5.14 for the three cases investigated (representing three different thickness of the microcapsule wall). In Table 5.15 more details of the compounds in the formulation are provided together with the properties that are relevant for this study.

Table 5.14: Microcapsule composition

	Case 1	**Case 2**	**Case 3**
	10% wall	**20% wall**	**30% wall**
inside capsule (donor)			
λ-cyhalothrin technical (84.6% pure)	74.98	74.98	74.98
Solvesso 100	147.63	121.38	95.13
capsule wall			
TDI	6.56	13.13	19.69
PMPPI	19.69	39.38	59.06
continuous phase (outside capsule)			
Surfactant 1	7.5	7.5	7.5
Surfactant 2	18.75	18.75	18.75
Water	461.25	461.25	461.25
Total mg of microcapsules	750	750	750

Table 5.15: Summary of some of the properties of the compounds

Compound	**CAS nr**	**Mw (g/mol)**	**Density** (g/cm^3)	**Details**
λ-cyhalothrin	91465-08-6	449.86	1.1494	AI
Solvesso 100	n/a	n/a	1.02	Mixture of C9-C10 dialkyl and trialkyl benzenes.
TDI	584-84-9	174.16	1.0847	Monomer
PMPPI	9016-87-9	381.31	1.225	Monomer
Surfactant 1	n/a	2990	1.19	
Surfactant 2	8061-51-6	n/a	1.146	
Water	7732-18-5	18.0152	1	Continuous phase

The release of AI from the described microcapsules has been studied (by Syngenta) and the results are given in Table 5.16. The AI is released into a mixture of hexane and ethanol with a composition of 90:10 by weight, with a total volume of 100 mL and at a temperature of 20 °C. This AI has very low water solubility but is on the other hand very soluble in n-hexane. Therefore, n-hexane was used within the release medium to accelerate the release of AI.

Table 5.16: Experimental data of AI release as a function of time.

t (h)	**% release**		
	10% wall	**20% wall**	**30% wall**
0.25	98.54	76.38	4.21
0.5	98.04	87.95	10.35
3	99.81	99.6	36.83

The next step is then, to analyze the experimental data in terms of the mathematical release model. Table 5.17 provides the variables needed by the release model that can be extracted from the description of the experiments, for the three cases investigated. Once again, the distribution of microcapsule sizes was not measured so it has been assumed based on other studies (Kubo et al. [3]).

The same procedure as in case studies 1 and 2 has also been used here for the calculation of the wall thickness from the ratio of wall material given in the experiment. The part that deserves special attention in this case study is the estimation of the properties or constitutive variables (diffusion and partition coefficients).

Table 5.17: Summary of the input data required for the mathematical release model.

Variable	**Case 1**	**Case 2**	**Case 3**
Wall %	10	20	30
h (m)	4.21×10^{-9}	10.18×10^{-9}	14.5×10^{-9}
r_{max} (m)	322×10^{-9}	342×10^{-9}	329×10^{-9}
r_{min} (m)	22×10^{-9}	42×10^{-9}	29×10^{-9}
r_{mean} (m)	122×10^{-9}	142×10^{-9}	129×10^{-9}
σ	3×10^{-8}	3×10^{-8}	3×10^{-8}
r_{step} (m)	1×10^{-8}	1×10^{-8}	1×10^{-8}
$V_r(m^3)$	100×10^{-6}	100×10^{-6}	100×10^{-6}
t (s)	10800	10800	10800
$C_{d,initial}(g/m^3)$	301.35×10^{3}	301.35×10^{3}	301.35×10^{3}
$V_d(m^3)$	0.249×10^{-6}	0.249×10^{-6}	0.249×10^{-6}

i) Prediction of the diffusion coefficient

The value of the diffusion coefficient is obtained from the Extended FV model. In Chapter 4 a case study dealing with the diffusion of λ-cyhalothrin in PE-VAc polymers has been presented. The results can now be used to provide some insight in the diffusivity predictions. There are two methods to estimate the diffusion coefficient depending on whether experimental diffusivity data is available or not. Both methods will be studied here. In the first place the estimation of the diffusion coefficient is attempted in a purely predictive manner (a), but given that some experimental data is available for the diffusivity of the same AI in another polymer, a semi-predictive methodology (b) can also be applied. In the latter approach, the parameters of the Extended FV model that are properties of the AI are obtained from experimental data (for another system).

(a) Predictive estimation of the diffusion coefficient (D)

In order to estimate the diffusion coefficient of the AI in a purely predictive manner all the Extended FV model parameters need to be estimated using the procedure outlined in chapter 4 (section 4.3). For the specific polymer of interest, the polyurea, the WLF parameters (C_1^{WLF}, C_2^{WLF}) or temperature dependent viscosity data are though not available, and it is therefore again modelled as a polyurethane. The values of the Extended FV model parameters estimated here are listed in Table 5.18 together with the estimated value for the diffusion coefficient at the temperature of the release experiments (293.15 K).

Table 5.18: Parameters obtained from pure prediction and diffusion coefficient value at 293.15 K.

Compound	**V(0K)** (cm^3/g)	K_{1i}/γ (cm^3/gK)	$K_{2i} - Tg_i$ **(K)**	D_0 (cm^2/s)	ξ
λ-cyhalothrin	0.68	1.36×10^{-3}	-206.46	4.75×10^{-5}	1.58
Polyurea (Polyurethane)	0.67	3.23×10^{-4}	-181.4	-	
D (cm^2/s) = 4.08×10^{-14}					

The estimated value of the diffusion coefficient is very small. This value can be compared, for example, with the diffusion coefficient calculated for HMDA (D = 1.23×10^{-9} (cm^2/s), in section 4.4.2.3), a compound with a linear shape similar to λ-cyhalothrin. HMDA is though smaller, so a higher diffusivity would be expected, but not such a big difference (five orders of magnitude). This value can also be compared with the diffusion coefficient predicted for Agrochemical A (D = 1.23×10^{-13} (cm^2/s), in section 5.3). λ-cyhalothrin is expected to have higher diffusivity than Agrochemical A, given that it is has a linear shape, but the predicted value contradicts this conclusion. It can be concluded, however, that while compared to HMDA the predicted value of the diffusion coefficient is at least qualitatively correct, the quantitative value is underpredicted.

(b) Semi-predictive estimation of the diffusion coefficient

In this case the previous study of diffusion of λ-cyhalothrin in PEVAc (section 4.4.2.2) is used. The parameter values obtained thereby (pre-exponential factor, D_0 and ratio of jumping units, ξ) can be used for this system (λ-cyhalothrin in polyurea) based on the fact that D_0 is a property of the AI, and from ξ, the value of the aspect ratio of the molecule can be calculated and used here. Then, based on these values the diffusion coefficient of λ-cyhalothrin in polyurea can be estimated in a predictive manner. The parameter values and the diffusion coefficient value obtained thereby at the temperature of interest (293.15 K) are reported in Table 5.19.

Table 5.19: Parameters obtained from semi-predictive methodology and diffusion coefficient value at 293.15 K.

Compound	**V(0K)** (cm^3/g)	K_{1i}/γ (cm^3/gK)	$K_{2i} - Tg_i$ **(K)**	D_0 (cm^2/s)	ξ
λ-cyhalothrin	0.68	1.36×10^{-3}	-206.46	1.94×10^{-3}	1.47
Polyurea (Polyurethane)	0.67	3.23×10^{-4}	-181.4	-	
D (cm^2/s) = 6.95×10^{-12}					

The diffusion coefficient obtained with the last method (b) is much higher than the previous one (from (a)). Now we see that the new predicted value is qualitatively correct with respect to both HMDA and Agrochemical A and is therefore quantitatively more accurate. The diffusion coefficient value reported in Table 5.19 will therefore be used in the following calculations.

ii) Prediction of the partition coefficients

In this part the prediction of the partition coefficient of the AI between the polymer and the solvents in the donor ($K_{m/d}$) and release medium ($K_{m/r}$) is attempted. The donor in this case is Solvesso 100 and the release medium is a solution of n-hexane-ethanol. The methodology followed has been described in chapter 3 (section 3.1). The activity coefficients of the AI in the respective solvents are estimated using the KT-UNIFAC model (Kang et al. [6]), while those in the polymer are estimated with the GC-Flory EoS model. The focus of this work has been on the GC-Flory EoS model which, after the extension performed, allows the representation of both the AI and the polymer and their group description is provided in Table 5.20. The AI (and the solvents) in turn, can also be described by KT-UNIFAC.

Table 5.20: AI and polyurea group description in terms of the GC-Flory EoS model.

λ-cyhalothrin		**Polyurea (from TDI)**		**Polyurea (from PMPPI)**	
MG	**SG**	**MG**	**SG**	**MG**	**SG**
CH_2	2 CH_3, 2 CH, 1 C	CONH	1 CONH	CONH	3 CONH
C=C	1 CH=C	CNH	1 CHNH	CNH	3 CHNH
aC	9 aCH, 2 aC	CH_2	1 CH_3	CH_2	2 CH_2
COO	1 COO	aCH	2 aC, 3 aCH	aCH	4 aC, 11 aCH
aCO	1 aC-O				
CF_2	1 CF_3				
Cl-(C=C)	1 Cl-(C=C)				
CCN	1 CHCN				

CHNH: this is an approximation given that aCHNH is not available.

Even though all the compounds can be described by the groups with the two mentioned models, not all the needed group parameters are available. Since this work has been focused on the extension of the GC-Flory EoS, the missing parameters for this model are highlighted in Table 5.21, where the missing group interaction parameters are indicated by (x). On the other hand for the KT-UNIFAC a significant number of group parameters were not available, mainly for the groups COO, aCO, Cl-(C=C) and CCN. Obviously, for both models

calculations without the missing group interaction parameters can introduce inaccuracies.

Table 5.21: Group parameters needed from GC-Flory EoS. (x) Missing parameters.

	CH_2	C=C	aCH	COO	aCO	CF_2	Cl-(C=C)	CCN	CONH	CNH
CH_2										
C=C										
aCH										
COO										
aCO						**x**			**x**	**x**
CF_2								**x**	**x**	**x**
Cl-(C=C)										**x**
CCN										**x**
CONH										**x**
CNH										

Nevertheless, the activity coefficients have been calculated ignoring the missing group-interaction parameters and the resulting values are presented in Table 5.22 and the corresponding partition coefficients given in Table 5.23. Note that Solvesso 100 consists of a mixture of C9 and C10 dialkyl and trialkyl benzenes but the actual composition is unknown. Therefore, the compound trimethylbenzene has been used to represent it, even though this can also introduce some inaccuracy.

Table 5.22: Activity coefficients of λ-cyhalothrin (1) in the compounds of interest (2)

Compound (2)	**Function**	Ω_1^∞ **in (2)**
Polyurea	Membrane	19.28
Solvesso 100	Donor solvent	0.053
hexane/ethanol	Release medium	6.77

Table 5.23: Partition coefficients of λ-cyhalothrin in the compounds of interest

	Polymer	**Solvent**	$K_{p/solv}$
$K_{m/r}$	Polyurea	hexane/ethanol	0.351
$K_{m/d}$	Polyurea	Solvesso 100	0.00275

These results will be analysed through the experimental release data, since

no other data is available to check them.

iii) Release calculations

The predicted properties (summarized in Table 5.24) are used in the mathematical release model together with the variables reported in Table 5.17 to study the release of λ-cyhalothrin from the polyurea microcapsules in a predictive manner.

Table 5.24: Properties needed in the controlled release model obtained from predictive methods.

Property	**Value**
$D(m^2/s)$	6.95×10^{-16}
$K_{m/r}$	0.351
$K_{m/d}$	0.00275

In the first attempt the same property values (reported in Table 5.17) are used for all three cases and the results are plotted in Fig. 5.11.

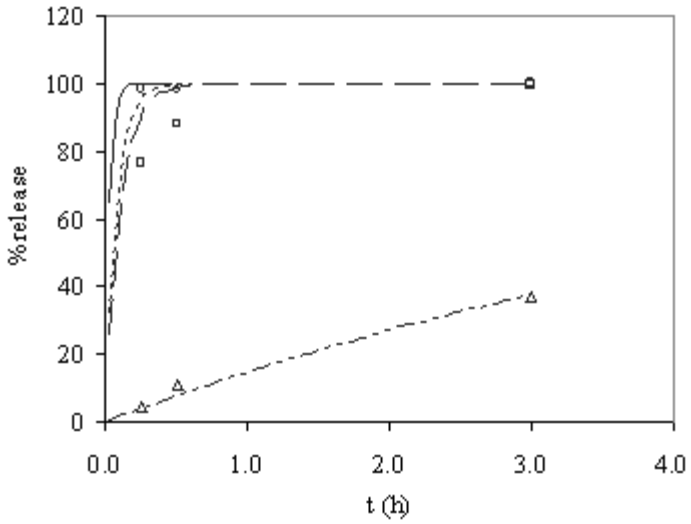

Figure 5.11: Comparison of experimental release data with the results from the model calculations. Experimental data: (○) Case 1 (10% wall), (□) Case 2 (20% wall), (△) Case 3 (30% wall). Model results: (—) Case 1 (10% wall), (- - -) Case 2 (20% wall), (– –) Case 3 (30% wall) and (– – –) Case 3 (30% wall) with $D = 1.1\times10^{-17}m^2/s$.

From this figure it can be observed that for the cases with the smallest thickness (Cases 1 and 2) the release is slightly overpredicted, while for the last case (Case 3) the percentage of AI released is much higher than the measured one.

For cases 1 and 2, a similar degree of cross-linking may be assumed, that is likely to be higher for these polyurea-based microcapsules than for the 'model' polymer used to predict the diffusion coefficient. As a higher degree of cross-linking decreases the diffusion coefficient, a better fit of the release data is obtained by decreasing its value to $2.9\times10^{-16}\mathrm{m}^2/\mathrm{s}$. The new results are shown in Fig. 5.12.

From Fig. 5.11 it can be observed that, the measured release data for case 3 is much lower than for cases 1 and 2. The wall thickness of the microcapsules in case 3 is higher than for the other two cases, and therefore a lower release is expected. However, the difference in thickness between the microcapsules in case 3 and in case 2 is equivalent to the difference between the microcapsules in case 1 and case 2. Therefore, the decrease in the amount of AI released from case 2 to case 3, would be expected to be of the same order as that from case 1 to case 2. This is, in fact, what the release model predicts. On the other hand, smaller microcapsules are usually expected to present faster release than the bigger ones. Then, the fact that the microcapsules in case 3 are smaller than the ones in case 2 should compensate for the decrease in release due to their greater thickness. The difference in release% between cases 2 and 3 cannot be explained by the effects described above.

Then, this reduction in the release% (from case 2 to case 3) is explained by a much higher degree of cross-linking of the microcapsule wall in case 3 (with respect to cases 1 and 2), which would significantly decrease the diffusion coefficient and thereby the release of the AI. This has been tested by using a smaller value of the diffusion coefficient in the release model calculations and the results are shown in both figures (Fig. 5.11 and Fig. 5.12) together with the original predictions. Now the amount of released AI can be perfectly modeled.

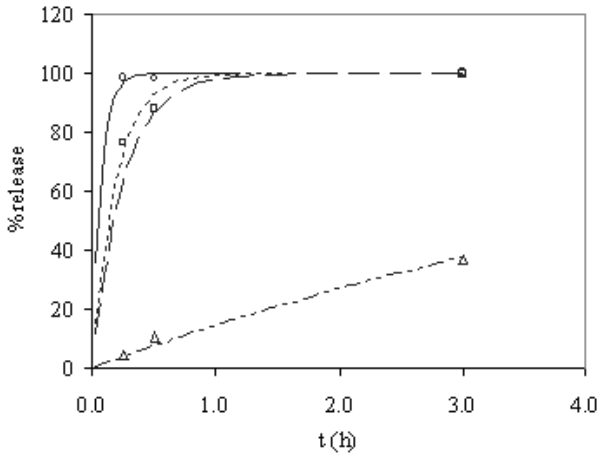

Figure 5.12: Comparison of experimental release data with the results from the model calculations. Experimental data: (○) Case 1 (10% wall), (□) Case 2 (20% wall), (△) Case 3 (30% wall). Model results: (—) Case 1 (10% wall), (- - -) Case 2 (20% wall), (– –) Case 3 (30% wall) and (– – –) Case 3 (30% wall) with D = 1.1×10^{-17}m^2/s.

Even though, it is known that the effect of cross-linking could be considered in a relatively simple manner through a tortuosity factor, that is, an enhancement of the distance that the molecules have to diffuse through, it cannot yet be considered in a predictive manner in the estimation of the diffusion coefficient. A number of experiments would be needed to do a thorough analysis of its specific effects.

Changes in the diffusivity of a penetrant within the same type of polymer but used in different microcapsules have been shown for example by Yadav et al. [7], also for polyurea membranes. Here, these differences were attributed to varying crystallinities of the polymer membrane. The effect of a higher degree of crystallinity is equivalent to that of a higher cross-linking, that is, a decrease in the diffusion coefficient value.

5.5 Conclusions

The case studies highlight the integration of the constitutive property models with the release models and their applicability to study the release of AIs from microcapsule devices in a predictive manner. The results could be assessed, at least qualitatively, and show the potential for use of this integrated framework in product design. Once the system to be studied has been selected, the properties are estimated through the adapted constitutive property models. Then, the amount of AI released as a function of time is calculated through the

developed release models for different alternatives. For example, for varying microcapsule sizes or wall thicknesses, and their effect on the release behaviour could be analyzed. This has been illustrated in the different scenarios treated within each of the case studies.

It has also been shown how different AI-solvent-polymer configurations, provide varying orders of release as a function of time, for example, only a few hours are needed to release Codeine and λ-cyhalothrin from the microcapsules while some days are required for the release of Agrochemical A. These case studies also provide an idea of how, without changing the type of polymer, but only changing the monomers or their compositions, the membrane morphology is altered (that is the effects of cross-linking, crystallinity,...) providing different solubilities and diffusivities, as seen from the different values for partition and diffusion coefficients used in each case. These in turn, result in different amounts of AI delivered. Also the different sizes and shapes of the AIs studied lead to very different values of the diffusion coefficients.

The effects of all these parameters that have been highlighted in this chapter provide the necessary information for the assessment of the alternatives that best suit the needs of the final application. These examples though, indicate the need for further work on the extension of the activity coefficient models for the prediction of the partition coefficients, since a lot more groups are needed to describe a wide range of AIs. Also, the need for better knowledge of the polymer membranes arises after observing how this affects the diffusion and release of the AIs.

Nomenclature

List of symbols

C_1^{WLF}, C_2^{WLF}	WLF equation parameters
$C_{d,initial}$	Initial concentration of AI in the donor
C_m	Concentration of AI in the membrane
C_r	Concentration of AI in the receiver
d	diameter
D	Diffusion coefficient
D_0	Constant pre-exponential factor
h	Thickness of the microcapsule wall
K	Partition coefficient of the AI between the polymer membrane and the donor or receiver compartment.
$K_{m/d}$	Partition coefficient of the AI between the donor and the polymer membrane
$K_{m/r}$	Partition coefficient of the AI between the polymer membrane and the release medium
$K_{p/solv}$	Partition coefficient between polymer and solvent
K_{1i}, K_{2i}	Free-volume parameters of compound i
Mw	Molecular weight
r	Microcapsule radius
t	Time
Tg	Glass transition temperature
V_d	Donor volume
V_r	Receiver volume
$V_i(0K)$	Volume of compound i at 0 K

Greek letters

δ	Solubility parameter
σ	Standard deviation
Ω_i^∞	Infinite dilution activity coefficient of compound i (weight basis)
ξ	ratio of molar volumes for the solvent and the polymer jumping units

Subscripts

d	Donor
i	Component i
$initial$	Initial value
m	Membrane
max	Maximum
$mean$	Mean value
min	Minimum
p	Polymer
r	Release medium
$solv$	Solvent

step	Step size (increment)
total	Total value

References

[1] Lukaszczyk, J. and Urbas,P. , Influence of the parameters of encapsulation process and of the structure of diisocyanates on the release of codeine from resinate encapsulated in polyurea by interfacial water promoted polyreaction, *React. Funct. Polym.* 1997, 33, 233-239.

[2] Ngai, K.L. and Plazek, D.J. (Chapter 25: pag. 341-362) in: *Physical properties of polymers handbook.* Mark, J.E., Woodbury, NY. AIP Press, 1996.

[3] Kubo,M., Harada,Y., Kawakatsu,T. and Yonemoto,T. Modeling of the formation kinetics of Polyurea microcapsules with size distribution by interfacial polycondensation, *J. Chem. Eng. Jpn.* 2001, 34, 12, 1506-1515.

[4] Scher, H.B., Rodson, M., Kuo-Shin, L., Microencapsulation of pesticides by interfacial polymerization utilizing Isocyanate or Aminoplast chemistry, *Pesti. Sci.* 1998, 54, 394-400.

[5] Peppas, N.A., Controlled drug bioavailability, vol. 1 (p. 203-237), *Mathematical modeling of diffusion processes in drug delivery polymeric systems.* New York, Wiley, 1984.

[6] Kang, J.W., Abildskov,J., Gani,R., Cobas,J., Estimation of Mixture Properties from First- and Second-Order Group Contributions with the UNIFAC Model, *Ind. Eng. Chem. Res.* 2002, 41(13), 3260.

[7] Yadav,S.K., Khilar,K.C. and Suresh,A.K., Microencapsulation in Polyurea shell: Kinetics and film structure, *AIChE J.* 1996, 42(9), 2616-2626.

6

Conclusions and Future work

6.1 Conclusions

An integrated framework for the study of the delivery of Active Ingredients (AIs) from controlled release devices in a completely predictive manner has been developed and presented in this work. The framework consists of predictive property models incorporated within the mathematical release models.

A mathematical model to study the AI delivery from a microcapsule has been developed and presented in detail. The applicability of the model has been highlighted through a case study. The model has been further improved to take into account the burst and lag time effects that may be encountered due to different storage and use conditions of the devices. This extended model has been tested with available measured data of AI release from microcapsules where the burst and lag time effects were observed. It has been proven for the release model and its extensions that, with the appropriate parameters, the models are able to accurately describe the delivery of different AIs from microcapsules.

Through a general analysis of the controlled release models the parameters/properties that are critical for the study of the AI delivery in a predictive manner have been identified. These are the diffusion coefficients of the AIs in the polymers and the partition coefficients of the AIs between the polymers and solvents in the formulation. Then, predictive property models for the estimation of both diffusion and partition coefficients have been developed. Each of the property models has been discussed and applied to large and complex molecules that are representative of pesticides.

The model proposed for the estimation of partition coefficients is based on activity coefficient calculations. The model selected to estimate the activity coefficients of AIs in polymers has been further extended and now allows for the description and estimation of activity coefficients of a much wider range of pesticide AIs (mainly within the pyrethroid group) and polymers (such as Polyamide). The new parameters of the activity coefficient model have been thoroughly tested to ensure their reliability. The approach proposed for the estimation of the partition coefficients has also been highlighted through ex-

amples involving complex molecules.

A predictive model for the estimation of diffusion coefficients of complex molecules in polymers has also been presented in this work. A very extensive analysis of the application of this predictive model has been performed on complex and large molecules that are considered to be representative of the pesticide type. The extended model has also been applied to some pesticide systems. It has been possible to accurately describe the temperature dependence of the diffusion coefficient in all the cases even though quantitative agreement was not always achieved. The reasons for this are related to inaccurate description of the polymer morphology (crystallinity and cross-linking) and directions for improvement are proposed in the following section.

The integration of the predictive property models with the model for the release from a microcapsule has been illustrated through three different examples of application. The predictive model for the diffusion coefficient has been successfully applied in the three cases while the predictive accuracy of the partition coefficient model could only be demonstrated in the last example through analysis of the predicted release behaviour.

To conclude, the main achievements of this thesis involve the extension and application of predictive models for estimation of solubility and diffusivity of large and complex pesticide AIs in polymers, where earlier, the calculations were limited to relatively small and simple molecules. The integration of the predictive property models with the controlled release models is considered a very valuable contribution in the area of controlled release technology, where the previous work has been focused on fitting of measured release data to mathematical release models to obtain the values of these properties. With the models presented in this work, the release of an AI can now be directly studied without the need of additional measurements to obtain the property values, since these are now estimated from predictive property models and the AI delivery is then obtained from the release model.

6.2 Future work

The integrated framework has been illustrated in this work through the controlled release model for a microcapsule. A very interesting contribution would be directed to applying the integration of the models to a greater range of controlled release devices, such as, matrices, tablets, etc. and test the applicability of the proposed approach.

With respect to the microcapsule model in particular, some further considerations can be taken into account:

i) The case of having a solution of different microcapsules has been taken into account in the current model through a normal distribution of the sizes of the microcapsules. First of all, in some cases the distribution might be observed to be different, maybe exponential. This could then, be modified in the model in order to improve the release predictions. On the other hand, the fact that the microcapsules have different sizes can mean that the wall thicknesses of the microcapsules also differ. Then, the normal distribution for the microcapsule sizes could be extended to the thicknesses. This can easily be introduced, if applicable, given that the wall thicknesses are in general obtained from the mean diameters. Then, instead of calculating a mean wall thickness, a thickness could be calculated for each diameter from the size distribution.

ii) Some work has been published in the literature regarding the modelling of the actual microencapsulation process (Yadav et al. [1], Kubo et al. [2]). The integration of the modelling of this part of the process would directly provide all the variables needed in the release model together with detailed information of the product (such as wall cross-linking, crystallinity, etc.). This would be a very important contribution towards developing a final integrated framework for product design and analysis.

Regarding the predictive approach proposed to estimate the partition coefficients, a further extension of the group parameter table of the model used to estimate activity coefficients of AIs in polymers is needed. Pesticide AIs are in general multifunctional compounds with complex structures. The variety of functional groups involved in the description of these compounds has not yet been covered by the activity coefficient models. Some of the groups that are relevant for an extension of the model include: aromatic amines, sulphur groups, phosphor, among others. Besides that, a similar extension of the models needed for estimation of activity coefficients of the AIs in solvents (UNIFAC and KT-UNIFAC) should also be performed and it would be a very valuable contribution for the overall applicability of this integrated framework.

In the area related to the prediction of the diffusion coefficients there are some limitations originated from the complex structure or morphology of the polymers. In general, the crystallinity and cross-linking of the polymer of interest are not known and this limits the predictive accuracy of the model

given that these two properties play a very important role in the diffusion process. These properties of the polymer generally cause a decrease of the diffusion coefficient due to an increase in the path length that the molecules have to diffuse through. Therefore these effects can, in principle, be taken into account in a relatively simple manner by introducing a tortuosity factor that would modify (increase) this path length. Some attempts have been made to incorporate a tortuosity factor (Lutzow et al. [3]) but a much greater amount of measured properties for the polymers of interest is required in order to develop a predictive form of the model that takes into account these effects.

Another very interesting addition in this area would be the incorporation of the effect of plasticizers within the predictive model. Some measurements and experimental correlations are available for specific plasticizing compounds but an extensive study that would allow the development of a predictive model valid for any plasticizer within any polymer is not currently available. Finally, with respect to the diffusing molecules, a better description of their shape and possibly the consideration of some descriptors regarding their flexibility could signify an improvement of the diffusion coefficient predictions, specially for large molecules such as the ones treated in this work.

And to conclude, a further assessment of the applicability of the integrated framework is suggested. The design of specific experiments where all the properties and variables needed by the release model are measured, would be very helpful in further improving the models and their applications.

The important issues related to the design of a specific experiment are discussed below. The principal objective of the experiment should be to validate the controlled release model for the delivery of an AI from a microcapsule based on the measurement of the amount of AI released as a function of time. However, a number of factors must be taken into account so that the validation can be accurately performed and the model assumptions verified. These are summarized in Table 6.1.

First of all, measurements of data related to the variables involved in the size distribution of the microcapsules in solution need to be included (see (1) in Table 6.1). Then, precise knowledge of the compounds present in the formulation and their composition in the final product is also needed so that thickness, volume and concentrations will be known (see (2) in Table 6.1). Finally, the properties that control the release, that is, the partition coefficient between the donor and the polymer ($K_{m/d}$) and the release medium and the polymer ($K_{m/r}$) together with the diffusion coefficient (see (3) in Table 6.1) should be independently measured. It is important that enough details on the compounds selected as AI, polymer and solvents be provided so that the applicability of the selected property models (group-parameter tables of the GC-Flory EoS model as well as the UNIFAC models) can be assessed. Also, the morphology of the polymer (crystallinity, cross-linking, glass transition temperature) and its viscosity-temperature dependence (either experimental data or the WLF-constants) needs to be known or measured so that the effects on diffusivity can be precisely assessed. Regarding the diffusivity measurements, the temperature

range needs to be specified and must be within the limitations of applicability of the Extended FV model to avoid external sources of error.

Table 6.1: Input data needed to validate the microcapsule release model

Variables	**Data needed by the model**
1. Normal distribution	
Release% vs time	Maximum radius Minimum radius Mean radius Standard deviation
2. Formulation and product	
Release% vs time	Wall thickness Volume of release medium Initial donor concentration
3. Properties needed by the release model	
Release% vs time	Diffusion coefficient $K_{m/r}$ $K_{m/d}$

In order to further improve the property models, detailed measurements are needed, not only of the values of the partition and diffusion coefficients, but also, precise knowledge of the compounds (solvents and AI) and polymers involved in the measurements. The information needed has been described above and is now summarized in Table 6.2.

Table 6.2: Measured data needed for improvement of the property models

Variables	**Needed by model**
1. Partition coefficients ($K_{m/r}$ and $K_{m/d}$)	
$K_{m/r}$	Activity coefficient of AI in solvent and polymer
$K_{m/d}$	Activity coefficient of AI in solvent and polymer
Activity coefficient in solvents	Molecular structure of solvent and AI Temperature Composition
Activity coefficient in polymers	Molecular structure of AI and polymer repeat unit Polymer molecular weight Temperature Composition
2. Diffusion coefficient	
Diffusion coefficient	Polymer crystallinity Polymer cross-linking Glass transition temperature of the polymer Viscosity (as a function of temperature) or WLF constants (C_1^{WLF}, C_2^{WLF})

With the data provided through specifically designed experiments (as highlighted in Table 6.2), the property models could be accurately validated and improved and their integration within the controlled release modelling area could be appropriately assessed.

References

[1] Yadav,S.K., Khilar,K.C. and Suresh,A.K. Microencapsulation in Polyurea shell: Kinetics and film structure, *AIChE J.* 1996, 42(9), 2616-2626.

[2] Kubo,M., Harada,Y., Kawakatsu,T. and Yonemoto,T. Modeling of the formation kinetics of Polyurea microcapsules with size distribution by interfacial polycondensation, *J. Chem. Eng. Jpn.* 2001, 34, 12, 1506-1515.

[3] Lützow,N., Tihminlioglu,A., Danner,R.P., Duda,J.L., De Haan,A., Warnier,G., Zielinski,J.M. Diffusion of toluene and n-heptane in polyethylenes of different crystallinity, *Polymer* 1999, 40, 2797-2803.

Appendices

A

Derivation of the equations for non-constant activity source

In this appendix the derivation of the equations for the Basic microcapsule model in section 2.3.1 are presented.

Consider the situation illustrated in Fig. A.1, where all of the Active Ingredient (AI) is initially contained in the donor compartment (that is the core of the microcapsule) and it is released through the polymer membrane to the receiver compartment, that is the release medium.

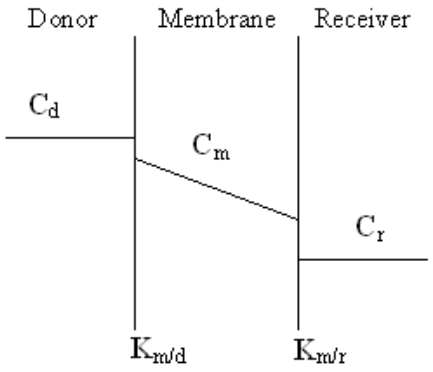

Figure A.1: Basic scenario for diffusion of an AI from the donor to the receiver compartment.

The equations to describe the release of the AI are based on Fick's law of diffusion (Eq. A.1) under the following assumptions:

i) Diffusion takes place through a very thin film, so Fick's law can be considered in one dimension only.

ii) The diffusion coefficient is considered independent of concentration.

$$J = -D\frac{dC}{dx} \tag{A.1}$$

This equation is now integrated in space (x) to give,

$$J = -D\frac{\Delta C}{\Delta x} \tag{A.2}$$

where, $\Delta C = C_{m,2} - C_{m,1}$
and, $\Delta x = h$

So, Eq. A.2 can be expressed as,

$$J = -\frac{D}{h}\left(C_{m,2} - C_{m,1}\right) \tag{A.3}$$

Now consider the definition of flux,

$$J = \frac{1}{A}\frac{dM_r}{dt} \tag{A.4}$$

And combine Eqs. A.4 and A.3 to obtain an expression for the derivative of the mass of released AI (M_r) with time,

$$\frac{1}{A}\frac{dM_r}{dt} = -\frac{D}{h}\left(C_{m,2} - C_{m,1}\right) \tag{A.5}$$

In order to obtain the same expression as in Eq. A.5 for the mass of AI remaining in the donor compartment (M_d) the mass balance is considered,

$$M_{total} = M_d + M_r \tag{A.6}$$

Then,

$$\frac{dM_{total}}{dt} = \frac{dM_d}{dt} + \frac{dM_r}{dt} \tag{A.7}$$

Where M_{total} is constant, thus:

$$\frac{dM_{total}}{dt} = 0 \qquad and \qquad \frac{dM_d}{dt} = -\frac{dM_r}{dt} \tag{A.8}$$

Then, the expression for the derivative of the mass in the donor with time is obtained from Eqs. A.5 and A.8,

$$\frac{1}{A}\frac{dM_d}{dt} = -\frac{D}{h}\left(C_{m,1} - C_{m,2}\right) \tag{A.9}$$

To avoid dealing with the membrane interfacial concentrations ($C_{m,1}, C_{m,2}$), the partition coefficients are defined,

$$K_{m/d} = \frac{C_{m,1}}{C_d} \rightarrow C_{m,1} = K_{m/d}C_d \tag{A.10}$$

$$K_{m/r} = \frac{C_{m,2}}{C_r} \rightarrow C_{m,2} = K_{m/r} C_r \tag{A.11}$$

These equations (Eq. A.10 and A.11) are then substituted in Eqs. A.5 and A.9 for the mass of AI in the receiver and in the donor respectively,

$$\frac{1}{A}\frac{dM_r}{dt} = \frac{D}{h}\left(K_{m/d} C_d - K_{m/r} C_r\right) \tag{A.12}$$

$$\frac{1}{A}\frac{dM_d}{dt} = -\frac{D}{h}\left(K_{m/d} C_d - K_{m/r} C_r\right) \tag{A.13}$$

Now, the analytical expressions for the variation with time, of the mass of AI in the donor and in the receiver will be respectively obtained.

i) AI in the donor:

The expression for the variation with time of the mass of AI in the donor will be obtained from the reorganized Eq. A.13,

$$\frac{dM_d}{dt} = -\frac{DA}{h}\left(K_{m/d} C_d - K_{m/r} C_r\right) \tag{A.14}$$

Now, use the definitions of concentrations (Eq. A.15) to express Eq. A.14 in terms of mass (Eq. A.16),

$$C_d = \frac{M_d}{V_d} \qquad and \qquad C_r = \frac{M_r}{V_r} \tag{A.15}$$

$$\frac{dM_d}{dt} = -\frac{DA}{h}\left(K_{m/d}\frac{M_d}{V_d} - K_{m/r}\frac{M_r}{V_r}\right) \tag{A.16}$$

In order to proceed with the derivations, Eq. A.16 must be given in terms of the mass of AI in the donor. For that, consider the mass balance in Eq. A.6, from where,

$M_r = M_{total} - M_d$

And substitute the above expression in Eq. A.16 to obtain,

$$\frac{dM_d}{dt} = -\frac{DA}{h}\left(K_{m/d}\frac{M_d}{V_d} - K_{m/r}\frac{(M_{total} - M_d)}{V_r}\right) \tag{A.17}$$

By reorganizing the above equation the following expression is obtained,

$$\frac{dM_d}{dt} = -\frac{DA}{hV_d}\left(M_d\left(K_{m/d} + K_{m/r}\frac{V_d}{V_r}\right) - K_{m/r} V_d \frac{M_{total}}{V_r}\right) \tag{A.18}$$

Before proceeding with the integration, some of the variables in Eq. A.18, that are not time-dependent, are grouped according to Eqs. A.19 and A.20 to simplifiy the derivations.

$$\beta = K_{m/d} + K_{m/r}\frac{V_d}{V_r} \tag{A.19}$$

$$\phi = K_{m/r}V_d\frac{M_{total}}{V_r} \tag{A.20}$$

So the final equation to be integrated is Eq. A.21, obtained from the combination of Eqs. A.19 and A.20 with Eq. A.18.

$$\frac{dM_d}{dt} = -\frac{DA}{hV_d}\left(M_d\beta - \phi\right) \tag{A.21}$$

Now integrate Eq. A.21 with time,

$$\int_{M_{d,0}}^{M_d}\frac{dM_d}{(M_d\beta-\phi)} = -\frac{DA}{hV_d}\int_{t_0}^{t}dt \rightarrow \left.\frac{\ln\left[(M_d\beta-\phi)\right]}{\beta}\right|_{M_{d,0}}^{M_d} = -\frac{DA}{hV_d}\left(t-t_0\right)$$

$$\rightarrow \frac{1}{\beta}\ln\left[\frac{(M_d\beta-\phi)}{(M_{d,0}\beta-\phi)}\right] = -\frac{DA}{hV_d}t \tag{A.22}$$

Consider that all the AI is initially in the donor compartment so,

$t_0 = 0; \quad M_{d,0} = M_{total}$

And then from Eq. A.22,

$$\ln\left[\frac{(M_d\beta-\phi)}{(M_{total}\beta-\phi)}\right] = -\frac{DA}{hV_d}\beta t \tag{A.23}$$

And reorganizing the above equation, the expression for the variation of the mass of AI in the donor with time is obtained,

$$M_d = M_{total}\exp\left(-\frac{DA}{hV_d}\beta t\right) + \frac{\phi}{\beta}\left(1-\exp\left(-\frac{DA}{hV_d}\beta t\right)\right) \tag{A.24}$$

Now, ungroup the variables from Eqs. A.19 and A.20, and divide by the donor volume (V_d) to obtain the final expression in terms of concentration in the donor (C_d), Eq. A.25.

$$C_d = \frac{K_{m/r}V_d}{K_{m/d}V_r + K_{m/r}V_d}C_{d,0}\left(1 - \exp\left(-\frac{DA}{hV_d}\left(K_{m/d} + K_{m/r}\frac{V_d}{V_r}\right)t\right)\right) + C_{d,0}\exp\left(-\frac{DA}{hV_d}\left(K_{m/d} + K_{m/r}\frac{V_d}{V_r}\right)t\right) \quad \text{(A.25)}$$

Now the explicit expression for the derivative of the donor concentration as a function of time (as provided in section 2.3.1) can be obtained from Eq. A.25.

First of all, the variables in the exponential term are grouped according to,

$$\alpha = \frac{DA}{hV_d}\left(K_{m/d} + K_{m/r}\frac{V_d}{V_r}\right) \quad \text{(A.26)}$$

And Eq. A.25 is then given by,

$$C_d = \frac{K_{m/r}V_d}{K_{m/d}V_r + K_{m/r}V_d}C_{d,0}\left(1 - \exp\left(-\alpha t\right)\right) + C_{d,0}\exp\left(-\alpha t\right) \quad \text{(A.27)}$$

Now, obtain the derivative,

$$\frac{dC_d}{dt} = \alpha C_{d,0}\exp\left(-\alpha t\right)\left(\frac{K_{m/r}V_d}{K_{m/d}V_r + K_{m/r}V_d} - 1\right)$$

And finally, ungroup the variables to obtain the equation,

$$\frac{dC_d}{dt} = -\frac{DA}{hV_d}K_{m/d}C_{d,0}\exp\left(-\frac{DA}{hV_d}\left(K_{m/d} + K_{m/r}\frac{V_d}{V_r}\right)t\right) \quad \text{(A.28)}$$

which is the one reported in section 2.3.1.

ii) AI in the receiver

The procedure to obtain the analytical expression for the mass of AI in the receiver as a function of time is completely equivalent to that presented in (i) for the concentration of the donor so only the main steps of the procedure will be indicated here.

The initial equation corresponds to the reorganized form of Eq. A.12, given as,

$$\frac{dM_r}{dt} = \frac{DA}{h}\left(K_{m/d}C_d - K_{m/r}C_r\right) \quad \text{(A.29)}$$

Express Eq. A.29 in terms of mass using Eq. A.15 to obtain,

$$\frac{dM_r}{dt} = -\frac{DA}{h}\left(K_{m/r}\frac{M_r}{V_r} - K_{m/d}\frac{M_d}{V_d}\right) \tag{A.30}$$

Then from the mass balance (Eq. A.6): $M_d = M_{total} - M_r$

And substitute in Eq. A.30 to obtain the expression in terms of the mass of AI in the receiver,

$$\frac{dM_r}{dt} = -\frac{DA}{h}\left(K_{m/r}\frac{M_r}{V_r} - K_{m/d}\frac{(M_{total} - M_r)}{V_d}\right) \tag{A.31}$$

Reorganize the above equation,

$$\frac{dM_r}{dt} = -\frac{DA}{h}\left(M_r\left(\frac{K_{m/r}}{V_r} + \frac{K_{m/d}}{V_d}\right) - \frac{K_{m/d}}{V_d}M_{total}\right) \tag{A.32}$$

Group the variables that are not time-dependent according to Eqs. A.33 and A.34.

$$\beta = \frac{K_{m/r}}{V_r} + \frac{K_{m/d}}{V_d} \tag{A.33}$$

$$\phi = \frac{K_{m/d}}{V_d}M_{total} \tag{A.34}$$

Then, Eq. A.32 becomes,

$$\frac{dM_r}{dt} = -\frac{DA}{h}\left(M_r\beta - \phi\right) \tag{A.35}$$

Integrate Eq. A.35 with time,

$$\int_{M_{r,0}}^{M_r}\frac{dM_r}{(M_r\beta - \phi)} = -\frac{DA}{h}\int_{t_0}^{t} dt \rightarrow \left.\frac{\ln\left[(M_r\beta - \phi)\right]}{\beta}\right|_{M_{r,0}}^{M_r} = -\frac{DA}{h}(t - t_0)$$

$$\rightarrow \ln\left[\frac{(M_r\beta - \phi)}{(M_{r,0}\beta - \phi)}\right] = -\frac{DA}{h}\beta t \tag{A.36}$$

Then consider again that all the AI is initially in the donor and therefore no AI is present in the receiver,

$t_0 = 0$; $M_{r,0} = 0$

Then, from Eq. A.36,

$$\ln\left[\frac{(M_r\beta-\phi)}{-\phi}\right]=-\frac{DA}{h}\beta t \tag{A.37}$$

And reorganizing the above equation the final expression for the variation of the mass of AI in the receiver with time is given by,

$$M_r=\frac{K_{m/d}V_rM_{total}}{K_{m/d}V_r+K_{m/r}V_d}\left(1-\exp\left(-\frac{DA}{hV_d}\left(K_{m/d}+K_{m/r}\frac{V_d}{V_r}\right)t\right)\right) \tag{A.38}$$

Or in terms of concentration,

$$\begin{aligned}C_r &= \frac{V_dK_{m/d}}{K_{m/d}V_r+K_{m/r}V_d}C_{d,0}\\ &\quad\left(1-\exp\left(-\frac{DA}{hV_d}\left(K_{m/d}+K_{m/r}\frac{V_d}{V_r}\right)t\right)\right)\end{aligned} \tag{A.39}$$

Finally, the explicit expression for the derivative is obtained in the same manner as for the mass of AI in the donor, and the expression obtained is,

$$\frac{dC_r}{dt}=\frac{DA}{hV_r}K_{m/d}C_{d,0}\exp\left(-\frac{DA}{hV_d}\left(K_{m/d}+K_{m/r}\frac{V_d}{V_r}\right)t\right) \tag{A.40}$$

Nomenclature

List of symbols

A	Surface area of membrane
C	Concentration
C_d	Concentration of AI in the donor compartment
$C_{d,0}$	Initial concentration of AI in the donor compartment
C_m	Concentration of AI in the membrane
$C_{m,1}$, $C_{m,2}$	Interfacial concentrations of AI in the membrane
C_r	Concentration of AI in the receiver compartment
D	Diffusion coefficient
h	Thickness through which diffusion occurs
J	Flux
$K_{m/d}$	Partition coefficient of the AI between the donor and the polymer membrane
$K_{m/r}$	Partition coefficient of the AI between the polymer membrane
M	Mass of AI
M_d	Mass of AI in the donor compartment
$M_{d,0}$	Initial mass of AI in the donor compartment
M_r	Mass of AI in the receiver compartment
$M_{r,0}$	Initial mass of AI in the receiver compartment
M_{total}	Total mass of AI
t	Time
V_d	Volume of the donor
V_r	Volume of the receiver
x	Direction of diffusion

Subscripts

0	Initial
d	Donor medium
m	Polymer membrane
r	Release medium
$total$	Total mass

B

Derivation of the burst and lag time equations

In this appendix the derivation of the equations for the microcapsule model considering burst and lag time effects described in section 2.3.2 are presented.

First, an analysis of the equations available in the literature (Kydonieus et al. [1]) is provided (i), and then the derivations to obtain the equations used in this work are presented (ii).

i) Literature equations (Kydonieus et al. [1])

The equations reported by Kydonieus et al. [1] for burst and lag time release correspond to Eq. B.1 and B.2 respectively.

$$\frac{J}{J_{\max}} = 1 + 2\exp\left(\frac{-D\pi^2 t}{h^2}\right) \tag{B.1}$$

$$\frac{J}{J_{\max}} = 1 - 2\exp\left(\frac{-D\pi^2 t}{h^2}\right) \tag{B.2}$$

Both equations consist of two terms. The first term is a constant thus representing zero-order release rate and the second term accounts for either the burst or the time lag effect, respectively. In the case were the release rate is zero-order after the initial burst or lag time effect the equations for the variation of mass of released AI as a function of time are obtained as detailed below.

i) Burst effects

Consider the definition of flux,

$$J = \frac{1}{A}\frac{dM_r}{dt} \tag{B.3}$$

Combine Eq. B.3 with Eq. B.1 to obtain,

$$J = \frac{1}{A}\frac{dM_r}{dt} = J_{\max}\left(1 + 2\exp\left(-\alpha' t\right)\right) \quad \text{(B.4)}$$
$$\text{where :} \quad \alpha' = \frac{D\pi^2}{h^2}$$

Now, integrate Eq. B.4 to obtain the mass of AI released as a function of time.

$$\frac{1}{AJ_{\max}}\int_{M_{r,0}}^{M_{r,t}} dM_r = \int_{t_0}^{t}\left(1 + 2\exp\left(-\alpha' t\right)\right)dt \rightarrow$$
$$\frac{1}{AJ_{\max}}\, M_r|_{M_{r,0}}^{M_{r,t}} = t|_{t_0}^{t} + 2\frac{\exp\left(-\alpha' t\right)}{-\alpha'}\Bigg|_{t_0}^{t} \quad \text{(B.5)}$$

From the consideration that all the AI is initially in the donor and none in the release medium,

$t_0 = 0; \quad M_{r,0} = 0$

Then, substituting in Eq. B.5,

$$\frac{1}{AJ_{\max}}M_{r,t} = t - \frac{2}{\alpha'}\left(\exp\left(-\alpha' t\right) - 1\right) \rightarrow$$
$$\rightarrow \quad M_{r,t} = J_{\max}A\left[t + \frac{2}{\alpha'}\left(1 - \exp\left(-\alpha' t\right)\right)\right] \quad \text{(B.6)}$$

Note that the equations have been modified (Eq. B.10) in order to incorporate the partitioning effect ($K_{m/d}$), in J_{max} and in α', related to the diffusion coefficient, where instead of considering 'D', the term considered is '$DK_{m/d}$', so,

$$J_{\max} = \frac{DC_{d,initial}}{h} \rightarrow J_{\max} = \frac{DC_{d,initial}}{h}K_{m/d} \quad \text{(B.7)}$$
$$\alpha' = \frac{D\pi^2}{h^2} \rightarrow \alpha' = \frac{D\pi^2}{h^2}K_{m/d} \quad \text{(B.8)}$$

ii) Lag time effects

The procedure to obtain the equation for the variation of the mass of AI released in the case of lag time effects, from Eq. B.2, is exactly equivalent to that presented for burst effects, and the final equation obtained is,

$$M_{r,t} = J_{\max} A \left[t - \frac{2}{\alpha'} \left(1 - \exp\left(-\alpha' t \right) \right) \right] \tag{B.9}$$

where,

$$J_{\max} = \frac{DC_{d,initial}}{h} K_{m/d}$$
$$\alpha' = \frac{D\pi^2}{h^2} K_{m/d}$$

In most of the cases dealing with microcapsules the release rate will not be zero-order but first order. Therefore the equations have to be modified in order to take this into account.

ii) Modification of literature equations

The procedure followed consists of removing the zero-order release term to substitute it by the first-order release term. From the derivations above, the analytical expressions for the mass of AI released as a function of time are available for burst and lag time release respectively (Eqs. B.10 and B.11).

$$M_{r,t} = J_{\max} A \left[t + \frac{2}{\alpha'} \left(1 - \exp\left(-\alpha' t \right) \right) \right] \tag{B.10}$$

$$M_{r,t} = J_{\max} A \left[t - \frac{2}{\alpha'} \left(1 - \exp\left(-\alpha' t \right) \right) \right] \tag{B.11}$$

where,

$$J_{\max} = \frac{DC_{d,initial}}{h} K_{m/d}$$
$$\alpha' = \frac{D\pi^2}{h^2} K_{m/d}$$

Then the above equations are combined with those representing the first order release rate (Eq. B.12) using the analytical solution of the derivatives from Appendix A.

$$M_r = C_r V_r = \frac{V_r C_{d,initial}}{\left(K_{m/r}/K_{m/d} + V_r/V_d \right)} \left(1 - \exp(-\alpha t) \right) \tag{B.12}$$

where,

$\alpha = \frac{DAK_{m/d}}{V_r h}\left(K_{m/r}/K_{m/d} + V_r/V_d\right)$

There is one consideration to be made, that is, the initial concentration used in the first-order release term is modified in order to account for the mass that is released (almost instantaneously) by burst (Eq. B.13), or not released initially in the case of time lag effect (Eq. B.14).

$C_{d,initial} = \frac{M'_{d,initial}}{V_d}$

where,

$M'_{d,initial} = M_{d,initial} - M_{burst/lag,\infty}$

And,

$$M_{burst,\infty} = \frac{2}{\alpha'} J_{\max} A \tag{B.13}$$

$$M_{lag,\infty} = -\frac{2}{\alpha'} J_{\max} A \tag{B.14}$$

The resulting equations for burst (Eq. B.15) and for lag time (Eq. B.16) effects are,

$$\begin{aligned} M_r(t) &= \frac{V_r C'_{d,initial}}{\left(K_{m/r}/K_{m/d} + V_r/V_d\right)}\left(1 - \exp(-\alpha t)\right) \\ &\quad + J_{\max} A \frac{2}{\alpha'}\left(1 - \exp\left(-\alpha' t\right)\right) \end{aligned} \tag{B.15}$$

$$\begin{aligned} M_r(t) &= \frac{V_r C'_{d,initial}}{\left(K_{m/r}/K_{m/d} + V_r/V_d\right)}\left(1 - \exp(-\alpha t)\right) \\ &\quad - J_{\max} A \frac{2}{\alpha'}\left(1 - \exp\left(-\alpha' t\right)\right) \end{aligned} \tag{B.16}$$

where,

$$\begin{aligned} J_{\max} &= \frac{DC_{d,initial}}{h} K_{m/d} \\ \alpha' &= \frac{D\pi^2}{h^2} K_{m/d} \\ \alpha &= \frac{DAK_{m/d}}{V_r h}\left(K_{m/r}/K_{m/d} + V_r/V_d\right) \end{aligned}$$

Nomenclature

List of symbols

A	Surface area through which diffusion takes place
C_d	Concentration of AI in the donor
$C_{d,initial}$	Initial concentration of AI in the donor
C_r	Concentration of AI in the receiver
D	Diffusion coefficient
h	Thickness of the microcapsule wall
J	Flux
J_{max}	Steady-state flux and the donor or receiver compartment.
$K_{m/d}$	Partition coefficient of the AI between the donor and the polymer membrane
$K_{m/r}$	Partition coefficient of the AI between the polymer membrane and the release medium
M	Mass of AI
M_d	Mass of AI in the donor
M_r	Mass of released AI
$M_{r,0}$	Initial mass of AI in the release medium
t	Time
V_d	Donor volume
V_r	Receiver volume

References

[1] Kydonieus, A.F., *Controlled release technologies: methods, theory and applications*. CRC Press, Inc. Boca Ratón, Florida, 1980.

C

Information of the compounds and polymers

In this appendix some details are provided to help in the identification of the compounds used in chapter 4.

In Tables C.1 to C.3 the compound names are identified with the corresponding CAS numbers and their abbreviations when appropriate.

Table C.1: Compounds used in diffusion studies and their corresponding CAS numbers

Compound	**CAS nr**	**Compound**	**CAS nr**
PNA	100-01-6	Methyl acetate	79-20-9
PAAB	60-09-3	Ethyl acetate	141-78-6
Disperse Yellow 7	6300-37-4	Propyl acetate	109-60-4
TTI	16291-99-9	Butyl acetate	123-86-4
ONSN	61599-59-5	n-Butane	106-97-8
ONSB	124604-84-8	iso-Butane	75-28-5
ONSA	124604-85-9	n-pentane	109-66-0
Orange3	730-40-5	iso-pentane	78-78-4
Red1	3025-52-3	Neopentane	463-82-1
Red4	n/a	n-dodecane	112-40-3
Dye I	n/a	n-hexadecane	544-76-3
Dye II	n/a	1,1-diphenylethane	612-00-0
ϵ-caprolactam	105-60-2	cyclohexane	110-82-7
NMP	872-50-4	2,2,5-trimethylhexane	3522-94-9
γ-butyrolactone	96-48-0	n-hexane	110-54-3
acetic acid	64-19-7	n-heptane	142-82-5
propionic acid	79-09-4	n-octane	111-65-9
THF	109-99-9		
λ-cyhalothrin	91465-08-6		
Permethrin	52645-53-1		

Table C.2: Compounds used in study of diffusion in plant cuticles

Abbreviation	**Compound**	**CAS nr**
n/a	Benzoic acid	65-85-0
2,4-D	(2,4-Dichlorophenoxy)acetic acid	94-75-7
PCP	Pentachlorophenol	87-86-5
n/a	Lindane	58-89-9
n/a	Triadimenol (*)	55219-65-3
n/a	Bitertanol (*)	55179-31-2
IAA	1H-Indole-3-acetic acid	87-51-4
n/a	Tebuconazole	107534-96-3
n/a	Bifenox	42576-02-3
WL-110547	1-(3-fluoromethylphenyl)-5-U-14C-phenoxy-1,2,3,4-tetrazole	n/a

Table C.3: Compounds used in study related to controlled release compounds

Abbreviation	**Compound**	**CAS nr**
HMDA	Hexamethylene diamine	124-09-4
DETA	Diethylene triamine	111-40-0

For the compounds for which the CAS number is not available, their structures are given in Table C.4.

Table C.4: Molecular structures of the compounds for which CAS numbers are not available

Compounds	**Molecular structures**
Red 4	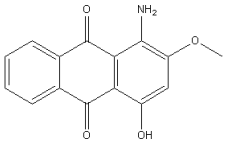
Dye I	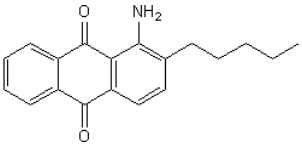
DyeII	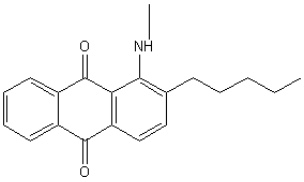

Finally, in Table C.5, the polymer abbreviations used in this chapter are given together with their corresponding names.

Table C.5: Polymer abbreviations

Abbreviation	**Polymer**
PS	Polystyrene
PC	Polycarbonate
PES	Poly(ethyl-styrene)
PMMA	Poly(methyl methacrylate)
PEMA	Poly(ethyl methacrylate)
PET	Poly(ethylene terephtalate)
iPP	Isotactic Polypropylene
PE	Polyethylene
PVAc	Poly(vinyl acetate)
Nylon 6	Polyamide 6
PSF	Polysulfone
PMA	Poly(methyl acrylate)
PIB	Polyisobutylene

D

Pesticide diffusion in plants

In order to extend the study of the applicability of the Extended FV model to pesticide compounds, the possibility of using measured data of diffusivity of these compounds in plant cuticles is considered in section 4.4.2.2 (chapter 4). The special nature of the experimental data and the form in which it is available (different experimental correlations) makes it necessary to apply some considerations so that it can be used for the purposes of this study, that is temperature dependent diffusivity data. The nature of the data and these considerations will be explained in detail in the present appendix.

Analysis of the experimental data available

In the literature of diffusion in plant cuticles, the experimental data is provided in the form of correlations of the diffusion coefficient, D (or the mobility, $k*$) of several compounds either with the solute molar volume at absolute zero (V(0K)), at a fixed temperature (25 °C), or just as a function of temperature. These correlations are summarized in Table D.1.

Table D.1: Summary of the experimental data available (in the form of correlations. V (0K) in cm^3/mol, and T in °C).

Data source	Data correlated	Property used to correlate	Property range of validity	Compounds	Membrane
[1]	D (25 °C)	V (0K)	$93 \sim 267$	Aromatics	Barley wax
[1]	D (25 °C)	V (0K)	$238 - 462$	Aliphatics	Barley wax
[2]	k* (25 °C)	V (0K)	$99 \sim 349$	Cyclics	Several CMs (and wax)
[2]	k*	T	$5 \sim 45$	2 cyclic compounds	1 CM 1 CM
[3]	k*	T V(0K)	25 - 70 (1) $130 \sim 349$	Pesticides	Several CMs
[4]	k* (25 °C)	V (0K)	$93 \sim 356$	Cyclics and aliphatics	Several CMs

CM: cuticular membrane (wax + cuticle)
(1)For Citrus a. It depends on the CM studied.

The relationship between the diffusion coefficient and the mobility is given by a proportionality factor that is the membrane thickness (Eq. D.1). For the purposes of this work the diffusion coefficient or the mobility correlations can be used indistinctively, this will be clarified in the next section.

$$D = k^* \Delta x_1 \Delta x_2 \tag{D.1}$$

i) Diffusion coefficient correlations as a function of molar volume

The correlations of both the diffusion coefficient and the mobility as a function of the molar volume have the general form given by Eq. D.2 (or Eq. D.3 in some cases).

$$\log_{10} D = a + \beta V(0K) \quad \text{or} \quad \log_{10} k^* = a + \beta V(0K) \tag{D.2}$$

$$\log_{10} D = a + \beta \log_{10} V(0K) \quad \text{or} \quad \log_{10} k^* = a + \beta \log_{10} V(0K) \tag{D.3}$$

In these correlations the parameter a represents the diffusion of a hypothetical molecule having zero molar volume. This parameter is independent of the polymer membrane (i.e. cuticle, wax, etc.) and is only a function of type of compound that is, cyclic or aliphatic. It includes the effect of tortuosity and the diffusion path. The second parameter, β represents the size selectivity of the barrier that is, the free volume available for diffusion. Thus, it only depends on the membrane and reflects its viscosity. The values of the correlation parameters are listed in Table D.2 for each of the sources available.

Table D.2: List of correlations with molar volume at 0 K (cm^3/mol), and T = 25 °C.

Type of compounds	**Property**	a	β	**Eq.**	**Ref.**
Pesticide	D (m^2/s)	-15.778	0.0077	D.2[3]	[1]
	D (m^2/s)	-10.64	-2.93	D.3	[1]
Aliphatic	D (m^2/s)	-11.946	0.021	D.2[3]	[1]
	D (m^2/s)	20.31	-15.72	D.3	[1]
Aliphatic (with double bonds)[1]	D (m^2/s)	56.217	-30.325	D.3	[1]
Cyclics	k* (1/s)	Depends on plant species	-0.0094[2]	D.2	[2]
Cyclics	k* (1/s)	4.28	-0.012	D.2	[4]
Aliphatics	k* (1/s)	3.19	-0.011	D.2	[4]

[1] Can also be represented with the correlation for 'Aliphatic molecules'

[2] Average value

[3] Correlation converted from: $\log_{10}\mathrm{D}(\mathrm{m}^2/\mathrm{s}) = \mathrm{a} + \mathrm{b}\log_{10}\mathrm{V}(0\mathrm{K})$ to $\log_{10}\mathrm{D}(\mathrm{m}^2/\mathrm{s}) = \mathrm{a} + \mathrm{bV}(0\mathrm{K})$

ii) Diffusion coefficient correlations as a function of temperature

The correlations that represent the mobility as a function of temperature are provided in Table D.3 in terms of the parameters, and follow an Arrhenius type of equation as shown in Eq. D.4. In these cases there is one single correlation for each compound diffusing in a specific plant cuticle.

$$\log_{10} k^* = a - b/T \tag{D.4}$$

Table D.3: List of correlations with temperature (in K) based on Eq. D.4.

Compounds	**Membrane**	a	b	**Ref.**
IAA	Strophantus G. (CM)	14.75	6.23×10^3	[2]
Tebuconazole	Strophantus G. (CM)	26.67	1.01×10^4	[2]
Pesticides	Several plant CMs	Several examples		[3]

iii) Combination of the molar volume and temperature correlations

Finally, the two types of correlations given in (i) and (ii) are combined through the size selectivity parameter (β in Eq. D.2). The procedure followed involves the calculation of the mobility of different compounds (concerning different molar volumes), at several temperatures. This is illustrated through the compounds in Buchholz et al. [2] represented in Fig. D.1.

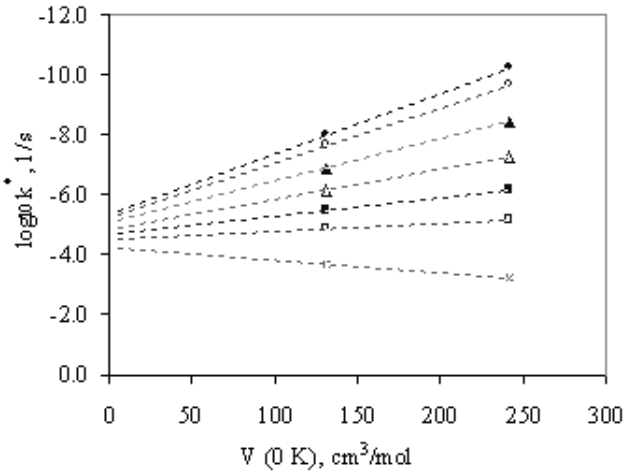

Figure D.1: Plot of mobility (logarithm) as a function of the molar volume at several temperatures. (•) T = 274.15 K; (○) T = 278.15 K; (▲) T = 288.15 K; (△) T = 298.15 K; (■) T = 308.15 K; (□) T = 318.15 K; (x) T = 338.15 K. (- - -) Regression lines.

In Fig. D.1, the size selectivity parameter (β) is the slope of the regression lines (based on Eq. D.2), and therefore a value of this parameter is obtained at each different temperature. Then, the size selectivity parameter can be correlated as a function of temperature (Fig. D.2).

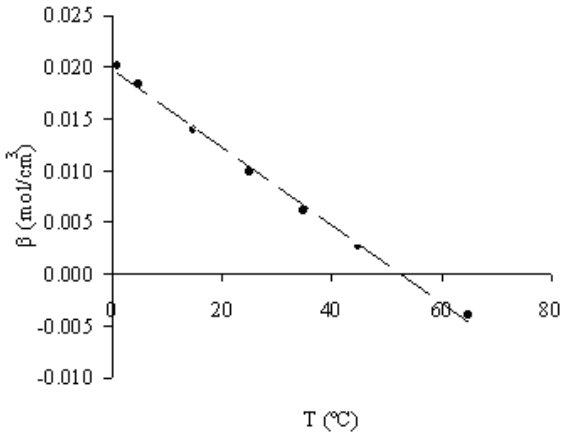

Figure D.2: Plot of β as a function of temperature. (•) Data; (– –) Regression line.

The same procedure is followed for the compounds in Baur et al. [3] and a similar correlation is obtained. The final equations are presented in Table D.4.

Table D.4: Summary of the combination of V(0K) and temperature correlations.

Compounds	Membrane	a	β (T)	Eq.	Ref.
Cyclics	Several plant (CM and wax)	Depends on plant species	0.02 - 0.0004 T(°C)	D.3	[2]
Pesticides	Citrus a.		0.0214 - 0.0003 T(°C)	D.3	[3]

The last step is the combination of the temperature dependence of the size selectivity parameter (β) to obtain the equations that provide the mobility/diffusivity data for each compound at different temperatures (Eqs. D.5, for pesticide compounds and D.6, for aliphatics).

$$\log_{10} D = -15.778 - [0.02 - 0.0004 \times T(^{\circ}C)]V(0K) \quad \text{(D.5)}$$

$$\log_{10} D = -11.946 - [0.02 - 0.0004 \times T(^{\circ}C)]V(0K) \quad \text{(D.6)}$$

It is worth noting that in this procedure diffusion coefficient (D) and the mobility ($k*$) correlations have been combined. As it can be seen in Table D.2, the values of the size selectivity parameter (β) are approximately the same for

all the correlations of the same type (Eq. D.2), whether they refer to diffusivity or to mobility. This parameter is also approximately the same for diffusion in different cuticular membranes and cuticular waxes. More details and data to confirm this can be found in Buchholz et al. [2]. Then, since the combination of the different correlations is done through the size selectivity parameter, the a parameters of the original correlations (Eqs. D.2, D.3) do not change.

Nomenclature

List of symbols

a, β	Parameters of the correlations
D	Diffusion coefficient
Δx_i	Thickness of membrane i
$k*$	Mobility
T	Temperature
$V(0K)$	Molar volume at 0 K

References

[1] Schreiber,L. and Schnherr,J., Mobilities of organic compounds in reconstituted cuticular wax of Barley leaves: Determination of diffusion coefficients, *Pesti. Sci.* 1993, 38, 353-361.

[2] Buchholz, A., Baur,P., Schnherr, J., Differences among plant species in cuticular permeabilities and solute mobilities are not caused by differential size selectivities, *Planta* 1998, 206, 322-328.

[3] Baur,P., Buchholz,A., Schnherr,J., Diffusion in plant cuticles as affected by temperature and size of organic solutes: similarity and diversity among species, *Plant Cell Environ.* 1997, 20, 982-994.

[4] Baur, P., Marzouk, H., Schönherr, J., Bauer, H., Mobilities of organic compounds in plant cuticles as affected by structure and molar volumes of chemicals and plant species, *Planta* 1996, 199, 404-412.

E

Considerations regarding the aspect ratio

One of the parameters needed in the Extended FV model is the aspect ratio of the diffusing compounds, that takes into account the shape of these compounds. In Vrentas et al. [1] the aspect ratio is defined based on the approximation of the molecules as a rectangular parallelepiped, with a square cross section of side A and height B. Vrentas et al. [1] obtained the values of the aspect ratio (B/A) from the ADAPT software [2] according to the following procedure:

i) Put the major plane of the molecule in the X-Y plane

ii) Determine the size of the rectangle which encloses the molecule and then two aspect ratios can be obtained,
a) The aspect ratio of the rectangle with minimum area that can enclose the molecule.
b) Aspect ratio of the rectangle enclosing the molecule, that maximizes B/A.
An average value between these two is finally used.

In this work, two different molecular modelling software have been used to obtain the values of the aspect ratio, these are: Accelrys [3] and Chem3D [4]. Both of these software provide values for the three dimensions of the molecule (lengths in the three spatial directions: L_1, L_2 and L_3) from which the ratios L_i/L_j (i, j = 1, 2 and 3) can be calculated. None of these ratios gives the same values of the aspect ratio reported by Vrentas et al. [1] but a correlation exists between them and is used in this work. The aspect ratios obtained from the software available for this work (L_i/L_j) are then correlated with the aspect ratios (B/A) reported by Vrentas et al. [1] for all the compounds reported.

The final correlations have the form given in Eq. E.1 and the values obtained for the parameters of this equation are provided in Table E.1.

$$B/A = a \times (L_i/L_j) + b \tag{E.1}$$

where,
a, b: regressed parameters
L_i/L_j: input aspect ratio calculated by each software (Accelrys and Chem3D)

B/A: resulting aspect ratio, equivalent to that in Vrentas et al. [1]

Table E.1: Resulting parameters for the correlation of aspect ratios.

L_i/L_j	**a**	**b**	r^2
Accelrys	0.0725	1.0992	0.9446
Chem3D	0.2929	0.8586	0.7866

References

[1] Vrentas, J.S.; Vrentas,C.M. and N.Faridi, Effect of solvent size on solvent self-diffusion in polymer-solvent systems, *Macromolecules* 1996, 29, 3272-3276.

[2] ADAPT Software, Chemistry Department, Pennsylvania State University.

[3] Accelrys Software Inc. 2001-2005.

[4] CS Chem3D Ultra, 2001. CambridgeSoft, 100 Cambridge Park Dr. Cambridge, MA 02140-2317 USA.